



**This electronic thesis or dissertation has been
downloaded from Explore Bristol Research,
<http://research-information.bristol.ac.uk>**

Author:
Walters, Jess L

Title:
Investigating Argonaute phosphorylation and miR-134 in Alzheimer's disease

General rights

Access to the thesis is subject to the Creative Commons Attribution - NonCommercial-No Derivatives 4.0 International Public License. A copy of this may be found at <https://creativecommons.org/licenses/by-nc-nd/4.0/legalcode>. This license sets out your rights and the restrictions that apply to your access to the thesis so it is important you read this before proceeding.

Take down policy

Some pages of this thesis may have been removed for copyright restrictions prior to having it been deposited in Explore Bristol Research. However, if you have discovered material within the thesis that you consider to be unlawful e.g. breaches of copyright (either yours or that of a third party) or any other law, including but not limited to those relating to patent, trademark, confidentiality, data protection, obscenity, defamation, libel, then please contact collections-metadata@bristol.ac.uk and include the following information in your message:

- Your contact details
- Bibliographic details for the item, including a URL
- An outline nature of the complaint

Your claim will be investigated and, where appropriate, the item in question will be removed from public view as soon as possible.



**This electronic thesis or dissertation has been
downloaded from Explore Bristol Research,
<http://research-information.bristol.ac.uk>**

Author:

Walters, Jess L

Title:

Investigating Argonaute phosphorylation and miR-134 in Alzheimer's disease

General rights

Access to the thesis is subject to the Creative Commons Attribution - NonCommercial-No Derivatives 4.0 International Public License. A copy of this may be found at <https://creativecommons.org/licenses/by-nc-nd/4.0/legalcode>. This license sets out your rights and the restrictions that apply to your access to the thesis so it is important you read this before proceeding.

Take down policy

Some pages of this thesis may have been removed for copyright restrictions prior to having it been deposited in Explore Bristol Research. However, if you have discovered material within the thesis that you consider to be unlawful e.g. breaches of copyright (either yours or that of a third party) or any other law, including but not limited to those relating to patent, trademark, confidentiality, data protection, obscenity, defamation, libel, then please contact collections-metadata@bristol.ac.uk and include the following information in your message:

- Your contact details
- Bibliographic details for the item, including a URL
- An outline nature of the complaint

Your claim will be investigated and, where appropriate, the item in question will be removed from public view as soon as possible.

Investigating Argonaute phosphorylation and miR-134 in Alzheimer's disease

Jessica Lynn Walters

December 2022

A dissertation submitted to the University of Bristol in accordance with the requirements of the degree of Doctor of Philosophy by advanced study in the School of Biochemistry, Faculty of Life Sciences



Word count: 30,318

Abstract

MicroRNAs (miRNAs) are small non-coding RNAs involved in RNA-mediated silencing of synaptic proteins via Argonaute (AGO) as part of the RNA-induced Silencing Complex (RISC). miRNAs are known to be involved in regulation of synapses and dendritic spine morphology and specific miRNAs have been implicated in the pathogenesis of Alzheimer's Disease (AD). However, how RISC protein machinery is affected by AD pathology is less well understood.

Limk kinase 1 (LIMK1) activity stabilises and maintains mature dendritic spine structure. miRNA-134 (miR-134) plays a role in shrinkage of dendritic spines following Long Term Depression (LTD) by targeting LIMK1 mRNA for translational silencing. Preliminary data from the Hanley lab indicated that phosphorylation of AGO at S387 and the association of AGO to the RISC is increased in the J20 mouse model of AD and in a primary neuronal culture model of AD. Furthermore, LIMK1 expression levels were found to be decreased in late stage cortical AD tissue. This thesis aimed to investigate the potential role of AGO2 phosphorylation and miR-134 in the synaptic dysfunction and dendritic spine loss seen in AD by determining at what point in the disease course these changes occur, and to produce a model in which rescue strategies targeting AGO2 phosphorylation could potentially be tested.

Technical challenges with the primary neuronal culture model used previously led me to use and characterise an alternative model using lentiviral expression of Amyloid Precursor Protein (APP) with AD-associated mutations and to design a method for quantifying miRNA activity in this model. Changes in levels of AGO2-S387 phosphorylation or LIMK1 expression seen in the previous model were not successfully reproduced, however, I demonstrated proof of concept for this novel miRNA activity assay.

Surprisingly, when I quantified LIMK1 expression levels in cortical samples from AD patients at Braak stages 1-6 by Western blotting I found no significant differences during the disease course. However, Western blotting of cortical and hippocampal samples from the J20 AD mouse model at 6months and 18months revealed that, despite no change in LIMK1 levels, pS387-AGO2 was significantly decreased. These results may indicate altered miRISC assembly and regulation in the AD hippocampus and provide a potentially important foundation for future research into the role of AGO2 phosphorylation in AD.

Acknowledgements

Thank you to Jon and to everyone in the Hanley and Henley labs. To my fellow post-graduate students: Fathima thank you for your kindness and for our chats. It's been such a pleasure working with and getting to know you. Georgiana and Siobhan thank you for all the colour and fun you brought to the lab. Luke and Elliott thank you for being friendly faces at our GW4 events, for working with me, and making me laugh.

Thank you from the bottom of my heart to all the ACORN Bristol branch members and staff for the multitude of ways over the past four years in which your boundless solidarity, drive and compassion has helped me to grow and given me hope at times when I was running low.

Thank you to my family for supporting me whilst I was writing up, especially to Skye and Max for taking me out on walks when I was drowning in writing.

To my friends: Thank you to my Mogg Street housemates Ben, Will, Dan and Sherman for making me feel so welcome and at home during that final crazy stretch in the lab. Thank you to Alex for being an almost indefatigable cheerleader, motivator, and true friend through all the pitfalls and peaks that led to my getting here in the first place. Thank you so much to Matt for all of the love and support you gave me through my imposter syndrome and everything else. You helped me so much more than you know. Thank you to Merlin and Ashley for weathering the scariest parts of the pandemic with me and bringing so much joy and silliness and squash plants into my life. It was a crazy and difficult time but we went into it as friends and came out of it as family. I could not have done it without you. Thank you to Molly and Baz for being my bedrock and, like always, keeping me sane whilst I did another crazy thing.

Last but certainly not least, thank you to Kev, for always answering my endless questions, cheerfully tolerating my griping and moaning, for all the nonsense and laughs, for the countless man-hours sunk into pep talks and for ultimately pulling me through to the end in one piece. You have been an incredible teacher, friend, and all round solid gold legend and I am eternally grateful to you for all your support.

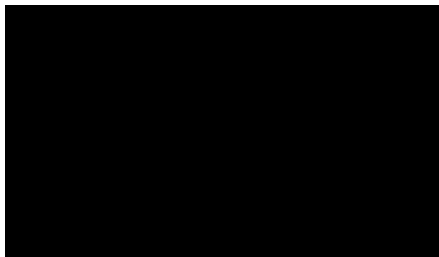
I would like to dedicate this thesis to Ken and to Haley.

This work was supported in part by grant MR/N0137941/1 for the GW4 BIOMED DTP, awarded to the Universities of Bath, Bristol, Cardiff and Exeter from the Medical Research Council (MRC)/UKRI

"In the middle of progress, in the middle of the fight, we learn how we must fight."

Author's Declaration

I declare that the work in this dissertation was carried out in accordance with the requirements of the University's Regulations and Code of Practice for Research Degree Programmes and that it has not been submitted for any other academic award. Except where indicated by specific reference in the text, the work is the candidate's own work. Work done in collaboration with, or with the assistance of, others, is indicated as such. Any views expressed in the dissertation are those of the author.



SIGNED: DATE:.....19.12.22.....

Table of Contents

| | |
|---|----|
| Abstract..... | 2 |
| Acknowledgements..... | 3 |
| List of Figures..... | 11 |
| List of Tables..... | 12 |
| List of Abbreviations..... | 12 |
| Chapter 1: Introduction..... | 17 |
| 1.1 Synaptic plasticity in learning and memory..... | 18 |
| 1.1.1 Synapses are the fundamental cellular units of learning and memory..... | 18 |
| 1.1.2 Dendritic spines house excitatory synapses..... | 18 |
| 1.1.3 Chemical synapses transmit electrical signals using neurotransmitters as chemical intermediates..... | 20 |
| 1.1.4 GABA is the major inhibitory neurotransmitter in the brain..... | 21 |
| 1.1.5 Glutamate is the major excitatory transmitter in the brain..... | 21 |
| 1.1.6 The strength of synaptic connections can be modified by activity..... | 22 |
| 1.1.7 NMDARs are major coordinators of synaptic plasticity..... | 22 |
| 1.1.8 Functional plasticity of a synapse is complemented by structural plasticity of the dendritic spine..... | 23 |
| 1.1.9 Overview of Long Term Potentiation..... | 24 |
| 1.1.10 Early phase Long Term Potentiation..... | 24 |
| 1.1.11 Late phase Long Term Potentiation..... | 25 |
| 1.1.12 Overview of Long Term Depression..... | 26 |
| 1.1.13 Synaptic plasticity underlies memory and learning..... | 26 |
| 1.1.14 Actin is the major cytoskeletal protein of the dendritic spine..... | 29 |
| 1.1.15 Structural plasticity of dendritic spines is orchestrated through actin modifiers..... | 29 |
| 1.1.16 Cofilin is essential for activity-dependent actin remodelling in synaptic plasticity..... | 31 |

| | |
|---|----|
| 1.1.17 Cofilin activity is regulated by Slingshot Homolog 1 and LIM kinase..... | 32 |
| 1.1.18 Cofilin regulation is important for dendritic spine morphology and function..... | 32 |
| 1.1.19 LIM kinase 1 activity is important for synaptic function..... | 33 |
| 1.1.20 Excessive cofilin activity is associated with dysregulated dendritic spine morphology..... | 34 |
| 1.2 Alzheimer's Disease is a progressive neurodegenerative disorder..... | 34 |
| 1.2.1 Alzheimer's Disease is the most common cause of dementia globally..... | 34 |
| 1.2.2 Alzheimer's Disease symptoms..... | 35 |
| 1.2.3 Alzheimer's Disease Pathology..... | 35 |
| 1.2.4 Neurofibrillary tangles progress through the brain in a stepwise manner in Alzheimer's Disease..... | 36 |
| 1.2.5 Amyloid dysregulation is the earliest molecular hallmark of Alzheimer's Disease..... | 37 |
| 1.2.6 Alzheimer's Disease genetics..... | 39 |
| 1.2.7 Amyloid Cascade Hypothesis..... | 40 |
| 1.2.8 Synapse loss is the earliest structural change in AD..... | 43 |
| 1.2.9 Dysregulation of dendritic spines is seen in models of AD..... | 45 |
| 1.2.10 LIM Kinase and cofilin are dysregulated in Alzheimer's Disease and its models..... | 47 |
| 1.3 Local translational control at the synapse by miRNA..... | 52 |
| 1.3.1 Localised translation occurs at the synapse..... | 52 |
| 1.3.2 mRNA is transported to dendritic spines..... | 53 |
| 1.3.3 mRNAs are subject to regulation by microRNAs..... | 54 |
| 1.3.4 miRNA and RISC machinery are present in the synapse..... | 55 |
| 1.3.5 AGO proteins..... | 57 |
| 1.3.6 Loading miRNA into AGO..... | 58 |
| 1.3.7 AGO target recognition and translational down-regulation..... | 59 |

| | |
|---|----|
| 1.3.8 RISC loading/binding partners..... | 60 |
| 1.3.9 Post translational modifications of AGO regulate function, localisation and stability..... | 60 |
| 1.3.10 AGO is regulated extensively by phosphorylation at number of residues..... | 61 |
| 1.3.11 miRNAs regulate synaptic plasticity..... | 65 |
| 1.3.12 miR-134 activity is important in neuronal function and synaptic plasticity..... | 66 |
| 1.3.13 RNA-induced Silencing Complex (RISC) machinery plays a role in synaptic plasticity..... | 68 |
| 1.3.14 Many miRNAs are involved in AD pathology..... | 70 |
| 1.4 Summary and Aims..... | 72 |
| 1.4.1 Summary..... | 72 |
| 1.4.2 Aims..... | 75 |
| Chapter 2: Materials and methods..... | 76 |
| 2.1 Materials..... | 77 |
| 2.1.1 Chemicals..... | 77 |
| 2.1.2 Bacterial culture reagents..... | 77 |
| 2.1.3 Eukaryotic cell culture reagents..... | 77 |
| 2.1.4 Molecular cloning reagents..... | 78 |
| 2.1.5 Protein biochemistry reagents..... | 78 |
| 2.1.6 Primary antibodies..... | 79 |
| 2.1.7 Secondary antibodies..... | 79 |
| 2.1.8 Consumables and equipment..... | 80 |
| 2.1.8.1 Plastic and glassware..... | 80 |
| 2.1.8.2 Electronic equipment..... | 80 |
| 2.2 Cell culture methods..... | 81 |
| 2.2.1 Eukaryotic cell culture..... | 81 |
| 2.2.1.1 HEK293T cells..... | 81 |

| | |
|--|----|
| 2.2.1.1.1 HEK293T cell passaging..... | 82 |
| 2.2.1.1.2 HEK293T cell transfection..... | 82 |
| 2.2.1.2 Primary neuronal culture..... | 83 |
| 2.2.1.2.1 Poly-D-lysine coating of cell culture plates..... | 83 |
| 2.2.1.2.2 Rat sacrifice and dissection of embryos..... | 83 |
| 2.2.1.2.3 Dissociation and plating of primary neurons..... | 84 |
| 2.3 Virus production..... | 85 |
| 2.3.1 HEK293T production..... | 85 |
| 2.3.2 HEK293T transfection for the production of lentiviruses..... | 85 |
| 2.3.3 Harvesting of lentivirus..... | 86 |
| 2.3.4 Viral transduction of primary neurons..... | 86 |
| 2.4 Molecular biology methods..... | 86 |
| 2.4.1 SDS-PAGE..... | 86 |
| 2.4.1.1 Preparation of brain tissue samples..... | 86 |
| 2.4.1.1.1 <i>Post-mortem</i> Human Brain tissue..... | 86 |
| 2.4.1.1.2 J20 mouse model brain tissue..... | 87 |
| 2.4.1.1.3 J20 mouse brain dissection..... | 87 |
| 2.4.1.1.4 Tissue homogenisation..... | 84 |
| 2.4.1.1.5 Bradford protein assay..... | 89 |
| 2.4.1.2 Lysis of primary neurons and HEK293T cells..... | 90 |
| 2.4.1.3 SDS-PAGE..... | 90 |
| 2.4.2 Western Blotting..... | 92 |
| 2.4.2.1 Immunoblotting..... | 92 |
| 2.4.2.2 Enhanced chemiluminescence detection..... | 92 |
| 2.4.2.3 Immunoblot Quantification and Analysis..... | 93 |

| | |
|--|------------|
| 2.4.2.4 Total Protein Stain..... | 93 |
| 2.4.3 Molecular Cloning..... | 94 |
| 2.4.3.1 Polymerase chain reaction (PCR)..... | 94 |
| 2.4.3.2 DNA gel electrophoresis..... | 95 |
| 2.4.3.3 DNA fragment purification..... | 95 |
| 2.4.3.4 Restriction digest..... | 95 |
| 2.4.3.5 DNA ligation..... | 96 |
| 2.4.3.6 Transformation of <i>E. Coli</i> | 96 |
| 2.4.3.7 Plasmid DNA amplification and purification..... | 97 |
| 2.4.3.8 Phenol chloroform precipitation..... | 97 |
| 2.4.3.9 Extraction of RNA from Rat brain tissue..... | 98 |
| 2.4.3.10 First strand cDNA synthesis..... | 99 |
| Chapter 3: Investigating Argonaute phosphorylation and LIMK1 expression in a primary neuronal culture model of Alzheimer's Disease..... | 101 |
| 3.1 Introduction..... | 102 |
| 3.1.1 A β causes synaptic dysfunction and loss in AD and its models..... | 102 |
| 3.1.2 Methods for modelling A β accumulation <i>in vitro</i> | 104 |
| 3.1.3 Aim..... | 106 |
| 3.2 Results..... | 106 |
| 3.2.1 Primary neuronal culture amyloidopathy model..... | 106 |
| 3.2.2 miRNA activity assay..... | 107 |
| 3.2.3 mCherry.PEST protein expression is decreased when conjugated to LIMK1 3'UTR and miR-134 precursor is overexpressed..... | 111 |
| 3.3 Discussion..... | 114 |
| 3.3.1 Primary neuronal culture amyloidopathy model..... | 114 |
| 3.3.2 Lentivirus based miRNA activity assay proof of concept..... | 116 |
| 3.3.3 Conclusions..... | 119 |

Chapter 4: Investigating Argonaute phosphorylation and LIMK1 expression in the J20 mouse model of Alzheimer's Disease.....120

| | |
|---|-----|
| 4.1 Introduction..... | 121 |
| 4.1.1 Animal models of AD are generated using EOAD-associated mutations of APP-related genes..... | 121 |
| 4.1.2 pS387-AGO2 and miR-134-mediated down-regulation of LIMK1 occurs in aged J20 mice..... | 123 |
| 4.1.3 Aim..... | 124 |
| 4.2 Results..... | 124 |
| 4.2.1 APP expression is increased in J20 mice..... | 124 |
| 4.2.2 pS387-AGO2 is increased in the hippocampus of J20 mice..... | 125 |
| 4.2.3 LIMK1 expression is unchanged in NL-F mice..... | 126 |
| 4.3 Discussion..... | 127 |
| 4.3.1 pS387-AGO2 levels are altered in the hippocampus of J20 mice..... | 127 |
| 4.3.2 Conclusions..... | 131 |

Chapter 5: Investigating LIMK1 expression in Alzheimer's Disease cortical tissue.....133

| | |
|--|-----|
| 5.1 Introduction..... | 134 |
| 5.1.1 AD models are unable to recapitulate all aspects of human AD..... | 134 |
| 5.1.2 Deposition of Neurofibrillary Tangles progresses linearly through the human brain during course of AD..... | 134 |
| 5.1.3 LIMK1 is down-regulated in LTD and in the AD brain..... | 135 |
| 5.1.4 Aim..... | 136 |
| 5.2 Results..... | 136 |

| | |
|---|-----|
| 5.2.1 Post mortem delay was not significantly different between test groups..... | 136 |
| 5.2.2 Cortical pTau is increased in late stage AD but LIMK1 expression is unaffected..... | 138 |
| 5.3 Discussion..... | 140 |
| 5.3.2 Cortical LIMK1 expression levels are unchanged during the course of AD..... | 140 |
| 5.3.3 Conclusions..... | 143 |
| Chapter 6: General Discussion..... | 144 |
| 6.1 Summary..... | 145 |
| 6.2 Conclusions..... | 147 |
| Chapter 8: References..... | 148 |
| Appendix: South West Dementia Brain Bank human sample data..... | 189 |

List of Figures:

| | |
|--|-----|
| Figure 1.1: Dendritic spine and filopodia morphology as recorded by Ramon y Cajal (1933)..... | 19 |
| Figure 1.2: Hyperphosphorylated tau spreads in a stereotyped manner through the brain..... | 37 |
| Figure 1.3: Processing of the transmembrane protein APP..... | 38 |
| Figure 1.4: Amyloid cascade hypothesis..... | 41 |
| Figure 1.5: Synaptic loss is correlated with performance on a number of tests of cognitive function used to quantify disease progression in AD patients..... | 44 |
| Figure 1.6: Biogenesis of miRNAs..... | 55 |
| Figure 1.7: AGO structure..... | 57 |
| Figure 1.8: Post-translational modifications of AGO..... | 61 |
| Figure 1.9: miRNAs have been found to be involved in AD via many different mechanisms..... | 71 |
| Figure 1.10: Schematic of hypothesised pS387-AGO2 and miR134-mediated synaptic loss in AD..... | 74 |
| Figure 3.1: Diagrammatic representation of recombinant genes created..... | 110 |

| | |
|---|-----|
| Figure 3.2: Expression of mCherry conjugated to a PEST sequence and the 3' UTR of LIMK1 is down-regulated by co-expression of pre-miR-134..... | 111 |
| Figure 3.3: Lentiviral expression of myc-tagged APP with EOAD-associated mutations in primary neuronal cultures does not lead to changes in pS387-AGO2 or LIMK1 expression..... | 113 |
| Figure 4.1: Changes in expression of APP in the cortical tissue of J20 mouse model at 6- and 18-months..... | 125 |
| Figure 4.2: Expression levels of proteins related to pS387-AGO2 and miR-134-mediated silencing of LIMK1 in hippocampal and cortical tissue of the J20 mouse model of AD at 6- and 18-months..... | 126 |
| Figure 4.3: Expression levels of LIMK1 in NL-F APP Knock in mouse model of AD..... | 127 |
| Figure 5.1: Post-mortem delay was not significantly different between Entorhinal (ER) (Early) stage, Limbic (L) (Mid) and Neocortical (NC) stage human AD samples..... | 138 |
| Figure 5.2: Cortical LIMK1 expression levels do not change during the course of AD as determined by pTau deposition and Braak stage..... | 139 |

List of Tables

| | |
|---|----|
| Table 1.1: Investigations into the role of cofilin and LIMK1 in AD and its models..... | 48 |
| Table 2.1: Suppliers and dilutions of primary antibodies used in Western blots..... | 79 |
| Table 2.2: Polymerase Chain Reaction parameters for thermocycler..... | 94 |

List of Abbreviations

| | |
|------|---|
| aa | Amino acid |
| AD | Alzheimer's Disease |
| ADF | Actin-depolymerizing factor |
| ADI | Alzheimer's Disease International |
| AGO | Argonaute |
| AICD | APP intracellular domain |
| AIP1 | Actin-interacting protein 1 |
| AMPA | α -amino-3-hydroxyl-5-methyl-4-isoxazole-propionate |
| AMPA | α -amino-3-hydroxyl-5-methyl-4-isoxazole-propionate receptor |

| | |
|----------------|--|
| ANKRD52 | Ankyrin repeat domain 52 |
| APP | Amyloid precursor protein |
| APT1 | Acyl protein thioesterase 1 |
| Arc | Activity-regulated cytoskeletal associated protein |
| A β | β amyloid |
| A β O | Amyloid β oligomers |
| BDNF | Brain-derived neurotrophic factor |
| Blessed IMC | Blessed Information-Memory-Concentration Test |
| BSA | Bovine Serum Albumin |
| C3PO | Translin |
| CamKII | Ca ²⁺ /calmodulin-dependent protein kinase II |
| CCR4 | Carbon catabolite repressor protein 4 |
| CDC33 | Myeloid cell surface antigen CD33 |
| CIP | Calf Intestinal Alkaline Phosphatase |
| cLTD | Chemical LTD |
| CLU | Clusterin |
| CREB | cAMP response element-binding protein |
| CSNK1A1 | Casein kinase 1 alpha 1 |
| DCP1 | Decapping by mRNA-decapping enzyme subunit |
| DDX6 | DEAD-Box Helicase 6 |
| DGCR8 | DiGeorge syndrome critical region 8 protein |
| DIV | Days <i>in vitro</i> |
| DMEM | Dulbecco's Modified Eagle's Medium |
| DMSO | Dimethyl sulfoxide |
| DRS | Dementia Rating Scale |
| <i>E. coli</i> | <i>Escherichia coli</i> |
| ECACC | The European Collection of Cell Cultures |

| | |
|-------------|---|
| ECL | Enhanced Chemiluminescence |
| EGFR | Epidermal growth factor receptor |
| EM | Electron Microscope |
| EOAD | Early onset Alzheimer's disease |
| EPSC | Excitatory post-synaptic current |
| EPSP | Excitatory Post Synaptic Potential |
| ER stage | Entorhinal stage |
| F-actin | Filamentous actin |
| FBS | Foetal bovine serum |
| FMRP | Fragile Mental Retardation Protein |
| GABA | Gamma-Aminobutyric acid |
| GABAR | Gamma-Aminobutyric acid receptor |
| G-actin | Globular actin |
| GRIA2 | Glutamate Ionotropic Receptor AMPA Type Subunit 2 |
| GTP | Guanosine triphosphate |
| HBSS | Hank's Buffered Salt Solution |
| HEK293 | Human Embryonic Kidney 293T cells |
| HRP | Horse Radish Peroxidase |
| HS | Horse serum |
| Hsc70/Hsp90 | Heat shock cognate 70/ Heat shock protein 90 |
| IPO8 | Importin 8 |
| iPSC | induced pluripotent stem cell |
| IPSC | Inhibitory post-synaptic current |
| IPSP | Inhibitory post synaptic potential |
| KO | Knock out |
| L stage | Limbic stage |
| LB | Luria-Bertani Broth |

| | |
|----------|--|
| LIMK | LIM kinase |
| LOAD | Late onset Alzheimer's disease |
| LTD | Long-term depression |
| LTM | Long term memories |
| LTP | Long-term depression |
| MAPK | p38 mitogen-activated kinase |
| MCI | Mild cognitive impairment |
| MEF | Mouse embryonic fibroblasts |
| MEF2 | Myocyte enhancing factor 2 |
| MEK | Mitogen-activated protein kinase |
| mGluR | Metabotropic glutamate receptor |
| miRNA | Micro RNA |
| MME | Mini mental State Exam |
| MOV10 | Moloney leukemia virus 10 |
| mRBP | mRNA-binding proteins |
| mRNA | Messenger ribonucleic acid |
| NC stage | Neocortical stage |
| NFT | Neurofibrillary tangles |
| NMDA | N-methyl-d-aspartate |
| NMDAR | N-methyl-d-aspartate receptor |
| P bodies | Processing bodies |
| PABPC | Polyadenylate-binding protein |
| pAGO2 | Phosphorylated AGO2 |
| PAK | p21 activated kinase |
| PAN | Poly(A)-nuclease deadenylation complex subunit |
| PBS | Phosphate-buffered saline |
| pCofilin | Phosphorylated cofilin |

| | |
|-------------|--|
| PCR | Polymerase chain reaction |
| PDL | Poly-D-Lysine |
| PEI | Polyethylenimine |
| PICALM | Phosphatidylinositol-binding clathrin assembly protein |
| PICK1 | Protein Interacting with C Kinase – 1 |
| PIWI | P-element Induced Wimpy testis |
| PKC | Protein kinase C |
| PKM ζ | Protein kinase C ζ type |
| pLIMK | Phosphorylated LIM kinase |
| PP6 | Protein phosphatase 6 |
| pre-miRNA | Precursor miRNA |
| pri-miRNA | Primary miRNA |
| PrPc | Cellular prion protein |
| PSD | Post-synaptic Density |
| PSD-95 | Post-synaptic Density protein 95 |
| PSEN1 | Presenilin 1 |
| PSEN2 | Presenilin 2 |
| pTau | Phosphorylated tau |
| PTP1B | Protein tyrosine phosphatase 1B |
| Pum | Pumilio |
| PVDF | Polyvinylidene difluoride |
| RACK1 | Receptor activated kinase 1 |
| REST | RE1-Silencing transcription factor |
| RISC | RNA induced silencing complex |
| ROCK | Rho kinase |
| RT | Room temperature |
| SDS | Sodium Dodecyl Sulphate |

| | |
|----------|--|
| SDS-PAGE | Sodium Dodecyl Sulphate-polyacrylamide gel electrophoresis |
| SHANK | SH3 and multiple ankyrin repeat domains protein |
| siRNA | Short interfering RNA |
| SIRT1 | Sirtuin-1 |
| SORL1 | Sortilin-related receptor LR11/SorLA |
| SSH1 | Slingshot homolog 1 |
| STM | Short term memories |
| SV | Synaptic Vesicle |
| SWDBB | South West Dementia Brain Bank |
| Syt-1 | Synaptotagmin-1 |
| Stx-1A | Syntaxin1A |
| TRBP | Transactivating response RNA-binding protein |
| TREM2 | Triggering receptor expressed on myeloid cells 2 |
| TREM2 | Triggering receptor expressed on myeloid cells 2 |
| UTR | Untranslated region |
| WT | Wild type |
| YY1 | Yin yang 1 |

Chapter 1: Introduction

1.1 Synaptic plasticity in learning and memory

1.1.1 Synapses are the fundamental cellular units of learning and memory

Neurons are the cells through which information storage and retrieval are primarily carried out in the central nervous system. Their morphology is complex and varies according to neuronal subtype but in simple terms most neurons can be described as polar cells, with one end responsible for receiving information and the other for transmitting information to other cells. Each neuron can make many thousands of connections with other neurons and in this way ~86 billion neurons form a network that constitutes the human brain ([Herculano-Houzel, 2012](#)).

Neurons communicate with one another through specialised junctions called synapses where information is transmitted directly as an electrical signal, or as a chemical signal that is translated into an electrical signal. These are called electrical and chemical synapses, respectively. The behaviour of a neural network or circuit can be characterised by the pattern and relative “strength” of the synaptic connections between the neurons within it. The brain’s ability to encode memories and learn behaviour hinges upon the capacity of its many neuronal networks to modulate this connectivity according to accumulated experience. Synapses therefore represent one of the most fundamental units of learning and memory ([Chklovskii *et al.*, 2004](#)).

1.1.2 Dendritic spines house excitatory synapses

Synapses were first postulated to be key mediators of memory and learning by Santiago Ramon y Cajal in 1888 who used Golgi staining and light microscopy to explore the morphology

Figure 1 consists of four diagrams labeled A, B, C, and D, illustrating the development of a dendritic tree. Diagram A shows a single axon with many small, simple dendrites. Diagram B shows a branching dendritic tree. Diagram C shows a more complex branching structure. Diagram D shows a highly branched, complex dendritic tree.

internal ultrastructure and that they consisted of a synaptic cleft lying between a pre- and post-synaptic bouton (Gray, 1959). At the post-synapse was a dense electron-rich region sitting at the head of the post-synaptic bouton facing the active zone of the presynapse - the post-synaptic density (PSD). The presynapse was shown to contain vesicles though at this time the function of these structures was unknown (Gray, 1959; Kennedy, 2000)

1.1.3 Chemical synapses transmit electrical signals using neurotransmitters as chemical intermediates

We now know that the synaptic vesicles (SVs) identified at the presynapse by Gray (1959) store the chemical mediators of electrical signals at the chemical synapse - neurotransmitters (Carlson *et al.* 1989; Burger *et al.* 1991). SVs within the presynaptic bouton are largely in one of two pools - the reserve pool within the bouton or the pool docked at the surface of the active zone ready for rapid release of neurotransmitters into the synaptic cleft (Rizzoli & Betz, 2005). Electrical signals are passed down the length of the cell via a change in membrane potential (Raghavan *et al.*, 2019). This property hinges on the transient opening of voltage-gated ion channels in the neuronal membrane. When an electrical signal, called an action potential, reaches the presynaptic active zone, voltage-gated calcium (Ca^{2+}) channels open (Llinás *et al.*, 1981; Augustine *et al.*, 1987). The consequent rise in intracellular Ca^{2+} levels triggers merging of the docked SVs with the pre-synaptic membrane, releasing the neurotransmitters within them into the synaptic cleft where they are able to bind with ligand-gated ion channels on the post-synaptic membrane (Heuser *et al.* 1979; Heidelberger *et al.*, 1994; Hilfiker *et al.*, 1999; Raghavan *et al.*, 2019). Depending on the ion channel, inward flow

through these can be either excitatory (i.e., depolarizing) or inhibitory (i.e., hyperpolarizing).

1.1.4 GABA is the major inhibitory neurotransmitter in the brain

Gamma-Aminobutyric Acid (GABA) receptors are activated by the neurotransmitter GABA and are responsible for most inhibitory transmission in the brain (Wilcox *et al.* 1994). There are two main subtypes of GABARs which contribute to inhibitory signalling - ionotropic GABA^ARs and metabotropic GABA^BRs. When bound to GABA the transmembrane channel of GABA^ARs opens, allowing an influx of Cl⁻ ions into the post-synapse and generating an inhibitory post synaptic potential (IPSP) (Wilcox *et al.* 1994). Pre-synaptically released GABA is also able to activate GABA^BRs which activate K⁺ channels to allow efflux of this positively charge ion (Sigel & Steinmann, 2012). The net effect of this is to hyperpolarise the cell, making a stronger depolarisation by excitatory signalling necessary to reach the threshold needed for an action potential to be propagated from the input neuron onwards.

1.1.5 Glutamate is the major excitatory transmitter in the brain

Glutamate is the major excitatory neurotransmitter in the brain (Megias *et al.*, 2001). The PSD of a glutamatergic synapse can contain three major types of ionotropic glutamate receptors: N-methyl-d-aspartate receptors (NMDARs) and α -amino-3-hydroxyl-5-methyl-4-isoxazole-propionate receptors (AMPA) and kainate receptors, so named for their synthetic agonists (NMDA, AMPA, and kainate, respectively). AMPARs are membrane channels that, once activated by pre-synaptically released glutamate, open to allow an inward current of monovalent cations (Na⁺ and K⁺) which generate changes in membrane potential or an

Excitatory Post Synaptic Potential (EPSP) (Kandel *et al.*, 2000; Citri & Malenka, 2007).

1.1.6 The strength of synaptic connections can be modified by activity

It is the cumulative effect of these changes in ion permeability at the many excitatory and inhibitory synaptic inputs of a neuron that determine whether an action potential is generated, propagating a received signal onwards to neurons downstream (Kandel *et al.*, 2000). The ion current through these channels is termed either an excitatory or inhibitory post-synaptic current (EPSC or IPSC, respectively). The strength of a synapse can be characterised by the magnitude of these currents in response to an action potential at the presynaptic neuron. At the presynapse the probability of SV release of neurotransmitters confers a change in EPSC/IPSC frequency, and at the postsynapse the amplitude of an EPSC/IPSC can be modified by changing surface expression of ionotropic neurotransmitter receptor channels. This capacity for activity-dependent adaptation of synaptic strengths is called synaptic plasticity.

1.1.7 NMDARs are major coordinators of synaptic plasticity

At the excitatory postsynapse this change in synaptic strength is proportional to the permeability of the post-synapse to cations which is co-ordinated largely via the insertion or removal of AMPARs at the PSD (Anggono & Huganir, 2012; Chater & Goda, 2014; Ehlers, 2000). A number of mechanisms for synaptic plasticity have been identified but the most prominent of these are that of long-term depression (LTD) and long term potentiation (LTP) which decrease or increase synaptic strength respectively (Bliss & Gardner-Medwin, 1973; Citri & Malenka, 2007).

NMDARs are a central player in the mechanisms underlying these changes. This is because NMDARs differ from AMPARs in that their membrane pore is blocked with an extracellular magnesium plug (Mayer *et al.*, 1984, Nowak *et al.*, 1984). NMDARs require strong depolarisation to remove this magnesium block and crucially also permit Ca^{2+} to enter the cell (Sabatini *et al.*, 2002; Yuste *et al.*, 2011). In this way, NMDARs act as coincidence detectors - only triggering the influx of Ca^{2+} and consequent intracellular signalling cascades when they are bound by glutamate in the presence of strong depolarisation.

1.1.8 Functional plasticity of a synapse is complemented by structural plasticity of the dendritic spine

Most excitatory synapses are housed within the dendritic spines structures first observed by Ramon y Cajal. This allows neurons to compartmentalise biochemical and electrical signals received from other neurons and therefore for synapses to act as discrete units of information transfer (Gray, 1959; Majewska *et al.*, 2000; Ashby *et al.*, 2006). The number of AMPARs present at the synapse is closely correlated with the volume of the dendritic spine that houses it (Nusser *et al.*, 1998; Takumi *et al.*, 1999; Matsuzaki *et al.*, 2001). Functional plasticity is complemented by changes in the density and morphology of dendritic spines, termed structural plasticity (Lamprecht & LeDoux, 2004; Carlisle & Kennedy, 2005; Alvarez & Sabatini, 2007; Bernardinelli *et al.*, 2014; ; Lai & Ip, 2013; Borovac *et al.*, 2018; Sheppard *et al.*, 2019). These structural changes can occur within minutes (Lendvai *et al.*, 2000). However, changes in spine morphology can also persist over longer periods or even permanently (Guang *et al.*, 2009). It can also be the case that both formation and elimination of dendritic spines are promoted simultaneously such that

there is a high turnover environment, with the ratio of these determining the overall effect on spine density (Jung & Herms, 2014).

1.1.9 Overview of Long Term Potentiation (LTP)

LTP is a positive feedback mechanism that underpins Hebb's famous axiom "cells that fire together, wire together." It is the process through which an increase in signalling at a synapse causes its connection to become strengthened, meaning that at an excitatory synapse an action potential in the pre-synaptic neuron leads to a stronger depolarisation in the post-synaptic membrane and therefore an increased probability of that action potential being propagated (Bliss & Collingridge, 1993). LTP was first discovered by Bliss and Lomo (1973) when conducting electrophysiological experiments on neurons from a region of the brain called the hippocampus. They found that high frequency stimulation of rabbit hippocampal neurons led to potentiation of synaptic transmission that lasted up to 10 h (Bliss & Lomo, 1973). This potentiation reflects an increase in EPSC amplitude, mediated largely by changes at the post-synapse (Cormier & Kelly, 1996).

1.1.10 Early phase Long Term Potentiation (LTP)

NMDARs permit the entry of Ca^{2+} into the post-synapse when bound to glutamate while the membrane is simultaneously strongly depolarised. When Ca^{2+} levels reach a critical threshold within the post-synapse LTP is induced through an intracellular signalling cascade. The early phase of LTP involves a number of protein kinases - particularly Ca^{2+} /calmodulin-dependent protein kinase II (CamKII) and protein kinase C (PKC) (Derkach *et al.*, 1999; Huganir

et al., 2000; Lisman et al., 2012). The result of this cascade is an increase in the single channel conductance of AMPARs and the incorporation of more AMPARs into the perisynaptic membrane, from which they laterally diffuse into the PSD and are anchored by scaffold proteins such as Post-synaptic Density protein 95 (PSD-95) (Benke et al. 1998; Derkach et al. 1999; Hayashi et al. 2000; Lee et al., 2000; Borgdoff & Choquet, 2002; Ren et al. 2013; Penn et al., 2017). This process leads to the activation of retrograde messengers which are released from the postsynaptic neuron into the synaptic cleft where they can bind presynaptic receptors and ultimately enhance SV release of glutamate (Sola et al. 2004; Regehr et al., 2009).

1.1.11 Late phase Long Term Potentiation (LTP)

Potentiation of signalling that persists more than 1 - 2 hours after LTP induction is considered “late phase LTP” and depends on localised dendritic protein synthesis (Sutton & Schuman, 2006, Reymann & Frey, 2007). In late phase LTP the dendritic spine and PSD are enlarged to accommodate these newly incorporated AMPARs in a NMDAR-dependent manner (Matsuzaki et al; 2004). A larger spine head allows for a greater synaptic surface for the insertion of AMPARs and NMDARs and as such AMPAR and NMDAR currents correlate linearly with the size of the spine head (Noguchi et al; 2005). This in turn triggers enlargement of the presynaptic active zone (Matsuzaki et al., 2004). In addition to increasing spine volume, spine density can also increase as a result of LTP protocols through the formation of new spines (Engert & Bonhoeffer, 1999; Maletic-Savatic et al., 1999).

1.1.12 Overview of Long Term Depression (LTD)

In contrast, LTD is induced by low-frequency stimulation. The two major receptors responsible for initiating LTD are metabotropic glutamate receptors (mGluRs) and again, NMDARs. mGluRs are coupled to intracellular guanosine triphosphate (GTP)-binding proteins through which they initiate downstream signalling cascades (Conn & Pinn, 1997). Low frequency stimulation leads to only a modest increase in NMDAR activation and therefore a modest increase in post-synaptic Ca^{2+} levels (Cummings *et al.*, 1996). This results in preferential activation of protein phosphatases (Cummings *et al.*, 1996). Phosphatase-driven signalling cascade induces the dissociation of AMPARs from the PSD, causing them to diffuse laterally to perisynaptic sites where they are endocytosed (Malinow & Malenka, 2002; Brecht & Nicoll, 2003; Collingridge *et al.*, 2004; Derkach *et al.*, 2007; Malenka & Bear, 2004). This reduction in synaptically localised AMPARs is concurrent with a reduction in protein synthesis and a decrease in dendritic spine volume (Nagerl *et al.*, 2004; Zhou *et al.*, 2004, Hsieh *et al.*, 2006). LTD can also lead to selective elimination of weak synapses (Wiegert & Oertner, 2013).

1.1.13 Synaptic plasticity underlies memory and learning

There are clear parallels between memory formation and synaptic plasticity processes (Nabavi *et al.*, 2014). Prolonged repetition increases potentiation and also strengthens memories. LTP is also facilitated by cooperativity and associativity (Nicoll *et al.*, 1988). When a critical number of synapses are simultaneously activated this facilitates potentiation. This is cooperativity. Associativity is a synaptic property that allows the potentiation of a weak input (a small number of synapses) when it is concurrent with a strong input (a large number of synapses). These properties of neuronal behaviour are cellular analogues of associative

learning.

The hippocampus is the brain region responsible for spatial and declarative memory and is the structure in which LTP was first described (Scoville *et al.*, 1957; Martin *et al.*, 2000; Squire, 2004; Morris, 2006). Unsurprisingly, this finding was followed by decades of intensive research into the role of LTP in memory formation. Early studies into the role of the hippocampus in memory found a clear link between memory formation and synaptic plasticity of hippocampal neurons. In 1982, hippocampal lesioning of rats was shown to lead to impairment of performance in spatial memory tasks, such as the Morris water maze, by Morris and colleagues (Morris *et al.*, 1982). They then went on to demonstrate that this impairment in spatial memory could also be induced pharmacologically by infusion of the NMDAR antagonist and known blocker of LTP, DL-AP5 into the intraventricular space (Morris *et al.*, 1986). Further evidence for the role of LTP and NMDARs in memory was the poor performance in spatial memory tasks of the transgenic mice generated by Tsien and colleagues (1996) in which a NMDAR subunit specific to NMDARs in the CA1 region of the hippocampus was knocked out (Tsien *et al.*, 1996). Conversely, in transgenic mice overexpressing the NMDAR subunit NR2B spatial learning and LTP were found to be enhanced (Tang *et al.*, 1999). As discussed above, CamKII is a Ca^{2+} -dependent protein kinase that is an important downstream effector of NMDAR activation in LTP. In CamKII knockout transgenic mice performance in tasks such as the Morris water maze and random-platform task (which depend on spatial memory formation) is impaired (Silva, Stevens, *et al.*, 1992; Silva, Paylor, *et al.*, 1992). This is concurrent with a reduction in hippocampal LTP, further underlining the importance of synaptic plasticity in memory (Silva, Stevens, *et al.*, 1992; Silva, Paylor, *et al.*, 1992).

1992). Another protein that facilitates LTP is Protein kinase C ζ type (PKM ζ), the pharmacological inhibition of which abolishes both LTP and long-lasting spatial memory (Pastalkova *et al.*, 2006). Later techniques developed such that *in vivo* electrophysiological evidence for LTP's role in memory could be demonstrated. In 2006 the proposed link between LTP and hippocampal memory formation was demonstrated in the mouse brain *in vivo* by Whitlock and colleagues who compared EPSPs of the CA1 hippocampal region in mice that had been trained using an inhibitory avoidance task compared to untrained mice. (Whitlock *et al.*, 2006). They found that EPSPs were enhanced and that in hippocampal synaptosomes from trained mice AMPARs were increased relative to controls, suggesting increased delivery to the synapse as a result of learning and memory formation (Whitlock *et al.*, 2006). The importance of LTD in learning and memory has also been demonstrated *in vivo*. For example, pharmacological inhibition of LTD in the CA1 hippocampal region was shown to block novel memory formation and the conversion of short term memories (STM) to long term memories (LTM) (Dong *et al.*, 2012). In a separate study, the same LTD inhibitors impeded performance in rats trained using a hidden platform task used to test spatial memory reversal - which is the loss of a redundant memory and important for learning (Dong *et al.*, 2013). Collectively, these data provide clear evidence for the important role that synaptic plasticity plays in memory formation and maintenance.

1.1.14 Actin is the major cytoskeletal protein of the dendritic spine

Unlike the dendritic shaft in which the core cytoskeletal elements are microtubules, in dendritic spines actin is the primary cytoskeletal protein (Landis & Rees, 1983). Actin is present in two forms: globular, monomeric G-actin and filamentous, polymeric F-actin (Dominguez &

Holmes, 2011). Depending on the structural requirements of the cell or cellular subcompartment, free G-actin is able to self-assemble to form F-actin polymers in an ATP hydrolysis-dependent manner or conversely F-actin can disassemble back into the monomer pool. These F-actin filaments are granted asymmetry by the arrangement of G-actin in a head-to-tail fashion, such that one end of the filament is “barbed” (+) and the other “pointed” (-) ([Pollard, 2003](#)). The barbed end is markedly more dynamic as it is able to be elongated with the addition of G-actin ten times faster than the pointed end ([Pollard, 2003](#)). The ratio of these processes can be quickly shifted in response to intra- or inter- cellular signals, facilitated by a number of actin-binding proteins ([Skruber *et al*; 2018](#)).

1.1.15 Structural plasticity of dendritic spines is orchestrated through actin modifiers

Actin filaments are organised in branching networks which are dynamically structured and restructured depending on activity ([Matus, 2000; Hotulainen & Hoogenraad, 2010](#)). This dynamic bidirectional regulation of the actin cytoskeleton within the dendritic spine neck and head plays an important role in synaptic plasticity ([Hlushchenko *et al.*, 2016](#)). Beneath the post-synaptic membrane lies the PSD - a dense disk-shaped array of proteins that orchestrate synaptic activity and plasticity ([Sheng & Hoogenraad, 2007](#)). The spine’s actin cytoskeleton lies directly beneath this, interacting with PSD scaffold proteins such as SH3 and multiple ankyrin repeat domains protein (SHANK) and PSD-95 via F-actin-binding proteins such as α -actinin and cortactin ([MacGillavry *et al.*, 2016; Matt *et al.*, 2018](#)). The pool of F-actin beneath the spine’s surface is much more dynamic and less stable than the internal pool of actin within the spine which acts as a scaffold to maintain its structure ([Hotulainen & Hoogenraad, 2010; Cingolani &](#)

Goda, 2008).

When high frequency stimulation is used to stimulate LTP G-actin and newly polymerised F-actin levels in the spine are increased (Bosch *et al.*, 2014; Okamoto *et al.*, 2004). Remodelling of the spine's actin cytoskeleton is set into action by redistribution of actin regulators to enlarge the spine head and expand the PSD in a process that can be divided into three stages (Bosch *et al.*, 2014). In the first 5 min following LTP induction actin stability is reduced to allow reorganisation (Bosch *et al.*, 2014). In this phase the spine head is enriched in actin modifiers able to sever (cofilin), cap (Actin-depolymerizing factor (ADF)/cofilin and actin-interacting protein 1 (AIP1)) or branch (Actin Related Protein 2/3 (ARP2/3) complex) actin filaments (Bosch *et al.*, 2014; Sekino *et al.*, 2006) while stabilisers that bundle or anchor F-actin (CaMKII β , drebrin, α -actinin) are translocated to the neck (Bosch *et al.*, 2014; Sekino *et al.*, 2006). This initial brief destabilisation of actin structure in the spine head facilitates remodelling by allowing access to other actin-binding factors and a treadmilling of actin to generate an expansive force (Sekino *et al.*, 2006; Honkura *et al.*, 2008; Bosch *et al.*, 2014). The second phase is characterised by stabilisation of spine structure as the concentration of stabilising factors in the spine head returns to basal levels (Bosch *et al.*, 2014). The third phase occurs by around 60 min after LTP induction and is the protein-synthesis dependent stage in which scaffold and other synaptic proteins are incorporated into the PSD (Tada *et al.*, 2005).

It is of note that although modifications in spine size accompany synaptic plasticity, they only serve to facilitate the insertion of more or less AMPARs and as such, modification of spine size

alone is insufficient to produce changes in synaptic transmission without concurrent changes in stimulation ([Hayashi & Majewska, 2005](#)).

1.1.16 Cofilin is essential for activity-dependent actin remodeling in synaptic plasticity

The actin-depolymerising factor (ADF) cofilin is a crucial player in activity-dependent actin remodelling in dendritic spines. Cofilin-1, cofilin-2 and ADF protein comprise the highly conserved ADF protein family and promote actin turnover by severing F-actin ([Bravo-Cordero *et al.*, 2014](#)). Cofilin is the main ADF family member in the human brain as mammalian neurons contain five to ten times less ADF protein than cofilin ([Minamide *et al.*, 2000](#); [Garvalov *et al.*, 2007](#)). Depolymerisation by cofilin can cause a decrease in net F-actin and therefore promote structural shrinkage, or it can serve to increase the pool of monomeric G-actin for use in remodelling and to create free barbed ends to facilitate growth ([Bamburg & Bernstein, 2016](#); [Hotulainen *et al.*, 2005](#)). LTP-induced activation of NMDARs leads to cofilin translocation to the spine where it forms new barbed ends on F-actin ([Oser & Condeelis, 2009](#)). These free barbed ends allow filament growth and are the preferred site for the ARP2/3 complex ([Ichetovkin *et al.*, 2002](#)). This protein complex initiates actin nucleation and branching ([Ichetovkin *et al.*, 2002](#)). The co-ordinated activity of ARP2/3 and cofilin is therefore crucial for the maintenance of spine expansion and has also been shown to be important for the delivery of proteins to the synaptic membrane such as AMPARs ([Pollard, 2016](#); [Hanley, 2014](#)).

1.1.17 Cofilin activity is regulated by Slingshot Homolog 1 and LIM kinase

Cofilin activity is regulated via phosphorylation at Ser3. LIM kinase (LIMK) phosphorylates this site, inactivating cofilin (Arber *et al.*, 1998). The LIM kinase protein family comprises LIMK1 and LIMK2 and lies downstream of the Rho-family GTPases (Dan *et al.*, 2001). They are known to be phosphorylated by Rac- and Cdc42-activated kinase p21 activated kinase (PAK) or Rho kinase (ROCK) and to be inactivated by phosphatases such as chronophin and slingshot homolog 1 (SSH1) (Dan *et al.*, 2001; Scott & Olson, 2007). They are active in their phosphorylated form and go on to phosphorylate and inactivate cofilin (Dan *et al.*, 2001). SSH1 is also the phosphatase that removes this phosphate to activate cofilin (Niwa *et al.*, 2002).

1.1.18 Cofilin regulation is important for dendritic spine morphology and function

Given the importance of actin remodelling in the dynamic morphology of dendritic spines, it is unsurprising that the role of cofilin and its upstream regulators in synaptic plasticity and memory have been extensively investigated. The process of LTP was shown to be dependent on cofilin, as demonstrated by the lack of potentiation in the CA1 neurons of hippocampal slices from cofilin knockout mice, alongside impaired spine morphology and deficits in associative learning (Rust *et al.*, 2006). This is likely due to cofilin's role in AMPAR diffusion and AMPAR subunit activation following LTP induction (Rust *et al.*, 2006; Gu *et al.*, 2010). However, when endogenous WT cofilin is replaced with mutant (S3A) constitutively active cofilin in neurons this causes spine size to be reduced and a relative increase in spines with an immature morphology (Shi *et al.*, 2009). Mature spine morphology returns to these neurons when transfected with phosphomimetic cofilin (S3D) (Shi *et al.*, 2009). In another study, knock down of cofilin expression with short interfering RNA (siRNA) induces a shift in spines

towards a filopodia-like morphology (Hotulainen *et al.*, 2009). Furthermore, conditional knock-out (KO) of cofilin in the excitatory neurons of the mouse brain was shown to lead to an increase in spine density and size and also to an impairment of late phase LTP and LTD (Rust *et al.*, 2010). Furthermore, in LTD phosphorylation of serine 3 in cofilin has been shown to mediate spine shrinkage (Nägerl *et al.*, 2004; Zhou *et al.*, 2004).

1.1.19 LIM kinase 1 activity is important for synaptic function

Indirect evidence of the importance of cofilin comes from studies into the role of its upstream regulators. LIMK1 is expressed throughout the body but predominantly in the brain (Proschel *et al.*, 1995; Foletta *et al.*, 2004) and has been implicated in neuritogenesis and synaptic plasticity (Meng *et al.*, 2002; Endo *et al.*, 2003; Rosso *et al.*, 2004). In LIMK1/2 KO mice cofilin phosphorylation is dramatically reduced and consequently these mice have impaired synaptic function and altered spine morphology (Meng *et al.*, 2002, 2004). In humans, partial loss of LIMK1 is believed to underlie the visuospatial cognitive deficits associated with Williams syndrome - a neurodevelopmental disorder which results from a chromosomal deletion on chromosome band 7q11.23 and therefore hemizygoty for genes within it - including LIMK1 (Bellugi *et al.*, 1999).

1.1.20 Excessive cofilin activity is associated with dysregulated dendritic spine morphology

Depending on the concentration and form of actin and actin binding proteins present, *in vitro* cofilin activity can promote either nucleation or depolymerisation of actin filaments (Andrianantoandro & Pollard, 2006). Collectively this evidence suggests that although cofilin

plays a role in both spine expansion and shrinkage in LTP and LTD respectively, when its activity is aberrantly elevated the balance of these two processes shifts towards inducing spine shrinkage. One explanation for this may be that in LTP cofilin serves to sever and destabilise actin such that other actin modifiers which are able to elongate actin are able to access the spine, however, in the absence of a concurrent increase in the activity of these elongating factors the net effect is the breakdown of actin structure and therefore spine stability and size.

1.2 Alzheimer's disease is a progressive neurodegenerative disorder

1.2.1 Alzheimer's Disease is the most common cause of dementia globally

Alzheimer's Disease (AD) is a chronic neurodegenerative disease for which, despite extensive research, effective treatment strategies have proved elusive due to its complex and multi-factorial pathology. The Alzheimer's Disease International's (ADI) 2021 report on the implementation of its global dementia action plan stated that over 50 million people globally are living with dementia. They predicted that this would increase to 82 million by 2030 and 152 million by 2050. The leading cause of dementia worldwide is AD which accounts for 60 - 70 % of cases (World Health Organisation). Drugs currently prescribed for AD include cholinesterase inhibitors galantamine, donepezil and rivastigmine and the NMDA receptor antagonist memantine. However, their effect on cognition is only moderate and they are only able to alleviate symptoms rather than to slow or halt neurodegeneration ([Hardy & Selkoe, 2002](#)). With the current annual cost of dementia care currently estimated to be US\$1 trillion globally and predicted to double by 2030 the dearth of effective AD treatments demonstrates the urgent need for a greater understanding of the aetiology of this disease ([Gauthier *et al.*, 2021](#)).

1.1.2 Alzheimer's Disease symptoms

Early AD symptoms include declarative and spatial memory problems, language processing and speech problems and neuropsychiatric issues such as depression and anxiety ([Alzheimer's Research UK](#)). As the disease progresses these problems become more pronounced, with patients becoming unable to recognise familiar places or people, having difficulty sleeping, problems with physical tasks such as walking and swallowing food ([Alzheimer's Research UK](#)). AD patients may also experience hallucinations and suffer from paranoia and seizures ([Alzheimer's Research UK](#)). Ultimately AD sufferers become unable to care for themselves and eventually the disease causes them to die ([Alzheimer's Research UK](#)). In summary, AD is a profoundly debilitating and ultimately fatal disease.

1.2.3 Alzheimer's Disease Pathology

The brains of AD patients undergo progressive neuronal loss in a stereotyped pattern, with detectable atrophy starting before symptom onset in the entorhinal and hippocampal regions ([Bobinski *et al.*, 2000](#)). Around two years later this starts to progress through the brain in a temporal-frontal sensorimotor sequence, sparing primary visual, sensorimotor, and frontal regions until late in the disease course ([Bobinski *et al.*, 2000](#); [Thompson *et al.*, 2003](#)).

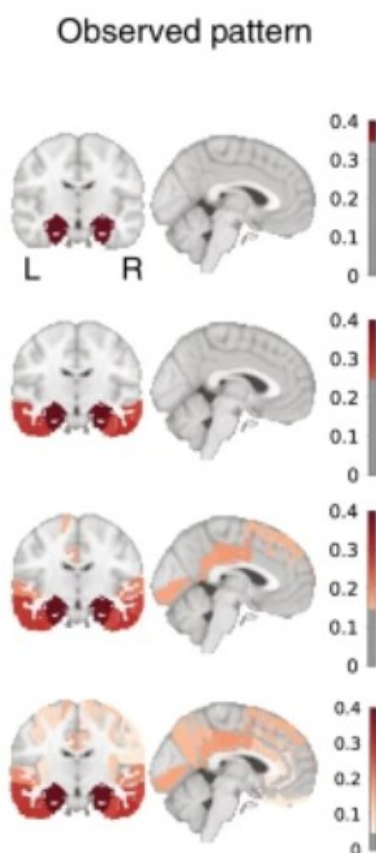
1.2.4 Neurofibrillary tangles progress through the brain in a stepwise manner in Alzheimer's Disease

In 1906 Alois Alzheimer identified the two types of insoluble protein aggregates that

characterise the AD brain - intracellular neurofibrillary tangles (NFTs) and extracellular senile plaques ([Hippius & Neundörfer 2003](#)). The spreading pattern of neuronal pathology from entorhinal through to neocortical regions is also reflected in the deposition of NFTs which have been found to be composed primarily of paired helical filaments of hyperphosphorylated tau ([Braak & Braak, 1991](#); [Hardy & Selkoe, 2002](#); [Kidd 1963](#); [Stoothoff & Johnson 2005](#)). In the healthy brain tau's function is as a microtubule binding protein but the excessive phosphorylation of tau seen in AD causes it to dissociate from microtubules and to form toxic aggregates ([Kidd, 1963](#); [Stoothoff & Johnson, 2005](#)). The degree of spread of tau pathology along this axis is correlated with measures of cognitive decline and as such is used to define disease progression as described through Braak staging ([Terry *et al.*, 1991](#); [Braak & Braak, 1997](#)) (**Figure 1.2**).

Figure 1.2: ([Vogel *et al.*, 2020](#))
Hyperphosphorylated tau
 baseline scans show tau represented from top to and VI as described by Braak colours on the scale represent the population.

1.2.5 Amyloid dysregulation is
hallmark of Alzheimer's
 Tau
 tangle formation is preceded



[al., 2020](#)
spreads in a stereotyped
 [18F]-flortaucipir tau-PET
 spreading pattern of tau,
 bottom by Braak stages I, II, V
 & Braak (1997). Warmer
 higher tau-positivity across
 the earliest molecular
 Disease
 hyperphosphorylation and
 by accumulation of senile

plaques which are primarily composed of β amyloid ($A\beta$) peptides derived from sequential cleavage of amyloid precursor protein (APP) (Hsiao *et al.*, 1996; Hardy and Selkoe, 2002) (**Figure 1.3**). APP is a type I integral transmembrane glycoprotein (Gralle & Ferreira, 2007). Of the three main APP isoforms, APP695 is an isoform consisting of 695 amino acids (aa) that makes up the majority of neuronal APP (Del Turco *et al.*, 2016). APP751 and APP770 consist of 751 and 770 amino acids respectively and make up the majority of glial APP (Moreno-Flores *et al.*, 2003; Premkumar & Kalaria, 1996).

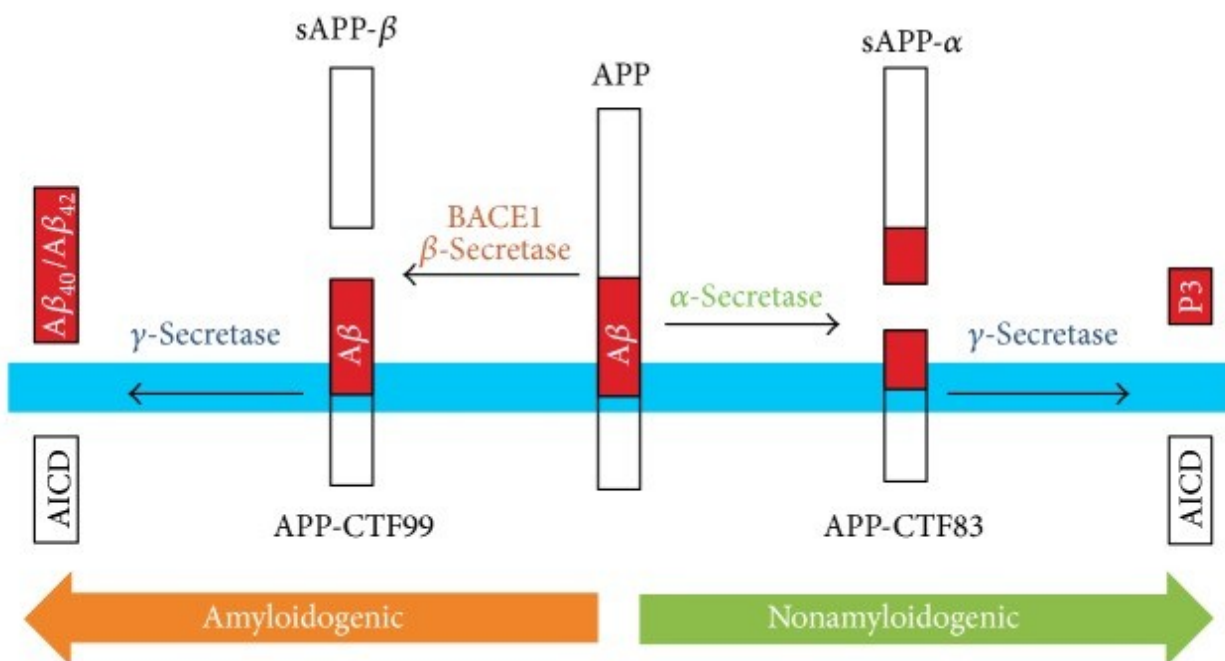


Figure 1.3: Processing of the transmembrane protein APP (Pajak *et al.*, 2016). Processing of the transmembrane protein APP involves sequential cleavage by β - or α -secretase within the luminal domain generating either β - or α -C-terminal fragments respectively (Kojro & Fahrenholz, 2005). These are then subsequently cleaved by γ -secretase to produce either $A\beta$ or p3 peptides respectively, which are released from the membrane into the extracellular space (Kojro & Fahrenholz, 2005). The latter process involving α -secretase and producing soluble APP α , p3 and the APP intracellular domain (AICD) is considered non-amyloidogenic (Kojro & Fahrenholz, 2005). The former process involving β -secretase and producing $A\beta$ isoforms ranging from 38-43 amino acid (aa), soluble APP β and AICD is considered the amyloidogenic APP

processing pathway (Golde *et al.*, 1992).

Most A β peptides produced via the amyloidogenic pathway are the 40aa A β^{1-40} but ~10% are the 42aa peptide A β^{1-42} , which is highly hydrophobic and aggregation prone (Jarrett *et al.*, 1993). A β aggregates form oligomers (A β O) of 10 – 200 kDa or insoluble A β fibrils found in the senile plaques characteristic of AD brains (Burdick *et al.*, 1992; Walsh *et al.*, 2002). It has been shown that the ratio of A β^{1-42} / A β^{1-40} more strongly correlates with AD pathology than total A β^{1-42} suggesting an interaction between these that is perturbed in the disease (Spies *et al.*, 2010; Lewczuk *et al.*, 2017; Hansson *et al.*, 2019). Evidence suggests that the increase in A β levels seen early in the disease course may in fact trigger tau pathology in AD. For example, in a 3D *in vitro* human neural cell culture system elevated A β levels were found to be sufficient to induce tau pathology (Choi *et al.*, 2014). It has also been shown that in human tau transgenic mice the injection of A β fibrils accelerates tau pathology (Bolmont *et al.*, 2007). Furthermore, in transgenic mice carrying both tau and APP-related genes with mutations that promote aggregation A β pathology is unchanged by the addition of mutant tau despite exaggerated tau pathology when A β production is enhanced (Gotz *et al.*, 2001).

1.2.6 Alzheimer's Disease genetics

Around 95% of AD cases are sporadic and late onset with symptoms typically appearing over the age of 65 (van der Flier & Scheltens, 2005). Sporadic late onset AD (LOAD) is believed to be the result of biological, environmental, genetic and epigenetic factors. The biggest risk factor for sporadic AD is age with AD affecting 3 % of 65 - 75 year olds, 17 % of 75 - 85 year olds, and 32 % of people over the age of 84 (Alzheimer's Association, 2019). There are however a

number of gene variants that have been identified as risk factors. The greatest genetic risk factor in LOAD is the $\epsilon 4$ gene variant of the ApoE gene (Belloy *et al.*, 2019). ApoE is a major lipid carrier in the brain and is involved in A β processing (Fagan *et al.*, 2002). Other risk genes include coding variants of Myeloid cell surface antigen CD33 (CD33) and the Triggering receptor expressed on myeloid cells 2 (TREM2) which are expressed in the microglial immune cells of the brain indicating the importance of these cells in modifying or potentially initiating AD (Bertram *et al.*, 2008; Guerreiro *et al.*, 2013; Jonsson *et al.*, 2013; Parhizkar *et al.*, 2019). Other genes involved in the trafficking and processing of APP have been shown to be risk loci such as Sortilin-related receptor LR11/SorLA (SORL1), Phosphatidylinositol-binding clathrin assembly protein (PICALM), and Clusterin (CLU) (Harold *et al.*, 2009; Holstege *et al.*, 2017). Some gene variants have also been identified as protective in AD such as a the $\epsilon 2$ variant of the ApoE gene and the APP with the mutation A673T (Corder *et al.*, 1994; Jonsson *et al.*, 2012). A rare variant of the GTPase Ras-related protein Rab-10 (RAB10 rs142787485) has also been identified as protective in AD (Ridge *et al.*, 2017; Tavana *et al.*, 2019). In contrast to LOAD, Early onset AD (EOAD) begins before the age of 65 and within this subpopulation there are familial forms of AD caused by autosomal dominant alleles of mutated genes including APP and genes associated with APP processing such as the γ -secretase subunits presenilin 1 (PSEN1) and presenilin 2 (PSEN2) (Bettens *et al.*, 2010; Levy-Lahad *et al.*, 1995).

1.2.7 Amyloid Cascade Hypothesis

The identification of causative mutations within the amyloid pathway and the observed presymptomatic accumulation of soluble and aggregated insoluble A β peptides within the

brains of Alzheimer's patients lead to the development of the Amyloid Cascade hypothesis (Hardy & Higgins, 1992). This hypothesis proposes that in AD APP processing is dysregulated and a greater ratio of the aggregation-prone 42 amino acid peptide $A\beta^{1-42}$ is produced relative to the 40 amino acid peptide $A\beta^{1-40}$. These

amyloid species begin to accumulate and aggregate, causing a cascade of events that lead to progressive neuritic and neuronal dysfunction, cell death and dementia

(Figure 1.4).

Figure 1.4: Amyloid (Hardy & Selkoe, 2002). This cascade of events that lead to AD pathology in people with EOAD genes was laid out by Hardy and Selkoe in 1992 who proposed that dysregulation of APP and consequent changes to amyloid production of the disease. The curved arrow highlights $A\beta$ oligomer production as key to synaptic and neuritic injury of neurons.

Since its inception

Hardy's Amyloid

been called in to

failure of several large clinical trials developing therapeutics that target APP processing and $A\beta$

accumulation (Tolar *et al.*, 2020) Further confounding evidence is that of the discovery of

cognitively normal people with extensive amyloid plaque deposition (Price & Morris, 1999).

Amyloid cascade hypothesis

Missense mutations in *APP*, *PS1*, or *PS2* genes



Increased $A\beta_{42}$ production and accumulation



$A\beta_{42}$ oligomerization and deposition as diffuse plaques



Subtle effects of $A\beta$ oligomers on synapses



Microglial and astrocytic activation (complement factors, cytokines, etc.)



Progressive synaptic and neuritic injury



Altered neuronal ionic homeostasis; oxidative injury



Altered kinase/phosphatase activities ➤ tangles



Widespread neuronal/neuritic dysfunction and cell death with transmitter deficits



Dementia

begin to accumulate and cascade of events that neuritic and neuronal death and dementia

cascade hypothesis (2002). This cascade of AD pathology in people laid out by Hardy and Selkoe proposed that dysregulation of APP and to amyloid production of the disease. The highlights $A\beta$ oligomer synaptic and neuritic

the validity of Selkoe and

cascade hypothesis has

question due to the

Furthermore, total plaque load is only poorly correlated at best with cognitive decline and synaptic pathology (Blennow *et al.*, 1996; Nelson *et al.*, 2012). However, many studies have demonstrated that A β oligomers and soluble forms of A β (A β -derived diffusible ligands), that accumulate prior to the larger fibrillar assemblies first identified as characteristic of the disease by Alois Alzheimer may be at the root of synaptic toxicity (Roher, Ball *et al.*, 1991; Roher, Palmer *et al.*, 1991; Lambert *et al.*, 1998). Indeed, both synthetic and naturally secreted A β oligomers have been shown to disrupt synaptic and cognitive function in animal models of AD (Cline *et al.*, 2018; Lambert *et al.*, 1998; Cleary *et al.*, 2005; Lesne *et al.*, 2006; Shankar *et al.*, 2008; Lesne *et al.*, 2013; Esparza *et al.*, 2013; Perez-Nievas *et al.*, 2013).

However, despite the poor correlation of A β load with cognitive decline relative to the NFTs, it is believed that by the time tau hyperphosphorylation and tangle formation has been initiated it is too late in the disease course to effectively intervene. Therefore, a greater understanding of the early stages of the disease is needed for effective intervention during this therapeutic window.

1.2.8 Synapse loss is the earliest structural change in AD

The earliest structural correlate of cognitive decline in AD is that of the loss of synapses which also precedes NFT formation (DeKowsky *et al.*, 1990; Terry *et al.*, 1991; Blennow *et al.*, 1996; DeKowsky *et al.*, 1996; Wilde *et al.*, 2016). At the subcellular level synapses serve as the functional units of learning and memory in the brain. It is no surprise therefore that the progressive loss of synapses in AD is correlated with a decline in cognitive function as measured by the Blessed Information-Memory-Concentration (IMC) Test, the Mini mental State Exam

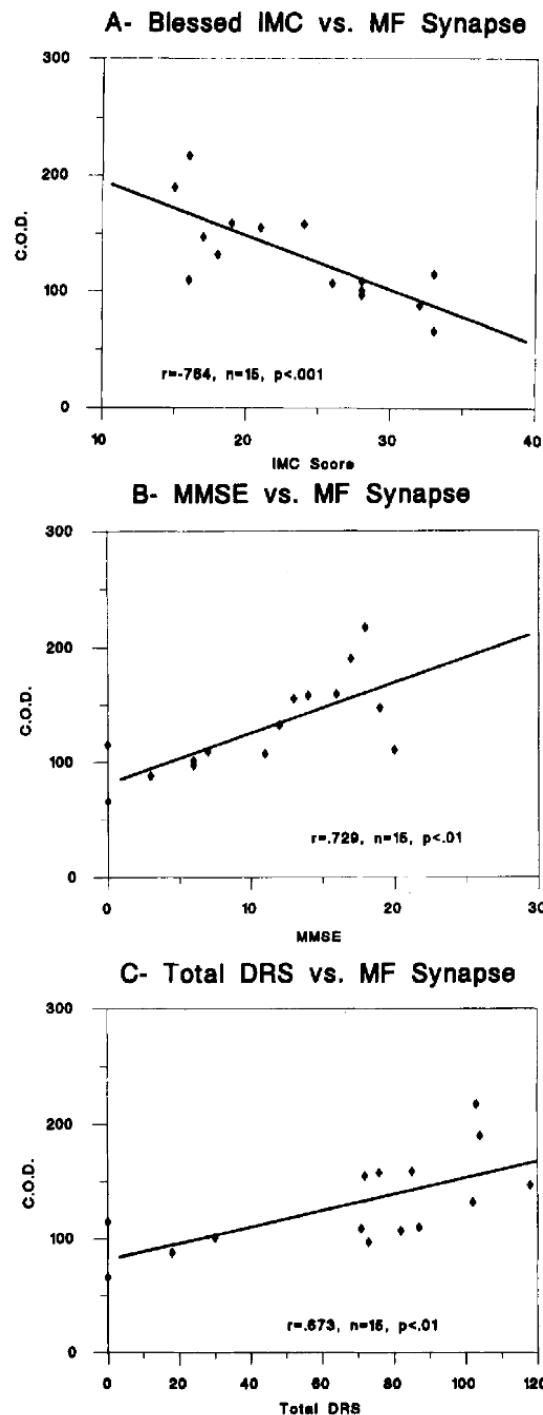
(MME), and the total Dementia Rating Scale (DRS) (DeKosky & Scheff, 1990; Terry *et al.*, 1991)

(Figure 1.5).

Figure 1.5:
with performance
cognitive function
progression in AD
(C.O.D.) of
AD patients was
antibody raised
synaptophysin to
loss was negatively
function as
Infomation-
Test, B) the Mini
and the total

Ultrastructural
patients revealed
cortical layer
number of
brain tissue
Moolman *et al.*
Impairment (MCI)
different types of
this condition
less hippocampal
controls, which

who finally developed AD (Scheff *et al.*, 2006). Furthermore, reduction in levels of proteins



Synaptic loss is correlated
on a number of tests of
used to quantify disease
patients. The optical density
midfrontal brain slices from
immunostained with an
against the synaptic marker
quantify synapses. Synaptic
correlated with cognitive
measured by A) the Blessed
Memory-Concentration (IMC)
mental State Exam (MME), C)
Dementia Rating Scale (DRS).

analyses in biopsies of AD
a 15-35% (depending on the
studied) reduction in the
synapses per neuron in AD
(DeKosky *et al.*, 1996;
2004). Mild Cognitive
precedes a number of
dementia and patients with
were found to have 18-25%
synapses than healthy
rose to 45-55% in patients

important for synaptic function such as synaptophysin, SNAP-25, synapsin 1, synaptobrevin and drebrin were found to be reduced in patients with MCI and early AD (Masliah *et al.*, 2001).

Collectively, these findings indicate that synaptic loss and dysfunction are early events in the course of AD pathology which has led to some describing AD as primarily an example of a synaptopathy and to call for future therapeutic interventions that target this aspect of the disease (Pozueta *et al.*, 2013).

1.2.9 Dysregulation of dendritic spines is seen in models of AD

A variety of methods are used to simulate AD in model systems ranging from exogenous application of A β and tau to cells and brain slices, to the generation of transgenic animals expressing EOAD-linked genes. The intrinsic link between the morphology and density of dendritic spines and synaptic strength and therefore learning and memory has naturally led to extensive investigation into the biochemical underpinning of these spine changes using these model systems.

In organotypic rat brain slices exposure to oligomeric A β induces NMDAR-dependent spine loss suggested to be due to activation of LTD-related processes (Hsieh *et al.*, 2006; Shrestha *et al.*, 2006; Shankar *et al.*, 2007;*;*). Spine loss is also seen *in vivo* following injection of soluble A β into the brains of wild type (WT) mice (Arbel-Ornath *et al.*, 2017).

The first mouse model of AD was the PDAPP mouse line generated by Games and colleagues (1995) by engineering a mouse that overexpresses human APP (>10fold murine APP expression) with the Indiana mutation (V17F) (Murrell *et al.*, 1991) using a neuron-specific promoter (PDGF). These mice develop AD-like pathology with many characteristic phenotypes such as A β deposits, neuritic plaques, loss of dendritic spines and synapses, astrogliosis and microgliosis (Games *et al.*, 1995). Since then, many mouse models have been produced utilising the FAD-linked mutations that led to EOAD in humans. Analysis of spine structure in these models has highlighted dysregulation of synapses and spines as a key feature of the A β -induced pathology. In the PDAPP mouse significant spine loss is seen even before a detectable increase in A β levels (Lanz *et al.*, 2003). Another example is that of the TG2576 mouse model which overexpresses human APP with the Swedish double mutation (K670N/M671L) (Mullan *et al.*, 1992) and these mice also have reduced spine density relative to controls, particularly proximal to A β plaques (Mucke *et al.*, 2000; Lanz *et al.*, 2003; Wu *et al.*, 2004; Jacobsen *et al.*, 2006; Spires *et al.*, 2005). Another well studied mouse model of AD is the J20 mouse produced by Mucke and colleagues (2000). This mouse overexpresses APP with both the Indiana and Swedish mutations and also exhibits marked spine loss in hippocampal neurons (Moolman *et al.*, 2004) Importantly, all of these mouse models develop reduced cognitive function and memory deficits (Hsiao *et al.*, 1996, Mucke *et al.*, 2000, Chen *et al.*, 2000). Furthermore, these memory deficits occur prior to plaque formation and even in mice overexpressing APP with a mutation that renders the A β peptide produced able to form soluble oligomers but unable to form plaques (Hsiao *et al.*, 1996, Mucke *et al.*, 2000, Chen *et al.*, 2000, Gerlai *et al.*, 2002; Gandy *et al.*, 2010). These findings therefore also provide further support for the notion that oligomers are the primary toxic

species in AD.

1.2.10 LIM Kinase and cofilin are dysregulated in Alzheimer's Disease and its models

Given the importance of the actin cytoskeleton in synaptic plasticity it is unsurprising that dysregulation of actin-related proteins such as cofilin and LIMK1 has been reported widely in a number of brain disorders. These include Williams syndrome ([Hoogenraad *et al.*, 2004](#)), drug addiction ([Rothenfluh & Cowan, 2013](#)), autism spectrum disorder ([Duffney *et al.*, 2015](#); [Sungur *et al.*, 2018](#)) and indeed neurodegenerative diseases including AD ([Liu *et al.*, 2019](#)).

However, the results of investigations into the role of cofilin and LIMK1 in AD and its models have produced conflicting results (**Table 1.1**).

| Study | Method | Outcome |
|---|---|--|
| Maloney <i>et al.</i>, 2005 | Primary neuronal cultures treated with A β 1–42 | Increased phosphorylation/deactivation of cofilin and cofilin rod formation |
| Heredia <i>et al.</i>, 2006 | 20 uM synthetic fibrillar A β ^{1–40} applied for 24 h to primary hippocampal neuronal cultures Immunofluorescence in human AD entorhinal cortex | FAB increased phosphorylated cofilin (pCofilin) and phosphorylated LIMK (pLIMK). Inhibition of LIMK reduced neuritic loss following fibrillar A β treatment. |

| | | |
|--|--|--|
| | | pLIMK was increased proximal to areas of high pathology (increased A β and hyperphosphorylated tau staining or lesions) |
| <u>Shankar <i>et al.</i>, 2007</u> | Cell derived (naturally secreted) A β oligomers (10 day chronic) applied to organotypic rat hippocampal slices | Neurons transfected with a plasmid containing phosphomimetic (inactive) cofilin reduced the spine loss seen when A β oligomers were applied. Calcineurin (activates SSH-1L which dephosphorylates and activates cofilin) was shown to be involved in this pathway. |
| <u>Davis <i>et al.</i>, 2011</u> | ~250 pM Synthetic A β trimers and dimers applied to primary neuronal cultures and organotypic hippocampal slices from rat pups | Increased pCofilin and cofilin rod formation. Adenoviral expression of WT or constitutively active LIMK reduced rod formation following A β application and expression of the phosphatases SSH-1L and CIN increased rod formation. |
| <u>Mendoza-Naranjo <i>et al.</i>, 2012</u> | Primary neuronal cultures treated with fibrillar A β | Increased LIMK phosphorylation despite decreased cofilin phosphorylation. Fibrillar A β induced changes to actin dynamics prevented by overexpression of SSH1 |
| <u>Woo <i>et al.</i>, 2012</u> | APP/PS1 mice | Increased cofilin phosphorylation/deactivation |
| <u>Barone <i>et al.</i>, 2014</u> | Human AD brain, APP/PS1 mice, normal ageing in WT mice, mouse primary cortical neurons, and mouse embryonic fibroblasts (MEF) | pCofilin (inactive) levels positively correlated with AD pathology. Increase in SSH-1L phosphorylation and no change in total LIMK or pLIMK levels. Gamma secretase KO in MEF reduced cofilin phosphorylation |

| | | |
|--------------------------------------|--|--|
| | | and SSH-1 phosphorylation with no effect on total or phosphorylated LIMK levels. |
| <u>Sun <i>et al.</i>, 2015</u> | APP/PS1 mice and AD brain | Identified an increase in cofilin-2 as an AD biomarker. |
| <u>Woo <i>et al.</i>, 2015</u> | 1 μ M A β ¹⁻⁴² oligomers for 2h in hippocampus derived HT22 cells and in primary cultured hippocampal neurons. APP/PS1 RanBP9 ^{+/-} mouse line generated. | Cofilin activation (dephosphorylation) is promoted by up-regulation of SSH-1 activity downstream of RanBP9. RanBP9 is increased fourfold in APP/PS1 mice relative to WT controls. Rescue of synaptic and memory loss in transgenic mice. |
| <u>Deng <i>et al.</i>, 2016</u> | 5 x FAD mouse model | Inhibition of cofilin dephosphorylation (competitive inhibition for phosphatases by use of peptide fragment of cofilin containing phosphorylation site) improved surface expression of AMPARs and NMDARs and cognitive deficits. |
| <u>Henderson <i>et al.</i>, 2016</u> | 250 nM synthetic A β 42 oligomers for 6 h in primary neuronal cultures | LIMK phosphorylation increased. |
| <u>Rush <i>et al.</i>, 2018</u> | 100 nm synthetic A β oligomers APP/PS1 mice Human AD | Elevated pCofilin in post-synapse enriched synaptosomes from human and APP/PS1 mice. Increased pCofilin and actin stabilisation following A β oligomer application. A ROCK inhibitor (Fasudil) rescued this effect and prevented A β blocking of Glutamate receptor A1 insertion at the PSD |
| <u>Liu <i>et al.</i>, 2019</u> | APP751 expressing Chinese Hamster Ovary 7wd10 cell line | Adenoviral knock down of cofilin in both cell lines reduced |

| | | |
|--------------------------------------|---|--|
| | and primary neuronal cultures APP/PS1:cofilin ^{+/-} mice | A β accumulation by increasing surface APP. Expression of phosphonull (active) and not phosphomimetic (inactive) cofilin reduced this effect. In the transgenic mouse, A β deposition was reduced in the cofilin knock down mice relative to APP/PS1 mice. Furthermore, microglia isolated from cofilin KD mice were more efficient at clearing A β . |
| <u>Henderson <i>et al.</i>, 2019</u> | Primary neuronal cultures 500nM synthetic A β ¹⁻⁴² oligomers for 6 h at DIV14 6 month J20 mice | LIMK1 inhibition rendered dendritic spines resilient to A β 42 oligomers and rescued hippocampal spine loss and morphologic aberrations in J20 mice. J20 mice have increased pLimK in the hippocampus. |
| <u>Sun <i>et al.</i>, 2019</u> | AD patient serum | Cofilin-2 levels and score in cognitive decline negatively correlated. |

Table 1.1: Investigations into the role of cofilin and LIMK1 in AD and its models

This may be due to the complex and multiphasic role of cofilin in synaptic plasticity or perhaps due to its involvement in other aspects of neuronal function. Processes which cofilin has been implicated in include microtubule binding, mitochondrial morphology and function (and oxidative stress (Klamt *et al.*, 2009; Rehklau *et al.*, 2017; Hoffman *et al.*, 2019; Woo *et al.*, 2019)). AD pathology has also been shown to affect cofilin's role in these processes outside of cytoskeletal maintenance. In AD mouse models cofilin has been shown to be targeted to mitochondria where it mediates cytochrome C release and subsequent apoptosis (Woo *et al.*, 2012; Roh *et al.*, 2013). Furthermore, as in many other neurodegenerative conditions, in AD

active/dephosphorylated cofilin forms rod shaped bundles in a 1:1 ratio with actin called cofilin rods (Minamide *et al.*, 2000; Maloney *et al.*, 2005; Davis *et al.*, 2011; Walsh *et al.*, 2014). The recruitment of cofilin into these inclusions also impairs neuronal function through loss of function and gain of toxic function pathways (Bamburg & Bernstein, 2016).

Another factor in the heterogeneity of results may be the variety of techniques used. There are various methods for probing human tissue and different studies may investigate different brain regions. Furthermore, no AD model is able to replicate all aspects of the disease and as such the strategy for modelling must be considered carefully to assess its physiological relevance. It is believed that the most appropriate window for therapeutic intervention is the prodromal stage of AD in which A β levels and synaptic dysfunction begin to increase prior to symptom onset (Masliah *et al.*, 2001; Hardy & Selkoe, 2002; Scheff *et al.*, 2006). As such, various methods are employed to artificially increase A β levels in model systems. These include expression of APP with FAD-linked mutations and application of naturally secreted or synthetically derived A β (Pike *et al.*, 1993; Millucci *et al.*, 2010). In cell models the method for introducing these APP genes can also vary. For example, lentiviral transduction or transfection can be used to simply overexpress the gene, or the endogenous gene can be knocked down and replaced with a mutant. These cells may be primary neuronal cultures or iPSC-derived. In both cell and animal models there can be differences in insert site and copy number of a gene. When applying A β monomeric or oligomeric may be chosen, however, the propensity of A β to spontaneously aggregate under various conditions can make it difficult to ensure a homogeneously monomeric pool (Lambert *et al.*, 1998; Podlisny *et al.*, 1998; Walsh *et al.*, 2001; Stine *et al.*, 2003; Bitan *et*

al., 2005; ,Hepler *et al.*, 2006; Nag *et al.*, 2011). The protocol used to produce these can also vary (*Jiminez et al.*, 2014). These can be applied to cell models at a variety of time points, concentrations and for varying durations. They can also be injected into the brains of animal models but again, alongside region-specific effects the above factors can influence results.

In summary, although LIMK1 and cofilin signalling has been demonstrated to be perturbed in AD, there is a lack of consensus around the ways in which they are affected. This may be due in part to the heterogeneity of approaches to modelling AD and therefore a carefully considered and multi-faceted approach is necessary in future investigations.

1.3 Local translational control at the synapse by miRNA

1.3.1 Localised translation occurs at the synapse

The size, complex morphology and functional compartmentalisation of neuronal cells necessitates mechanisms for highly localised coordination of cellular processes. Intracellular signals must also be transmitted along great distances as neurons are the largest known cells in the body, reaching lengths of meters in some animals. One such mechanism for overcoming these challenges is localised translation of messenger RNAs (mRNAs). Local translation of subregion specific proteins allows spatiotemporal control of localised proteomes in response to inter- and intra- cellular signals. mRNA localisation to nerve terminals was first hypothesised in the 60s following studies in which localised protein synthesis within synapses was demonstrated using metabolic labelling in isolated synaptosomes (*Autilio et al.*, 1968) This process and underlying pathways have been well researched since and in fact RNAseq studies have

estimated that around 2500 mRNAs are enriched in hippocampal dendrites and axons ready for rapid local expression (Cajigas *et al.*, 2012).

1.3.2 mRNA is transported to dendritic spines

The processing of mRNA is initiated the moment it is transcribed and is coordinated by many mRNA-binding proteins (mRBPs). The first step of mRNA trafficking is binding of mRNA by specialised *trans*-acting RBPs that interact with regions usually within the 3' untranslated region (UTR) of the mRNA. These *cis*-acting elements play a role in determining the destination of trafficked mRNA (Kislauskis and Singer, 1992). Depending on whether mRNAs are transported singly or as part of a cluster in an RNA granule, this trafficking of assembled mRBPs can be performed through interactions with molecular chaperones, adaptor proteins and motor proteins which translocate them in a microtubule-dependent manner (Krichevsky & Kosik, 2001; Batish *et al.*, 2012; Xing & Bassell, 2013; Buchan, 2014). Ribosomes present in both pre- and post- synaptic terminals and in axons facilitate translation of these distal mRNAs (Shigeoka *et al.*, 2016; Hafner *et al.*, 2019). Poly-ribosomes have also been shown to migrate into dendritic spines during LTD (Ostroff *et al.*, 2002). Cue-dependent local translation has been demonstrated to be important in a number of neuronal processes such as in developing growth cones and synaptic signalling, and interruption of this process is associated with neuropathologies such as Amyotrophic Lateral Sclerosis, Spinal Muscular Atrophy and Fragile X Syndrome (Zhang & Poo, 2002; Taylor *et al.*, 2013; Thelen & Kye, 2020; Sasaki *et al.*, 2020).

1.3.3 mRNAs are subject to regulation by microRNAs

These trafficked mRNAs are also subject to localised epigenetic regulation. MicroRNAs (miRNAs) are small non-coding RNAs that each target a specific range of mRNAs for RNA-induced silencing (**Figure 1.6**) (Friedman *et al.*, 2009). These regulatory RNAs are ~22nt in length and contain a seed sequence, partially or completely complementary to a number of target mRNAs, usually within their 3' UTR (Meister, 2013). It is through this complementarity that miRNAs are able to guide a RNA-induced silencing complex (RISC) to specific mRNA targets in order to selectively suppress protein expression either via transient inhibition of the translation process or direct cleavage of the mRNA itself (Horman *et al.*, 2014).

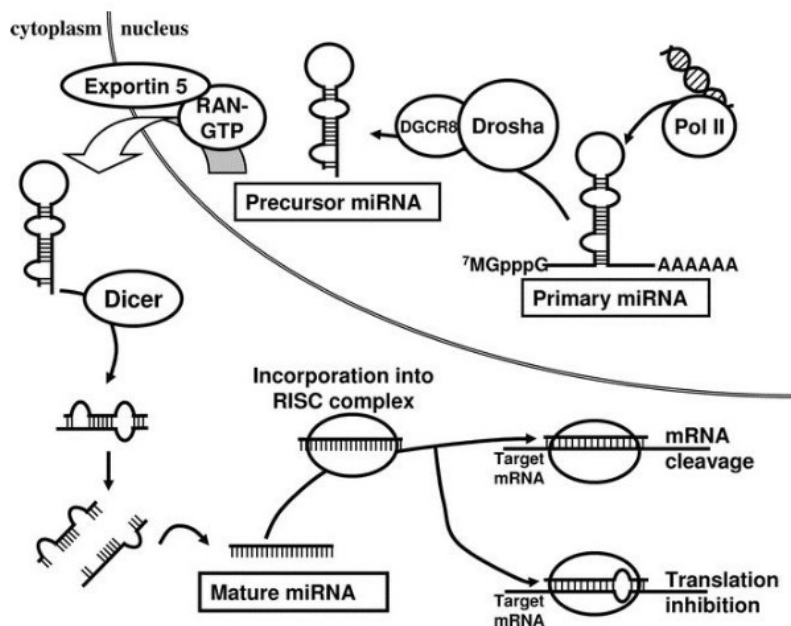


Figure 1.6: Biogenesis of miRNA (Chuang & Jones, 2007). Biogenesis of miRNAs begins in the nucleus where primary miRNA (pri-miRNA) of several thousand bases in length is transcribed by RNA polymerase II (Lee *et al.*, 2004). This is recognised and cut by a Drosha-containing complex called the Microprocessor to produce stem-loop precursor miRNA (pre-miRNA) of ~70 nucleotides in length (Lee *et al.*, 2002). This pre-miRNA can be transported out of the nucleus and into the cytoplasm by Exportin 5 where it is cleaved a final time by Dicer to produce mature

miRNA duplexes (Yi *et al.*, 2003). With the assistance of Dicer and a Heat shock cognate 70/Heat shock protein 90 (Hsc70/Hsp90) chaperone machinery, miRNA is loaded into an Argonaute protein (AGO) - a vital component of the RISC (Kobayashi & Tomari, 2016). One strand of the miRNA duplex is then degraded to enable it to bind with partial or complete complementarity to its target mRNA (Meister, 2013). Other RISC components include GW182, Pumilio2 (Pum2) and Moloney leukemia virus (MOV10) and are key for silencing of targeted mRNA (Du and Zamore, 2005).

1.3.4 miRNA and RISC machinery are present in the synapse

The mammalian brain uniquely expresses more miRNAs than any other tissue (Landgraf *et al.*, 2007). These miRNAs are differentially distributed across brain regions and a large number have been found to be enriched specifically at dendrites and at synapses (Pichardo-Casas *et al.*, 2012; Hu & Li, 2017) This indicates specialisation of miRNA function from the levels of tissue and brain region through to cellular sub-compartment.

If local translation requires active transport of specific mRNAs to target regions it follows that the miRNA must also be transported to its mRNA targets. Though miRNA targeting has long been known to be present and essential for cell function the mechanisms for miRNA transport are less well understood (Meister, 2013; Sheu-Gruttadauria & MacRae, 2017; Daugaard & Hansen, 2017). mRNA transport molecules were contained in fractions in which pri-miRNAs and the Microprocessor proteins Drosha and DiGeorge syndrome critical region 8 (DGCR8) were found to be enriched and cytosolic Drosha is known to be associated with the kinesin heavy chain suggesting that miRNA precursors may be transported in a similar manner to mRNAs (Lugli *et al.*, 2012). Furthermore, Fragile Mental Retardation Protein (FMRP) is known for its role coordinating local protein translation and has been found bound to several brain-enriched

miRNAs (Edbauer *et al.*, 2010). One defined miRNA transport mechanism is that of miR-134. The DEAH-box helicase DHX-36 has been shown to interact with the terminal loop of pre-miR-134 to mediate its transport to dendrites and this interaction is necessary for target silencing and downstream effects (Bicker *et al.*, 2013).

The presence of Drosha and DGCR8 proteins that comprise the microprocessor responsible for processing pri-mRNAs has been shown in synaptic fractions and isolated PSDs tightly associated with pre-miRNAs (Lugli *et al.*, 2012). Furthermore, Dicer has been found to be present in synapses and, unlike mature miRNAs and the RISC which are predominantly located in the soluble compartment, it is strongly localised to the PSD where it acts as a scaffold for biogenesis of mature miRNAs in dendritic spines (Lugli *et al.*, 2005, 2008). This also indicates that, as with pre-miR-134, miRNA arrives at its target destination in its precursor form before being processed to produce mature miRNAs for loading into the RISC.

1.3.5 AGO proteins

Roles for miRNA-mediated silencing have been identified in a wide range of fundamental cellular processes, including homeostasis, differentiation and proliferation (Aalto & Pasquinelli, 2012; Sheu-Gruttadauria & MacRae, 2017). The core RISC component and key protein effector element in siRNA-mediated gene regulation is the Argonaute protein family. In humans the Argonaute family of proteins consists of four argonaute (AGO) proteins and four P-element Induced Wimpy testis (PIWI) proteins. These proteins and their homologs are present in almost all eukaryotes, bacteria and archaea (Tolia & Joshua-Tor, 2007) and are highly conserved

structurally and functionally despite low sequence homology ([Swarts *et al.*, 2014](#); [Olina *et al.*, 2018](#)) (**Figure 1.7**).

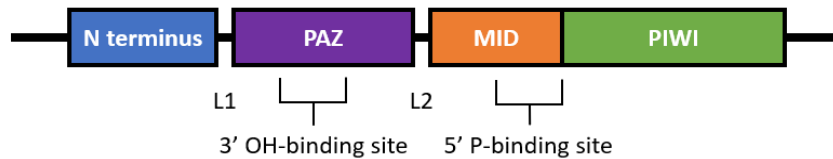


Figure 1.7: AGO structure. AGO proteins structurally consist of two lobes joined by a hinge region. The first of these lobes is comprised of the N-terminal and Piwi-Argonaute-Zwille (PAZ) domains and the second of the middle (MID) and PIWI domains ([Swarts *et al.*, 2014](#); [Parker, 2010](#)). The hinge region connecting these two lobes is made up of Linker 1 (L1) and Linker 2 (L2) ([Swarts *et al.*, 2014](#)). Conformational change following small RNA binding is coordinated via this hinging region. The 3' end of miRNA binds with the PAZ domain and the 5' end into the MID domain.

1.3.6 Loading miRNA into AGO

In most cases, to guide RNA-silencing machinery to target specific miRNA targets the appropriate miRNA must be loaded into AGO. Hsc70/Hsp90 chaperone machinery are required for ATP-dependent loading of RNA duplexes into AGO ([Iwasaki *et al.*, 2010](#)). Transactivating response RNA-binding protein (TRBP) is also necessary for loading miRNA in its double-stranded form into Ago and acts as an asymmetry sensor to locate and select the guide strand of the miRNA to be retained ([Noland *et al.*, 2011](#)). This selection process has been suggested to be a mechanism through which the activity of small RNA subtypes may be regulated as different AGO proteins preferentially bind to particular subpopulations of miRNAs ([Czech & Hannon, 2011](#)).

AGO is able to directly bind small RNA, anchoring the 3' end into a binding pocket located on the PAZ domain ([Jung *et al.*, 2013](#)) and the 5' end into another on the MID domain, facilitated

by a highly conserved tyrosine residue within its binding pocket (Jinek & Doudna, 2009; Boland *et al.*, 2011). Insertion of the hydroxy ends of miRNA into the PAZ domain protects them from degradation (Tian *et al.*, 2011; Park *et al.*, 2017) The N-terminal domain is also required for loading and helps to unwind the RNA duplex (Meister, 2013). Conformational changes in AGO cause the N-terminal domain to wedge between the strands of the RNA duplex, causing it to open up (Meister, 2013). AGO2 bears similarities to RNase H in that its PIWI domain has several highly conserved amino acids that form a slicer activity centre along with a Mg^{2+} cation and an unstructured loop within the N-terminal domain which is able to slice mRNA when there is 100% miRNA:mRNA complementarity (Jinek & Doudna, 2009; Nakanishi *et al.*, 2012; Wilkomm *et al.*, 2017). In mammals the only AGO protein with this slicer activity centre is AGO2, however, AGO3 has also been shown to be able to cleave mRNA by an alternative mechanism (Liu *et al.*, 2004; Park *et al.*, 2017). The other AGO proteins are not catalytically active and can therefore take longer to remove the passenger strand. C3PO (also known as translin) is another endonuclease that removes the passenger strand once it has been nicked, leaving the single guide strand loaded into the complex and able to base pair with its targets. (Ye *et al.*, 2011; Liu *et al.*, 2009).

1.3.7 AGO target recognition and translational down-regulation

AGO scans mRNA targets by diffusing laterally along it, assisted by loose protein-nucleic acid interactions, and is able to bypass secondary RNA structures and protein barriers to achieve this (Cui *et al.*, 2019). AGO proteins do not directly interact with mRNA and the binding of miRNA alone is insufficient for stable association of mRNA with the miRISC (Cui *et al.*, 2019).

Translational silencing is dependent therefore on the other components of the RISC. The GW182 protein family is so named for the presence of many glycine-tryptophan repeat regions through which it binds to AGO proteins (Zhang *et al.*, 2018). When AGO is bound to miRNA its affinity for GW182 is enhanced and the latter is able to act as a flexible scaffold for the RISC, recruiting other RNA binding proteins (Jonas & Elisa Izaurralde, 2015). These downstream effectors can inhibit mRNA translation in a number of ways. In some cases polyadenylate-binding protein (PABPC) bound to GW182 recruits poly(A)-nuclease deadenylation complex subunit 2 (PAN2)–PAN3 and carbon catabolite repressor protein 4 (CCR4)–NOT complexes (Behm-Ansmant *et al.*, 2006; Chen *et al.*, 2009; Braun *et al.*, 2011; Chekulaeva *et al.*, 2011; Fabian *et al.*, 2011). These promote deadenylation of mRNA which in turn permits decapping by mRNA-decapping enzyme subunit 1 (DCP1)–DCP2 complex and finally degradation by the 5' to 3' exoribonuclease (XRN1) (Li *et al.*, 2011; Medina *et al.*, 2014). However, although mRNA degradation is believed the dominant mechanism for miRNA-mediated silencing at steady state in mammalian cells, mRNA is not always degraded by the RISC (Eichhorn *et al.*, 2014). Temporary inhibition can allow a pause in expression which is able to rapidly return upon release of mRNA to the translational pool (Schratt *et al.*, 2006; Wakiyama *et al.*, 2007; Mudashetty *et al.*, 2011).

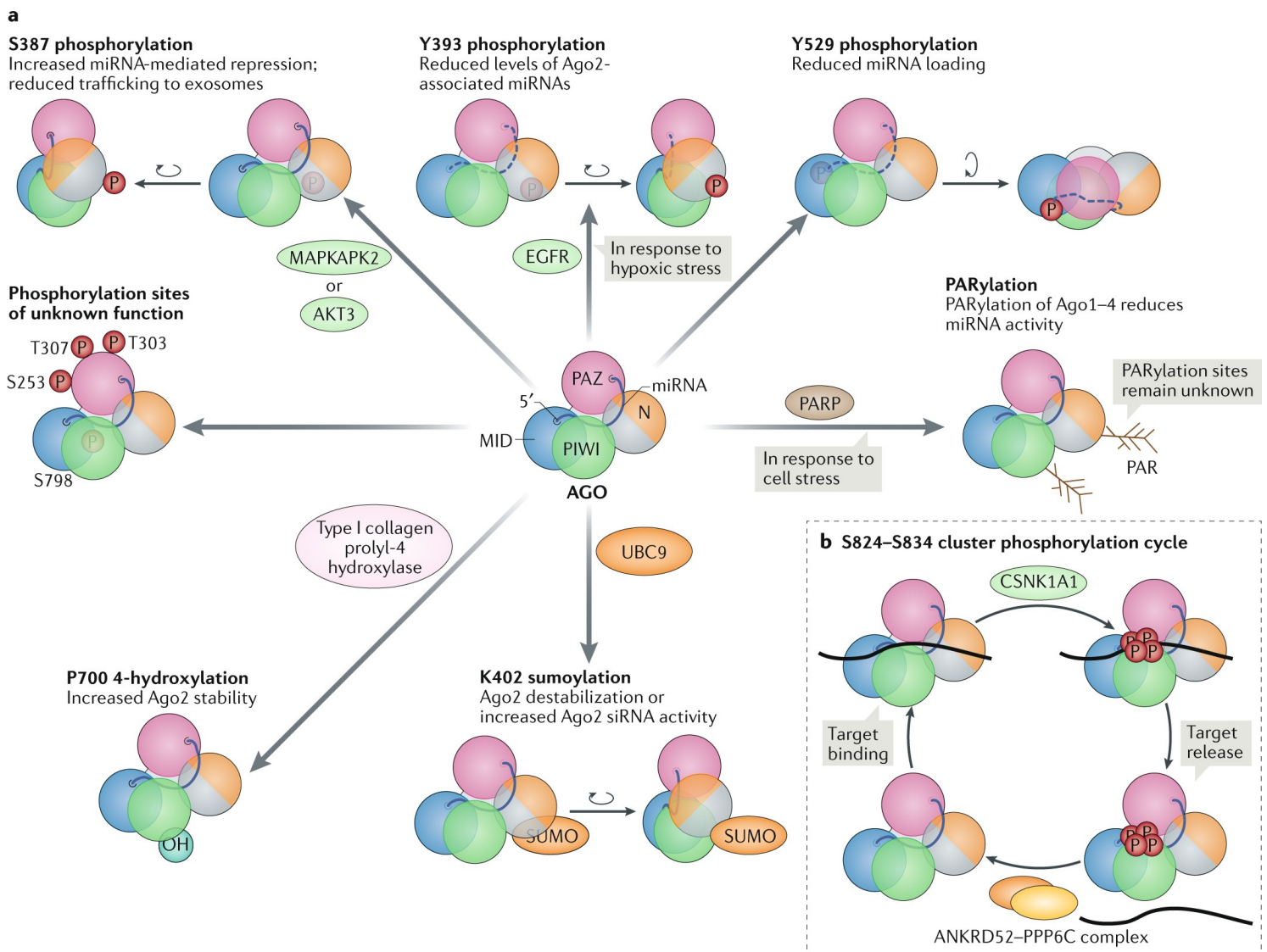
1.3.8 RISC loading/binding partners

Other RISC proteins have been shown to participate indirectly in RNA-induced silencing. For example, Pum regulates E2F3 mRNA by binding to its 3'UTR, leading to an increase in the activity of a number of miRNAs that target it (Miles *et al.*, 2012; van Kouwenhove *et al.*, 2011). Importin 8 (IPO8) and receptor or activated kinase 1 (RACK1) facilitate targeting of AGO to

specific mRNAs or to simply to sites of translation, respectively (Weinnman *et al.*, 2013; Jannot *et al.*, 2011). LIM domain containing proteins LIMD1, Ajuba and WTIP are necessary to stabilise the complex (James *et al.*, 2010).

1.3.9 Post translational modifications of AGO regulate function, localisation and stability

Post translational modifications of proteins allow another layer of regulation to fine tune



protein interactions and pathways (Seet *et al.*, 2006). Extensive post-translational modification

of AGO2 has been demonstrated and shown to affect its miRNA activity, localisation and

stability (Meister, 2013; Gebert & Macrae, 2019) (**Figure 1.8**).

Figure 1.8: Post-translational modifications of AGO (Gebert & Macrae, 2019). AGO2 modifications include hydroxylation at Proline700 (P700) which increases AGO2 stability (Qi *et al.*, 2008), nitrosylation at Cysteine691 (C691) which disrupts miRNA activity by reducing AGO2 association with GW182 (Seth *et al.*, 2019); ubiquitylation which reduces AGO2 stability and consequently represses miRNA activity (Bronevetsky *et al.*, 2013; Rybak *et al.*, 2009); Poly(ADP-ribose)ylation (PARylation) which reduces miRNA activity (Seo *et al.*, 2013); sumoylation of Lysine402 (K402) which has been reported to affect AGO2 stability (Sahin *et al.*, 2014); and acetylation at a number of lysine residues which was found to recruit the miR191b1 precursor to AGO2 (Zhang *et al.*, 2019). Phosphorylation of several residues has been attributed to various functions including regulating miRNA loading and release, AGO localisation and association with other RISC proteins.

1.3.10 AGO is regulated extensively by phosphorylation at number of residues

One of the most basic and important mechanisms for regulating protein activity is phosphorylation. This is a reversible modification in which a phosphate group (PO_4) is added to the polar group R of amino acids such as threonine, tyrosine or serine by a protein termed a kinase (Ardito *et al.*, 2017). The addition of a phosphate can lead to conformational changes in the protein and therefore changes in affinity and activity (Ardito *et al.*, 2017). AGO2 has a number of phosphorylation sites which have been implicated in its function and localisation (**Figure 1.8**).

Multi-site sequential phosphorylation of four highly conserved residues in the AGO2 PIWI domain from Serine824 (S824) to Serine834 (S834) by Casein kinase 1 alpha 1 (CSNK1A1) is triggered when AGO binds to its target (Golden *et al.*, 2017). Phosphorylation at these sites leads to dissociation of the bound miRNA. These sites are then dephosphorylated by the Ankyrin repeat domain 52 (ANKRD52) – Protein phosphatase 6 (PPP6C) complex (Golden *et al.*,

2017). This cycle promotes dissociation of miRNA from the RISC to free the complex for binding to other miRNAs (Golden *et al.*, 2017). Global miRNA-mediated repression is inhibited if this process is stalled. Through this mechanism target binding may be self-limiting by causing a conformational change that exposes the CSNK1A1 binding site. The triggering of a dissociation process following target binding allows loaded miRNA to bind to and inhibit translation of multiple targets. The presence of silencing factors such as CCR4-NOT deadenylase complex and DEAD-Box Helicase 6 (DDX6) have also been suggested to assist in signalling silencing completion and in triggering phosphorylation of AGO at these sites to stimulate release of miRNA:AGO from its target (Golden *et al.*, 2017).

Phosphorylation of AGO2 at Serine798 (S798) was found to eliminate localisation of processing bodies (P-bodies) and stress granules (cytoplasmic RNA granules which serve as sites of RNA processing) but surprisingly the reduction seen in RNA-induced silencing was only modest (Lopez-Orozco *et al.*, 2015). This suggests multiple coordinated mechanisms are responsible for translocation and function of AGO2.

Phosphorylation of Tyrosine529 (Y529) within the AGO2 MID domain prevents binding efficiency of the 5' end of miRNA due to the negative charge change which has been shown to be important for macrophage activation following parasite invasion (Rüdel *et al.*, 2011; Mazumder *et al.*, 2013).

Mutation of a cluster of AGO2 phosphorylation sites from Tyrosine555 (Y555) to Serine561

(S561) (located on a loop proximal to the mRNA binding site) strongly impairs silencing activity and eliminated localisation to P bodies ([Quévillon Huberdeau *et al.*, 2017](#)) AGO2 Serine253 (S253), Threonine303 (Tyrosine303) and Threonine307 (T307) are phosphorylation sites that lie within the PAZ domain ([Rüdel *et al.*, 2011](#)). When this site is mutated AGO2 is unable to bind miRNAs but can repress translation when artificially tethered to them ([Rüdel *et al.*, 2011](#)).

Tyrosine393 (Y393) of the AGO2 L2 linker region is phosphorylated by the epidermal growth factor receptor (EGFR) following hypoxia ([Shen *et al.*, 2013](#)). This was found to reduce Dicer:AGO2 interaction and processing of precursor miRNAs to mature miRNAs ([Shen *et al.*, 2013](#)). This study also demonstrated the importance of a long-loop structure in precursor miRNA in pY393-AGO2-mediated miRNA maturation ([Shen *et al.*, 2013](#)). Protein tyrosine phosphatase 1B (PTP1B) is also able to phosphorylate AGO2 Y393, which was also shown to inhibit loading of miRNAs ([Yang *et al.*, 2014](#)).

In HeLa cells phosphorylation of Serine387 (S387) in the L2 linker region of AGO2 by Akt has been shown to act as a molecular switch between the two mechanisms through which AGO2 can reduce target mRNA translation - direct cleavage of target mRNA and translational repression through association with other RISC proteins ([Horman *et al.*, 2014](#)). AGO2 has been shown to be present in exosomes, used for intercellular communication ([McKenzie *et al.*, 2016](#)) Phosphorylation of S387 by mitogen-activated protein kinases (MEKs) I and II reduces this exosomal secretion of AGO2 ([McKenzie *et al.*, 2016](#)). Phosphorylation of S387 by p38 mitogen-activated kinase (MAPK) has been associated with an increase in localisation of AGO2 to P-

bodies (Lopez-Orozco et al; 2015; Zeng *et al.*, 2008) This is in accordance with previous work in the Hanley lab which demonstrated that in neurons induction of cLTD with NMDA led to Akt-mediated phosphorylation at this site and not only an increase in association between AGO2 and the RISC scaffold protein GW182 but to an increase in activity of miR-134 (Rajgor *et al.*, 2018). The variety of kinases found to phosphorylate and regulate AGO2 function and localisation at this site demonstrates that AGO2 is under the influence of a number of different pathways and underlines its importance in RNA-induced silencing.

Collectively, these data show the importance and complexity of post-translational modification of AGO2, particularly phosphorylation. However, most of our understanding of AGO2 phosphorylation comes from studies using cell lines such as HEK293 or HeLa cells. Future investigations into the role of these pAGO2 in whole animals and human samples may shed light on the role that AGO2 phosphorylation may play in disease.

1.3.11 miRNAs regulate synaptic plasticity

To simulate NMDAR-related LTD in cultured neurons a bath application of NMDA at an appropriate concentration is used. This is one form of chemical LTD or cLTD. Investigations into the transcriptome following cLTD have shown that it is profoundly changed, with many up- or down-regulated miRNAs known to target key synaptic proteins (Park & Tang, 2009; Wibrand *et al.*, 2010; Kye *et al.*, 2011; Hu *et al.*, 2014; Olde Loohuis *et al.*, 2012; Reza-Zaldivar *et al.*, 2020; Hanley, 2021). These findings highlight the importance of miRNA in synaptic plasticity.

Of the many miRNAs found to participate in synaptic plasticity a number have been shown to

coordinate structural remodelling of spines. For example, [Hu and colleagues \(2014\)](#) investigated changes in the miRNA transcriptome following cLTD and highlighted miR-191 activity as necessary for actin remodelling mediated maintenance of spine shrinkage and miR-135 as important in AMPAR trafficking - both important components of lasting LTD. miR-501-3p plays an important role in neuronal development by targeting the AMPAR subunit GluA1 ([Hu *et al.*, 2015](#)) miR501-3p activity has also been shown to increase 60 min after cLTD induction and to be necessary for the consequent reduction in spine size suggesting a role in maintaining LTD-related changes at the synapse ([Hu *et al.*, 2015](#); Hanley, 2021). Translational inhibition by miR-132 is involved in dendritic spine formation via modulation of the Rac1-Pak actin remodeling pathway ([Impey *et al.*, 2010](#)). miR-188 positively regulates spine size and structure in targeting the semaphorin 3F receptor Nrp-2 - a negative regulator of spine development ([Lee *et al.*, 2012](#)). So too does miR-375 which enhances Brain-derived neurotrophic factor (BDNF) activity by targeting the RNA-binding protein HuD ([Abdelmohsen *et al.*, 2010](#)). miR-9 activity also promotes dendritic growth by targeting the transcriptional repressor RE1-Silencing transcription factor (REST) which itself represses miR-132 expression ([Giusti *et al.*, 2014](#); [Hwang *et al.*, 2014](#)). In contrast, miR-34a is a negative regulator of dendritic outgrowth ([Agostini *et al.*, 2011a, 2011b](#)). miR-34a has been shown to be important for amygdala-dependent fear memory consolidation ([Dias *et al.*, 2014](#)). miR-29a/b regulates dendritic spine maturation by targeting ARPC3, a subunit of the actin nucleating ARP2/3 complex ([Lippi *et al.*, 2011](#)). The activity-regulated cytoskeletal associated protein (Arc) is also a key player in spine dynamics and is the target of numerous miRNAs ([Wibrand *et al.*, 2012](#)).

1.3.12 miR-134 activity is important in neuronal function and synaptic plasticity

Of particular interest in this study is the brain-enriched miRNA miR-134 ([Schratt *et al.*, 2006](#)). miR-134 represents the first miRNA found to be enriched in dendrites in a landmark paper by Schratt and colleagues in 2006. They used fluorescence *in situ* hybridisation (FISH) to demonstrate that miR-134 is present in a punctate pattern along dendrites - indicative of presence at synapses. Specifically, it is localised to the post synaptic compartment where it targets LIMK1 mRNA. Overexpression of miR-134 was found to lead to shrinkage of dendritic spines. This effect could be rescued by overexpression of LIMK1 or by application of BDNF with the latter activating the mTor kinase pathway. This miR-134-mediated repression of LIMK1 translation was later demonstrated to play an important role in spine shrinkage in cLTD and in other types of synaptic plasticity ([Fiore *et al.*, 2014](#); [Rajgor *et al.*, 2018](#)). Specifically, phosphorylation of AGO2 S387 was found to follow the induction of cLTD, causing AGO2:GW182 interactions and miR-134 activity to increase ([Rajgor *et al.*, 2018](#)). This led to shrinkage of dendritic spines ([Rajgor *et al.*, 2018](#)).

The histone deacetylase, Sirtuin-1 (SIRT1) also regulates synaptic plasticity by repressing expression of miR-134 through the formation of a complex with the transcription factor yin yang 1 (YY1) which binds upstream of the miR134 locus ([Gao *et al.*, 2010](#)). Knockdown of SIRT1 leads to up-regulation of miR-134 expression and increased targeting of cAMP response element-binding protein (CREB) - a transcription factor that is important for synaptic plasticity ([Gao *et al.*, 2010](#)). This results in an impairment of synaptic plasticity and memory which can be reversed by inhibition of miR-134. SIRT1 both targets and is a target of other miRNAs ([Zovoilis *et al.*, 2011](#);

Liu et al., 2013). This is evidence of a complex network of cross-regulation and feedback systems that helps to regulate synaptic activity. Furthermore, inhibition of miR-134 was found to have a neuroprotective effect in kainate-induced epileptic seizures, indicating the importance of these coordinated signalling mechanisms in healthy brain functioning (Jimenez-Mateos et al., 2012).

The AMPAR-trafficking protein Protein Interacting with C Kinase - 1 (PICK1) dampens miR134 activity by promoting the localisation of AGO2 to recycling endosomes (Antoniou et al., 2014). This PICK1-mediated inhibition is relieved by cLTD, allowing miR-134 to inhibit LIMK translation and consequently, spine size. This represents one mechanism by which an inert pool of miRNA can be retained at the synapse and activated following synaptic signalling.

Another miR-134 target important for neuronal function is Pum2 - an RBP involved in RNA silencing (Fiore et al., 2009). Activity-dependent outgrowth of dendrites has been shown to be dependent on activation of myocyte enhancing factor 2 (MEF2) which increases transcription of the miR-379–410 cluster in which pri-miR-134 resides (Fiore et al., 2009). This increases miR-134-mediated repression of Pum2 translation and consequently increased dendritogenesis (Fiore et al., 2009). This is in striking contrast to its effect in dendritic spines in which it induces shrinkage but is perhaps due to differing effects on local cytoskeletal proteins as, unlike in the actin-rich dendritic spines, in dendrites these are primarily microtubules. Another inhibitor of mature miR-134 production is the Rett syndrome gene product MeCP2 which inhibits processing of pri-miR-134 by the DGCR8/Drosha complex and consequently also modulates dendritic growth (Cheng et al., 2014). Another role of BDNF in regulation of mechanism for miR-

134-mediated signalling is also in dendritic outgrowth ([Zampa et al., 2018](#)). BDNF stimulation has been shown to induce targeting of pre-miR-134 to dendrites by the RNA binding protein (RBP) DEAH-box helicase DHX36 which recognises and binds to specific region of its terminal loop ([Bicker et al., 2013](#); [Zampa et al., 2018](#)). The counteractive effects of these molecules may represent a self-limiting mechanism for growth after it has been initiated by BDNF.

1.3.13 RNA-induced Silencing Complex (RISC) machinery plays a role in synaptic plasticity

Although the focus of most miRNA studies is specific miRNA transcripts there is growing evidence that RISC proteins' activity can be regulated by synaptic activity and play an important role in synaptic plasticity and memory.

Dicer is present in the PSD of the dendritic spine ([Lugli et al., 2005](#)). cLTD in induction in hippocampal slices and calcium treatment of synaptoneurosomes causes it to be released along with AGO in a calpain-dependent manner ([Lugli et al., 2005](#)). Conditional knock-out of the microprocessor subunit DGCR8 leads to deficits in inhibitory signalling in the mouse prefrontal cortex ([Hsu et al., 2012](#)). miRNAs can be produced not only from the drosha-containing microprocessor but through alternative routes such as spliced introns ([Westholm & Lai, 2011](#)) so a knock-out of DGCR8 does not lead to completely diminished miRNA activity. In contrast, conditional KO of neuronal Dicer led to more severe morphological abnormalities ([Hsu et al., 2012](#)) however another study found that Dicer knockdown led to increased learning and memory, presumed due to the increase in synaptic-plasticity associated proteins found in the resulting elongated filopodia-like dendritic spines (Konopka et al., 2010).

Ubiquitination of the RISC component MOV10 is triggered following NMDAR activation causing it to be degraded and consequently a reduction in activity for a number of miRNAs including miR-138 and miR-134 ([Banerjee *et al.*, 2009](#)). miR-138 targets acyl protein thioesterase 1 (APT1), an enzyme that is involved in regulation of multiple synaptic proteins via palmitoylation ([Siegel *et al.*, 2009](#)). This results in palmitoylated G protein subunit G α 12/13, causing it to dissociate from the plasma membrane and trigger the RhoA signaling pathway which causes shrinkage of dendritic spines ([Siegel *et al.*, 2009](#)). In addition to its role in synaptic plasticity, MOV10 transcription has been shown to increase following contextual conditioning, suggesting a mechanism for replenishing degraded MOV10 protein and indicating its importance in memory not only cellular processes but in memory ([Kye *et al.*, 2011](#)).

Phosphorylated FMRP is found in a complex AGO2 bound to miR-125a in dendritic spines ([Muddashetty *et al.*, 2011](#)). This interaction promotes translational repression of the PSD scaffold protein PSD95 ([Muddashetty *et al.*, 2011](#)). mGluRs are another type of glutamate receptor that participate in synaptic plasticity. mGluR activation leads to dephosphorylation of FMRP, causing it to dissociate from this complex and therefore induces derepression of PSD95 translation ([Muddashetty *et al.*, 2011](#)). This depression of PSD95 in turn leads to an increase in spine density ([Muddashetty *et al.*, 2011](#); [Edbauer *et al.*, 2010](#)).

As discussed above, AGO2 has also been shown to play a role in miR-134-mediated down-regulation of LIMK1 following cLTD ([Rajgor *et al.*, 2018](#)). Further evidence for the importance of

AGO2 in memory comes from *in vivo* experiments in which AGO2 was knocked down in the dorsal hippocampus of C57BL/6 mice (Batassa *et al.*, 2010). These mice had short- and long-term impairment of contextual fear memories demonstrating the importance of AGO2 and RNA-induced silencing in regulating the processes that underpin memory formation.

1.3.14 Many miRNAs are involved in AD pathology

The high relative concentration of miRNA in the brain and the involvement of miRNA-mediated translational regulation across such a wide range of cellular processes has naturally led to extensive research into the role of miRNAs in neurological disease. These studies have implicated dysregulated miRNA activity in numerous disorders, including AD where they have been shown to be involved in APP processing, tau phosphorylation, inflammation, neurotransmitter dysregulation and deregulation of the cell cycle (**Figure 1.9**) (Garza-Manero *et al.*, 2013; Aksoy-Aksel *et al.*, 2014; Hemachandra Reddy *et al.*, 2016; Hu & Li, 2017; Thomas *et al.*, 2018; Perkovic *et al.*, 2021).

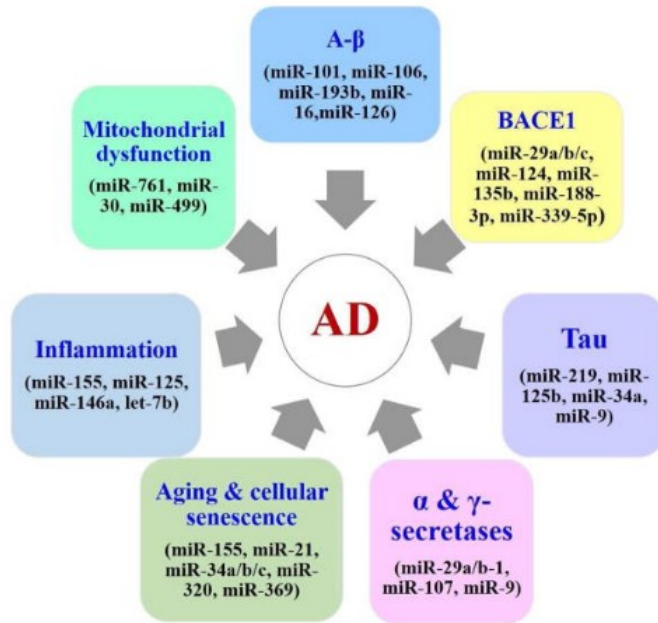


Figure 1.9: miRNAs have been found to be involved in AD via many different mechanisms (Reddy *et al.*, 2017). These include miRNAs that target genes key AD related genes such as BACE1, tau and APP but also other proteins involved in other peripheral cellular processes that contribute to ADs pathology.

Many of these are also known to play a role in structural plasticity. In the Tg2576 mouse model of AD miR-206 is overexpressed (Lee *et al.*, 2012). miR-206 targets BDNF for down-regulation, repressing its positive effect on LTP and cognitive function. Inhibition of miR-206 in these mice enhances expression of the synaptic marker synaptophysin (Lee *et al.*, 2012). miR-574 overexpression is seen in APP/PS1 mice along with loss of synapses in the hippocampus and this overexpression is negatively correlated with cognitive function (Li *et al.*, 2015). This is believed to be due to targeting by miR-574 of Nrn1 - a neurotrophin involved in the formation and stabilisation of dendritic spines (Fujino *et al.*, 2011). miR-34a is overexpressed in AD (Sarkar *et al.*, 2019). Sarkar and colleagues (2019) generated a heterozygous, conditional miR-34a overexpression mouse. Again, cognitive function was negatively correlated with miR-34a

expression and was concurrent with the presence of characteristic pathologic hallmarks of AD - hyperphosphorylated tau and A β . This mouse model also has altered spine morphology due to targeting of synaptic proteins Synaptotagmin-1 (Syt-1) and Syntaxin1A (Stx-1A) (Agostini *et al.*, 2011). miR-30b expression negatively effects synaptic integrity by down-regulating EphrinB2, SIRT1, and Glutamate Ionotropic Receptor AMPA Type Subunit 2 (GRIA2) and is overexpressed in AD patients' brains and the 5xFAD model of AD (Song *et al.*, 2019). Furthermore, hippocampal overexpression of miRNA-30b leads to impairment of synaptic plasticity and memory and a reduction spine density (Song *et al.*, 2019). Overexpression of miRNA-125b was found to increase phosphorylation of tau in primary neurons and to impair learning when injected into the hippocampus of WT mice (Banzhaf-Strathmann *et al.*, 2014).

1.4 Summary and aims

1.4.1 Summary

Synaptic loss is correlated with cognitive decline and is the earliest structural correlate of disease progression in AD. Understanding the mechanisms that underlie synaptic loss may lead to more effective therapeutic strategies for the disease.

Although there is abundant evidence of the involvement of miRNA in neurological disease, our understanding of the role of the protein components of the RISC is considerably limited.

Furthermore, despite the brain expressing the vast majority of all known miRNAs, most of our understanding of regulation of RISC proteins by post-translational modifications comes from non-neuronal cell lines (Landgraf *et al.*, 2007).

Previously this lab demonstrated that cLTD stimulation in cultured neurons led to a cascade of signalling in which phosphorylation of AGO2 by Akt at S387 led to an increase in association of AGO2 with binding partner GW182 and a rapid increase specifically in miRNA-134 activity (Rajgor *et al.*, 2018). LIMK1 expression decreased and consequently so did spine density and synaptic strength. Furthermore, this process was found to be necessary for the dendritic spine shrinkage observed following NMDA-stimulated cLTD.

The discovery of the role of phosphorylation of AGO in LTD-associated spine shrinkage led to the hypothesis that aberrant regulation of RISC machinery via post-translational modifications such as phosphorylation may contribute to spine loss seen in AD and its models. Specifically, that there may be an increase in phosphorylation of AGO at S387 and consequently an increase in miR134-mediated silencing of LIMK1 mRNA expression (**Figure 1.10**).

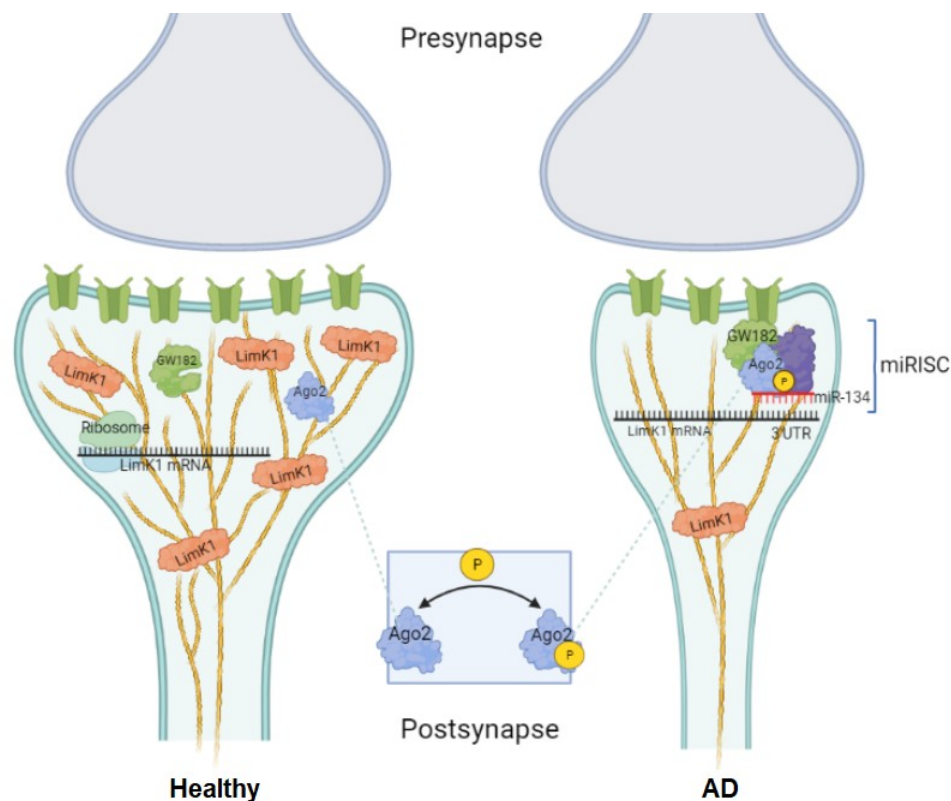


Figure 1.10: Schematic of hypothesised pS387-AGO2 and miR134-mediated synaptic loss in AD. In AD increased A β levels may induce AGO2 phosphorylation at S387 which increases binding of AGO2 to GW182, elevating miR-134 repression of LIMK1 mRNA translation. LIMK1 serves to phosphorylate and inactivate cofilin, a negative regulator of spine size. Derepression of cofilin by pS387-AGO2 and miR-134-mediated translational inhibition of LIMK1 mRNA thereby may contribute to the spine shrinkage and loss seen in AD.

A pilot study was conducted by members of the Hanley lab group to determine whether these changes are present in the hAPP-J20 mouse model of amyloidopathy (Mucke *et al.*, 2000).

Argonaute phosphorylation at S387 and interactions with GW182 were found to be significantly increased and LIMK1 expression significantly decreased in the brains of 18-month J20 mouse cortex relative to age-matched WT controls (personal communication). These results reflected those found in a primary neuronal cultures overexpressing of hAPP in which miR-134-mediated LIMK1 silencing was found to be significantly increased. Further to this, *post-mortem* human brain tissue from patients with AD was found to have lower LIMK protein expression than in age-

matched controls (personal communication).

Data from this lab published previously has demonstrated that replacing endogenous AGO2 with a phospho-null mutant (S387A) rendered cultured neurons resistant to shrinkage of dendritic spines and reduced excitatory post-synaptic current amplitudes following cLTD ([Rajgor *et al.*, 2018](#)). This suggests that inhibiting Argonaute phosphorylation may be a viable strategy for reducing deficits in synaptic transmission and dendritic spine morphology seen in AD.

1.4.2 Aims

The aims of my PhD project were therefore to:

- Produce a cellular model of AD in which rescue strategies targeting pS387-AGO2-mediated miR-134 activity could be tested.
- Determine whether changes seen in the pilot experiments occur early in the disease course or are only present in late stage in the J20 mouse model of AD by producing a time course of changes to pS387-AGO2 and LIMK1 levels
- Determine whether change in LIMK1 levels observed in the pilot experiments occur early in the disease course or are only present in late stage of AD by quantifying LIMK1 in early, mid and late stage AD brain samples.

Chapter 2: Materials and Methods

2.1 Materials

2.1.1 Chemicals

Reagents were supplied by Sigma-Aldrich unless stated otherwise. Fisher Scientific supplied all acids and solvents unless stated otherwise.

2.1.2 Bacterial culture reagents

All competent bacterial strains used were *Escherichia coli* (*E. coli*). For cloning the DH5 α (Western) strain was used (Thermo Fisher). For preparation of DNA the XL1-Blue (Genotype: *recA1, endA1, gyrA96, hsdR17, supE44, relA1, lac*) strain was used (Thermo Fisher). Bacteria were cultivated in standard Luria-Bertani (LB) broth (Thermo Fisher). Agar plates used for cloning were made using LB and 1.5 % agar (Sigma Aldrich). Growth media and plate agar was supplemented with either ampicillin (100 μg / ml) or kanamycin (25 μg / ml) as appropriate.

2.1.3 Eukaryotic cell culture reagents

Human Embryonic Kidney (HEK) 293T cells (HEK293) were purchased from The European Collection of Cell Cultures (ECACC). Stocks were stored in Dulbecco's Modified Eagle's Medium (DMEM) (Sigma-Aldrich) and 1 % dimethyl sulfoxide (DMSO) in liquid nitrogen. Dulbecco's Modified Eagle's Medium (DMEM) used for HEK293 cells was supplied by Sigma-Aldrich and supplemented with Heat-inactivated foetal bovine serum (FBS) from Biosera. Neurobasal media used for primary neuronal cultures was purchased from Gibco (Life Sciences) and supplemented with horse serum (HS) from Sigma Aldrich. Penicillin/Streptomycin and Poly-D-Lysine (PDL) Hydrobromide were also supplied by Sigma Aldrich. B27 supplement and glutamax were from

Gibco. Cell culture grade RNase-free water was purchased from Gibco. Cell culture grade RNase-free 10 x PBS stock solution was from Gibco. Lipofectamine 2000 reagent was purchased from Thermo Fisher.

2.1.4 Molecular cloning reagents

DNA was prepared using GeneJET Gel Extraction, Miniprep and Midiprep kits (Thermoscientific). Polymerase chain reaction (PCR) was performed using KOD Hot Start DNA Polymerase kit (Merck Millipore). Restriction enzymes and Calf Intestinal Alkaline Phosphatase (CIP) were obtained from New England Biolabs (NEB). DNA gel electrophoresis was performed using agarose (Bioline) gels prepared in house to appropriate concentration. DNA molecular weight marker (1 kb) and 6 x DNA loading buffer were purchased from Bio Line and New England Biolabs (NEB) respectively. Merck Millipore supplied Calbiochem Omnipur Phenol:Chloroform:Isoamyl alcohol 25:24:1.

2.1.5 Protein biochemistry reagents

1:100 Phosphatase inhibitor Cocktail 1 & 2 and EDTA-free protease inhibitors were obtained from Thermo Scientific. Molecular weight marker used in protein gel electrophoresis was PageRuler prestained molecular weight marker (Thermo Scientific). Acrylamide gels were made in house using 30 % acrylamide obtained from Geneflow Limited. Membrane used for Western blotting was Immobilon PVDF (polyvinylidene difluoride) with a pore size of 0.45 µm (Merck Millipore). Bovine Serum Albumin (BSA) was purchased from Sigma Aldrich. Enhanced Chemiluminescence (ECL) substrates used in Western blotting were Luminata Classico HRP

substrate and Luminata Crescendo HRP substrate supplied by Merck Millipore, and SuperSignal® West Pico and West Femto Enhanced Chemiluminescence (ECL) substrates supplied by Thermo Scientific. CL-XPosure™ X-ray film was used to develop Western blots (Thermo Scientific).

2.1.6 Primary antibodies

Primary antibodies were diluted in 5 % BSA in PBS-T (1x Phosphate Buffered Saline, 0.1 % Tween) (**Table 2.1**)

| Antibody | Species | Dilution | Supplier | Cat no. |
|---------------------------------|---------|----------|-----------------|------------|
| Actin | Mouse | 1:5000 | Sigma Aldrich | A5441 |
| Amyloid Precursor Protein (APP) | Rabbit | 1:1000 | Merck Millipore | ab5300 |
| Argonaute 2 (AGO2) | Rabbit | 1:500 | Cell Signalling | 2897S |
| GAPDH | Mouse | 1:5000 | Cell Signalling | ab8245 |
| LIM kinase 1 (LIMK1) | Rabbit | 1:1000 | Cell Signalling | 3842S |
| p-S387 AGO2 | Rabbit | 1:1000 | AbCam | ab215744 |
| pTau | Rabbit | 1:5000 | Abcam | 28866-1-AP |
| Myc | Mouse | 1:2000 | Santa Cruz | sc-40 |

Table 2.1: Suppliers and dilutions of primary antibodies used in Western blots

2.1.7 Secondary antibodies

Horse Radish Peroxide (HRP) secondary antibodies used for Western blotting were anti-mouse and anti-rabbit purchased (GE Healthcare) and were diluted 1:10,000 in 5 % BSA in PBS-T.

2.1.8 Consumables and equipment

2.1.8.1 Plastic and glassware

0.5 ml and 1.5 ml microcentrifuge tubes were purchased from Sarstedt and 0.05 ml thin wall tubes for PCR were supplied by Starlabs. Plastic Gilson pipette tips (10-1500 µl) were purchased from Starlabs. Gel loading tips (200 µl) were from Thermo Fisher. Plastic conical tubes, serological pipettes, cell culture flasks, plates and dishes were supplied by Greiner Bio One. Terumo supplied syringes and needles. Syringe filters of 0.25 µm and 0.45 µm pore size were obtained from Sartorius. Plastic cuvettes for spectrophotometer were from Thermo Scientific.

2.1.8.2 Electronic equipment

Microscopes used for dissection and cell culture were from Leica. Power packs for protein electrophoresis were from Bio-Rad laboratories and for DNA electrophoresis were MupidJ gel apparatus. Benchtop microcentrifuge used was from Eppendorf. Centrifuges were either Jouan or Beckman-Coulter. The SRX-101A automatic medical X-ray film developer from Konica was used to develop X-ray films used following Western blotting. PCR was performed using the MJ Research PTC-2000 thermal cycler. Spectrophotometry was performed using an Amersham Pharmacia Biotech spectrophotometer. Sterile laminar flow hoods for cell culture were from Holten LaminAir. Incubators for culturing of eukaryotic cells were from RS Biotech. DNA yield was quantified with the NanoDrop™ Spectrophotometer (Thermo Fisher) using the software NanoDrop 1000 (version 3.8.1). Canon CanoScan LiDE 300 Flatbed Scanner was used to scan X-ray film from Western blots.

2.2 Cell culture methods

All procedures described were performed using aseptic technique and within sterile laminar flow hoods to prevent infection. Cell cultures were kept in incubators at 37°C with 5 % CO₂ and at 90 % humidity. Media and reagents were warmed to 37 °C in a water bath prior to use to minimise shock to cells.

2.2.1 Eukaryotic cell culture

2.2.1.1 HEK293T cells

A 1 ml aliquot of stock HEK293T cells was removed from liquid nitrogen cryo-storage and placed in a 37 °C water bath. Once thawed this was then transferred to 15 ml conical tube containing 10 ml Complete DMEM (10 % FBS in DMEM) supplemented with 1 % Penicillin/Streptomycin. Cells were mixed with a 5 ml pipette before being centrifuged at 1500 x g for 2 min at room temperature (RT). The media was aspirated and 1 ml Complete DMEM was added. The cell pellet was resuspended with a 5 ml serological pipette and then transferred again to a T75 culture flask containing 10 ml Complete DMEM. This flask was then incubated overnight to allow cells to attach. The following day the media was aspirated replaced with 20 ml Complete DMEM.

2.2.1.1.1 HEK293T cell passaging

HEK293T cells were passaged once they reached 80-90% confluency (generally every 3-4 days). The media was aspirated, and the cells were washed gently twice with 10 ml 1x PBS. PBS

was then aspirated and replaced with 1 ml 0.05 % trypsin-EDTA to detach adherent cells from the flask. The cells were incubated at 37 °C for 3 min before 9 ml of Complete DMEM was added to competitively inhibit trypsin activity. Cells were resuspended and then transferred to a 15 ml conical tube. They were centrifuged at 2000 x g for 2 min 30 sec at RT to pellet cells. The media was then aspirated, and cells were resuspended in 10 ml of Complete DMEM. 1 ml of resuspended cells was transferred to a new T75 flask containing 20 ml Complete DMEM. The flask was then incubated.

2.2.1.1.2 HEK293T cell transfection

Media used for transfection was sterile filtered before use. Cells in a T75 flask were grown to 80-90 % confluency and passaged as above. The cell number of the remaining resuspended cells was counted and calculated by diluting cells 1:10 in 0.4 % Trypan Blue and using a haemocytometer. 5×10^5 cells were added to 2 ml of Complete DMEM in the well of a 6-well plate and incubated overnight. The following day the cells were at 70-90% confluency and able to be transfected. An appropriate amount of DNA for the given experiment/ purpose of transfection was calculated and added to 100 µl of plain DMEM in a 1.5 ml microfuge tube. Likewise, the transfection agent used varied according to the given experiment/ purpose of transfection. For the production of lentiviruses 12 µg / ml polyethylenimine (PEI) was used and for the testing of miRNA assay constructs Lipofectamine was used. 1.5 µl of the appropriate transfection agent per 1 µg DNA. This was placed into 100 µl of plain DMEM and vortexed briefly and then incubated at RT for 5 min. The DNA-DMEM mixture was then added to this microfuge and vortexed briefly again. The transfection agent and DNA mixture was then

incubated for 30 min at RT. This was then inverted 2-3 times to mix before being added dropwise to a well of the 6-well plate. These volumes are for one well only and were scaled up to account for extra conditions/wells.

2.2.2.4 Primary neuronal culture

2.2.1.2.1 Poly-D-lysine coating of cell culture plates

6-well plates were coated in PDL by adding 1.5 ml of 0.5 mg/ml PDL in sterile cell culture grade H₂O to each well. This was incubated overnight in a cell culture incubator (37 °C, 90 % humidity) before being washed three times in sterile cell culture grade H₂O. H₂O was then replaced with 2 ml plating media (Neurobasal® medium, 5 % HS, 2 % B27, 1 % Glutamax and 1 % Penicillin/Streptomycin) and incubated in a cell culture incubator until needed. 1 h prior to plating of neuronal cells plating media was replaced with 2ml fresh plating media.

2.2.1.2.2 Rat sacrifice and dissection of embryos

All work involving animals was carried out in a manner compliant with the Home Office Act (1986). Isoflurane (Henry Schein) supplemented with O₂ was used to anaesthetise pregnant Wistar rats bred either in-house or at Charles River at E17. Cervical dislocation of the anaesthetised dams was performed to humanely sacrifice them according to Home Office Schedule 1 regulations. Dissection tools and work surfaces were sterilised with 70 % ethanol in H₂O. The abdomen of the animal was sterilised with 70 % ethanol before incision and extraction of embryos. These were placed into a 10 cm dish containing 30 ml Hank's Buffered Salt Solution (HBSS). Embryos were humanely sacrificed by decapitation and removed heads were placed in

fresh HBSS for dissection. Forceps were used under a dissection microscope to open the skull and remove then brain. The meninges and midbrain were then removed, and the two cortical hemispheres separated so that the hippocampus could be excised. The cortices were placed in a 35 mm dish containing 5 ml HBSS.

2.2.1.2.3 Dissociation and plating of primary neurons

Following dissection of E18 rat embryos, the cortices were cut lengthwise using a sterile scalpel blade several times. They were then transferred to a 50 ml conical tube and washed three times in 30 ml of HBSS. The final wash of HBSS was aspirated and replaced with HBSS containing 0.005 % trypsin-EDTA. The tube was then placed in a water bath and incubated at 37 °C for 15 min with occasional mixing. Following trypsinisation, the trypsin solution was aspirated, and the tissue was washed three times in 30 ml of HBSS. The tissue was then washed a final time in 3 ml plating media. The tissue then was then triturated with a 5 ml serological pipette in 5 ml fresh plating media. After trituration a further 15 ml plating media was added and mixed with a 25 ml serological pipette. To remove remaining debris this was then strained into a new 50 ml conical tube using a 70 µm mesh cell strainer (Greiner Bio-One). To count the dissociated cortical cells they were diluted 1:10 in 0.4 % Trypan Blue solution. This was transferred to a haemocytometer for counting using a dissection microscope. 5×10^5 cells were plated per well in a PDL-coated 6-well dish containing 2 ml plating media per well. The cells were then incubated in a cell incubator overnight before replacing the plating media with 2 ml feeding media (Neurobasal® medium, % HS, 2% B27, 1% Glutamax). At 7 days *in vitro* (DIV7) neurons were fed with 0.5 ml feeding medium supplemented with 1 µM of the antimitotic

fluorodeoxyuridine to inhibit glial growth 0.5 ml of feeding media was then added every seven days.

2.3 Virus production

2.3.1 HEK293T production

All media used in lentiviral plasmid transfection was sterile filtered with a 0.25 µm filter prior to use. Lentiviruses were produced in HEK293T cells grown in conditions described in **Section 2.2.1.1**. 2×10^6 cells were plated in 60 mm cell culture dishes containing 5 ml Complete DMEM and incubated in a cell culture incubator overnight.

2.3.2 HEK293T transfection for the production of lentiviruses

Cells were transfected the next day at 70-90% confluence. The lentiviruses produced are not able to replicate independently so the transfection mix included 1 µg pMD2.G lentiviral packaging vector (Addgene) and 3 µg p8.91 helper vector (Addgene) to permit viral particle assembly. This was added to a 5 ml plastic bijou containing 1 ml of plain DMEM. 4 µg XLG viral vector containing the gene of interest was also added. This was briefly vortexed to mix. 1 µg / µl PEI was added 1 ml plain DMEM to a final concentration of 24 µg / ml in a 15 ml conical tube. This was briefly vortexed and incubated at RT before being transferred to the DNA:DMEM solution. This was vortexed briefly and incubated at RT for 30 min. The media was aspirated from the 60 mm dish of cells and replaced with this transfection mix. The cells were incubated in a cell culture incubator for 4 h. Transfection mix was then aspirated and replaced with 3 ml complete DMEM. Cells were incubated in the cell culture incubator for 48-72 h to allow viral

proteins to be expressed and assembled.

2.3.3 Harvesting of lentivirus

Media containing lentiviruses was transferred from HEK293T cells to a 15 ml conical tube. Cell debris was pelleted by centrifugation at 2000 x g for 10 min. The media was then filtered using a 0.45 µm filter into a fresh 15 ml conical tube. Lentivirus was then stored at 4 °C until needed for up to a week.

2.3.4 Viral transduction of primary neurons

Aliquots of lentivirus suspended in DMEM were stored at 4 °C no longer than seven days. 0.5 ml of the appropriate virus was added to each well of a 6-well plate of cortical neurons at DIV7. Cells were lysed at DIV14 for downstream applications.

2.4 Molecular biology methods

2.4.1 SDS-PAGE

2.4.1.1 Preparation of brain tissue samples

2.4.1.1.1 *Post-mortem* Human Brain tissue

Use of *post-mortem* human brain tissue was approved by the Research Ethics committee and provided by the South West Dementia Brain Bank (SWDBB). 2 g tissue from frontal cortex BA10 area of 60 humans was used (Mean age, 86; Mean Post-mortem delay (PMD), 28.2 h). These were divided equally into three age-matched groups according to their annotated Braak stage which is determined by histopathological analysis of NFT deposition (performed by

SWDBB). The three groups were: Braak stage I-II or Entorhinal (ER) stage AD ; Braak stage III-IV or Limbic (L) system stage; Braak stage V-VI or Neocortical (NC) stage Specification can be found in **Appendix Table 1**. Samples were stored at -80 °C.

2.4.1.1.2 J20 mouse model brain tissue

J20 mouse model mice were obtained from the lab of Professor Jon Brown at the University of Exeter under his Project Licence. NL-F mice were obtained from the lab of Mick Craig at the University of Exeter under his Project Licence. 6 x 6-month old J20 mice and 6 x age-matched controls, and 6 x 18-month old J20 mice and 6 x age-matched controls. Genotyping to confirm disease phenotype was carried out at the University of Exeter.

2.4.1.1.3 Mouse brain dissection

All dissection tools were sterilised with 70 % ethanol in H₂O placed on dry ice before use. Animals were humanely sacrificed by cervical dislocation. The skull was carefully cut open with a sterile scalpel blade and the brain was removed and placed onto a piece of filter paper on a dissection board. The cerebellum, hippocampi and cortices were dissected sequentially and immediately placed on a piece of aluminium foil kept on dry ice to snap freeze. The frozen tissue was then placed in a labelled 0.5 ml microfuge tube that had been pre-cooled in dry ice. The tube was then placed in the dry ice. Filter paper and aluminium foil was changed after each animal to avoid cross contamination of tissue. Once dissection and snap freezing had been completed the box of dry ice was sealed and transported to University of Bristol from Professor Jon Brown's lab at the University of Exeter. Here samples were stored at -80 °C.

2.4.1.1.4 Tissue homogenisation

Post-translational modifications of proteins are less stable than proteins and as these were the focus of this research a method for homogenisation in which thawing of tissue was minimised was chosen. A pestle and mortar were stored overnight at -80 °C. Liquid nitrogen in two dewars, an ice box of dry ice and ice box of wet ice were collected. All tools were kept on dry ice and wiped clean with tissue and sterilised with ethanol prior to use and between samples. 0.5ml microfuge tubes were labelled and pre-cooled on dry ice. Lysis buffer (150 mM NaCl, 50 mM Tris HCl pH7.4, 1 % Triton TX-100, 0.1 % W/V SDS, 1:100 Phosphatase inhibitor Cocktail 1 & 2 (Thermo Scientific) and EDTA-free protease inhibitors (Thermo Scientific)) was pre-cooled on wet ice. Human AD brain samples were processed in batches of 15 samples per day and each 15 was prepared in an alternating order: first an ER sample, then a L sample, then a NC sample and so on. This was to avoid both human or environmental differences that may be introduced by preparing sample groups on different days, or in time-sensitive changes that occur during the preparation process, skewing the results. Similarly, J20 mouse brain tissue was prepared in an alternating order, though all samples from a single brain region and time point could be processed in one batch. For human brain tissue, homogenisation was carried out in a laminar hood and a N95 mask (3M) was worn to protect against inhaling brain tissue. To remove frozen human brain tissue from the tube provided by the SWDBB a spoon was used. Frozen J20 mouse brain tissue was removed from the microfuge and placed on the dissection board coated in aluminium foil and an appropriate amount was cut using a scalpel blade. Remaining frozen

tissue was quickly returned to -80 °C. The tissue removed for homogenisation was placed onto the mortar. Liquid nitrogen was poured onto sample and allowed to boil off. The mortar was moved out of dry ice and onto a work surface only while grinding frozen tissue. The pestle was placed for ~10 sec into liquid nitrogen to cool it before grinding the frozen tissue into a fine powder. This was then transferred to a labelled 1.5 ml microfuge tube. The tube was immediately dropped into the second dewar of liquid nitrogen for temporary storage while other samples were processed. Each sample was retrieved from the liquid nitrogen and 350 µl chilled lysis buffer was added. The sample was then sonicated five times for 2 sec with 5 sec incubation in ice between sonication steps. Once all the samples for that batch had been sonicated they were left on ice for 20 min to allow solubilisation before centrifugation at 4 °C for 20 min at 14,000 x g. The supernatant was removed and placed into new pre-chilled 1.5 ml microfuge and the centrifugation step was repeated. The supernatant was then transferred to a new 1.5 ml microfuge tube and kept on wet ice. 5 µl brain homogenate was taken for protein quantification by Bradford assay. Once protein concentration was quantified, 50 µl was taken from each sample and diluted in the appropriate volume of lysis buffer to a concentration of 1.3 mg/ml. 4 x Laemmli sample buffer (250 mM Tris-HCl, pH 6.8; 40% (v/v) glycerol; 8% SDS; 0.02% bromophenol blue in H₂O) was then added to a ratio of 1:3 and the samples were boiled for 10 min at 95 °C. Samples in Laemmli buffer were stored at -20 °C and remaining brain homogenate was stored at -80 °C.

2.4.1.1.5 Bradford protein assay

Protein concentration of brain tissue homogenate was quantified using a Bradford assay.

Bradford reagent (Bio-Rad) was diluted 1:5 with H₂O. A protein concentration standard was prepared for this by dissolving 1 mg BSA in 1 ml lysis buffer and then using this for a 1:2 serial dilution in lysis buffer. 5 µl of each of the standards and each of the protein samples to be measured was then transferred to separate 1.5 ml microfuge tubes. 990 µl of the diluted Bradford reagent was then quickly added to each of the microfuge tubes. These tubes were then immediately closed and inverted 3 - 5 times to mix. These were incubated at RT for 5 min. This process is time sensitive and therefore no more than 15 tubes were quantified at one time to avoid a significant delay between adding Bradford reagent to the protein standards and samples to be measured. After this 5 min had elapsed the tubes were poured into cuvettes and immediately placed into a spectrophotometer. The absorbance of each sample at 595 nm was measured. A standard curve was calculated using the absorbance values for the BSA protein standards. The absorbance of the sample was then compared to this curve to determine its protein concentration. Where the protein concentrations of the sample fell outside of this linear range the sample was diluted by a suitable factor using lysis buffer and the assay was performed again.

2.4.1.2 Lysis of primary neurons and HEK293T cells

Cells were lysed directly in 1 x Laemmli sample buffer and scraped with a cell scraper before being transferred into a 1.5 ml microfuge tube. This was then boiled for 10 min at 95 °C.

2.4.1.4 SDS-PAGE

Sample lysates were subjected to Sodium Dodecyl Sulphate (SDS)-polyacrylamide gel

electrophoresis (SDS-PAGE) to separate proteins by molecular weight. This was performed using the Bio-Rad Mini-Protean system. 8 - 10 % acrylamide gels were used depending on the molecular weight of key sample proteins to be quantified. Gels were prepared using 1.5 mm glass plates which were filled firstly with acrylamide resolving gel solution (375 mM Tris-HCl pH 8.8, 8 – 10 % acrylamide, 0.1% SDS, 0.1% APS and 0.01% TEMED) to roughly 1.5 cm below the top. 700 µl ethanol was then carefully added to ensure the polymerised gel would be level. Once polymerised (~30 min) the ethanol was removed. The gel was rinsed with H₂O and dried using a piece of filter paper. An acrylamide stacking gel solution (125 mM Tris-HCl pH 6.8, 5 % acrylamide, 0.1 % SDS, 0.1 % APS, 0.01 % TEMED) was then used to fill the remaining space above the resolving gel and a 15- or 10-well comb was inserted depending on the number of samples to be added.

Following polymerisation of the stacking gel (~30 min) the gel was assembled into an electrode and placed into an electrophoresis tank containing SDS-PAGE running buffer (25 mM Tris, 250 mM glycine and 0.1 % SDS in ddH₂O). The tank was topped up with SDS-PAGE running buffer and the comb was removed from the gels. 5 µl molecular weight marker and 10-30 µg (depending on relative abundance or quality of antibody for proteins of interest) of sample lysates in Laemmli sample buffer were loaded into the wells using gel loading tips. The apparatus was connected to a power pack set to 100 V until the protein marker had separated. The voltage was then increased to 150V until the Laemmli sample buffer dye front reached the bottom of the gel.

When SDS-PAGE was completed an Immobilon-PVDF membrane was cut to size and activated in methanol on an agitator for 2 min. Sponges were immersed in transfer buffer (50 mM Tris, 40 mM glycine and 20 % methanol in H₂O) for 5 min. The gel was removed from the electrophoresis tank and submerged in transfer buffer. The plates were separated and the stacking gel removed. The wet transfer cassette was then assembled with the gel laid on top of the PVDF membrane and both sandwiched between filter paper and transfer cassette sponges. The cassette was then placed into an electrode, with the PVDF membrane facing towards the anode. This was then placed into an electrophoresis tank. The ice pack was also placed into the tank which was then filled with transfer buffer. The tank was placed on a magnetic stirrer and connected to a power pack set to 400mA for 70min.

2.4.2 Western Blotting

2.4.2.1 Immunoblotting

Following transfer, the membrane now containing sample proteins was rinsed in PBS-T before blocking for 1 h at RT in 5 % BSA in PBS-T. After blocking, the membrane was incubated with gentle agitation for 1 h at RT or overnight at 4 °C in the appropriate primary antibody at the concentration described in **Table 2.1**. Membranes were then washed three times in PBS-T for 5 min at RT with gentle agitation to remove excess primary antibody. Membranes were then incubated for 1 h in appropriate secondary antibody in 5 % BSA in PBS-T. After incubation in secondary antibody, the membrane was washed three times for 10 min at RT with gentle agitation to remove unbound antibody.

2.4.2.2 Enhanced chemiluminescence detection

To visualise proteins following incubation with primary and secondary antibodies, membranes were incubated for 1 min at RT in one of the following ECL substrates in order of sensitivity with the first being the lowest: SuperSignal® West Pico, Luminata Classico, Luminata Crescendo or SuperSignal® West Femto. Membranes were then placed between two sheets of acetate and closed inside a developing cassette (Amersham). To detect HRP signal the cassette was taken to a dark room where X-ray film was placed inside for varying times (10 sec - 10 min). The X-ray film was then developed using an automatic medical X-ray processor. Where necessary membranes were stripped of antibodies using Restore™ Stripping Buffer (Thermo Scientific) for 10 min at RT followed by five 10 min washes in PBS-T at RT - all with gentle agitation.

2.4.2.3 Immunoblot Quantification and Analysis

X-ray film was scanned and densitometry analysis was performed using the ImageJ (Fiji) Gel Analysis tool. The area under the peak for each band was used to determine its relative pixel intensity. These values were then transferred to Microsoft Excel for normalisation to loading control values. Statistical analysis was performed using Graph Prism. Data are presented as a percentage of control \pm SEM. Significance is presented such that * $p < 0.05$, ** $p < 0.01$, and *** $p < 0.001$.

2.4.2.4 Total Protein Stain

For membranes containing proteins from brain homogenates total protein was

measured to use as a loading control. This was performed using Li-Cor Total Protein Stain (TPS). After transfer membrane was rinsed in H₂O. Excess H₂O was removed by carefully tapping the corner of the membrane on a piece of tissue paper, being careful to avoid contact between the protein containing region of the membrane and the tissue. The membrane was then incubated in TPS for 5 min in the dark at RT with gentle agitation. Revert™ Total Protein Stain Wash Solution was then used to wash the membrane two times for 30 sec with gentle agitation. The membrane was then rinsed in H₂O and placed onto an Odyssey FC detection system tray and inserted into the machine. TPS was detected with a Solid-state Laser Diode at 700 nm excitation for 2 min. Total protein was then quantified as pixel intensity per lane using Image Studio (LI-COR).

2.4.3 Molecular Cloning

2.4.3.1 Polymerase chain reaction (PCR)

For each reaction a PCR mix (1×KOD polymerase buffer containing 1.5 mM MgSO₄, 0.2 mM of each dNTP) was produced. To this 10 ng of template DNA and 1 unit of a high fidelity Hot KOD polymerase) was added. Forward and reverse primers were ordered from Eurofins as oligonucleotides. These were added to a final concentration of 0.3 μM in a final volume of 50 μl. H₂O was added as necessary to make up the volume to 50 μl. This was added to 0.05 ml thin-walled PCR tube and mixed gently by pipetting. This was then placed in a thermocycler and run according to the parameters laid out in **Table 2.2**.

| | |
|--|-------------|
| | Target size |
|--|-------------|

| | < 500 bp | 500 – 1000 bp | 1000 – 3000 bp | > 3000 bp |
|-----------------------|------------------|------------------|------------------|------------------|
| Polymerase activation | 95 °C for 2 min | | | |
| Denaturing | 95 °C for 20 s | | | |
| Annealing | 55 °C for 10 s | | | |
| Extension | 70°C for 10 s/kb | 70°C for 15 s/kb | 70°C for 20 s/kb | 70°C for 25 s/kb |

Table 2.2: Polymerase Chain Reaction parameters for thermocycler.

2.4.3.2 DNA gel electrophoresis

PCR products and vectors were separated by size using gel electrophoresis to check success of cloning and for the presence of degradation. 0.8 % or 1.5 % agarose gels were chosen depending on the size of DNA fragment (0.8% being used for 1000-10,000 bp and 1.5% for >1000 bp). These gels were made using 0.5 µg / ml ethidium bromide to aid in DNA visualisation. 1 µl 6 x DNA loading dye was added to 5 µl DNA sample and run alongside 6 µl 1 kb Hyperladder at 135 V for 15 - 30 min in 0.5 x TAE buffer. DNA bands were visualised using a UV transilluminator.

2.4.3.3 DNA fragment purification

The GeneJET™ Gel Extraction kit was used according to the manufacturer's instructions to extract DNA fragments suspended in PCR mix.

2.4.3.4 Restriction digest

Restriction enzyme digests were performed using 20 units of restriction endonucleases

in NEB buffer. 3 µg of vector plasmid DNA or 50 µl PCR product were added to this. To prevent religation of the vector plasmid 20 units of CIP was added to remove the 5'phosphate groups (Vector plasmid mix only). These were then made up to a final volume of 100 µl using H₂O. These were incubated in 1.5 ml microfuge tubes or 4 h at 37 °C. The resulting digested DNA was then purified.

2.4.3.5 DNA ligation

Following restriction digestion, 5 µl of the linearised DNA fragments was run on an agarose gel. The relative signal of the vector and insert bands was used to estimate the vector:insert molar ratio. The vector and insert were diluted to allow 1 µl of each to be added to a 0.05 µl microfuge tube with a 3:1 insert:vector molar ratio. To this 2 µl T4 ligase solution 1 (Tamara) was added. To control for religation of the vector plasmid a control ligation was set up in parallel in which the insert was replaced with 1 µl H₂O.

2.4.3.6 Transformation of *E. Coli*

Chemically competent DH5α strain *E. coli* were prepared using the Inoue method and were used for cloning. Commercially available chemically competent XL1-Blue *E. coli* were used for producing DNA for use in transfections. Both were stored at -80°C. 50 µl aliquots of competent *E. coli* were thawed on ice. A volume of plasmid construct containing 10-100 ng of DNA but no more than 10 % of the final volume was added to 10-50 µl of competent cells. The tube was flicked 1 - 3 times to mix and then incubated on ice for 20 or 30 min for XL1-Blue and DH5α cells respectively. They were then heat-shocked in a water bath at 42 °C for 45 sec or 130

sec for XL1-Blue and DH5 α cells respectively and immediately placed back in ice for 2 min. 200 μ l LB broth was added and the cells were incubated at 37 °C for 1 h. 20 μ l of this was then spread on an LB agar plate containing the antibiotic for which the plasmid conferred resistance. The agar plate was then incubated overnight at 37 °C.

2.4.3.7 Plasmid DNA amplification and purification

A miniprep produces 50 μ l 50-300 ng/ μ l DNA in H₂O and was used to screen for successful cloning. A midiprep produces 350 μ l 500-1500 ng/ μ l DNA in H₂O and was used to amplify DNA for use in transfection. Bacterial colonies on agar plates were selected for amplification and picked using a 200 μ l pipette tip, then cultured in LB broth containing the appropriate antibiotic overnight at 37 °C in a shaking incubator. For minipreps 3 ml LB broth was used in a 15 ml conical tube. For midipreps 100 ml of LB broth in a 500 ml glass conical flask was used. GeneJET™ Plasmid Miniprep Kit and the GeneJET™ Plasmid Midiprep Kit were used according to the manufacturer's instructions. To quantify DNA yield the NanoDrop NanoDrop™ Spectrophotometer (Thermo Fisher) was used to measure absorbance at 260 nm and 280 nm and NanoDrop 1000 software was used to automatically calculate ratio for yield and purity.

2.4.3.8 Phenol chloroform precipitation

An equal volume of 25:24:1 Phenol:chloroform:isoamyl was added to the DNA sample. This was centrifuged for 5 min at 16,000 \times g at RT. The upper aqueous phase was transferred to a fresh 1.5 ml microfuge tube. 2.5 x volume of ethanol and a 0.5 x volume of 7.5M ammonium acetate was added to the reserved upper phase. This was then incubated overnight

at -20°C or for 1 h at -80°C to precipitate the DNA. The sample was then centrifuged for 30 min at $16,000 \times g$ at 4°C to pellet the DNA. The supernatant was discarded. 150 μL of 70 % ethanol in H_2O was added and DNA was resuspended by pipetting up and down using a 200 μL pipette tip. The sample was then centrifuged for 2 min at $16,000 \times g$ at 4°C . The supernatant was discarded. The ethanol wash step was repeated once more. The pellet was allowed to air dry at room temperature for 5 – 10 min in laminar flow hood. The pellet was then resuspended in 200 μL of H_2O by pipetting up and down.

2.4.3.9 Extraction of RNA from Rat brain tissue

Rat brain tissue was obtained by dissecting the brain of the dam sacrificed for the production of embryonic primary neuronal cultures described in **Section 2.2.1.2**. The brain was removed, transferred to a 50 ml conical tube and stored at -80°C . RNaseZap RNase Decontamination solution (Invitrogen) was used to remove RNase contamination from work surface prior to RNA extraction. RNA extraction was performed in laminar flow hood. Aseptic technique was also used to reduce RNase contamination. The frozen brain tissue was removed from the conical tube and placed on a dissection board covered with aluminium foil. A sterile scalpel blade was used to remove 50-100 μg of tissue which was transferred to a 1.5 ml microfuge tube. 1 ml TRIzol Reagent (Invitrogen) was added to the tube and the tissue was homogenised using a disposable pestle. This was then incubated for 5 min at RT to allow dissociation of nucleoprotein complexes. 0.2 ml of chloroform was then added. This was incubated for 3 min before centrifuging for 15 min at $12,000 \times g$ at 4°C . The result of this phase separation leads to a colourless aqueous upper phase, an interphase and red phenol-

chloroform lower phase. The RNA-containing aqueous phase was carefully removed with a 200 µl pipette tip and transferred to a new 1.5 ml microfuge tube. 0.5 ml of isopropanol was added to this and incubated for 10 min. This was then centrifuged for 10 min at 12,000 x g at 4 °C to pellet RNA. The supernatant was discarded. The RNA pellet was resuspended in 75% ethanol in RNase-free H₂O. by pipetting up and down. The RNA sample was then briefly vortexed before centrifuging for 5 min at 7500 x g at 4 °C. The supernatant was discarded and the RNA pellet was allowed to air dry in a laminar flow hood for 10min. The pellet was then resuspended in 50 µl RNase-free water. RNA yield was quantified using the NanoDrop™ Spectrophotometer (ThermoFisher) and NanoDrop 1000 software to measure light absorption at 260 nm and 280 nm and to calculate the A260/A280 ratio.

2.4.3.10 First strand cDNA synthesis

cDNA synthesis was performed using the RevertAid First Strand cDNA synthesis kit (Thermo Fisher). All reagents were stored -80 °C. After thawing they were mixed by pipetting up and down then briefly centrifuged and kept on ice while in use. RNaseZap RNase Decontamination solution (Invitrogen) was used to remove RNase contamination from work surface prior to cDNA synthesis. Aseptic technique was also used to reduce RNase contamination. 5 µg template RNA was added to a 1.5 ml microfuge. To this 1 µl supplied Random Hexamer primer and an appropriate volume of nuclease-free water to make up a total volume of 12 µl. To this the following was added in this order: 4 µl 5 x Reaction Buffer, 20 units RiboLock RNase Inhibitor, 10 µl 10 mM dNTP mix and finally 1 µl / 200 units RevertAid M-MuLV Reverse Transcriptase. This was pipetted up and down with a 200ul pipette to mix and then

briefly centrifuged before incubating for 5 min at RT. The sample tube was then placed in a heat block for 1 h at 42 °C. The reaction was terminated by heating at 70 °C for 5 min. PCR amplification of first strand performed as described in **Section 2.4.3.1** using 2 µl of the first strand cDNA synthesis reaction mixture. A control was also used in which the cDNA mixture was replaced with H₂O.

Chapter 3: Investigating Argonaute phosphorylation and LimK in a primary neuronal culture AD model

3.1 Introduction

3.1.1 A β causes synaptic dysfunction and loss in AD and its models

Decades of intensive research has revealed many pathological changes that occur in AD and contribute to its progression and symptoms including mitochondrial dysfunction, excessive microglial activation and inflammation, synaptic signalling dysfunction, synaptic and neuritic injury and of course the formation of the pathological hallmarks of AD - increased A β production and accumulation, and tau hyperphosphorylation and NFT formation (Hardy & Selkoe, 2002). Despite this, the hurdle of identifying the chronology and interconnectivity of these many complicated changes remains to be surmounted. It is, however, known that a decrease in hippocampal and fronto-cortical synapses precedes symptom onset and even detectable NFT and plaque formation (Selkoe, 2002). Prior to the presence of amyloid plaques A β begins to aggregate into soluble intermediary assemblies - A β oligomers (A β O) (Ferrone *et al.*, 1990).

The most abundant APP peptide species in AD brains are the A β sequences comprised of 40 or 42 amino acids (A β 40 and A β 42 respectively) (Millucci *et al.*, 2010; Pike *et al.*, 1993). Indeed, both endogenous and synthetic forms of these peptides have been shown to self-assemble in aqueous medium to form higher order aggregates such as A β O (Nag *et al.*, 2011). High resolution imaging has revealed that A β O are present within individual spines of AD patients and AD animal models (Koffie *et al.*, 2009, 2012; Pickett *et al.*, 2016). Furthermore, they have been shown to interact with numerous synaptic receptors including EphrinB2, NgR1, cellular prion protein (PrPc) (Um *et al.*, 2012), neuroligins (Dinamarca *et al.*, 2011), insulin receptors (Zhao & Townsend, 2009), and ionotropic and metabotropic glutamate receptors (De

Felice et al., 2007; Um et al., 2013). Extensive study into the relative toxicity of different A β species has indicated that these A β O represent the most toxic (Izzo et al., 2014; Vargas et al., 2014; Lee et al., 2017). They have been correlated with impairment of synaptic plasticity and spine loss in the AD brain and both animal and cellular models of AD (Lue et al., 1999; Calabrese et al., 2007; Lacor et al., 2007; Shankar et al., 2008; Bao et al., 2012; Koffie et al., 2012; Lourenco et al., 2013; Arbel-Ornath et al., 2017; Wang et al., 2017; Batista et al., 2018). The effect of A β O is very potent and rapid, with application of physiological concentrations of A β O *in vitro* leading to down-regulation of synaptic proteins crucial for learning and memory occurring within hours and higher concentrations to neuronal death (Calabrese et al., 2007; Lacor et al., 2007; Wang et al., 2017). A β O have also been shown to inhibit LTP and promote LTD - a factor which may contribute to spine shrinkage and loss (Zhou et al., 2004; Jo et al., 2011; Vargas et al., 2014). One mechanism for enacting this is by reducing pre-synaptic transmitter release (Branco & Staras, 2009). They have also been shown to bind to and activate NMDARs, causing intracellular and synaptic dysregulation (De Felice et al., 2007; Decker et al., 2010). It has been suggested that the cascade of dysregulation initiated by the accumulation of A β O may produce a positive feedback loop in which neuronal dysfunction leads to increase in production of A β and therefore an increase in A β O formation and so on (Tabner et al., 2005; Ferreira et al., 2014). Synaptic loss is correlated with reduced cognitive function and disease progression in AD and with it being the earliest structural change and concurrent with A β O accumulation, researchers have laboured to find the precise mechanism through which these may be related (Terry et al., 1991; Selkoe, 2002). However, this mechanism remains elusive.

3.1.2 Methods for modelling A β accumulation *in vitro*

Cell culture models represent the simplest model systems and as such are incredibly valuable in unpicking disease-related changes at the molecular level. Proof of concept in a cell-based system serves as the basic starting point of any translational pipeline. A method for culturing primary neurons was first developed by [Banker & Cowan \(1977\)](#) who isolated neuronal cells from rat embryos at 18- or 19-days (E18/19). These cultures are relatively pure, containing very few glial cells. This technique has since become the one of the most popular methods for *in vitro* AD modelling and has provided substantial data to inform our current understanding of mechanisms that underlie the disease ([Kaeche & Banker, 2006](#); [Fontana *et al.*, 2020](#)).

In some studies, synthetically or endogenously derived A β peptides or oligomers are applied to neuronal cultures to model conditions found in early AD pathology ([Fontana *et al.*, 2020](#)).

However, this method can present problems due to the propensity of A β to self-aggregate into various higher order structures and therefore the form of A β can be difficult to control for ([Vadukul *et al.*, 2021](#)). Furthermore, although A β plaques are extracellular, A β peptides of course originate in the cell and as such are subjected to and affect various subcellular processes before being excreted from the cell to form extracellular plaques ([O'Brien & Wong, 2011](#)).

Application of A β peptides to neuronal cultures is a method that is able to reproduce aspects of the end point of A β -related pathology but is arguably less physiologically representative of A β production, secretion and oligomerisation.

In modelling neurological disease, expression of key proteins can be induced in a multiplicity of

ways to better simulate disease conditions (Karra & Dahm, 2010). A β production can be increased through over expression of WT APP (Kamenetz *et al.*, 2003). However, APP overexpression may produce artefacts due to the effects of overexpression on the function of APP and other APP-derived non-amyloidogenic peptides (Saito *et al.*, 2014). Various methods are employed in AD models to try to circumvent this problem. One potential solution is to compare the effect of over expression of WT APP to equivalent expression of an APP mutant with a mutation at the β -secretase site which selectively eliminates production of the amyloidogenic 42- and 40-aa peptides (Citron *et al.*, 1995). However, although this allows isolation of the effect of these particular peptides it of course does not eliminate the overexpression of other APP-derived peptides and the downstream effects of their increased expression. Another is to express APP in which mutations known to increase production of these peptides are present. This rationale was used in producing the NLGF mouse model in which hAPP is expressed at endogenous levels but the presence of three mutations (Swedish “NL”, the Iberian “F”, and the Arctic “G” mutations) A β production (Swedish), increase the ratio of the 42-aa peptide relative to 40-aa peptide (Iberian mutation) and finally increase the propensity of A β to aggregate, thereby reducing its proteolytic degradation (Arctic mutation) (Kamino *et al.*, 1992; Mullan *et al.*, 1992; Guerreiro *et al.*, 2010). Similar to the related NL-F mouse model, in the NLGF model amyloid plaques are produced and a loss of synapses is seen, however this pathology is accelerated (Saito *et al.*, 2014).

Excessive shrinkage and loss of dendritic spines housing synapses is a key characteristic of the pathology of AD but is also seen as a part of healthy brain function through the process of LTD,

an important component of synaptic plasticity (Zhou *et al.*, 2004). Rajgor *et al.* (2018) identified phosphorylation of AGO2 at S387 and miR-134 induced down-regulation of LIMK1 as important in LTD-related spine shrinkage in primary neuronal cultures. Furthermore, data from preliminary experiments in primary neuronal cultures indicated that this LTD mechanism may be aberrantly activated in AD pathology. When APP was overexpressed an increase in pS387-AGO2 was seen, concurrent with an increase in association between AGO2 and the RISC scaffold protein GW182 and an increase in miR134 activity.

3.1.3 Aim

The aim for this section of my PhD was to produce a primary neuronal culture AD model in which changes to pS387-AGO2 and miR-134 activity found to be activated in pilot experiments could be reproduced and potentially rescued.

3.2 Results

3.2.1 Primary neuronal culture amyloidopathy model

Determining the efficacy of dampening AGO2 activity in protecting against spine shrinkage in AD necessitates a model for A β induced spine shrinkage. Initially, I attempted to reproduce the model used in preliminary experiments from the lab that supported the hypothesis that pS387-AGO2 related changes occur in AD. These pilot experiments were performed using a model in which primary neuronal cultures were transfected with either GFP, myc-tagged WT APP, or myc-tagged APP in which a mutation (M671V) at the BACE cleavage site prevents production of the amyloidogenic APP fragment species.

However, in order to visualise spines this method would involve co-transfection of primary neuronal cultures with a plasmid expressing these APP genes and also a plasmid to express a fluorescent protein as a morphological marker such as mRuby or mCherry. I found that cell viability was prohibitively low following neuronal transfection with lipofectamine (L2K) (data not shown).

In neurons, transfection efficiency of a transfection agent like lipofectamine is relatively low, but high for lentiviruses, which are retroviruses also capable of transducing non-mitotic cells (Karra & Dahm, 2010). Furthermore, I found lentiviral transduction to be a much better tolerated method for introducing DNA to primary neuronal cultures. Therefore, an alternative model was designed in which primary neuronal cultures were first transduced with lentiviruses expressing endogenous APP-directed shRNA bi-cistronically with a GFP reporter and shRNA-resistant C-terminally myc-tagged APP that was either WT, contained the Swedish mutation (Mullan *et al.*, 1992) or the NLGF triple mutation (Saito *et al.*, 2014) (referred to hereafter as WT APP, SweAPP and NLGF APP viruses respectively) or a scrambled shRNA sequence bicistronically with a GFP reporter as a control. In this system, endogenous APP is knocked down via the APP-directed shRNA and this is then replaced with myc-tagged APP such that the effect of these mutations could be isolated and observed. The lentiviral plasmids used to produce these were kindly donated by Dr Kevin Wilkinson.

3.2.2 miRNA activity assay

In the previous model the Promega Dual Luciferase Reporter Assay System was used to quantify changes in specific miRNA activity levels. This assay involves co-transfection with two luciferase constructs - one expressing firefly luciferase conjugated to a regulatory element of interest and another expressing *Renilla* luciferase which acts as a control for transfection efficiency. In this case the regulatory element used was the 3' UTR of LIMK1 mRNA in which the miR-134 seed sequence was either intact or mutated to act as a control. Following transfection with the luciferase constructs, changes in expressed luciferase bioluminescence following application of the luciferase substrate can be measured by a luminometer and used to infer changes in specific miRNA activity in different conditions.

However, this protocol also involves transfection. To circumvent potential issues with cell viability following transfection I designed an assay to quantify miRNA activity levels by Western blot also using lentiviruses as a vector rather than a lipofectamine transfection. My aim was to produce an assay using lentiviral transduction in which changes in expression of a fluorescent reporter due to changes in activity of a specific miRNA could be measured by Western blot. Unlike in primary neurons, in HEK293T cells lipofectamine transfection efficiency is very high and transfection protocols are well tolerated. I therefore chose to use direct transfection of HEK293T cells to streamline testing of this concept before moving forward.

The cloning vector that I chose to use was pEGFP with some alterations. Firstly, in this vector the EGFP sequence has been replaced with an mCherry sequence. This is because future experiments using this primary neuronal culture AD model will involve rescue strategies using

lentiviruses expressing GFP-tagged mutant AGO2. Additionally, the MScI site usually present in mCherry has been removed for ease of downstream cloning.

A potential stumbling block in the production of this assay is the stability of fluorescent proteins which are typically ~24 h (Li *et al.*, 1998). This stability facilitates accumulation and detection in cells, however, this property limits their use in applications that require high reporter turnover where changes in expression may be difficult to detect in the background of accumulated protein. Regions rich in proline (P), glutamic acid (E), serine (S), and threonine (T) are termed PEST sequences and are associated with increased protein turnover (Li *et al.*, 1998). This feature can be utilised to increase the turnover of a protein to allow for detection of changes in expression over a smaller timescale (Li *et al.*, 1998). I extracted RNA from rat brain tissue and used this to synthesise cDNA. I used this to amplify the PEST sequence from rat ornithine decarboxylase, adding a XhoI site to the 5' end (forward) and an EcoRI site to the 3' end (reverse) so that I could digest and ligate this to the 3' end of the mCherry sequence **Figure 3.1**. This destabilised mCherry plasmid served as my control. I then used PCR to amplify the LIMK1 3' UTR region containing the miR-134 seed sequence from luciferase constructs first used in and kindly donated to the lab by the Schratt lab who first reported a role of miR-134 in LIMK1 mRNA signalling (Schratt *et al.*, 2006). I designed primers for this amplification such that there was an EcoRI restriction site on the 5' end and a SalI restriction site on the 3' end. I was then able to digest and ligate this to the 3' end of the PEST sequence **Figure 3.1**.

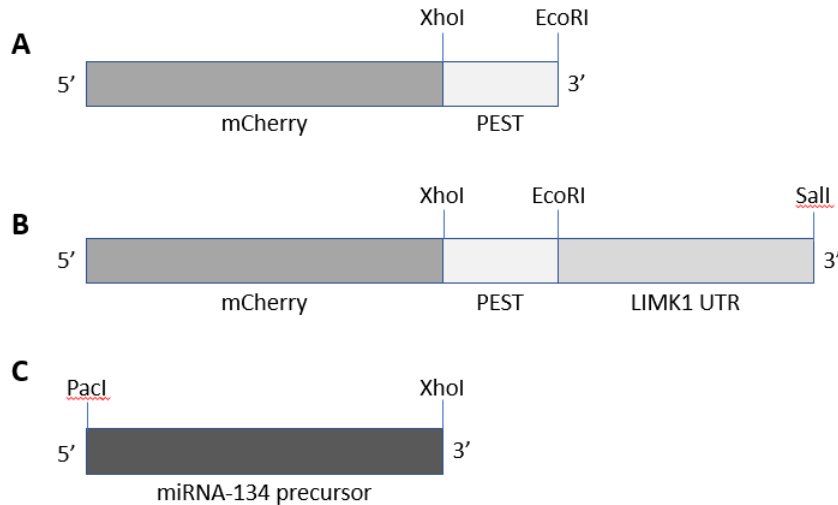


Figure 3.1 Diagrammatic representation of recombinant genes created (A) control construct in which the PEST sequence of rat ornithine decarboxylase (ODC) was amplified with XhoI (at 5' end) and EcoRI (at 3' end) a (B) as (A) but conjugated to the LIMK1 3' UTR sequence with a Sall site at the 3' end, and (C) miR-134 precursor amplified with a PacI site (at 5' end) and XhoI site (at 3' end). The backbone vector was pEGFP in which GFP had been replaced with mCherry.

The 3' UTR of mRNA is an important site for regulation by many different regulatory mechanisms ([Mayr, 2019](#)). To determine whether changes in expression specific to miR-134 activity are able to produce a detectable change in mCherry expression when it is fused to the LIMK1 3'UTR I concurrently overexpressed the miR134 precursor by co-transfecting with a separate plasmid ([Schratt *et al.*, 2006](#); [Olde Loohuis *et al.*; 2015](#)). To produce this cDNA extracted from rat brain tissue was used to amplify the miR134 precursor with a PacI restriction site on the 5' end and a XhoI restriction site on the 3' end (**Figure 3.1**). This allowed me to digest and ligate the insert into a pcDNA3.1 backbone.

I transfected HEK293 cells with the Cherry.PEST (\pm LIMK1 UTR) constructs with/without the miR-134 precursor plasmid to artificially increase miR-134 levels ([Olde Loohuis *et al.*, 2015](#)). 48 h

after transfection I lysed the cells in denaturing conditions and performed a western blot using these lysates to determine whether an increase in miR-134 activity induced by expression of the miR-134 precursor could be detected via a decrease in expression of mCherry when it is fused to the LIMK1 3'UTR.

3.2.3 mCherry.PEST protein expression is decreased when conjugated to LIMK1 3'UTR and miR-134 precursor is overexpressed

mCherry.PEST expression was not significantly reduced by co-expression of pre-miR-134 when LIMK1 3' UTR was not present (**Figure 3.2**). However, when mCherry.PEST was conjugated to the LIMK1 3' UTR mCherry expression decreased by 68% (± 15.11 , $n = 4$ $P < 0.001$) when co-expressed with pre-miR-134 compared to expression alone (**Figure 3.2**).

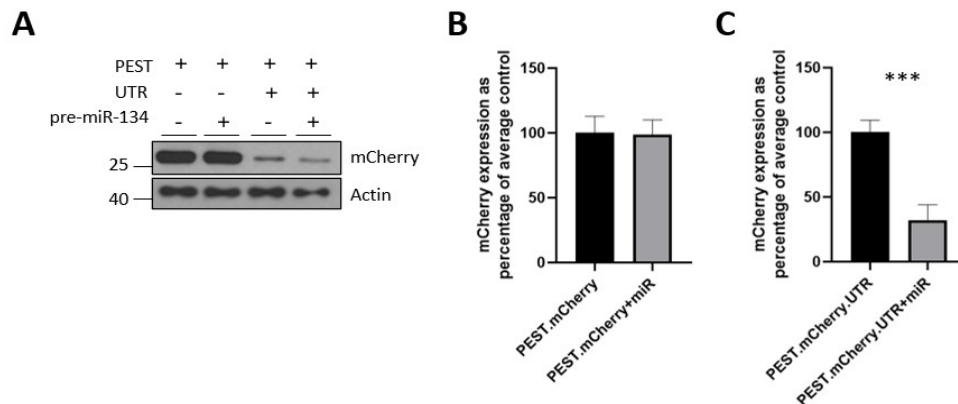


Figure 3.2: Expression of mCherry conjugated to a PEST sequence and the 3' UTR of LIMK1 is down-regulated by co-expression of pre-miR-134. (A) Western blots showing the expression of mCherry and actin in HEK293T cells transfected with plasmids expressing mCherry conjugated to a PEST sequence, and also with or without the 3' UTR of LIMK1, with and without expression of pre-miR-134. (B) Quantification of mCherry.PEST expression with co-expression of pre-miR-134 expressed as percentage of average control ($n = 4$; error bars, s.e.m). (C) Quantification of mCherry.PEST expression when conjugated to 3'UTR of LIMK1 with co-expression of pre-miR-134 expressed as percentage of average control ($n = 4$; *** $p < 0.001$, Student t -test; error bars, s.e.m). Expression bands were normalised to corresponding actin expression band.

Concurrently, the lentivirus-induced cellular amyloidopathy model was characterised - the first step being to determine whether changes seen in the previous model were able to be reproduced. Primary neuronal cultures were transduced with the lentiviruses described above at DIV7 and lysed in denaturing conditions at DIV14. Cell lysates were subjected to Western blot and the resulting blots were probed with antibodies raised against APP and myc to determine transduction efficacy. They were also probed with antibodies raised against LIMK1, AGO2, and pS387-AGO2 to investigate whether changes seen in the previous model were able to be reproduced.

APP was knocked down 91% ($n = 3$, $p = 0.02$) by the shAPP and APP was replaced with myc-tagged sh-resistant APP to levels that were not significantly different to the scrambled shRNA control in all cases (**Figure 3.3 B**). Of the myc-tagged APP mutants myc expression was significantly decreased in the NLGF APP lentivirus transduced cells by 24% ($n = 3$, $P = 0.03$) relative to the WT APP control (**Figure 3.3 C**). However, LIMK1, AGO2, and pS387-Ago2 levels did not significantly change in any condition relative to the control (**Figure 3.3 D, E, F, G**).

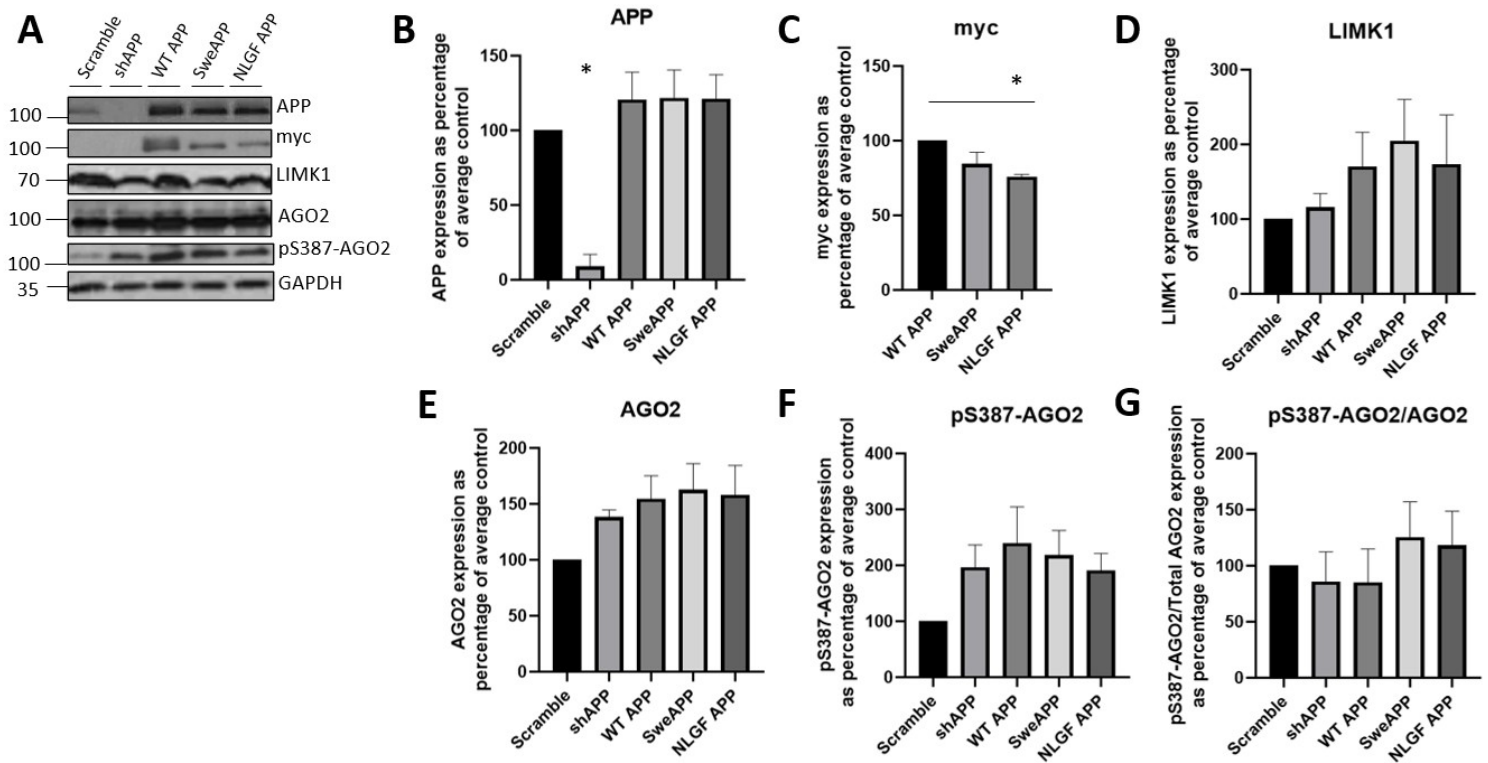


Figure 3.3: Lentiviral expression of myc-tagged APP with EOAD-associated mutations in primary neuronal cultures does not lead to changes in pS387-AGO2 or LIMK1 expression. (Normalised to actin and expressed as percentage of average control) (A) Western blots showing expression levels of key proteins in primary neurons transduced with lentiviruses expressing myc-tagged APP with EOAD-associated mutations. (B) Quantification of APP in primary neurons transduced with lentiviruses expressing myc-tagged APP with EOAD-associated mutations ($n = 3$; $*p = 0.02$, One-way ANOVA, Bonferroni multiple comparisons test; error bars, s.e.m.). (C) Quantification of myc in primary neurons transduced with lentiviruses expressing myc-tagged APP with EOAD-associated mutations ($n = 5$; $*p = 0.03$, One-way ANOVA, Bonferroni multiple comparisons test; error bars, s.e.m.). (D) Quantification of LIMK1 in primary neurons transduced with lentiviruses expressing myc-tagged APP with EOAD-associated mutations ($n = 5$; error bars, s.e.m.). (E) Quantification of AGO2 in primary neurons transduced with lentiviruses expressing myc-tagged APP with EOAD-associated mutations ($n = 5$; error bars, s.e.m.). (F) Quantification of pS387-AGO2 in primary neurons transduced with lentiviruses expressing myc-tagged APP with EOAD-associated mutations ($n = 5$; error bars, s.e.m.). (G) Quantification of pS387-AGO2/AGO2 in primary neurons transduced with lentiviruses expressing myc-tagged APP with EOAD-associated mutations ($n = 5$; error bars, s.e.m.). All expression bands were normalised to corresponding GAPDH expression band and data are presented as percentage of average scrambled shRNA control.

3.3 Discussion

3.3.1 Primary neuronal culture amyloidopathy model

The method for simulating early AD-related amyloidopathy used in this study did not reproduce the effects on LIMK1 expression or pS387-AGO2 seen in preliminary experiments using an alternative method in which APP was overexpressed. It is of note that spine loss is less dramatic in transgenic mouse models of amyloidosis *in vivo* relative to loss following bath application of A β in *ex vivo* preparations which has been suggested to be due to compensatory mechanisms that are able to alleviate effects when the build up is slow (Subramanian *et al.*, 2020). Similarly, in this model APP levels are not significantly different from the control and therefore the emergence of a disease phenotype depends on the gradual accumulation of A β caused by the APP mutations present. Compensatory mechanisms may therefore be able to be activated sufficiently to reduce the toxic effect of changes in A β production. Unlike in this primary neuronal model, however, in model animals these proposed compensatory mechanisms are unable to prevent the production of a disease phenotype. This may be because although the APP mutations used are known to increase levels of A β 40 and A β 42 APP cleavage products and to lead to cognitive abnormalities and A β plaque formation in animal models and in human AD, these pathologies occur over the scale of a lifetime rather than the short few weeks during which primary neuronal cultures are used for experiments (Kamino *et al.*, 1992; Mullan *et al.*, 1992; Guerreiro *et al.*, 2010). It is important therefore to determine whether these changes accumulate sufficiently during this period to induce AD-like changes so that this may be used as a model. Future characterisation and development of this method could involve quantification of A β over time as has been achieved through mass spectrometry analysis of A β

species in induced pluripotent stem cell (iPSC) models of the brain in health and disease (Arber *et al.*, 2021). Furthermore, the method use for lentiviral production did not allow for quantification of viral titre, and as such, variable MOI may have influenced results.

A further confounding factor may lie in the simplicity of the system. Although having neuronal cultures containing very few glial cells can be useful in isolating neuron specific effects, many AD-related pathologies have been linked to glia. Glia play a crucial role in forming synapses and in their function and capacity to adapt to different conditions (Allen & Barres, 2009). Historically neurons have been the focus of AD pathophysiology but in more recent years research has demonstrated the importance of glial cells in this process (Whitehouse *et al.*, 1982; Hansen *et al.*, 2018; Carter *et al.*, 2019). Particularly given that certain alleles of the Triggering receptor expressed on myeloid cells 2 (TREM2) and Myeloid cell surface antigen CD33 (CD33) genes confer some of the highest risk in LOAD it is likely that glial cells are key players in AD pathology (Bertram *et al.*, 2008; Guerreiro *et al.*, 2013; Jonsson *et al.*, 2013; Parhizkar *et al.*, 2019). Their reduced presence in this system may reduce the effect of A β , particularly of the neuroinflammatory immune cells, microglia. In examining the role of cofilin regulation in AD it is of note that microglia isolated from APP/PS1:cofilin+/-mice have been shown to be more efficient at clearing A β (Liu *et al.*, 2019). This underlines the importance of glial cells in AD and therefore in AD research. A system in which they are present could be crucial to understanding the impact of dysregulation in the LIMK1:cofilin pathway.

Another aspect of brain physiology that is not able to be modelled in this way is its 3D structure.

Particularly where manipulations of 2D cell culture systems such as transfection involve partial changing of media as this will also remove secreted A β , impeding oligomerisation. Furthermore, should glial cells be present, a 2D structure such as a culture system does not permit interactions between different cell types to the same degree as the 3D structure of *in vivo* tissue (D'Avanzo *et al.*, 2015). To overcome these limitations 3D systems have been developed such as matrix-embedded cells (Choi *et al.*, 2014; Papadimitriou *et al.*, 2018) or scaffold-free self-organising structures such as neurospheroids and organoids (Lancaster *et al.*, 2013; Yoon *et al.*, 2019). 3D cellular models of AD have been shown to recapitulate both core AD biomarkers (A β plaques and NFTs) and used to test rescue strategies for the associated pathological changes (Choi *et al.*, 2014; Papadimitriou *et al.*, 2018). This may indicate that, particularly in modelling diseases characterised by extracellular aggregation, 3D models are better able to represent physiological conditions and as such may be a more useful system to consider moving forward.

3.3.2 Lentivirus based miRNA activity assay proof of concept

In addition to producing a model of cellular changes in AD I also aimed to design and test an assay which was able to detect changes in specific miRNA activity without the use of transfection of neuronal cultures with lipofectamine. It is important to have baseline cell health to be uncompromised in your control condition in order to make meaningful comparisons with other experimental conditions, however, when cells are being used for the imaging of dendritic spines the importance of maintaining cell health is particularly key as spines are very sensitive to cellular stress (Penzes *et al.*, 2011). Despite extensive attempts at protocol optimisation the use of lipofectamine as a transfection reagent proved prohibitively stressful for reliable imaging

of spines even in control conditions. Furthermore, should I have achieved an optimised protocol in which cells were suitably unstressed after one round of lipofectamine transfection, in projected future experiments they would potentially need to undergo further rounds to test whether the effects of A β could be rescued by knockdown of endogenous AGO2 and expression of phospho-null mutant AGO2.

The gene delivery efficiency of lentiviral transduction is 10-30 fold higher than lipofectamine transfection and in my experiments did not noticeably affect cell viability ([Karra & Dahm, 2010](#)). This made lentiviral transduction an attractive candidate for this assay. Proof of concept was demonstrated in HEK293T cells in which overexpression of pre-miR-134 lead to a 68 % (\pm 15.11, n = 4 P<0.001) decrease in mCherry.PEST expression. This result is promising, however, there are a number of factors to consider before moving forward.

Although increased miR-134 activity and targeting of the LIMK1 3' UTR for translational down-regulation is likely to be the cause of the down-regulation of mCherry.PEST when miR-134 precursor is overexpressed it is possible that this may be due to an alternative mechanism. miRNAs participate in complex networks of regulation such that activity of one can affect the activity of another ([Ghibaudi *et al.*, 2017](#)). To rule out an indirect effect by other regulatory elements when pre-miR-134 is expressed a plasmid construct should be produced in which the miR-134 seed sequence is mutated so that miR-134 is unable to bind. If the down-regulation seen is due to increased miR-134 activity mutation of this seed sequence should eliminate the effect.

Another important future experiment will be a comparison between mCherry expression with and without the ODC PEST sequence. Should it be the case that overexpression of pre-miR-134 leads to an increase in miR-134 activity that far exceeds changes that occur in physiological conditions the assay may be insufficiently sensitive to detect them. An important component of the assay's sensitivity is the vulnerability of mCherry.PEST to changes in expression so optimising this will be crucial.

Another area for optimisation is the 3' UTR region of the mCherry.PEST.UTR construct. The 3' UTR region of mRNA is an important coordinator of extensive post-transcriptional regulation ([Mayr, 2019](#)). Therefore, to eliminate confounding off target effects it may prove prudent to reduce the size of the regions flanking the miRNA seed sequence. However, the 3' UTR can be important for regulating mRNA localisation ([Martin & Ephrussi, 2009](#); [Macdonad & Struhl, 1988](#)). For example, in neurons dendritic targeting of BDNF and CamKII mRNA has been shown to be dependent on their 3'UTR ([An *et al.*, 2008](#); [Miller *et al.*, 2002](#)). They also contain *cis*-elements to which *trans*-acting RBPs bind ([Chen *et al.*, 2001](#); [Brennan & Steitz, 2001](#); [Barreau *et al.*, 2005](#)). Therefore, there may be RBP interactions that facilitate site recognition. Should elimination of the flanking regions prevent effective miRNA activity-mediated down-regulation of the fluorescent reporter protein at the synapse they could be reduced in a stepwise fashion to determine the minimum sequence necessary to retain efficient miRNA binding.

Once these factors have been considered the next steps in the development of this assay will be

to transfer the constructs into a lentiviral vector such as XLG. This can then be used to produce lentiviruses for use in primary neuronal cultures. This system has the advantage of an established method for inducing a physiological increase in miR-134 activity through cLTD with which to test the sensitivity of the assay ([Rajgor *et al.*, 2018](#)).

3.3.3 Conclusions

In summary, lentivirus induced expression of EOAD-linked mutant APP alleles to endogenous levels in primary neurons was insufficient to reproduce the changes to AGO2 phosphorylation and LIMK1 expression seen in the model used in pilot experiments. It is unclear whether this is because this model is insufficient to produce AD-like pathology or whether the pilot data was anomalous to the APP overexpression model used. Going forward immunoprecipitation and quantification of excreted A β in this model may shed light on this.

Significant down-regulation of mCherry expression in HEK cells transfected with the plasmid components of the miRNA assay system described here suggests this may be a viable technique for use in neurons. The next steps with this project will be to transfer the constructs into a lentiviral plasmid backbone such as XLG. The assay can then be tested in neurons by transducing them with lentiviruses produced using these constructs.

Chapter 4: Investigating Argonaute phosphorylation and LimK expression in the J20 mouse model

4.1 Introduction

4.1.1 Animal models of AD are generated using EOAD-associated mutations of APP-related genes

Genetically, AD patients fall broadly into one of two categories. The first of these is that of sporadic late-onset AD (LOAD) which is influenced by common gene variants which only modestly increase AD risk individually ([Lambert *et al.*, 2013](#)). [Ballenguez *et al.*, 2022](#) performed a two-stage genome-wide association study comparing AD patients, people identified as having parents with AD (AD-by-proxy) who had not yet developed AD, and controls (111,326 cases, 677,366 controls). Their analysis identified 75 risk loci and implicated ~250 genes in AD risk. These genes represent a range of different functional roles including immune- and lipid-related processes, and in the degradation of APP proteins. This demonstrates the complex aetiology of sporadic LOAD. The second category is that of familial early-onset AD (EOAD) caused by rare but highly penetrant variants of either APP or presenilin1 or 2 ([Cacace *et al.*, 2016](#)). The latter form the catalytic subunit of γ -secretase - the secretase responsible for producing the APP-derived 40- and 42 aa peptides found to form the A β plaques characteristic of AD ([Jarrett *et al.*, 1993](#)). The discovery of these disease-associated mutations led to the development of the amyloid hypothesis which implicates APP cleavage products in AD's aetiology ([Hardy & Selkoe, 2002](#)). Consequently, these mutations have been utilised extensively to generate animal models of AD pathology.

[Mucke and colleagues](#) generated the J20 (PDGF-APPSw,Ind) mouse model in 2000 by expressing human APP (hAPP) carrying the FAD-linked double mutation KM->NL (Swedish)

(Mullan *et al.*, 1992) and the V717F mutation (Indiana) (Murrell *et al.*, 1991) driven by the platelet-derived growth factor β chain promoter for neuron-specific expression (Sasahara *et al.*, 1991). The insertion site has been mapped to chromosome 16, within the first intron of the Zinc Finger And BTB Domain Containing 20 (ZBTB20) gene (Fisher *et al.*, 2017). Despite decreased ZBTB20 mRNA expression in young J20 mice relative to WT littermates, protein levels are unaffected and as such the phenotype is most likely exclusively due to the expression of mutant hAPP (Fisher *et al.*, 2017). This APP mutation leads to an increase in A β levels relative to mice expressing equivalent levels of WT hAPP, with increased levels detected from 6 weeks and amyloid plaques present from five months of age (Mullan *et al.*, 1992). Neuronal loss from the CA1 region of the hippocampus is seen from 12 weeks (Wright *et al.*, 2013). Similarly, at three months loss of synapses is seen (Hong *et al.*, 2016). This synaptic dysregulation is also reflected in electrophysiological changes, as demonstrated by Saganich *et al.* (2006) who found deficits in basal synaptic transmission from 3 months. They also reported a smaller average amplitude of field EPSPs and LTP deficits at the Schaffer collateral to CA1 synapse. Dendritic spines are small protrusions from dendrites that house the majority of excitatory synapses in the brain. Loss of spines and swollen dystrophic neurites seen in 11-month J20 mice are similar to morphological abnormalities in neurons in hippocampal tissue from AD patients (Moolman *et al.*, 2004). Although dendritic pruning is a part of healthy brain function (Subramanian *et al.*, 2020; Merlini *et al.*, 2019) excessive loss of dendritic spines leads to cognitive impairment (Terry *et al.*, 1991). It is no surprise therefore that from 4 months J20 mice perform significantly worse than age matched controls in the radial arm maze test (Wright *et al.*, 2013) and Morris water maze test (Cheng *et al.*, 2007) indicating deficits in spatial reference memory.

4.1.2 pS387-AGO2 and miR-134-mediated down-regulation of LIMK1 occurs in aged J20 mice

miRNAs are small non-coding RNAs that guide the RISC to target mRNAs for translational repression. A considerable majority of miRNAs are expressed in the brain where they have been shown to be involved in a range of processes and miRNA dysregulation has been associated with numerous neurological disorders ([Kamal *et al.*, 2015](#)). Previous work in the Hanley lab ([Rajgor *et al.*, 2018](#)) demonstrated that upon NMDA-induced LTD, AGO2 is phosphorylated at S387, leading to increased AGO2 association with RISC components and activity of miR-134. LIMK1 mRNA is a known target of miR-134 and its expression was decreased following cLTD induction in a pS387-AGO2 and miR-134 activity dependent manner. LIMK1 promotes actin cytoskeleton stability by phosphorylating cofilin, the activity of which depolymerises F-actin. Rajgor *et al.* suggested that the shrinkage of dendritic spines associated with LTD, and reproduced in their cLTD experiments, was due to actin depolymerisation caused by cofilin disinhibition via miR134-mediated LimK1 translational inhibition. LIMK1:cofilin signaling has been shown to be perturbed in animal models of AD (**Table 1.1**). This lead to the hypothesis that aberrant phosphorylation of AGO2 in AD and its models may underlie the observed spine loss and synaptic dysregulation. Data from pilot experiments in 18-month old J20 mice showed a reduction in LIMK1 concurrent with an increase in phosphorylation of AGO2 at S387 and in association of AGO2 and the RISC scaffolding protein GW182.

4.1.3 Aim

Following pilot data in 18-month old J20 mice that found a reduction in LIMK1 levels concurrent with an increase in phosphorylation of AGO2 at S387 I aimed to determine whether these changes to AGO2 phosphorylation and LIMK1 expression occur in the early or late stage of the disease course.

4.2 Results

4.2.1 APP expression is increased in J20 mice

To determine the time course of changes to pS387-AGO2 and LIMK1 expression in J20 mice cortical and hippocampal tissue were collected from 6- and 18-month J20 mice and age-matched controls and Western blotted firstly to quantify APP to confirm the disease phenotype. APP expression was increased by 131% ($\pm 12\%$; $n = 6$; **** $p < 0.0001$, Student t -test) in 6-month J20 mice and 225% ($\pm 26\%$, $n = 4$, **** $p < 0.0001$) in 18-month J20 mice relative to controls (**Figure 4.1**). These results aligned with the assigned genotypes.

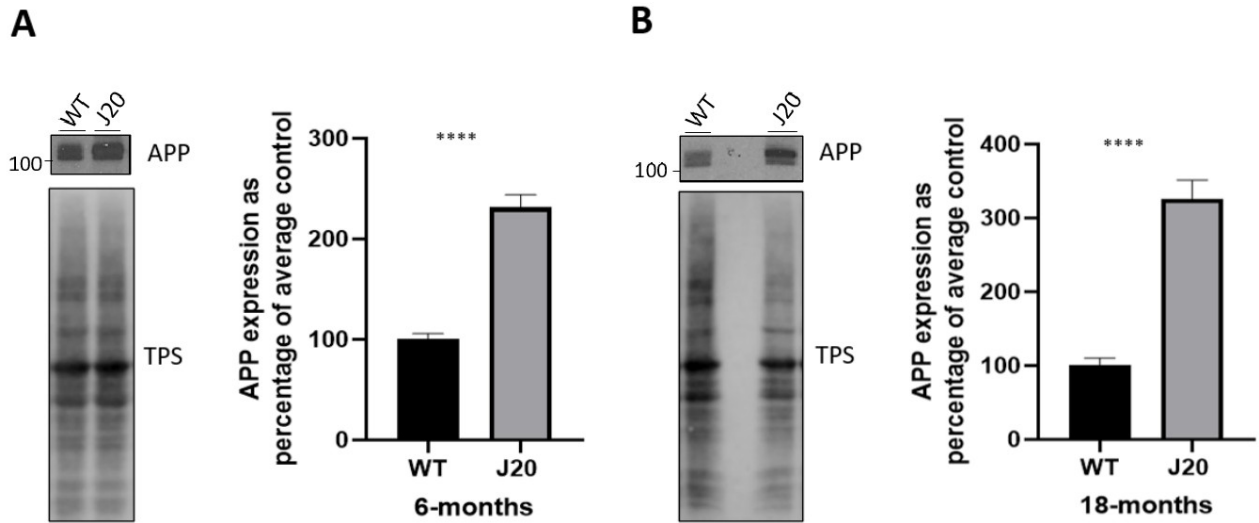


Figure 4.1: Changes in expression of APP in the cortical tissue of J20 mouse model at 6- and 18-months. (A) Western blot quantification of cortical APP expression in 6-month J20 mouse model ($n = 6$; **** $p < 0.0001$, Student t -test, error bars: s.e.m.) **(B)** Western blot quantification of cortical APP expression in 18-month J20 mouse model ($n = 4$; **** $p < 0.0001$, Student t -test, error bars: s.e.m.). Expression bands were normalised to corresponding total protein (TPS, LICOR). Data presented as percentage of average control.. Error bars are s.e.m.

4.2.2 pS387-AGO2 is increased in the hippocampus of J20 mice

Tissue from these animals was also homogenised and subject to Western blotting. The resulting membranes were then probed for LIMK1, AGO2 and pS387-AGO2. LIMK1 levels were found to be equivalent in J20 mice relative to controls at both 6- and 18-months and in both brain regions (**Figure 4.2**). No significant differences in total and relative levels of pS387-AGO2 were found in cortical tissue from either time point, however, phosphorylation of AGO2 at S387 was found to be decreased by 25% ($\pm 9\%$, $P = 0.02$) at 6 months and 47% ($\pm 18\%$, $P = 0.02$) at 18-months in the hippocampus of J20 mice relative to controls (**Figure 4.2 D, E**). In the hippocampus at 18-months total pS387-AGO2 was decreased by 37% (± 13 , $p = 0.01$) despite no significant change in total AGO2 (**Figure 4.2 E**).

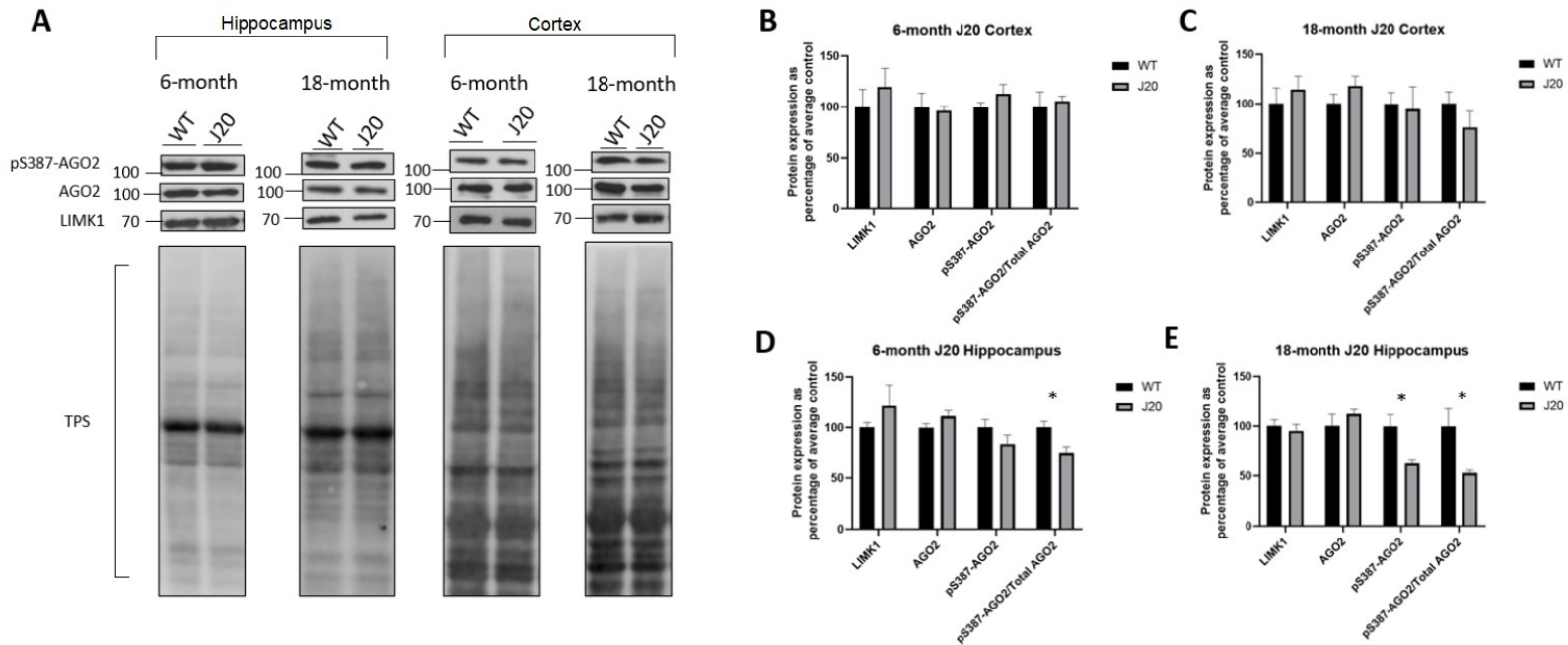


Figure 4.2: Expression levels of proteins related to pS387-AGO2 and miR-134-mediated silencing of LIMK1 in hippocampal and cortical tissue of the J20 mouse model of AD at 6- and 18-months (A) Western blots showing expression of LIMK1, AGO2, pS387-AGO2 and pS387-AGO2/Total AGO2 in 6- and 18-month J20 mouse cortex and hippocampus. (B) Western blot quantification of total LIMK1, AGO2, pS387-AGO2 and pS387-AGO2/Total AGO2 in 6-month J20 mouse cortex (n = 6; error bars, s.e.m.) (C) Western blot quantification of total LIMK1, AGO2, pS387-AGO2 and pS387-AGO2/Total AGO2 in 18-month J20 mouse cortex (n = 6; error bars, s.e.m.) (D) Western blot quantification of total LIMK1, AGO2, pS387-AGO2 and pS387-AGO2/Total AGO2 in 6-month J20 mouse hippocampus (n = 4; *p < 0.05, Student *t*-test; error bars, s.e.m.) (E) Western blot quantification of total LIMK1, AGO2, pS387-AGO2 and pS387-AGO2/Total AGO2 in 18-month J20 mouse hippocampus (n = 6; *p < 0.05, Student *t*-test; error bars, s.e.m.) Expression bands were normalised to corresponding total protein (TPS, LICOR). Data presented as percentage of average control. Error bars are s.e.m.

4.2.3 LIMK1 expression is unchanged in NL-F mice

Due to differences in the site of insertion, gene copy number, and mutation present, certain animal models may present with anomalous phenotypes (Saito *et al.*, 2014). The NL-F APP

Knock in mouse model of AD expresses endogenous levels of APP with the Swedish mutation described above and I716F (Iberian) mutation ([Saito *et al.*, 2014](#)). Cortical samples were also collected from NL-F APP Knock in mice at 18-months and age-matched controls (n = 6) to ascertain whether this result was anomalous to the J20 mouse model. These samples were subjected to western blot and probed for LIMK1. LIMK1 expression levels did not differ significantly relative to age-matched controls (**Figure 4.3**).

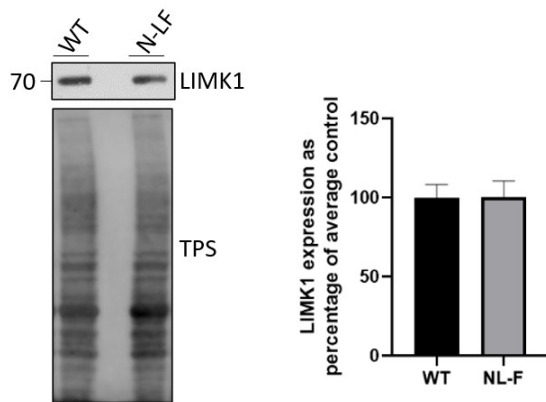


Figure 4.3: Expression levels of LIMK1 in NL-F APP Knock in mouse model of AD (n = 6; error bars, s.e.m.) Expression bands were normalised to corresponding total protein (TPS, LICOR). Data presented as percentage of average WT.

4.3 Discussion

4.3.1 pS387-AGO2 levels are altered in the hippocampus of J20 mice

Significant reductions in spine density and volume are seen in AD brains and their models - including J20 mice ([Pozueta *et al.*, 2013](#); [Moolman *et al.*, 2004](#)). These morphological changes have electrophysiological consequences and confer an enhancement in LTD and a reduction in LTP as larger spine heads can accommodate a greater number of AMPARs and consequently confer greater excitability at that synapse ([Saganich *et al.* 2006](#)). Morphological

changes in dendritic spines are co ordinated via modulation of the actin cytoskeleton. This led to the hypothesis that the LTD-associated role of pS387-AGO2 and miR-134 in regulating the LIMK1:cofilin signalling pathway discovered previously in the lab may be overactivated in AD and its models, causing excessive and pathological spine loss ([Rajgor *et al.*, 2018](#)).

Preliminary data from the Hanley lab showed that in the J20 cortex there is an increase in phosphorylation of AGO2 at S387 and in association between AGO2 and the RISC scaffold protein GW182 concurrent with a decrease in expression of the miR-134 target LIMK1 supporting the hypothesis that pS387-Ago dependent LTD related processes are aberrantly activated in AD. To determine whether these changes occur early in the disease course and contribute to the disease aetiology or only appear at later stages cortical and hippocampal tissue from 6-month (n = 4) and 18-month (n = 6) J20 mice and age-matched controls was homogenised, subjected to Western blotting and probed for relevant proteins. The J20 mouse model overexpresses APP so firstly, APP levels were quantified to confirm disease phenotype (Mucke *et al.*, 2000). APP expression increased by 131% ($\pm 12\%$) in 6-month J20 mice and 225% ($\pm 26\%$) in 18-month J20 mice relative to controls. Surprisingly however, the pilot data showing a decrease in LIMK1 expression in the J20 mouse relative to controls were not reproduced. No reduction in LIMK1 expression was found at either 6- or 18- months in J20 cortical or hippocampal tissue relative to that of controls. Samples from an alternative model - the NL-F APP Knock in mouse model of AD were also probed for LIMK1 to determine whether this result was an anomaly of the J20 model (Saito *et al.*, 2014). However, neither were levels altered relative to control mice in the NL-F APP knock in model. These findings were however in line

with those of previous studies investigating the LIMK-Cofilin pathway in mouse AD models in which LIMK1 levels were found to be unchanged relative to controls (Barone *et al.*, 2014; Henderson *et al.*, 2019).

Interestingly, although phosphorylation of AGO2 at S387 remained the same in cortex in J20 mice relative to controls at 6- and 18-months, it was significantly decreased in the hippocampus by 25% ($\pm 9\%$, $p = 0.02$) at 6 months and 47% ($\pm 18\%$, $p = 0.02$) at 18-months. At 18-months this effect is more pronounced with relative levels of pS387-Ago2 but also total levels of pS387-Ago2 decreased by 37% (± 11.92 , $p = 0.01$) in J20 mouse hippocampus. This concurrent reduction in relative pS387-AGO2 and total pS387-AGO2 despite no change in total AGO2 levels may indicate specific degradation of AGO2 phosphorylated at this site. This is in agreement with previous work demonstrating a role for phosphorylation of S387 in degradation of AGO2 during LTD (Paradis & Boehm, 2018). It is known that hydroxylation at P700 and sumoylation of K402 are also post-translational modifications that can affect AGO2 stability (Qi *et al.*, 2008; Sahin *et al.*, 2014). In the context of AD S387 might also represent a site for regulation of AGO2 stability. The specific vulnerability of the hippocampus to this change in pS387-AGO2 is particularly interesting as this brain region is known to be responsible for processing and retrieving memories and is also the region affected the earliest and most heavily by AD pathology (Gurvits *et al.*, 1996; Scoville & Milner, 1957; O'Keefe & Dostrovsky, 1971; MacDonald *et al.*, 2011).

Work by Rajgor *et al.*, (2018) suggested that during LTD an increase in pS387-AGO2 leads to an increase in miR-134 activity. The absence of changes in expression of LIMK in the J20 mouse

brain despite a decrease in pS387-Ago2 may be due to a number of other factors. Precise regulation of the activity of cofilin in synaptic plasticity is crucial to healthy synaptic function and as such homeostatic mechanisms may come into play if the expression of a key player in this pathway is perturbed. This could be enacted through an increase in total expression to compensate for miR-134 targeting of LIMK1 mRNA. Alternatively, a reduction in LIMK1 activity may trigger a reduction in LIMK1 turnover through changes to mechanisms such as ubiquitination which targets proteins for degradation ([Hershko & Ciechanover, 1998](#)).

Another consideration in this is the promiscuity of miRNAs. A single miRNA can have many targets. Another layer of regulation may be present in which a subpopulation of miR-134 targets are selected for silencing. Indeed, editing of miRNA has been extensively reported and is suggested to allow greater specificity in target recognition ([Correia *et al.*, 2019](#)). miRNAs can also be subject to signal mediated silencing, for example by target-directed miRNA silencing (TDMS) in which specialised RNAs bind to miRNA to form a bipartite duplex with a flexible linker. AGO cannot accommodate this duplex, which causes it to bend at the linker region, exposing the 3' end of the miRNA to enzymatic degradation ([Sheu-Gruttadauria *et al.*, 2019](#)). Expression of other non-coding RNAs that can act as miRNA sponges such as circular RNAs and pseudogenes and long ncRNAs can also reduce miRNA activity ([Gjorgjieva *et al.*, 2019](#)). These processes all represent mechanisms by which an increase in activity of a specific miRNA can be negated.

Although total levels were unchanged these results do not rule out an effect limited to dendritic

spines. If translational inhibition by miR-134 was regulated such that it was highly localised to spines or dendrites, this effect may not be evident in data produced using a Western blot which quantifies total lysate protein levels. Given that specific mechanisms for trafficking of mRNA, miRNA and RISC machinery to the synapse have been demonstrated, in addition to subcompartment specific regulatory pathways it may also be the case that spatial control of these processes could occur on a much smaller scale. For example, other work has shown that the relative distribution of SSH1 and LIMK1 within a dendritic spine is key to lamellipodia formation and neuronal migration (Nagata-Ohashi *et al.*, 2004). This suggests that rather than total levels, alternative configurations of the relative concentrations of these proteins within the dendritic spine can play an important role in the net effect of their activity. Therefore, although there no changes were seen in LIMK1 at the whole tissue level, in future work immunohistochemistry of J20 hippocampal slices or synapotosomal sub-fractionation of tissue could be used to determine whether there are highly localised changes to LIMK1 levels within the spine.

4.3.2 Conclusions

Surprisingly, I was not able to reproduce findings from the pilot study and therefore these results do not support the hypothesis that pS387-AGO2 and miR134-mediated down-regulation of LIMK1 play a role in spine loss in the J20 mouse model. Furthermore, reduced phosphorylation of AGO2-S387 in the absence of altered LIMK1 expression indicates that although LIMK1 expression can be altered by miR-134 activity (Schratt *et al.*, 2006), in the J20 mouse this is insufficient to affect total LIMK1 levels. However, whether other targets of miR-

134 or other miRNAs preferentially recruited by pS387-AGO2 are involved in the AD pathology warrants further investigation. It also cannot be ruled out that this altered regulation of AGO2 may confer changes within the very localised context of the dendritic spine. The specific reduction in AGO2 phosphorylated at S387 in the J20 mouse model hippocampus at 18-months may also indicate targeting of AGO2 with this modification for degradation in AD.

Chapter 5: Investigating LIMK1 in Alzheimer's Disease cortical tissue

5.1 Introduction

5.1.1 AD models are unable to recapitulate all aspects of human AD

Experimental models expressing EAOD-linked APP, PSEN1 and PSEN2 mutations in cells or whole animals are vital tools in research, but ultimately are limited. They cannot reflect all aspects of human brain physiology and also its susceptibility to human-specific pathways associated with AD. One important indicator of this is that despite producing sometimes very high levels of A β , mouse models do not lead to the production of NFTs (Myers & McGonigle, 2019). The murine ortholog of tau has key sequence differences that render it highly resistant to aggregation relative to human tau (Gilley *et al.*, 2012). To generate mouse models in which NFTs are present, mutant tau variants are expressed alongside mutant APP, however these are mechanistically distinct from amyloid accumulation and aggregation (Lewis *et al.*, 2001). It is therefore important to consider, where possible, using human-derived tissue and models to determine disease mechanisms.

5.1.2 Deposition of Neurofibrillary Tangles progresses linearly through the human brain during course of AD

Hyperphosphorylated tau protein deposition has been demonstrated to spread in a stepwise fashion through brain networks through examination of *post mortem* AD patient brain tissue (Braak & Braak, 1991) and in PET scans of MCI and AD patients (Cho *et al.*, 2016). Tau accumulation starts in the medial temporal regions and then progresses to the basal and lateral temporal, inferior parietal, posterior cingulate, and other association cortices and finally to the primary cortex (Cho *et al.*, 2016). In contrast, amyloid accumulates diffusely through the

neocortex and cortical thinning only occurs at advanced tau stages (Cho *et al.*, 2016; Thal *et al.*, 2002). These stages of NFT progression through the brain were described by Braak (1991) as following a broad pattern in six stages, with Braak stages I and II being when entorhinal regions are primarily affected, Braak stages III and IV when limbic regions are also involved and the final Braak stages V and VI where there is NFT accumulation right through to the neocortical regions. The stage of NFT progression also correlates with general cognitive status and can be used to confirm disease stage (Cho *et al.*, 2016).

5.1.3 LIMK1 is down-regulated in LTD and in the AD brain

LIMK1 is a crucial component of synaptic plasticity and neuronal function (Meng *et al.*, 2002; Todorovski *et al.*, 2015; Lunardi *et al.*, 2018; Rajgor *et al.*, 2018). It has been demonstrated to be down-regulated during LTD in healthy neuronal function via pS387-AGO2-dependent miR-134 activity (Rajgor *et al.*, 2018). LTD is associated with shrinkage of the dendritic spines that house excitatory synapses (Zhou *et al.*, 2004). Excessive synaptic loss is also one of the earliest changes in AD and the best correlate of cognitive decline (DeKosky & Scheff, 1990, Terry *et al.*, 1991). This led to the hypothesis that this LTD-associated mechanism for spine reduction may be aberrantly activated in AD and therefore contributing to this disease feature. Preliminary results from Braak stage VI AD patient cortical tissue showed that LIMK1 levels are indeed reduced in late stage AD relative to controls.

5.3.4 Aim

To determine whether LIMK1 expression decreases in AD in the entorhinal, limbic or neocortical stage of NFT deposition in AD.

5.2 Results

5.2.1 *Post mortem* delay was not significantly different between test groups

Post mortem cortical tissue from 60 age-matched AD patients (range: 74 - 96) was obtained from the South West Dementia Brain Bank. These were divided into disease course stages according to Braak staging (Entorhinal stages, NFT (I - II); Limbic stages, NFT (III - IV) and Neocortical stages (V - VI)) (Braak, 1991) with each group making up 20 of the total 60 samples. This tissue was homogenised in denaturing conditions and subjected to Western blot. Relative total protein was quantified with Licor Total Protein stain (TPS) used as a loading control.

Protein degradation increases with *post mortem* delay and can therefore skew results. *Post mortem* delay was compared across groups and no significant differences were found (**Figure 5.1**).

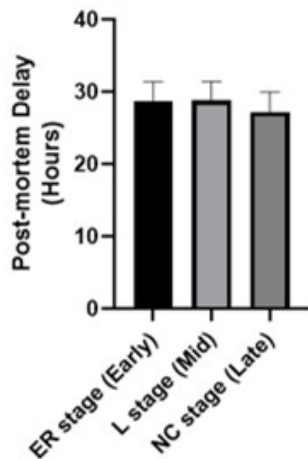


Figure 5.1: Post-mortem delay was not significantly different between Entorhinal (ER) (Early) stage, Limbic (L) (Mid) and Neocortical (NC) stage human AD samples. (n = 20; error bars, s.e.m.)

5.2.2 Cortical pTau is increased in late stage AD but LIMK1 expression is unaffected

Braak staging is based upon the progressive formation of NFTs made up of hyperphosphorylated tau that deposit firstly in the entorhinal cortex and then through the brain in a stereotyped manner ([Braak, 1991](#)). Of these samples four from each group were randomly selected to confirm assigned Braak staging by probing for phosphorylated tau (pTau). pTau was found to increase significantly in the neocortical (NC) stage relative to the limbic (L) stage (254% $P = 0.044$) and NC relative to entorhinal (ER) stage (380% $P = 0.0045$) (**Figure 5.2 A**)

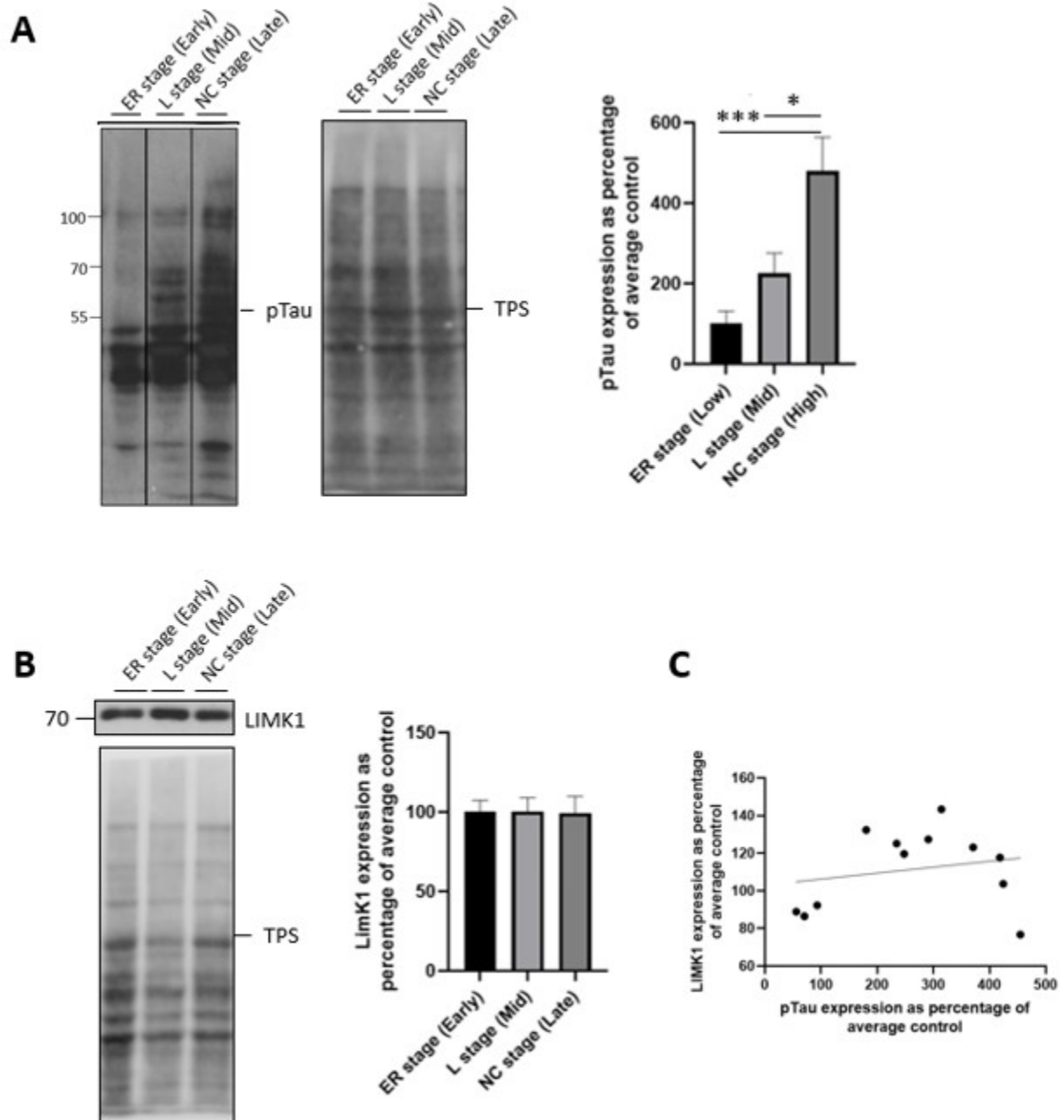


Figure 5.2: Cortical LIMK1 expression levels do not change during the course of AD as determined by pTau deposition and Braak stage. A) pTau expression levels in Entorhinal (ER) (Early) stage, Limbic (L) (Mid) and Neocortical (NC) stage human AD samples ($n = 5$; $***p < 0.001$, $*p < 0.05$, One-way ANOVA, Bonferroni multiple comparisons test; error bars, s.e.m.) **B)** LIMK1 expression levels in Entorhinal (ER) (Early) stage, Limbic (L) (Mid) and Neocortical (NC) stage human AD samples ($n = 20$, error bars, s.e.m.) **C)** Scatterplot showing correlation between expression levels of pTau and LIMK1. ($n = 5$; $r = 0.06$)

Previous work in the lab demonstrated the role of pS387-Ago2 and miR134-mediated LIMK1 down-regulation in LTD-associated shrinkage of dendritic spines and lead to the hypothesis that this mechanism may underlie spine loss in AD. This was supported by pilot experiments in which LIMK1 was found to decrease in late stage AD. Surprisingly however, LIMK1 levels were analysed and no significant difference was found between control and AD conditions at any disease course stage (ER/L/NC) (**Figure 5.2 B**). Furthermore, LIMK1 levels were also not found to be correlated pTau levels (**Figure 5.2 C**).

5.3 Discussion

5.3.2 Cortical LIMK1 expression levels are unchanged during the course of AD

Preliminary data indicated that in late stage AD there is a reduction in cortical LIMK1 expression in AD. To explore when in the disease course this change occurs LIMK1 levels were quantified by Western blot in cortical tissue from 60 AD patients acquired from the SWDBB. These were divided equally into groups (n = 20) according to the progression of pTau inclusions through the brain, either restricted to entorhinal cortex (Early stage: Braak I-II), spread to the limbic regions (Mid stage: Braak III-IV) or through the brain to neocortical regions (Late stage: Braak V-VI) (Braak & Braak, 1991). No significant differences were found in *post mortem* delay between groups indicating that the results were not skewed by uneven distribution of protein degradation.

To investigate the accuracy of assigned Braak stage a random selection of four samples from each group were probed for one of the hallmark AD protein aggregates - NFTs. These are made

up of hyperphosphorylated tau so quantification of this pTau was used as a proxy measurement of NFT deposition. The trend was an increase with Braak group, however, there was no significant difference between Early and Mid stage samples. This suggests a greater variability of pTau deposition within groups than between them which may be due to the fact that these samples are cortical and in these earlier stages pTau deposition has not stably progressed to this region. This is supported by the 254% increase of pTau found in NC/late stage samples relative to L/mid and 380% increase relative to ER/early stage. The finding of increasing cortical pTau levels with assigned Braak stages indicates accurate assignment of Braak stage.

Contrary to previous findings, cortical LIMK1 levels did not differ significantly in NC/late stage relative to ER/early stage AD. LIMK1 levels were also not correlated with pTau levels suggesting that variations in these did not skew the results. This result is however in line with that of Heredia *et al.* (2006) who found that total LIMK1 expression levels did not change in the AD brain.

There are many different factors which can negatively impact reproducibility, particularly when working with human tissue. Although these samples were age-matched and did not differ significantly in *post-mortem* delay there may be other factors that were not controlled for that may affect results. These include the presence or absence of genes that confer a greater risk of AD, or protection against it such as the well-studied APOE alleles (Serrano-Pozo *et al.*, 2021). Uneven distribution of APOE4 carriers across groups in Phase 2b trial cast doubts on the efficacy of the IgG1 monoclonal antibody based treatment that targets soluble aggregated amyloid β

(A β) Lecanemab (BAN2401) in 2018 (Alzforum). This highlights the importance of controlling for confounding factors when analysing results. In addition to genetic risk factors there are a number of modifiable factors that have been shown to affect AD risk. A meta-analysis by Xu and colleagues (2015) with a pooled population of > 5000 people revealed that diseases such as osteoporosis, heart conditions such as atherosclerosis, hypertension, hypotension and a history of myocardial infarction all increased the risk of developing AD. A history of Type II Diabetes was also shown to be positively correlated with AD. This is unsurprising as it has long been associated with insulin resistance and diabetes, leading some to suggest that AD represents a third type of diabetes (Burillo *et al.*, 2021). Furthermore, diabetes drugs have been shown to ameliorate the negative effect of Type II diabetes on cognitive function and have been suggested to be potential candidates for AD drugs (Boccardi *et al.*, 2019). Should this prove true the use of these drugs could affect molecular mechanisms involved in LIMK1 expression. Conversely, having a history of cancer or metabolic syndrome was associated with a reduced risk of developing AD. Medical treatment with NSAIDs, statins or oestrogen were all found to reduce AD risk. Lifestyle factors also play a role. High intake of folate, vitamin C, vitamin E, caffeine or a mediterranean-type diet were all dietary factors negatively correlated with AD risk. Low BMI was shown to be a risk factor. Educational attainment was found to reduce risk. In future work, additional data regarding the presence or absence of these conditions within subgroups would allow for more confident conclusions to be drawn.

Another potential confounding factor is potential variations in tau deposition. Although the staging method described by Braak and Braak (1991) derived from histopathological analysis of

ex vivo brain slices has been demonstrated in vivo with tau-PET imaging studies a number of examples since have emerged in which the tau spreading pattern does not fit perfectly into this system (Schwarz *et al.*, 2016; Scholl *et al.*, 2016). These include an AD phenotype in which the medial temporal lobe is spared despite extensive cortical tau deposition and a phenotype in which the most prominent tau pathology is found in the limbic medial temporal cortex (Murray *et al.*, 2011; Whitwell *et al.*, 2012; Ferreira *et al.*, 2020;). Furthermore, different AD subtypes have been attributed to different rates of atrophy and cognitive decline (Risacher *et al.*, 2017; Ossenkoppele *et al.*, 2020). It has been suggested that defining these subtypes will be an important step in refining research into AD pathology (Vogel *et al.*, 2021).

5.3.3 Conclusions

Despite the findings of the pilot experiments in late stage AD, these results do not support the hypothesis that LIMK1 expression is altered during the course AD. Unlike model systems, humans are highly variable in lifestyle, genetic make up and even amongst AD sufferers, in AD phenotype. To reduce issues with reproducibility these confounding factors must be identified and controlled for as thoroughly as possible.

Chapter 6: General Discussion

6.1 Summary

Firstly, I attempted to reproduce pS387-AGO2 and miR-134-mediated changes seen in cLTD and in a primary neuronal model of AD overexpressing WT APP and using a BACE1 site mutant APP as a control. The lipofectamine protocol used to produce this model proved too stressful for cultured neurons in my hands. I therefore chose to use an alternative strategy for producing a primary neuronal model using lentiviruses, produced using lentiviral plasmid constructs kindly donated by Dr Kevin Wilkinson. With these, I was able to almost entirely knock down endogenous APP and replace it to endogenous levels with myc-tagged APP that was either WT or carried the EOAD-linked Swedish mutation, or the Swedish, Iberian and Arctic mutations in combination. This lead to no observable changes in cell viability. However, this also did not confer the same effects on phosphorylation of AGO2 at S387 or LIMK1 levels seen in the previous model.

The pilot data had also used a dual luciferase assay which would again require transfection. I decided to design a miRNA activity assay that also involved lentiviruses, in this case expressing a reporter protein (mCherry) that could be quantified by Western blot. The sequence of this reporter protein was conjugated to a degron sequence (ODC PEST) to increase protein turnover and thereby sensitivity to changes in expression caused by miRNA activity. To this I also conjugated the 3' UTR of LIMK1 containing the target sequence complementary to miR-134 so that reporter protein expression was subject to regulation by miR-134 activity. To test the design concept I transfected HEK293T cells with these plasmid constructs either with or without another plasmid expressing pre-miR-134. When pre-miR-134 was overexpressed mCherry

expression decreased significantly by 68%.

I considered that although my cellular model had not reproduced the results of the pilot experiments this was most likely due to the difference in protocol used to produce the model. I moved forward to a whole animal model - the J20 mouse model of AD. Pilot experiments using tissue from 18-month old J20 mice had also found changes in protein expression levels supporting the hypothesis that excessive phosphorylation of AGO2 at S387 increases miR-134-mediated silencing of LIMK1, leading to the suggestion that this may contribute to spine loss seen in AD and its models and therefore represent an avenue for therapeutic intervention. However, the therapeutic window for AD is considered to be the prodromal stage, prior to extensive neuropathology. I aimed to determine whether these changes occur early in the disease course or only in late stages. Surprisingly, the pilot data were not reproduced. I found no change in LIMK1 levels and a significant decrease in phosphorylation of AGO2 S387 in the hippocampus of both 6- and 18-month old J20 mice of 25% and 47% respectively.

Although animal models are better able to model the intact human brain than cellular models they are still unable to recapitulate all aspects of neurological disease. Pilot experiments using late stage human AD cortical tissue had found a decrease in LIMK1 expression supporting the general hypothesis. As in the J20 mice I aimed to determine whether this occurs only in late stage AD or if it occurs earlier and as such is a potential candidate for maximally effective therapeutic intervention. However, I found no difference in LIMK1 expression between early (Braak stage I - II), mid (Braak stage III-IV) and late (Braak stage V - VI) AD.

6.2 Conclusions

My primary aim was to investigate the roles of AGO2 phosphorylation and miR-134 in synaptic dysfunction in AD. Although the data shown here does not support the initial hypothesis that pS387-AGO2 and miR-134 mediated down-regulation of LIMK1 is involved in shrinkage of dendritic spines in AD the finding that there is specific reduction in pS387-AGO2 in hippocampal tissue from J20 mouse model mice at both 6- and 18-months is intriguing. The hippocampus plays a well-established role in memory and is one of the first and most heavily affected regions in AD pathology. This is the first finding in J20 mice as young as 6-months of changes to phosphorylation of AGO2. Here I have also demonstrated proof of concept for a lentivirus-based miRNA activity assay. This may be a useful tool in determining what other miRNAs may be involved in primary neuronal models of AD in future.

Chapter 8: References

- Aalto, A. P., & Pasquinelli, A. E. (2012). Small non-coding RNAs mount a silent revolution in gene expression. *Current opinion in cell biology*, 24(3), 333-340.
<https://doi.org/10.1016/j.ceb.2012.03.006>
- Abdelmohsen, K., Hutchison, E. R., Lee, E. K., Kuwano, Y., Kim, M. M., Masuda, K., . . . Gorospe, M. (2010). miR-375 inhibits differentiation of neurites by lowering HuD levels. *Molecular and cellular biology*, 30(17), 4197-4210. <https://doi.org/10.1128/MCB.00316-10>
- Agostini, M., Tucci, P., Killick, R., Candi, E., Sayan, B. S., Rivetti di val Cervo, P., . . . Melino, G. (2011). Neuronal differentiation by TAp73 is mediated by microRNA-34a regulation of synaptic protein targets. *Proceedings of the National Academy of Sciences*, 108(52), 21093-21098. <https://doi.org/10.1073/pnas.1112061109>
- Allen, N. J., & Barres, B. A. (2009). Glia — more than just brain glue. *Nature*, 457(7230), 675-677. <https://doi.org/10.1038/457675a>
- Alvarez, V. A., & Sabatini, B. L. (2007). Anatomical and Physiological Plasticity of Dendritic Spines. *Annual Review of Neuroscience*, 30(1), 79-97.
<https://doi.org/10.1146/annurev.neuro.30.051606.094222>
- Alzforum. Lecanemab. In <https://www.alzforum.org/therapeutics/lecanemab> [Accessed on 12.10.22].
- Alzheimer's, A. (2019). 2019 Alzheimer's disease facts and figures. *Alzheimer's & Dementia*, 15(3), 321-387. <https://doi.org/10.1016/j.jalz.2019.01.010>
- Alzheimer's Research, U. K. Alzheimer's Symptoms. In Available at: <https://www.alzheimersresearchuk.org/dementia-information/types-of-dementia/alzheimers-disease/symptoms/> [Accessed on 14.08.22].
- An, J. J., Gharami, K., Liao, G.-Y., Woo, N. H., Lau, A. G., Vanevski, F., . . . Xu, B. (2008). Distinct role of long 3' UTR BDNF mRNA in spine morphology and synaptic plasticity in hippocampal neurons. *Cell*, 134(1), 175-187. <https://doi.org/10.1016/j.cell.2008.05.045>
- Andrianantoandro, E., & Pollard, T. D. (2006). Mechanism of Actin Filament Turnover by Severing and Nucleation at Different Concentrations of ADF/Cofilin. *Molecular Cell*, 24(1), 13-23.
<https://doi.org/10.1016/j.molcel.2006.08.006>
- Anggono, V., & Huganir, R. L. (2012). Regulation of AMPA receptor trafficking and synaptic plasticity. *Current Opinion in Neurobiology*, 22(3), 461-469.
<https://doi.org/10.1016/j.conb.2011.12.006>
- Antoniou, A., Baptista, M., Carney, N., & Hanley, J. G. (2014). PICK1 links Argonaute 2 to endosomes in neuronal dendrites and regulates miRNA activity. *EMBO reports*, 15(5), 548-556. <https://doi.org/10.1002/embr.201337631>
- Arbel-Ornath, M., Hudry, E., Boivin, J. R., Hashimoto, T., Takeda, S., Kuchibhotla, K. V., . . . Bacskaï, B. J. (2017). Soluble oligomeric amyloid- β induces calcium dyshomeostasis that precedes synapse loss in the living mouse brain. *Molecular Neurodegeneration*, 12(1), 27-27. <https://doi.org/10.1186/s13024-017-0169-9>
- Arber, C., Alatz, A., Leckey, C. A., Paterson, R. W., Zetterberg, H., & Wray, S. (2021). Mass

- spectrometry analysis of tau and amyloid-beta in iPSC-derived models of Alzheimer's disease and dementia. *Journal of neurochemistry*, 159(2), 305-317.
<https://doi.org/10.1111/jnc.15315>
- Arber, S., Barbayannis, F. A., Hanser, H., Schneider, C., Stanyon, C. A., Bernard, O., & Caroni, P. (1998). Regulation of actin dynamics through phosphorylation of cofilin by LIM-kinase. *Nature*, 393(6687), 805-809. <https://doi.org/10.1038/31729>
- Ardito, F., Giuliani, M., Perrone, D., Troiano, G., & Muzio, L. L. (2017). The crucial role of protein phosphorylation in cell signaling and its use as targeted therapy (Review). *International Journal of Molecular Medicine*, 40(2), 271-280. <https://doi.org/10.3892/ijmm.2017.3036>
- Arosio, B., Casati, M., Pucci, M., Sun, Y., Liang, L., Dong, M., . . . Gao, H. (2019). Cofilin 2 in Serum as a Novel Biomarker for Alzheimer's Disease in Han Chinese.
<https://doi.org/10.3389/fnagi.2019.00214>
- Ashby, M. C., Maier, S. R., Nishimune, A., & Henley, J. M. (2006). Lateral diffusion drives constitutive exchange of AMPA receptors at dendritic spines and is regulated by spine morphology. *The Journal of neuroscience : the official journal of the Society for Neuroscience*, 26(26), 7046-7055. <https://doi.org/10.1523/JNEUROSCI.1235-06.2006>
- Augustine, G. J., Charlton, M. P., & Smith, S. J. (1987). Calcium Action in Synaptic Transmitter Release. *Annual Review of Neuroscience*, 10(1), 633-693.
<https://doi.org/10.1146/annurev.ne.10.030187.003221>
- Autilio, L. A., Appel, S. H., Pettis, P., & Gambetti, P. L. (1968). Biochemical studies of synapses in vitro. I. Protein synthesis. *Biochemistry*, 7(7), 2615-2622.
<https://doi.org/10.1021/bi00847a025>
- Bamburg, J. R., & Bernstein, B. W. (2016). Actin dynamics and cofilin-actin rods in alzheimer disease. *Cytoskeleton*, 73(9), 477-497. <https://doi.org/10.1002/cm.21282>
- Banerjee, S., Neveu, P., & Kosik, K. S. (2009). A Coordinated Local Translational Control Point at the Synapse Involving Relief from Silencing and MOV10 Degradation. *Neuron*, 64(6), 871-884. <https://doi.org/10.1016/j.neuron.2009.11.023>
- Banker, G. A., & Cowan, W. M. (1977). Rat hippocampal neurons in dispersed cell culture. *Brain research*, 126(3), 397-342. [https://doi.org/10.1016/0006-8993\(77\)90594-7](https://doi.org/10.1016/0006-8993(77)90594-7)
- Banzhaf-Strathmann, J., Benito, E., May, S., Arzberger, T., Tahirovic, S., Kretzschmar, H., . . . Edbauer, D. (2014). Micro RNA -125b induces tau hyperphosphorylation and cognitive deficits in Alzheimer's disease. *The EMBO Journal*, 33(15), 1667-1680.
<https://doi.org/10.15252/embj.201387576>
- Bao, F., Wicklund, L., Lacor, P. N., Klein, W. L., Nordberg, A., & Marutle, A. (2012). Different β -amyloid oligomer assemblies in Alzheimer brains correlate with age of disease onset and impaired cholinergic activity. *Neurobiology of Aging*, 33(4), 825.e821-825.e813.
<https://doi.org/10.1016/j.neurobiolaging.2011.05.003>
- Barbarino, P., Lynch, C., Watchman, K., Dabas, L., Arthurton, L., Blom, M., . . . Ritchie, L. *From Plan to Impact IV Progress towards targets of the WHO Global action plan on dementia Contributors.*
- Barone, E., Mosser, S., & Fraering, P. C. (2014). Inactivation of brain Cofilin-1 by age, Alzheimer's

- disease and γ -secretase. *Biochimica et Biophysica Acta (BBA) - Molecular Basis of Disease*, 1842(12), 2500-2509. <https://doi.org/10.1016/J.BBADIS.2014.10.004>
- Barreau, C., Paillard, L., & Osborne, H. B. (2005). AU-rich elements and associated factors: are there unifying principles? *Nucleic acids research*, 33(22), 7138-7150. <https://doi.org/10.1093/nar/gki1012>
- Batassa, E. M., Costanzi, M., Saraulli, D., Scardigli, R., Barbato, C., Cogoni, C., & Cestari, V. (2010). RISC activity in hippocampus is essential for contextual memory. *Neuroscience letters*, 471(3), 185-188. <https://doi.org/10.1016/j.neulet.2010.01.038>
- Batish, M., van den Bogaard, P., Kramer, F. R., & Tyagi, S. (2012). Neuronal mRNAs travel singly into dendrites. *Proceedings of the National Academy of Sciences of the United States of America*, 109(12), 4645-4650. <https://doi.org/10.1073/pnas.1111226109>
- Batista, A. F., Forny-Germano, L., Clarke, J. R., Lyra E Silva, N. M., Brito-Moreira, J., Boehnke, S. E., . . . De Felice, F. G. (2018). The diabetes drug liraglutide reverses cognitive impairment in mice and attenuates insulin receptor and synaptic pathology in a non-human primate model of Alzheimer's disease. *The Journal of pathology*, 245(1), 85-100. <https://doi.org/10.1002/path.5056>
- Behm-Ansmant, I., Rehwinkel, J., Doerks, T., Stark, A., Bork, P., & Izaurralde, E. (2006). mRNA degradation by miRNAs and GW182 requires both CCR4:NOT deadenylase and DCP1:DCP2 decapping complexes. *Genes & development*, 20(14), 1885-1898. <https://doi.org/10.1101/gad.1424106>
- Belloy, M. E., Napolioni, V., & Greicius, M. D. (2019). A Quarter Century of APOE and Alzheimer's Disease: Progress to Date and the Path Forward. *Neuron*, 101(5), 820-838. <https://doi.org/10.1016/j.neuron.2019.01.056>
- Bellugi, U., Lichtenberger, L., Mills, D., Galaburda, A., & Korenberg, J. R. (1999). Bridging cognition, the brain and molecular genetics: evidence from Williams syndrome. *Trends in Neurosciences*, 22(5), 197-207. [https://doi.org/10.1016/S0166-2236\(99\)01397-1](https://doi.org/10.1016/S0166-2236(99)01397-1)
- Benke, T. A., Lüthi, A., Isaac, J. T. R., & Collingridge, G. L. (1998). Modulation of AMPA receptor unitary conductance by synaptic activity. *Nature*, 393(6687), 793-797. <https://doi.org/10.1038/31709>
- Bernardinelli, Y., Randall, J., Janett, E., Nikonenko, I., König, S., Jones, Emma V., . . . Muller, D. (2014). Activity-Dependent Structural Plasticity of Perisynaptic Astrocytic Domains Promotes Excitatory Synapse Stability. *Current Biology*, 24(15), 1679-1688. <https://doi.org/10.1016/j.cub.2014.06.025>
- Bertram, L., Lange, C., Mullin, K., Parkinson, M., Hsiao, M., Hogan, M. F., . . . Tanzi, R. E. (2008). Genome-wide association analysis reveals putative Alzheimer's disease susceptibility loci in addition to APOE. *American journal of human genetics*, 83(5), 623-632. <https://doi.org/10.1016/j.ajhg.2008.10.008>
- Bertram, L., & Tanzi, R. E. (2008). Thirty years of Alzheimer's disease genetics: the implications of systematic meta-analyses. *Nature Reviews Neuroscience*, 9(10), 768-778. <https://doi.org/10.1038/nrn2494>
- Bettens, K., Sleegers, K., & Van Broeckhoven, C. (2010). Current status on Alzheimer disease

- molecular genetics: from past, to present, to future. *Human Molecular Genetics*, 19(R1), R4-R11. <https://doi.org/10.1093/hmg/ddq142>
- Bicker, S., Khudayberdiev, S., Weiß, K., Zocher, K., Baumeister, S., & Schratt, G. (2013). The DEAH-box helicase DHX36 mediates dendritic localization of the neuronal precursor-microRNA-134. *Genes & Development*, 27(9), 991-996. <https://doi.org/10.1101/gad.211243.112>
- Bicker, S., Lackinger, M., Weiß, K., & Schratt, G. (2014). MicroRNA-132, -134, and -138: a microRNA troika rules in neuronal dendrites. *Cellular and molecular life sciences : CMLS*, 71(20), 3987-4005. <https://doi.org/10.1007/S00018-014-1671-7/TABLES/2>
- Bitan, G., Fradinger, E. A., Spring, S. M., & Teplow, D. B. (2005). Neurotoxic protein oligomers--what you see is not always what you get. *Amyloid : the international journal of experimental and clinical investigation : the official journal of the International Society of Amyloidosis*, 12(2), 88-95. <https://doi.org/10.1080/13506120500106958>
- Blennow, K., Bogdanovic, N., Alafuzoff, I., Ekman, R., & Davidsson, P. (1996). Synaptic pathology in Alzheimer's disease: Relation to severity of dementia, but not to senile plaques, neurofibrillary tangles, or the ApoE4 allele. *Journal of Neural Transmission*, 103(5), 603-618. <https://doi.org/10.1007/BF01273157>
- Bliss, T. V., & Collingridge, G. L. (1993). A synaptic model of memory: long-term potentiation in the hippocampus. *Nature*, 361(6407), 31-39. <https://doi.org/10.1038/361031a0>
- Bliss, T. V. P., & Lømo, T. (1973). Long-lasting potentiation of synaptic transmission in the dentate area of the anaesthetized rabbit following stimulation of the perforant path. *The Journal of physiology*, 232(2), 331-356. <https://doi.org/10.1113/JPHYSIOL.1973.SP010273>
- Bobinski, M., de Leon, M. J., Wegiel, J., DeSanti, S., Convit, A., Saint Louis, L. A., . . . Wisniewski, H. M. (1999). The histological validation of post mortem magnetic resonance imaging-determined hippocampal volume in Alzheimer's disease. *Neuroscience*, 95(3), 721-725. [https://doi.org/10.1016/S0306-4522\(99\)00476-5](https://doi.org/10.1016/S0306-4522(99)00476-5)
- Boccardi, V., Murasecco, I., & Mecocci, P. (2019). Diabetes drugs in the fight against Alzheimer's disease. *Ageing Research Reviews*, 54, 100936-100936. <https://doi.org/10.1016/j.arr.2019.100936>
- Boland, A., Huntzinger, E., Schmidt, S., Izaurralde, E., & Weichenrieder, O. (2011). Crystal structure of the MID-PIWI lobe of a eukaryotic Argonaute protein. *Proceedings of the National Academy of Sciences of the United States of America*, 108(26), 10466-10471. <https://doi.org/10.1073/pnas.1103946108>
- Bolmont, T., Clavaguera, F., Meyer-Luehmann, M., Herzog, M. C., Radde, R., Staufenbiel, M., . . . Jucker, M. (2007). Induction of Tau Pathology by Intracerebral Infusion of Amyloid- β -Containing Brain Extract and by Amyloid- β Deposition in APP \times Tau Transgenic Mice. *The American Journal of Pathology*, 171(6), 2012-2020. <https://doi.org/10.2353/ajpath.2007.070403>
- Borgdorff, A. J., & Choquet, D. (2002). Regulation of AMPA receptor lateral movements. *Nature*, 417(6889), 649-653. <https://doi.org/10.1038/nature00780>
- Borovac, J., Bosch, M., & Okamoto, K. (2018). Regulation of actin dynamics during structural plasticity of dendritic spines: Signaling messengers and actin-binding proteins. *Molecular*

- and Cellular Neuroscience*, 91, 122-130. <https://doi.org/10.1016/j.mcn.2018.07.001>
- Bosch, M., Castro, J., Saneyoshi, T., Matsuno, H., Sur, M., & Hayashi, Y. (2014). Structural and molecular remodeling of dendritic spine substructures during long-term potentiation. *Neuron*, 82(2), 444-459. <https://doi.org/10.1016/J.NEURON.2014.03.021>
- Braak, H., & Braak, E. (1991). Neuropathological stageing of Alzheimer-related changes. *Acta Neuropathologica*, 82(4), 239-259. <https://doi.org/10.1007/BF00308809>
- Braak, H., & Braak, E. (1997). Frequency of Stages of Alzheimer-Related Lesions in Different Age Categories. *Neurobiology of Aging*, 18(4), 351-357. [https://doi.org/10.1016/S0197-4580\(97\)00056-0](https://doi.org/10.1016/S0197-4580(97)00056-0)
- Branco, T., & Staras, K. (2009). The probability of neurotransmitter release: variability and feedback control at single synapses. *Nature Reviews Neuroscience*, 10(5), 373-383. <https://doi.org/10.1038/nrn2634>
- Braun, Joerg E., Huntzinger, E., Fauser, M., & Izaurralde, E. (2011). GW182 Proteins Directly Recruit Cytoplasmic Deadenylation Complexes to miRNA Targets. *Molecular Cell*, 44(1), 120-133. <https://doi.org/10.1016/j.molcel.2011.09.007>
- Bravo-Cordero, J. J., Magalhaes, M. A. O., Eddy, R. J., Hodgson, L., & Condeelis, J. (2013). Functions of cofilin in cell locomotion and invasion. *Nature Reviews Molecular Cell Biology*, 14(7), 405-415. <https://doi.org/10.1038/nrm3609>
- Bredt, D. S., & Nicoll, R. A. (2003). AMPA Receptor Trafficking at Excitatory Synapses. *Neuron*, 40(2), 361-379. [https://doi.org/10.1016/S0896-6273\(03\)00640-8](https://doi.org/10.1016/S0896-6273(03)00640-8)
- Brennan, C. M., & Steitz, J. A. (2001). HuR and mRNA stability. *Cellular and molecular life sciences : CMLS*, 58(2), 266-277. <https://doi.org/10.1007/PL00000854>
- Bridge, K. S., Shah, K. M., Li, Y., Foxler, D. E., Wong, S. C. K., Miller, D. C., . . . Sharp, T. V. (2017). Argonaute Utilization for miRNA Silencing Is Determined by Phosphorylation-Dependent Recruitment of LIM-Domain-Containing Proteins. *Cell reports*, 20(1), 173-187. <https://doi.org/10.1016/j.celrep.2017.06.027>
- Bronevetsky, Y., Villarino, A. V., Eisley, C. J., Barbeau, R., Barczak, A. J., Heinz, G. A., . . . Ansel, K. M. (2013). T cell activation induces proteasomal degradation of Argonaute and rapid remodeling of the microRNA repertoire. *The Journal of experimental medicine*, 210(2), 417-432. <https://doi.org/10.1084/jem.20111717>
- Buchan, J. R. (2014). mRNP granules. *RNA Biology*, 11(8), 1019-1030. <https://doi.org/10.4161/15476286.2014.972208>
- Burdick, D., Soreghan, B., Kwon, M., Kosmoski, J., Knauer, M., Henschen, A., . . . Glabe, C. (1992). Assembly and aggregation properties of synthetic Alzheimer's A4/beta amyloid peptide analogs. *The Journal of biological chemistry*, 267(1), 546-554.
- Burger, P. M., Hell, J., Mehl, E., Krasel, C., Lottspeich, F., & Jahn, R. (1991). GABA and glycine in synaptic vesicles: storage and transport characteristics. *Neuron*, 7(2), 287-293. [https://doi.org/10.1016/0896-6273\(91\)90267-4](https://doi.org/10.1016/0896-6273(91)90267-4)
- Burillo, J., Marqués, P., Jiménez, B., González-Blanco, C., Benito, M., & Guillén, C. (2021). Insulin Resistance and Diabetes Mellitus in Alzheimer's Disease. *Cells*, 10(5). <https://doi.org/10.3390/cells10051236>

- Cacace, R., Slegers, K., & Van Broeckhoven, C. (2016). Molecular genetics of early-onset Alzheimer's disease revisited. *Alzheimer's & Dementia*, 12(6), 733-748. <https://doi.org/10.1016/J.JALZ.2016.01.012>
- Cajigas, Iván J., Tushev, G., Will, Tristan J., tom Dieck, S., Fuerst, N., & Schuman, Erin M. (2012). The Local Transcriptome in the Synaptic Neuropil Revealed by Deep Sequencing and High-Resolution Imaging. *Neuron*, 74(3), 453-466. <https://doi.org/10.1016/j.neuron.2012.02.036>
- Calabrese, B., Shaked, G. M., Tabarean, I. V., Braga, J., Koo, E. H., & Halpain, S. (2007). Rapid, concurrent alterations in pre- and postsynaptic structure induced by naturally-secreted amyloid- β protein. *Molecular and Cellular Neuroscience*, 35(2), 183-193. <https://doi.org/10.1016/j.mcn.2007.02.006>
- Carlisle, H. J., & Kennedy, M. B. (2005). Spine architecture and synaptic plasticity. *Trends in Neurosciences*, 28(4), 182-187. <https://doi.org/10.1016/j.tins.2005.01.008>
- Carlson, M. D., Kish, P. E., & Ueda, T. (1989). Characterization of the solubilized and reconstituted ATP-dependent vesicular glutamate uptake system. *The Journal of biological chemistry*, 264(13), 7369-7376.
- Carter, S. F., Herholz, K., Rosa-Neto, P., Pellerin, L., Nordberg, A., & Zimmer, E. R. (2019). Astrocyte Biomarkers in Alzheimer's Disease. *Trends in Molecular Medicine*, 25(2), 77-95. <https://doi.org/10.1016/j.molmed.2018.11.006>
- Chater, T. E., & Goda, Y. (2014). The role of AMPA receptors in postsynaptic mechanisms of synaptic plasticity. *Frontiers in Cellular Neuroscience*, 8. <https://doi.org/10.3389/fncel.2014.00401>
- Chekulaeva, M., Mathys, H., Zipprich, J. T., Attig, J., Colic, M., Parker, R., & Filipowicz, W. (2011). miRNA repression involves GW182-mediated recruitment of CCR4-NOT through conserved W-containing motifs. *Nature structural & molecular biology*, 18(11), 1218-1226. <https://doi.org/10.1038/nsmb.2166>
- Chen, C.-Y., Gherzi, R., Ong, S.-E., Chan, E. L., Raijmakers, R., Pruijn, G. J. M., . . . Karin, M. (2001). AU Binding Proteins Recruit the Exosome to Degrade ARE-Containing mRNAs. *Cell*, 107(4), 451-464. [https://doi.org/10.1016/S0092-8674\(01\)00578-5](https://doi.org/10.1016/S0092-8674(01)00578-5)
- Chen, C.-Y. A., Zheng, D., Xia, Z., & Shyu, A.-B. (2009). Ago-TNRC6 triggers microRNA-mediated decay by promoting two deadenylation steps. *Nature structural & molecular biology*, 16(11), 1160-1166. <https://doi.org/10.1038/nsmb.1709>
- Chen, Q. S., Kagan, B. L., Hirakura, Y., & Xie, C. W. (2000). Impairment of hippocampal long-term potentiation by Alzheimer amyloid beta-peptides. *Journal of neuroscience research*, 60(1), 65-72. [https://doi.org/10.1002/\(SICI\)1097-4547\(20000401\)60:1<65::AID-JNR7>3.0.CO;2-Q](https://doi.org/10.1002/(SICI)1097-4547(20000401)60:1<65::AID-JNR7>3.0.CO;2-Q)
- Cheng, I. H., Searce-Levie, K., Legleiter, J., Palop, J. J., Gerstein, H., Bien-Ly, N., . . . Mucke, L. (2007). Accelerating Amyloid- β Fibrillization Reduces Oligomer Levels and Functional Deficits in Alzheimer Disease Mouse Models. *Journal of Biological Chemistry*, 282(33), 23818-23828. <https://doi.org/10.1074/JBC.M701078200>
- Cheng, T.-L., Wang, Z., Liao, Q., Zhu, Y., Zhou, W.-H., Xu, W., & Qiu, Z. (2014). MeCP2 Suppresses

- Nuclear MicroRNA Processing and Dendritic Growth by Regulating the DGCR8/Drosha Complex. *Developmental Cell*, 28(5), 547-560.
<https://doi.org/10.1016/j.devcel.2014.01.032>
- Chklovskii, D. B., Mel, B. W., & Svoboda, K. (2004). Cortical rewiring and information storage. *Nature*, 431(7010), 782-788. <https://doi.org/10.1038/nature03012>
- Cho, H., Choi, J. Y., Hwang, M. S., Kim, Y. J., Lee, H. M., Lee, H. S., . . . Lyoo, C. H. (2016). In vivo cortical spreading pattern of tau and amyloid in the Alzheimer disease spectrum. *Annals of Neurology*, 80(2), 247-258. <https://doi.org/10.1002/ana.24711>
- Choi, S. H., Kim, Y. H., Hebisch, M., Sliwinski, C., Lee, S., D'Avanzo, C., . . . Kim, D. Y. (2014). A three-dimensional human neural cell culture model of Alzheimer's disease. *Nature*, 515(7526), 274-278. <https://doi.org/10.1038/nature13800>
- Chowdhury, D., & Hell, J. W. (2018). Homeostatic synaptic scaling: molecular regulators of synaptic AMPA-type glutamate receptors. *F1000Research*, 7, 234-234.
<https://doi.org/10.12688/F1000RESEARCH.13561.1>
- Chuang, J. C., & Jones, P. A. (2007). Epigenetics and MicroRNAs. *Pediatric Research*, 61(5 Part 2), 24R-29R. <https://doi.org/10.1203/pdr.0b013e3180457684>
- Cingolani, L. A., & Goda, Y. (2008). Actin in action: the interplay between the actin cytoskeleton and synaptic efficacy. *Nature Reviews Neuroscience*, 9(5), 344-356.
<https://doi.org/10.1038/nrn2373>
- Citri, A., & Malenka, R. C. (2008). Synaptic plasticity: multiple forms, functions, and mechanisms. *Neuropsychopharmacology : official publication of the American College of Neuropsychopharmacology*, 33(1), 18-41. <https://doi.org/10.1038/sj.npp.1301559>
- Cleary, J. P., Walsh, D. M., Hofmeister, J. J., Shankar, G. M., Kuskowski, M. A., Selkoe, D. J., & Ashe, K. H. (2005). Natural oligomers of the amyloid- β protein specifically disrupt cognitive function. *Nature Neuroscience*, 8(1), 79-84. <https://doi.org/10.1038/nn1372>
- Cline, E. N., Bicca, M. A., Viola, K. L., & Klein, W. L. (2018). The Amyloid- β Oligomer Hypothesis: Beginning of the Third Decade. *Journal of Alzheimer's Disease*, 64(s1), S567-S610.
<https://doi.org/10.3233/JAD-179941>
- Collingridge, G. L., Isaac, J. T. R., & Wang, Y. T. (2004). Receptor trafficking and synaptic plasticity. *Nature Reviews Neuroscience*, 5(12), 952-962. <https://doi.org/10.1038/nrn1556>
- Conn, P. J., & Pin, J.-P. (1997). Pharmacology and functions of metabotropic glutamate receptors. *Annual Review of Pharmacology and Toxicology*, 37(1), 205-237.
<https://doi.org/10.1146/annurev.pharmtox.37.1.205>
- Corder, E. H., Saunders, A. M., Risch, N. J., Strittmatter, W. J., Schmechel, D. E., Gaskell, P. C., . . . Pericak-Vance, M. A. (1994). Protective effect of apolipoprotein E type 2 allele for late onset Alzheimer disease. *Nature Genetics*, 7(2), 180-184.
<https://doi.org/10.1038/ng0694-180>
- Cormier, R. J., & Kelly, P. T. (1996). Glutamate-induced long-term potentiation enhances spontaneous EPSC amplitude but not frequency. *Journal of neurophysiology*, 75(5), 1909-1918. <https://doi.org/10.1152/jn.1996.75.5.1909>
- Correia de Sousa, M., Gjorgjieva, M., Dolicka, D., Sobolewski, C., & Foti, M. (2019). Deciphering

- miRNAs' Action through miRNA Editing. *International journal of molecular sciences*, 20(24). <https://doi.org/10.3390/ijms20246249>
- Cui, T. J., & Joo, C. (2019). Facilitated diffusion of Argonaute-mediated target search. *RNA Biology*, 16(9), 1093-1107. <https://doi.org/10.1080/15476286.2019.1616353>
- Cui, T. J., Klein, M., Hegge, J. W., Chandradoss, S. D., Van Der Oost, J., Depken, M., & Joo, C. Argonaute bypasses cellular obstacles without hindrance during target search. <https://doi.org/10.1038/s41467-019-12415-y>
- Cummings, J. A., Mulkey, R. M., Nicoll, R. A., & Malenka, R. C. (1996). Ca²⁺ Signaling Requirements for Long-Term Depression in the Hippocampus. *Neuron*, 16(4), 825-833. [https://doi.org/10.1016/S0896-6273\(00\)80102-6](https://doi.org/10.1016/S0896-6273(00)80102-6)
- Czech, B., & Hannon, G. J. (2011). Small RNA sorting: matchmaking for Argonautes. *Nature reviews. Genetics*, 12(1), 19-31. <https://doi.org/10.1038/nrg2916>
- D'Avanzo, C., Aronson, J., Kim, Y. H., Choi, S. H., Tanzi, R. E., & Kim, D. Y. (2015). Alzheimer's in 3D culture: Challenges and perspectives. *BioEssays*, 37(10), 1139-1148. <https://doi.org/10.1002/bies.201500063>
- Dalby, B. (2004). Advanced transfection with Lipofectamine 2000 reagent: primary neurons, siRNA, and high-throughput applications. *Methods*, 33(2), 95-103. <https://doi.org/10.1016/j.ymeth.2003.11.023>
- Dan, C., Kelly, A., Bernard, O., & Minden, A. (2001). Cytoskeletal Changes Regulated by the PAK4 Serine/Threonine Kinase Are Mediated by LIM Kinase 1 and Cofilin. *Journal of Biological Chemistry*, 276(34), 32115-32121. <https://doi.org/10.1074/jbc.M100871200>
- Daugaard, I., & Hansen, T. B. (2017). Biogenesis and Function of Ago-Associated RNAs. *Trends in Genetics*, 33(3), 208-219. <https://doi.org/10.1016/j.tig.2017.01.003>
- Davis, R. C., Marsden, I. T., Maloney, M. T., Minamide, L. S., Podlisny, M., Selkoe, D. J., & Bamberg, J. R. (2011). Amyloid beta dimers/trimers potently induce cofilin-actin rods that are inhibited by maintaining cofilin-phosphorylation. *Molecular Neurodegeneration*, 6(1), 10-10. <https://doi.org/10.1186/1750-1326-6-10>
- De Felice, F. G., Velasco, P. T., Lambert, M. P., Viola, K., Fernandez, S. J., Ferreira, S. T., & Klein, W. L. (2007). Aβ Oligomers Induce Neuronal Oxidative Stress through an N-Methyl-D-aspartate Receptor-dependent Mechanism That Is Blocked by the Alzheimer Drug Memantine. *Journal of Biological Chemistry*, 282(15), 11590-11601. <https://doi.org/10.1074/jbc.M607483200>
- De Wilde, M. C., Overk, C. R., Sijben, J. W., & Masliah, E. (2016). Meta-analysis of synaptic pathology in Alzheimer's disease reveals selective molecular vesicular machinery vulnerability. *Alzheimer's & dementia : the journal of the Alzheimer's Association*, 12(6), 633-644. <https://doi.org/10.1016/J.JALZ.2015.12.005>
- Decker, H., Lo, K. Y., Unger, S. M., Ferreira, S. T., & Silverman, M. A. (2010). Amyloid- Peptide Oligomers Disrupt Axonal Transport through an NMDA Receptor-Dependent Mechanism That Is Mediated by Glycogen Synthase Kinase 3 in Primary Cultured Hippocampal Neurons. *Journal of Neuroscience*, 30(27), 9166-9171. <https://doi.org/10.1523/JNEUROSCI.1074-10.2010>

- DeKosky, S. T., & Scheff, S. W. (1990). Synapse loss in frontal cortex biopsies in Alzheimer's disease: correlation with cognitive severity. *Annals of neurology*, 27(5), 457-464. <https://doi.org/10.1002/ANA.410270502>
- DeKosky, S. T., Scheff, S. W., & Styren, S. D. (1996). Structural correlates of cognition in dementia: quantification and assessment of synapse change. *Neurodegeneration : a journal for neurodegenerative disorders, neuroprotection, and neuroregeneration*, 5(4), 417-421. <https://doi.org/10.1006/NEUR.1996.0056>
- Del Turco, D., Paul, M. H., Schlaudraff, J., Hick, M., Endres, K., Müller, U. C., & Deller, T. (2016). Region-Specific Differences in Amyloid Precursor Protein Expression in the Mouse Hippocampus. *Frontiers in Molecular Neuroscience*, 9. <https://doi.org/10.3389/fnmol.2016.00134>
- Deng, Y., Wei, J., Cheng, J., Zhong, P., Xiong, Z., Liu, A., . . . Yan, Z. (2016). Partial Amelioration of Synaptic and Cognitive Deficits by Inhibiting Cofilin Dephosphorylation in an Animal Model of Alzheimer's Disease. *Journal of Alzheimer's disease : JAD*, 53(4), 1419-1432. <https://doi.org/10.3233/JAD-160167>
- Derkach, V., Barria, A., & Soderling, T. R. (1999). Ca²⁺/calmodulin-kinase II enhances channel conductance of α -amino-3-hydroxy-5-methyl-4-isoxazolepropionate type glutamate receptors. *Proceedings of the National Academy of Sciences*, 96(6), 3269-3274. <https://doi.org/10.1073/pnas.96.6.3269>
- Derkach, V. A., Oh, M. C., Guire, E. S., & Soderling, T. R. (2007). Regulatory mechanisms of AMPA receptors in synaptic plasticity. *Nature Reviews Neuroscience*, 8(2), 101-113. <https://doi.org/10.1038/nrn2055>
- Dias, Brian G., Goodman, Jared V., Ahluwalia, R., Easton, Audrey E., Andero, R., & Ressler, Kerry J. (2014). Amygdala-Dependent Fear Memory Consolidation via miR-34a and Notch Signaling. *Neuron*, 83(4), 906-918. <https://doi.org/10.1016/j.neuron.2014.07.019>
- Dinamarca, M. C., Weinstein, D., Monasterio, O., & Inestrosa, N. C. (2011). The Synaptic Protein Neuroligin-1 Interacts with the Amyloid β -Peptide. Is There a Role in Alzheimer's Disease? *Biochemistry*, 50(38), 8127-8137. <https://doi.org/10.1021/bi201246t>
- Dominguez, R., & Holmes, K. C. (2011). Actin structure and function. *Annual review of biophysics*, 40, 169-186. <https://doi.org/10.1146/annurev-biophys-042910-155359>
- Dong, Z., Bai, Y., Wu, X., Li, H., Gong, B., Howland, J. G., . . . Wang, Y. T. (2013). Hippocampal long-term depression mediates spatial reversal learning in the Morris water maze. *Neuropharmacology*, 64, 65-73. <https://doi.org/10.1016/j.neuropharm.2012.06.027>
- Dong, Z., Gong, B., Li, H., Bai, Y., Wu, X., Huang, Y., . . . Wang, Y. T. (2012). Mechanisms of hippocampal long-term depression are required for memory enhancement by novelty exploration. *The Journal of neuroscience : the official journal of the Society for Neuroscience*, 32(35), 11980-11990. <https://doi.org/10.1523/JNEUROSCI.0984-12.2012>
- Dorostkar, M. M., Zou, C., Blazquez-Llorca, L., & Herms, J. (2015). Analyzing dendritic spine pathology in Alzheimer's disease: problems and opportunities. *Acta Neuropathol*, 3, 1-19. <https://doi.org/10.1007/s00401-015-1449-5>
- Drinnenberg, I. A., Weinberg, D. E., Xie, K. T., Mower, J. P., Wolfe, K. H., Fink, G. R., & Bartel, D. P.

- (2009). RNAi in budding yeast. *Science (New York, N.Y.)*, 326(5952), 544-544. <https://doi.org/10.1126/SCIENCE.1176945>
- Du, T., & Zamore, P. D. (2005). microPrimer: the biogenesis and function of microRNA. *Development*, 132(21), 4645-4652. <https://doi.org/10.1242/dev.02070>
- Duffney, L. J., Zhong, P., Wei, J., Matas, E., Cheng, J., Qin, L., . . . Yan, Z. (2015). Autism-like Deficits in Shank3-Deficient Mice Are Rescued by Targeting Actin Regulators. *Cell reports*, 11(9), 1400-1413. <https://doi.org/10.1016/j.celrep.2015.04.064>
- Edbauer, D., Neilson, J. R., Foster, K. A., Wang, C.-F., Seeburg, D. P., Batterton, M. N., . . . Sheng, M. (2010). Regulation of Synaptic Structure and Function by FMRP-Associated MicroRNAs miR-125b and miR-132. *Neuron*, 65(3), 373-384. <https://doi.org/10.1016/j.neuron.2010.01.005>
- Ehlers, M. D. (2000). Reinsertion or degradation of AMPA receptors determined by activity-dependent endocytic sorting. *Neuron*, 28(2), 511-525. [https://doi.org/10.1016/s0896-6273\(00\)00129-x](https://doi.org/10.1016/s0896-6273(00)00129-x)
- Eichhorn, S. W., Guo, H., McGeary, S. E., Rodriguez-Mias, R. A., Shin, C., Baek, D., . . . Bartel, D. P. (2014). mRNA destabilization is the dominant effect of mammalian microRNAs by the time substantial repression ensues. *Molecular cell*, 56(1), 104-115. <https://doi.org/10.1016/j.molcel.2014.08.028>
- Endo, M., Ohashi, K., Sasaki, Y., Goshima, Y., Niwa, R., Uemura, T., & Mizuno, K. (2003). Control of Growth Cone Motility and Morphology by LIM Kinase and Slingshot via Phosphorylation and Dephosphorylation of Cofilin. *The Journal of Neuroscience*, 23(7), 2527-2537. <https://doi.org/10.1523/JNEUROSCI.23-07-02527.2003>
- Engert, F., & Bonhoeffer, T. (1999). Dendritic spine changes associated with hippocampal long-term synaptic plasticity. *Nature*, 399(6731), 66-70. <https://doi.org/10.1038/19978>
- Esparza, T. J., Zhao, H., Cirrito, J. R., Cairns, N. J., Bateman, R. J., Holtzman, D. M., & Brody, D. L. (2013). Amyloid-beta oligomerization in Alzheimer dementia versus high-pathology controls. *Annals of Neurology*, 73(1), 104-119. <https://doi.org/10.1002/ana.23748>
- Esquerda-Canals, G., Montoliu-Gaya, L., Güell-Bosch, J., & Villegas, S. (2017). Mouse Models of Alzheimer's Disease. *Journal of Alzheimer's Disease*, 57, 1171-1183. <https://doi.org/10.3233/JAD-170045>
- Fabian, M. R., Cieplak, M. K., Frank, F., Morita, M., Green, J., Srikumar, T., . . . Sonenberg, N. (2011). miRNA-mediated deadenylation is orchestrated by GW182 through two conserved motifs that interact with CCR4-NOT. *Nature structural & molecular biology*, 18(11), 1211-1217. <https://doi.org/10.1038/nsmb.2149>
- Fagan, A. M., Watson, M., Parsadanian, M., Bales, K. R., Paul, S. M., & Holtzman, D. M. (2002). Human and Murine ApoE Markedly Alters A β Metabolism before and after Plaque Formation in a Mouse Model of Alzheimer's Disease. *Neurobiology of Disease*, 9(3), 305-318. <https://doi.org/10.1006/NBDI.2002.0483>
- Ferreira, D., Nordberg, A., & Westman, E. (2020). Biological subtypes of Alzheimer disease. *Neurology*, 94(10), 436-448. <https://doi.org/10.1212/WNL.0000000000009058>
- Ferreira, D., Perestelo-Pañez, L., Westman, E., Wahlund, L.-O., Sarráa, A., & Serrano-Aguilar, P.

- (2014). Meta-Review of CSF Core Biomarkers in Alzheimer's Disease: The State-of-the-Art after the New Revised Diagnostic Criteria. *Frontiers in Aging Neuroscience*, 6. <https://doi.org/10.3389/fnagi.2014.00047>
- Ferrone, F. (1999). [17] Analysis of protein aggregation kinetics. In (pp. 256-274). [https://doi.org/10.1016/S0076-6879\(99\)09019-9](https://doi.org/10.1016/S0076-6879(99)09019-9)
- Fiala, J. C., Feinberg, M., Popov, V., & Harris, K. M. (1998). Synaptogenesis Via Dendritic Filopodia in Developing Hippocampal Area CA1. *The Journal of Neuroscience*, 18(21), 8900-8911. <https://doi.org/10.1523/JNEUROSCI.18-21-08900.1998>
- Fiore, R., Khudayberdiev, S., Christensen, M., Siegel, G., Flavell, S. W., Kim, T.-K., . . . Schratt, G. (2009). Mef2-mediated transcription of the miR379–410 cluster regulates activity-dependent dendritogenesis by fine-tuning Pumilio2 protein levels. *The EMBO Journal*, 28(6), 697-710. <https://doi.org/10.1038/emboj.2009.10>
- Fiore, R., Rajman, M., Schwale, C., Bicker, S., Antoniou, A., Bruehl, C., . . . Schratt, G. (2014). MiR-134-dependent regulation of Pumilio-2 is necessary for homeostatic synaptic depression. *The EMBO journal*, 33(19), 2231-2246. <https://doi.org/10.15252/embj.201487921>
- Fisher, E. M. C., Wiseman, F. K., Tosh, J. L., Rickman, M., Rhymes, E., Norona, F. E., . . . Isaacs, A. M. (2017). The integration site of the APP transgene in the J20 mouse model of Alzheimer's disease. *Wellcome Open Research*, 2. <https://doi.org/10.12688/WELLCOMEOPENRES.12237.2>
- Foletta, V. C., Moussi, N., Sarmiere, P. D., Bamburg, J. R., & Bernard, O. (2004). LIM kinase 1, a key regulator of actin dynamics, is widely expressed in embryonic and adult tissues. *Experimental Cell Research*, 294(2), 392-405. <https://doi.org/10.1016/j.yexcr.2003.11.024>
- Fontana, I. C., Zimmer, A. R., Rocha, A. S., Gosmann, G., Souza, D. O., Lourenco, M. V., . . . Zimmer, E. R. (2020). Amyloid- β oligomers in cellular models of Alzheimer's disease. *Journal of neurochemistry*, 155(4), 348-369. <https://doi.org/10.1111/jnc.15030>
- Frey, U., & Morris, R. G. M. (1997). Synaptic tagging and long-term potentiation. *Nature*, 385(6616), 533-536. <https://doi.org/10.1038/385533a0>
- Friedman, R. C., Farh, K. K.-H., Burge, C. B., & Bartel, D. P. (2009). Most mammalian mRNAs are conserved targets of microRNAs. *Genome Research*, 19(1), 92-105. <https://doi.org/10.1101/gr.082701.108>
- Frisoni, G. B., Prestia, A., Rasser, P. E., Bonetti, M., & Thompson, P. M. (2009). In vivo mapping of incremental cortical atrophy from incipient to overt Alzheimer's disease. *Journal of Neurology*, 256(6), 916-924. <https://doi.org/10.1007/S00415-009-5040-7/TABLES/3>
- Fujino, T., Leslie, J. H., Eavri, R., Chen, J. L., Lin, W. C., Flanders, G. H., . . . Nedivi, E. (2011). CPG15 regulates synapse stability in the developing and adult brain. *Genes & Development*, 25(24), 2674-2685. <https://doi.org/10.1101/gad.176172.111>
- Games, D., Adams, D., Alessandrini, R., Barbour, R., Borthellette, P., Blackwell, C., . . . Zhao, J. (1995). Alzheimer-type neuropathology in transgenic mice overexpressing V717F β -amyloid precursor protein. *Nature* 1995 373:6514, 373(6514), 523-527. <https://doi.org/10.1038/373523a0>

- Gandy, S., Simon, A. J., Steele, J. W., Lublin, A. L., Lah, J. J., Walker, L. C., . . . Ehrlich, M. E. (2010). Days to criterion as an indicator of toxicity associated with human Alzheimer amyloid- β oligomers. *Annals of Neurology*, n/a-n/a. <https://doi.org/10.1002/ana.22052>
- Gao, J., Wang, W.-Y., Mao, Y.-W., Gräff, J., Guan, J.-S., Pan, L., . . . Tsai, L.-H. (2010). A novel pathway regulates memory and plasticity via SIRT1 and miR-134. *Nature*, 466(7310), 1105-1109. <https://doi.org/10.1038/nature09271>
- García-López, P., García-Marín, V., & Freire, M. (2007). The discovery of dendritic spines by Cajal in 1888 and its relevance in the present neuroscience. *Progress in Neurobiology*, 83(2), 110-130. <https://doi.org/10.1016/j.pneurobio.2007.06.002>
- Garvalov, B. K., Flynn, K. C., Neukirchen, D., Meyn, L., Teusch, N., Wu, X., . . . Bradke, F. (2007). Cdc42 Regulates Cofilin during the Establishment of Neuronal Polarity. *Journal of Neuroscience*, 27(48), 13117-13129. <https://doi.org/10.1523/JNEUROSCI.3322-07.2007>
- Garza-Manero, S., Pichardo-Casas, I., Arias, C., Vaca, L., & Zepeda, A. (2014). Selective distribution and dynamic modulation of miRNAs in the synapse and its possible role in Alzheimer's Disease. *Brain research*, 1584, 80-93. <https://doi.org/10.1016/j.brainres.2013.12.009>
- Gauthier, S. R.-N. P. M. J. A. W. C. (2021). *World Alzheimer Report 2021: Journey through the diagnosis of dementia*.
- Gebert, L. F. R., & MacRae, I. J. (2019). Regulation of microRNA function in animals. *Nature Reviews Molecular Cell Biology*, 20(1), 21-37. <https://doi.org/10.1038/s41580-018-0045-7>
- Gerlai, R., Fitch, T., Bales, K. R., & Gitter, B. D. (2002). Behavioral impairment of APPV717F mice in fear conditioning: is it only cognition? *Behavioural Brain Research*, 136(2), 503-509. [https://doi.org/10.1016/S0166-4328\(02\)00198-5](https://doi.org/10.1016/S0166-4328(02)00198-5)
- Ghibaudi, M., Boido, M., & Vercelli, A. (2017). Functional integration of complex miRNA networks in central and peripheral lesion and axonal regeneration. *Progress in Neurobiology*, 158, 69-93. <https://doi.org/10.1016/j.pneurobio.2017.07.005>
- Gilley, J., Seereeram, A., Ando, K., Mosely, S., Andrews, S., Kerschensteiner, M., . . . Coleman, M. P. (2012). Age-dependent axonal transport and locomotor changes and tau hypophosphorylation in a "P301L" tau knockin mouse. *Neurobiology of Aging*, 33(3), 621.e621-621.e615. <https://doi.org/10.1016/j.neurobiolaging.2011.02.014>
- Giuditta, A., Dettbarn, W. D., & Brzin, M. (1968). Protein synthesis in the isolated giant axon of the squid. *Proceedings of the National Academy of Sciences of the United States of America*, 59(4), 1284-1287. <https://doi.org/10.1073/pnas.59.4.1284>
- Giusti, S. A., Vogl, A. M., Brockmann, M. M., Vercelli, C. A., Rein, M. L., Trümbach, D., . . . Refojo, D. (2014). MicroRNA-9 controls dendritic development by targeting REST. *eLife*, 3. <https://doi.org/10.7554/eLife.02755>
- Gjorgjieva, M., Sobolewski, C., Dolicka, D., Correia de Sousa, M., & Foti, M. (2019). miRNAs and NAFLD: from pathophysiology to therapy. *Gut*, 68(11), 2065-2079. <https://doi.org/10.1136/gutjnl-2018-318146>
- Golde, T. E., Estus, S., Younkin, L. H., Selkoe, D. J., & Younkin, S. G. (1992). Processing of the

- Amyloid Protein Precursor to Potentially Amyloidogenic Derivatives. *Science*, 255(5045), 728-730. <https://doi.org/10.1126/science.1738847>
- Golden, R. J., Chen, B., Li, T., Braun, J., Manjunath, H., Chen, X., . . . Mendell, J. T. (2017). An Argonaute phosphorylation cycle promotes microRNA-mediated silencing. *Nature*, 542(7640), 197-202. <https://doi.org/10.1038/nature21025>
- Götz, J., Chen, F., van Dorpe, J., & Nitsch, R. M. (2001). Formation of Neurofibrillary Tangles in P301L Tau Transgenic Mice Induced by A β 42 Fibrils. *Science*, 293(5534), 1491-1495. <https://doi.org/10.1126/science.1062097>
- Gralle, M., & Ferreira, S. T. (2007). Structure and functions of the human amyloid precursor protein: The whole is more than the sum of its parts. *Progress in Neurobiology*, 82(1), 11-32. <https://doi.org/10.1016/j.pneurobio.2007.02.001>
- Gray, E. G. (1959). Electron Microscopy of Synaptic Contacts on Dendrite Spines of the Cerebral Cortex. *Nature*, 183(4675), 1592-1593. <https://doi.org/10.1038/1831592a0>
- Gu, J., Lee, C. W., Fan, Y., Komlos, D., Tang, X., Sun, C., . . . Zheng, J. Q. (2010). ADF/cofilin-mediated actin dynamics regulate AMPA receptor trafficking during synaptic plasticity. *Nature Neuroscience*, 13(10), 1208-1215. <https://doi.org/10.1038/nn.2634>
- Guerreiro, R., Wojtas, A., Bras, J., Carrasquillo, M., Rogaeva, E., Majounie, E., . . . Alzheimer Genetic Analysis, G. (2013). TREM2 variants in Alzheimer's disease. *The New England journal of medicine*, 368(2), 117-127. <https://doi.org/10.1056/NEJMoa1211851>
- Guerreiro, R. J., Baquero, M., Blesa, R., Boada, M., Brás, J. M., Bullido, M. J., . . . Clarimón, J. (2010). Genetic screening of Alzheimer's disease genes in Iberian and African samples yields novel mutations in presenilins and APP. *Neurobiology of Aging*, 31(5), 725-731. <https://doi.org/10.1016/j.neurobiolaging.2008.06.012>
- Gurvits, T. V., Shenton, M. E., Hokama, H., Ohta, H., Lasko, N. B., Gilbertson, M. W., . . . Pitman, R. K. (1996). Magnetic resonance imaging study of hippocampal volume in chronic, combat-related posttraumatic stress disorder. *Biological Psychiatry*, 40(11), 1091-1099. [https://doi.org/10.1016/S0006-3223\(96\)00229-6](https://doi.org/10.1016/S0006-3223(96)00229-6)
- Götz, J., Bodea, L. G., & Goedert, M. (2018). Rodent models for Alzheimer disease. *Nature Reviews Neuroscience* 2018 19:10, 19(10), 583-598. <https://doi.org/10.1038/s41583-018-0054-8>
- Hafner, A.-S., Donlin-Asp, P. G., Leitch, B., Herzog, E., & Schuman, E. M. (2019). Local protein synthesis is a ubiquitous feature of neuronal pre- and postsynaptic compartments. *Science*, 364(6441). <https://doi.org/10.1126/science.aau3644>
- Halasz, E., Townes-Anderson, E., & Wang, W. (2020). LIM kinases in synaptic plasticity and their potential as therapeutic targets. In *Neural Regeneration Research* (Vol. 15, pp. 1471-1472): Wolters Kluwer Medknow Publications.
- Hanley, J. G. (2014). Actin-dependent mechanisms in AMPA receptor trafficking. *Frontiers in Cellular Neuroscience*, 8. <https://doi.org/10.3389/fncel.2014.00381>
- Hanley, J. G. (2021). Regulation of AMPAR expression by microRNAs. *Neuropharmacology*, 197, 108723-108723. <https://doi.org/10.1016/j.neuropharm.2021.108723>
- Hansen, D. V., Hanson, J. E., & Sheng, M. (2018). Microglia in Alzheimer's disease. *Journal of Cell*

- Biology*, 217(2), 459-472. <https://doi.org/10.1083/jcb.201709069>
- Hansson, O., Lehmann, S., Otto, M., Zetterberg, H., & Lewczuk, P. (2019). Advantages and disadvantages of the use of the CSF Amyloid β (A β) 42/40 ratio in the diagnosis of Alzheimer's Disease. *Alzheimer's Research & Therapy*, 11(1), 34-34. <https://doi.org/10.1186/s13195-019-0485-0>
- Hardy, J., & Selkoe, D. J. (2002). The amyloid hypothesis of Alzheimer's disease: Progress and problems on the road to therapeutics. In *Science* (Vol. 297, pp. 353-356).
- Hardy, J. A., & Higgins, G. A. (1992). Alzheimer's Disease: The Amyloid Cascade Hypothesis. *Science*, 256(5054), 184-185. <https://doi.org/10.1126/science.1566067>
- Harold, D., Abraham, R., Hollingworth, P., Sims, R., Gerrish, A., Hamshere, M. L., . . . Williams, J. (2009). Genome-wide association study identifies variants at CLU and PICALM associated with Alzheimer's disease. *Nature Genetics*, 41(10), 1088-1093. <https://doi.org/10.1038/ng.440>
- Harris, K. M., & Kater, S. B. (1994). Dendritic Spines: Cellular Specializations Imparting Both Stability and Flexibility to Synaptic Function. *Annual Review of Neuroscience*, 17(1), 341-371. <https://doi.org/10.1146/annurev.ne.17.030194.002013>
- Hayashi, Y., & Majewska, A. K. (2005). Dendritic Spine Geometry: Functional Implication and Regulation. *Neuron*, 46(4), 529-532. <https://doi.org/10.1016/j.neuron.2005.05.006>
- Hayashi, Y., Shi, S.-H., Esteban, J. A., Piccini, A., Poncer, J.-C., & Malinow, R. (2000). Driving AMPA Receptors into Synapses by LTP and CaMKII: Requirement for GluR1 and PDZ Domain Interaction. *Science*, 287(5461), 2262-2267. <https://doi.org/10.1126/science.287.5461.2262>
- Hebb, D. O. (1949). *The organization of behavior; a neuropsychological theory*. Wiley.
- Heidelberger, R., Heinemann, C., Neher, E., & Matthews, G. (1994). Calcium dependence of the rate of exocytosis in a synaptic terminal. *Nature*, 371(6497), 513-515. <https://doi.org/10.1038/371513a0>
- Henderson, B. W., Gentry, E. G., Rush, T., Troncoso, J. C., Thambisetty, M., Montine, T. J., & Herskowitz, J. H. (2016). Rho-associated protein kinase 1 (ROCK1) is increased in Alzheimer's disease and ROCK1 depletion reduces amyloid- β levels in brain. *Journal of neurochemistry*, 138(4), 525-531. <https://doi.org/10.1111/jnc.13688>
- Henderson, B. W., Greathouse, K. M., Ramdas, R., Walker, C. K., Rao, T. C., Bach, S. V., . . . Herskowitz, J. H. (2019). *Pharmacologic inhibition of LIMK1 provides dendritic spine resilience against α -amyloid* (Sci. Signal, Issue. <https://www.science.org>
- Hepler, R. W., Grimm, K. M., Nahas, D. D., Breese, R., Dodson, E. C., Acton, P., . . . Joyce, J. G. (2006). Solution state characterization of amyloid beta-derived diffusible ligands. *Biochemistry*, 45(51), 15157-15167. <https://doi.org/10.1021/bi061850f>
- Herculano-Houzel, S. (2012). The remarkable, yet not extraordinary, human brain as a scaled-up primate brain and its associated cost. *Proceedings of the National Academy of Sciences*, 109(supplement_1), 10661-10668. <https://doi.org/10.1073/pnas.1201895109>
- Heredia, L., Helguera, P., De Olmos, S., Kedikian, G., Vigo, F. S., LaFerla, F., . . . Lorenzo, A. (2006). Phosphorylation of Actin-Depolymerizing Factor/Cofilin by LIM-Kinase Mediates Amyloid

- β -Induced Degeneration: A Potential Mechanism of Neuronal Dystrophy in Alzheimer's Disease. *The Journal of Neuroscience*, 26(24), 6533-6533.
<https://doi.org/10.1523/JNEUROSCI.5567-05.2006>
- Hershko, A., & Ciechanover, A. (1998). The ubiquitin system. *Annual review of biochemistry*, 67, 425-479. <https://doi.org/10.1146/annurev.biochem.67.1.425>
- Heuser, J. E., Reese, T. S., Dennis, M. J., Jan, Y., Jan, L., & Evans, L. (1979). Synaptic vesicle exocytosis captured by quick freezing and correlated with quantal transmitter release. *Journal of Cell Biology*, 81(2), 275-300. <https://doi.org/10.1083/jcb.81.2.275>
- Hilfiker, S., Greengard, P., & Augustine, G. J. (1999). Coupling calcium to SNARE-mediated synaptic vesicle fusion. *Nature Neuroscience*, 2(2), 104-106.
<https://doi.org/10.1038/5659>
- Hippius, H., & Neundörfer, G. (2003). The discovery of Alzheimer's disease. *Dialogues in Clinical Neuroscience*, 5(1), 101-108. <https://doi.org/10.31887/DCNS.2003.5.1/hippius>
- Hlushchenko, I., Koskinen, M., & Hotulainen, P. (2016). Dendritic spine actin dynamics in neuronal maturation and synaptic plasticity. *Cytoskeleton*, 73(9), 435-441.
<https://doi.org/10.1002/cm.21280>
- Hoffmann, L., Rust, M. B., & Culmsee, C. (2019). Actin(g) on mitochondria - a role for cofilin1 in neuronal cell death pathways. *Biological chemistry*, 400(9), 1089-1097.
<https://doi.org/10.1515/hsz-2019-0120>
- Holstege, H., van der Lee, S. J., Hulsman, M., Wong, T. H., van Rooij, J. G. J., Weiss, M., . . . Scheltens, P. (2017). Characterization of pathogenic SORL1 genetic variants for association with Alzheimer's disease: a clinical interpretation strategy. *European Journal of Human Genetics*, 25(8), 973-981. <https://doi.org/10.1038/ejhg.2017.87>
- Hong, S., Beja-Glasser, V. F., Nfonoyim, B. M., Frouin, A., Li, S., Ramakrishnan, S., . . . Stevens, B. Complement and Microglia Mediate Early Synapse Loss in Alzheimer Mouse Models HHS Public Access. <https://doi.org/10.1126/science.aad8373>
- Hong, S., Beja-Glasser, V. F., Nfonoyim, B. M., Frouin, A., Li, S., Ramakrishnan, S., . . . Stevens, B. (2016). Complement and microglia mediate early synapse loss in Alzheimer mouse models. *Science (New York, N.Y.)*, 352(6286), 712-716.
<https://doi.org/10.1126/science.aad8373>
- Honkura, N., Matsuzaki, M., Noguchi, J., Ellis-Davies, G. C. R., & Kasai, H. (2008). The Subspine Organization of Actin Fibers Regulates the Structure and Plasticity of Dendritic Spines. *Neuron*, 57(5), 719-729. <https://doi.org/10.1016/J.NEURON.2008.01.013>
- Hoogenraad, C. C., Akhmanova, A., Galjart, N., & De Zeeuw, C. I. (2004). LIMK1 and CLIP-115: linking cytoskeletal defects to Williams syndrome. *BioEssays : news and reviews in molecular, cellular and developmental biology*, 26(2), 141-150.
<https://doi.org/10.1002/bies.10402>
- Horman, S. R., Janas, M. M., Litterst, C., Wang, B., MacRae, I. J., Sever, M. J., . . . Orth, A. P. (2013). Akt-mediated phosphorylation of Argonaute 2 down-regulates cleavage and up-regulates translational repression of microRNA targets. *Molecular cell*, 50(3), 356-356.
<https://doi.org/10.1016/J.MOLCEL.2013.03.015>

- Hotulainen, P., & Hoogenraad, C. C. (2010). Actin in dendritic spines: connecting dynamics to function. *Journal of Cell Biology*, 189(4), 619-629.
<https://doi.org/10.1083/jcb.201003008>
- Hotulainen, P., Llano, O., Smirnov, S., Tanhuanpää, K., Faix, J., Rivera, C., & Lappalainen, P. (2009). Defining mechanisms of actin polymerization and depolymerization during dendritic spine morphogenesis. *Journal of Cell Biology*, 185(2), 323-339.
<https://doi.org/10.1083/jcb.200809046>
- Hotulainen, P., Paunola, E., Vartiainen, M. K., & Lappalainen, P. (2005). Actin-depolymerizing Factor and Cofilin-1 Play Overlapping Roles in Promoting Rapid F-Actin Depolymerization in Mammalian Nonmuscle Cells. *Molecular Biology of the Cell*, 16(2), 649-664.
<https://doi.org/10.1091/mbc.e04-07-0555>
- Hsiao, K., Chapman, P., Nilsen, S., Eckman, C., Harigaya, Y., Younkin, S., . . . Cole, G. (1996). Correlative memory deficits, Abeta elevation, and amyloid plaques in transgenic mice. *Science (New York, N.Y.)*, 274(5284), 99-102.
<https://doi.org/10.1126/SCIENCE.274.5284.99>
- Hsieh, H., Boehm, J., Sato, C., Iwatsubo, T., Tomita, T., Sisodia, S., & Malinow, R. (2006). AMPAR Removal Underlies A β -Induced Synaptic Depression and Dendritic Spine Loss. *Neuron*, 52(5), 831-843. <https://doi.org/10.1016/j.neuron.2006.10.035>
- Hsu, H. W., Rodriguez-Ortiz, C. J., Lim, S. L., Zumkehr, J., Kilian, J. G., Vidal, J., & Kitazawa, M. (2019). Copper-Induced Upregulation of MicroRNAs Directs the Suppression of Endothelial LRP1 in Alzheimer's Disease Model. *Toxicological Sciences*, 170(1), 144-144.
<https://doi.org/10.1093/TOXSCI/KFZ084>
- Hsu, R., Schofield, C. M., Dela Cruz, C. G., Jones-Davis, D. M., Bbleloch, R., & Ullian, E. M. (2012). Loss of microRNAs in pyramidal neurons leads to specific changes in inhibitory synaptic transmission in the prefrontal cortex. *Molecular and Cellular Neuroscience*, 50(3-4), 283-292. <https://doi.org/10.1016/j.mcn.2012.06.002>
- Hu, Z., & Li, Z. (2017). miRNAs in synapse development and synaptic plasticity. *Current Opinion in Neurobiology*, 45, 24-31. <https://doi.org/10.1016/j.conb.2017.02.014>
- Hu, Z., Yu, D., Gu, Q.-h., Yang, Y., Tu, K., Zhu, J., & Li, Z. (2014). miR-191 and miR-135 are required for long-lasting spine remodelling associated with synaptic long-term depression. *Nature communications*, 5, 3263-3263. <https://doi.org/10.1038/ncomms4263>
- Hu, Z., Zhao, J., Hu, T., Luo, Y., Zhu, J., & Li, Z. (2015). miR-501-3p mediates the activity-dependent regulation of the expression of AMPA receptor subunit GluA1. *The Journal of cell biology*, 208(7), 949-959. <https://doi.org/10.1083/jcb.201404092>
- Hwang, J.-Y., Kaneko, N., Noh, K.-M., Pontarelli, F., & Zukin, R. S. (2014). The gene silencing transcription factor REST represses miR-132 expression in hippocampal neurons destined to die. *Journal of molecular biology*, 426(20), 3454-3466.
<https://doi.org/10.1016/j.jmb.2014.07.032>
- Ichetovkin, I., Grant, W., & Condeelis, J. (2002). Cofilin Produces Newly Polymerized Actin Filaments that Are Preferred for Dendritic Nucleation by the Arp2/3 Complex. *Current Biology*, 12(1), 79-84. [https://doi.org/10.1016/S0960-9822\(01\)00629-7](https://doi.org/10.1016/S0960-9822(01)00629-7)

- Impey, S., Davare, M., Lesiak, A., Lasiek, A., Fortin, D., Ando, H., . . . Wayman, G. A. (2010). An activity-induced microRNA controls dendritic spine formation by regulating Rac1-PAK signaling. *Molecular and cellular neurosciences*, 43(1), 146-156. <https://doi.org/10.1016/j.mcn.2009.10.005>
- Ingelsson, M., Fukumoto, H., Newell, K. L., Growdon, J. H., Hedley-Whyte, E. T., Frosch, M. P., . . . Irizarry, M. C. (2004). Early Abeta accumulation and progressive synaptic loss, gliosis, and tangle formation in AD brain. *Neurology*, 62(6), 925-931. <https://doi.org/10.1212/01.WNL.0000115115.98960.37>
- Iwasaki, S., Kobayashi, M., Yoda, M., Sakaguchi, Y., Katsuma, S., Suzuki, T., & Tomari, Y. (2010). Hsc70/Hsp90 chaperone machinery mediates ATP-dependent RISC loading of small RNA duplexes. *Molecular cell*, 39(2), 292-299. <https://doi.org/10.1016/j.molcel.2010.05.015>
- Izzo, N. J., Xu, J., Zeng, C., Kirk, M. J., Mozzoni, K., Silky, C., . . . Catalano, S. M. (2014). Alzheimer's therapeutics targeting amyloid beta 1-42 oligomers II: Sigma-2/PGRMC1 receptors mediate Abeta 42 oligomer binding and synaptotoxicity. *PloS one*, 9(11), e111899-e111899. <https://doi.org/10.1371/journal.pone.0111899>
- Jack, C. R., Knopman, D. S., Jagust, W. J., Shaw, L. M., Aisen, P. S., Weiner, M. W., . . . Trojanowski, J. Q. (2010). Hypothetical model of dynamic biomarkers of the Alzheimer's pathological cascade. *Lancet neurology*, 9(1), 119-119. [https://doi.org/10.1016/S1474-4422\(09\)70299-6](https://doi.org/10.1016/S1474-4422(09)70299-6)
- Jacobsen, J. S., Wu, C.-C., Redwine, J. M., Comery, T. A., Arias, R., Bowlby, M., . . . Bloom, F. E. (2006). Early-onset behavioral and synaptic deficits in a mouse model of Alzheimer's disease. *Proceedings of the National Academy of Sciences*, 103(13), 5161-5166. <https://doi.org/10.1073/pnas.0600948103>
- James, V., Zhang, Y., Foxler, D. E., de Moor, C. H., Kong, Y. W., Webb, T. M., . . . Sharp, T. V. (2010). LIM-domain proteins, LIMD1, Ajuba, and WTIP are required for microRNA-mediated gene silencing. *Proceedings of the National Academy of Sciences*, 107(28), 12499-12504. <https://doi.org/10.1073/pnas.0914987107>
- Jannot, G., Bajan, S., Giguère, N. J., Bouasker, S., Banville, I. H., Piquet, S., . . . Simard, M. J. (2011). The ribosomal protein RACK1 is required for microRNA function in both *C. elegans* and humans. *EMBO reports*, 12(6), 581-586. <https://doi.org/10.1038/embo.2011.66>
- Jansen, I. E., Savage, J. E., Watanabe, K., Bryois, J., Williams, D. M., Steinberg, S., . . . Posthuma, D. (2019). Genome-wide meta-analysis identifies new loci and functional pathways influencing Alzheimer's disease risk. *Nature Genetics* 2019 51:3, 51(3), 404-413. <https://doi.org/10.1038/s41588-018-0311-9>
- Jarrett, J. T., Berger, E. P., & Lansbury, P. T. (1993). Accelerated Publications The Carboxy Terminus of the β Amyloid Protein Is Critical for the Seeding of Amyloid Formation: Implications for the Pathogenesis of Alzheimer's Disease* 1".
- Jimenez, S., Navarro, V., Moyano, J., Sanchez-Mico, M., Torres, M., Davila, J. C., . . . Vitorica, J. (2014). Disruption of amyloid plaques integrity affects the soluble oligomers content from Alzheimer disease brains. *PloS one*, 9(12), e114041-e114041.

- <https://doi.org/10.1371/journal.pone.0114041>
- Jimenez-Mateos, E. M., Engel, T., Merino-Serrais, P., McKiernan, R. C., Tanaka, K., Mouri, G., . . . Henshall, D. C. (2012). Silencing microRNA-134 produces neuroprotective and prolonged seizure-suppressive effects. *Nature Medicine*, 18(7), 1087-1094.
<https://doi.org/10.1038/nm.2834>
- Jinek, M., & Doudna, J. A. (2009). A three-dimensional view of the molecular machinery of RNA interference. In *Nature* (Vol. 457, pp. 405-412).
- Jonas, S., & Izaurralde, E. (2015). Towards a molecular understanding of microRNA-mediated gene silencing. *Nature Reviews Genetics* 2015 16:7, 16(7), 421-433.
<https://doi.org/10.1038/nrg3965>
- Jones, E. G., & Powell, T. P. S. (1969). Morphological Variations in the Dendritic Spines of the Neocortex. *Journal of Cell Science*, 5(2), 509-529. <https://doi.org/10.1242/jcs.5.2.509>
- Jonsson, T., Atwal, J. K., Steinberg, S., Snaedal, J., Jonsson, P. V., Bjornsson, S., . . . Stefansson, K. (2012). A mutation in APP protects against Alzheimer's disease and age-related cognitive decline. *Nature*, 488(7409), 96-99. <https://doi.org/10.1038/nature11283>
- Jonsson, T., Stefansson, H., Steinberg, S., Jonsdottir, I., Jonsson, P. V., Snaedal, J., . . . Stefansson, K. (2013). Variant of TREM2 associated with the risk of Alzheimer's disease. *The New England journal of medicine*, 368(2), 107-116. <https://doi.org/10.1056/NEJMoa1211103>
- Jung, C. K. E., & Herms, J. (2014). Structural Dynamics of Dendritic Spines are Influenced by an Environmental Enrichment: An In Vivo Imaging Study. *Cerebral Cortex*, 24(2), 377-384.
<https://doi.org/10.1093/cercor/bhs317>
- Jung, S.-R., Kim, E., Hwang, W., Shin, S., Song, J.-J., & Hohng, S. (2013). Dynamic Anchoring of the 3'-End of the Guide Strand Controls the Target Dissociation of Argonaute-Guide Complex. *Journal of the American Chemical Society*, 135(45), 16865-16871.
<https://doi.org/10.1021/ja403138d>
- Kaech, S., & Banker, G. (2006). Culturing hippocampal neurons. *Nature Protocols*, 1(5), 2406-2415. <https://doi.org/10.1038/nprot.2006.356>
- Kamal, M. A., Mushtaq, G., & Greig, N. H. (2015). Current Update on Synopsis of miRNA Dysregulation in Neurological Disorders. *CNS & neurological disorders drug targets*, 14(4), 492-501. <https://doi.org/10.2174/1871527314666150225143637>
- Kamenetz, F., Tomita, T., Hsieh, H., Seabrook, G., Borchelt, D., Iwatsubo, T., . . . Malinow, R. (2003). APP Processing and Synaptic Function. *Neuron*, 37(6), 925-937.
[https://doi.org/10.1016/S0896-6273\(03\)00124-7](https://doi.org/10.1016/S0896-6273(03)00124-7)
- Kamino, K., Orr, H. T., Payami, H., Wijsman, E. M., Alonso, M. E., Pulst, S. M., . . . White, J. A. (1992). Linkage and mutational analysis of familial Alzheimer disease kindreds for the APP gene region. *American journal of human genetics*, 51(5), 998-1014.
- Kandel, E. R. (2001). The molecular biology of memory storage: A dialogue between genes and synapses. *Science*, 294(5544), 1030-1038. <https://doi.org/10.1126/SCIENCE.1067020>
- Kandel, E. S. J. J. T. (2000). *Principles of Neural Science* (4th ed.). McGraw-Hill Health Professions Division.
- Kang, D. E., & Woo, J. A. (2019). Cofilin, a Master Node Regulating Cytoskeletal Pathogenesis in

- Alzheimer's Disease. *Journal of Alzheimer's Disease*, 72(Suppl 1), S131-S131.
<https://doi.org/10.3233/JAD-190585>
- Karra, D., & Dahm, R. (2010). Transfection Techniques for Neuronal Cells. *Journal of Neuroscience*, 30(18), 6171-6177. <https://doi.org/10.1523/JNEUROSCI.0183-10.2010>
- Kawahara, Y., & Mieda-Sato, A. (2012). TDP-43 promotes microRNA biogenesis as a component of the Drosha and Dicer complexes. *Proceedings of the National Academy of Sciences of the United States of America*, 109(9), 3347-3352.
<https://doi.org/10.1073/pnas.1112427109>
- Kennedy, H. J., Kros, C. J., & Meech, R. W. (2000). Sodium independent regulation of intracellular calcium in inner hair cells from neonatal CD-1 mice. *Journal of Physiology*, 523, 94-95.
- Kennedy, M. B. (2000). Signal-Processing Machines at the Postsynaptic Density. *Science*, 290(5492), 750-754. <https://doi.org/10.1126/science.290.5492.750>
- Kidd, M. (1963). Paired Helical Filaments in Electron Microscopy of Alzheimer's Disease. *Nature*, 197(4863), 192-193. <https://doi.org/10.1038/197192b0>
- Kirkwood, C. M., Ciuchta, J., Ikonovic, M. D., Fish, K. N., Abrahamson, E. E., Murray, P. S., . . . Sweet, R. A. (2013). Dendritic Spine Density, Morphology, and Fibrillar Actin Content Surrounding Amyloid- β Plaques in a Mouse Model of Amyloid- β Deposition. *Journal of neuropathology and experimental neurology*, 72(8), 791-791.
<https://doi.org/10.1097/NEN.0B013E31829ECC89>
- Kislauskis, E., & Singer, R. (1992). Determinants of mRNA localization. *Current Opinion in Cell Biology*, 4(6), 975-978. [https://doi.org/10.1016/0955-0674\(92\)90128-Y](https://doi.org/10.1016/0955-0674(92)90128-Y)
- Klamt, F., Zdanov, S., Levine, R. L., Pariser, A., Zhang, Y., Zhang, B., . . . Shacter, E. (2009). Oxidant-induced apoptosis is mediated by oxidation of the actin-regulatory protein cofilin. *Nature cell biology*, 11(10), 1241-1246. <https://doi.org/10.1038/ncb1968>
- Kobayashi, H., & Tomari, Y. (2016). RISC assembly: Coordination between small RNAs and Argonaute proteins. *Biochimica et Biophysica Acta (BBA) - Gene Regulatory Mechanisms*, 1859(1), 71-81. <https://doi.org/10.1016/j.bbagrm.2015.08.007>
- Koffie, R. M., Hashimoto, T., Tai, H.-C., Kay, K. R., Serrano-Pozo, A., Joyner, D., . . . Spires-Jones, T. L. (2012). Apolipoprotein E4 effects in Alzheimer's disease are mediated by synaptotoxic oligomeric amyloid- β . *Brain*, 135(7), 2155-2168. <https://doi.org/10.1093/brain/aws127>
- Koffie, R. M., Meyer-Luehmann, M., Hashimoto, T., Adams, K. W., Mielke, M. L., Garcia-Alloza, M., . . . Spires-Jones, T. L. (2009). Oligomeric amyloid β associates with postsynaptic densities and correlates with excitatory synapse loss near senile plaques. *Proceedings of the National Academy of Sciences*, 106(10), 4012-4017.
<https://doi.org/10.1073/pnas.0811698106>
- Kojro, E., & Fahrenholz, F. The Non-Amyloidogenic Pathway: Structure and Function of α -Secretases. In *Alzheimer's Disease* (pp. 105-127). Springer US.
https://doi.org/10.1007/0-387-23226-5_5
- Krichevsky, A. M., & Kosik, K. S. (2001). Neuronal RNA granules: a link between RNA localization and stimulation-dependent translation. *Neuron*, 32(4), 683-696.
[https://doi.org/10.1016/s0896-6273\(01\)00508-6](https://doi.org/10.1016/s0896-6273(01)00508-6)

- Kwak, P. B., & Tomari, Y. (2012). The N domain of Argonaute drives duplex unwinding during RISC assembly. <https://doi.org/10.1038/nsmb.2232>
- Kye, M. J., Neveu, P., Lee, Y.-S., Zhou, M., Steen, J. A., Sahin, M., . . . Silva, A. J. (2011). NMDA mediated contextual conditioning changes miRNA expression. *PLoS one*, 6(9), e24682-e24682. <https://doi.org/10.1371/journal.pone.0024682>
- Lacor, P. N., Buniel, M. C., Furlow, P. W., Sanz Clemente, A., Velasco, P. T., Wood, M., . . . Klein, W. L. (2007). A Oligomer-Induced Aberrations in Synapse Composition, Shape, and Density Provide a Molecular Basis for Loss of Connectivity in Alzheimer's Disease. *Journal of Neuroscience*, 27(4), 796-807. <https://doi.org/10.1523/JNEUROSCI.3501-06.2007>
- Lai, K.-O., & Ip, N. Y. (2013). Structural plasticity of dendritic spines: The underlying mechanisms and its dysregulation in brain disorders. *Biochimica et Biophysica Acta (BBA) - Molecular Basis of Disease*, 1832(12), 2257-2263. <https://doi.org/10.1016/j.bbadis.2013.08.012>
- Lambert, J.-C., Ibrahim-Verbaas, C. A., Harold, D., Naj, A. C., Sims, R., Bellenguez, C., . . . Amouyel, P. (2013). Meta-analysis of 74,046 individuals identifies 11 new susceptibility loci for Alzheimer's disease. <https://doi.org/10.1038/ng.2802>
- Lambert, M. P., Barlow, A. K., Chromy, B. A., Edwards, C., Freed, R., Liosatos, M., . . . Klein, W. L. (1998). Diffusible, nonfibrillar ligands derived from A β ₁₋₄₂ are potent central nervous system neurotoxins. *Proceedings of the National Academy of Sciences*, 95(11), 6448-6453. <https://doi.org/10.1073/pnas.95.11.6448>
- Lamprecht, R., & LeDoux, J. (2004). Structural plasticity and memory. *Nature Reviews Neuroscience*, 5(1), 45-54. <https://doi.org/10.1038/nrn1301>
- Lancaster, M. A., Renner, M., Martin, C.-A., Wenzel, D., Bicknell, L. S., Hurles, M. E., . . . Knoblich, J. A. (2013). Cerebral organoids model human brain development and microcephaly. *Nature*, 501(7467), 373-379. <https://doi.org/10.1038/nature12517>
- Landgraf, P., Rusu, M., Sheridan, R., Sewer, A., Iovino, N., Aravin, A., . . . Tuschl, T. (2007). A Mammalian microRNA Expression Atlas Based on Small RNA Library Sequencing. *Cell*, 129(7), 1401-1414. <https://doi.org/10.1016/j.cell.2007.04.040>
- Landis, D. M., & Reese, T. S. (1983). Cytoplasmic organization in cerebellar dendritic spines. *Journal of Cell Biology*, 97(4), 1169-1178. <https://doi.org/10.1083/jcb.97.4.1169>
- Lanz, T. A., Carter, D. B., & Merchant, K. M. (2003). Dendritic spine loss in the hippocampus of young PDAPP and Tg2576 mice and its prevention by the ApoE2 genotype. *Neurobiology of Disease*, 13(3), 246-253. [https://doi.org/10.1016/S0969-9961\(03\)00079-2](https://doi.org/10.1016/S0969-9961(03)00079-2)
- Lazarev, V. F., Tsolaki, M., Mikhaylova, E. R., Benken, K. A., Shevtsov, M. A., Nikotina, A. D., . . . Nudler, E. (2021). Extracellular GAPDH Promotes Alzheimer Disease Progression by Enhancing Amyloid- β Aggregation and Cytotoxicity. *Aging and disease*, 12(5), 1223-1237. <https://doi.org/10.14336/AD.2020.1230>
- Leal, G., Comprido, D., & Duarte, C. B. (2014). BDNF-induced local protein synthesis and synaptic plasticity. *Neuropharmacology*, 76, 639-656. <https://doi.org/10.1016/j.neuropharm.2013.04.005>
- Lee, H.-K., Barbarosie, M., Kameyama, K., Bear, M. F., & Huganir, R. L. (2000). Regulation of distinct AMPA receptor phosphorylation sites during bidirectional synaptic plasticity.

- Nature*, 405(6789), 955-959. <https://doi.org/10.1038/35016089>
- Lee, K., Kim, J.-H., Kwon, O.-B., An, K., Ryu, J., Cho, K., . . . Kim, H.-S. (2012). An activity-regulated microRNA, miR-188, controls dendritic plasticity and synaptic transmission by downregulating neuropilin-2. *The Journal of neuroscience : the official journal of the Society for Neuroscience*, 32(16), 5678-5687. <https://doi.org/10.1523/JNEUROSCI.6471-11.2012>
- Lee, S.-T., Chu, K., Jung, K.-H., Kim, J. H., Huh, J.-Y., Yoon, H., . . . Roh, J.-K. (2012). miR-206 regulates brain-derived neurotrophic factor in Alzheimer disease model. *Annals of Neurology*, 72(2), 269-277. <https://doi.org/10.1002/ana.23588>
- Lee, S. J. C., Nam, E., Lee, H. J., Savelieff, M. G., & Lim, M. H. (2017). Towards an understanding of amyloid- β oligomers: characterization, toxicity mechanisms, and inhibitors. *Chemical Society Reviews*, 46(2), 310-323. <https://doi.org/10.1039/C6CS00731G>
- Lee, Y., Jeon, K., Lee, J.-T., Kim, S., & Kim, V. N. (2002). MicroRNA maturation: stepwise processing and subcellular localization. *The EMBO journal*, 21(17), 4663-4670. <https://doi.org/10.1093/emboj/cdf476>
- Lee, Y., Kim, M., Han, J., Yeom, K.-H., Lee, S., Baek, S. H., & Kim, V. N. (2004). MicroRNA genes are transcribed by RNA polymerase II. *The EMBO Journal*, 23(20), 4051-4060. <https://doi.org/10.1038/sj.emboj.7600385>
- Lendvai, B., Stern, E. A., Chen, B., & Svoboda, K. (2000). Experience-dependent plasticity of dendritic spines in the developing rat barrel cortex in vivo. *Nature*, 404(6780), 876-881. <https://doi.org/10.1038/35009107>
- Lesné, S., Koh, M. T., Kotilinek, L., Kaye, R., Glabe, C. G., Yang, A., . . . Ashe, K. H. (2006). A specific amyloid- β protein assembly in the brain impairs memory. *Nature*, 440(7082), 352-357. <https://doi.org/10.1038/nature04533>
- Lesné, S. E., Sherman, M. A., Grant, M., Kuskowski, M., Schneider, J. A., Bennett, D. A., & Ashe, K. H. (2013). Brain amyloid- β oligomers in ageing and Alzheimer's disease. *Brain*, 136(5), 1383-1398. <https://doi.org/10.1093/brain/awt062>
- Levy-Lahad, E., Wasco, W., Poorkaj, P., Romano, D. M., Oshima, J., Pettingell, W. H., . . . Tanzi, R. E. (1995). Candidate Gene for the Chromosome 1 Familial Alzheimer's Disease Locus. *Science*, 269(5226), 973-977. <https://doi.org/10.1126/science.7638622>
- Lewczuk, P., Matzen, A., Blennow, K., Parnetti, L., Molinuevo, J. L., Eusebi, P., . . . Fagan, A. M. (2016). Cerebrospinal Fluid A β 42/40 Corresponds Better than A β 42 to Amyloid PET in Alzheimer's Disease. *Journal of Alzheimer's Disease*, 55(2), 813-822. <https://doi.org/10.3233/JAD-160722>
- Lewis, J., Dickson, D. W., Lin, W.-L., Chisholm, L., Corral, A., Jones, G., . . . McGowan, E. (2001). Enhanced Neurofibrillary Degeneration in Transgenic Mice Expressing Mutant Tau and APP. *Science*, 293(5534), 1487-1491. <https://doi.org/10.1126/science.1058189>
- Li, F., Wei, G., Bai, Y., Li, Y., Huang, F., Lin, J., . . . Chen, D. F. (2015). MicroRNA-574 is involved in cognitive impairment in 5-month-old APP/PS1 mice through regulation of neuritin. *Brain Research*, 1627, 177-188. <https://doi.org/10.1016/j.brainres.2015.09.022>
- Li, X., Zhao, X., Fang, Y., Jiang, X., Duong, T., Fan, C., . . . Kain, S. R. (1998). Generation of

- destabilized green fluorescent protein as a transcription reporter. *The Journal of biological chemistry*, 273(52), 34970-34975. <https://doi.org/10.1074/jbc.273.52.34970>
- Li, Y., Song, M., & Kiledjian, M. (2011). Differential utilization of decapping enzymes in mammalian mRNA decay pathways. *RNA*, 17(3), 419-428. <https://doi.org/10.1261/rna.2439811>
- Lippi, G., Steinert, J. R., Marczylo, E. L., D'Oro, S., Fiore, R., Forsythe, I. D., . . . Young, K. W. (2011). Targeting of the Arpc3 actin nucleation factor by miR-29a/b regulates dendritic spine morphology. *The Journal of cell biology*, 194(6), 889-904. <https://doi.org/10.1083/jcb.201103006>
- Lisman, J., Yasuda, R., & Raghavachari, S. (2012). Mechanisms of CaMKII action in long-term potentiation. *Nature reviews. Neuroscience*, 13(3), 169-182. <https://doi.org/10.1038/nrn3192>
- Liu, C.-M., Wang, R.-Y., Saijilafu, Jiao, Z.-X., Zhang, B.-Y., & Zhou, F.-Q. (2013). MicroRNA-138 and SIRT1 form a mutual negative feedback loop to regulate mammalian axon regeneration. *Genes & Development*, 27(13), 1473-1483. <https://doi.org/10.1101/gad.209619.112>
- Liu, J., Carmell, M. A., Rivas, F. V., Marsden, C. G., Thomson, J. M., Song, J.-J., . . . Hannon, G. J. (2004). Argonaute2 is the catalytic engine of mammalian RNAi. *Science (New York, N.Y.)*, 305(5689), 1437-1441. <https://doi.org/10.1126/science.1102513>
- Liu, T., Woo, J.-A. A., Yan, Y., LePochat, P., Bukhari, M. Z., & Kang, D. E. (2019). Dual role of cofilin in APP trafficking and amyloid- β clearance. *FASEB journal : official publication of the Federation of American Societies for Experimental Biology*, 33(12), 14234-14247. <https://doi.org/10.1096/fj.201901268R>
- Liu, Y., Ye, X., Jiang, F., Liang, C., Chen, D., Peng, J., . . . Liu, Q. (2009). C3PO, an endoribonuclease that promotes RNAi by facilitating RISC activation. *Science (New York, N.Y.)*, 325(5941), 750-753. <https://doi.org/10.1126/science.1176325>
- Llinás, R., Steinberg, I. Z., & Walton, K. (1981). Relationship between presynaptic calcium current and postsynaptic potential in squid giant synapse. *Biophysical journal*, 33(3), 323-351. [https://doi.org/10.1016/S0006-3495\(81\)84899-0](https://doi.org/10.1016/S0006-3495(81)84899-0)
- Lopez-Orozco, J., Pare, J. M., Holme, A. L., Chaulk, S. G., Fahlman, R. P., & Hobman, T. C. (2015). Functional analyses of phosphorylation events in human Argonaute 2. *RNA (New York, N.Y.)*, 21(12), 2030-2038. <https://doi.org/10.1261/rna.053207.115>
- Lourenco, Mychael V., Clarke, Julia R., Frozza, Rudimar L., Bomfim, Theresa R., Forny-Germano, L., Batista, André F., . . . De Felice, Fernanda G. (2013). TNF- α Mediates PKR-Dependent Memory Impairment and Brain IRS-1 Inhibition Induced by Alzheimer's β -Amyloid Oligomers in Mice and Monkeys. *Cell Metabolism*, 18(6), 831-843. <https://doi.org/10.1016/j.cmet.2013.11.002>
- Lue, L.-F., Kuo, Y.-M., Roher, A. E., Brachova, L., Shen, Y., Sue, L., . . . Rogers, J. (1999). Soluble Amyloid β Peptide Concentration as a Predictor of Synaptic Change in Alzheimer's Disease. *The American Journal of Pathology*, 155(3), 853-862. [https://doi.org/10.1016/S0002-9440\(10\)65184-X](https://doi.org/10.1016/S0002-9440(10)65184-X)
- Lugli, G., Larson, J., Demars, M. P., & Smalheiser, N. R. (2012). Primary microRNA precursor

- transcripts are localized at post-synaptic densities in adult mouse forebrain. *Journal of Neurochemistry*, 123(4), 459-466. <https://doi.org/10.1111/j.1471-4159.2012.07921.x>
- Lugli, G., Larson, J., Martone, M. E., Jones, Y., & Smalheiser, N. R. (2005). Dicer and eIF2c are enriched at postsynaptic densities in adult mouse brain and are modified by neuronal activity in a calpain-dependent manner. *Journal of Neurochemistry*, 94(4), 896-905. <https://doi.org/10.1111/J.1471-4159.2005.03224.X>
- Lugli, G., Torvik, V. I., Larson, J., & Smalheiser, N. R. (2008). Expression of microRNAs and their precursors in synaptic fractions of adult mouse forebrain. *Journal of Neurochemistry*, 106(2), 650-661. <https://doi.org/10.1111/j.1471-4159.2008.05413.x>
- Lunardi, P., Sachser, R. M., Sierra, R. O., Pedraza, L. K., Medina, C., de la Fuente, V., . . . de Oliveira Alvares, L. (2018). Effects of Hippocampal LIMK Inhibition on Memory Acquisition, Consolidation, Retrieval, Reconsolidation, and Extinction. *Molecular Neurobiology*, 55(2), 958-967. <https://doi.org/10.1007/s12035-016-0361-x>
- M. Vargas, L., Leal, N., Estrada, L. D., González, A., Serrano, F., Araya, K., . . . Alvarez, A. R. (2014). EphA4 Activation of c-Abl Mediates Synaptic Loss and LTP Blockade Caused by Amyloid- β Oligomers. *PLoS ONE*, 9(3), e92309-e92309. <https://doi.org/10.1371/journal.pone.0092309>
- Ma, N., Tie, C., Yu, B., Zhang, W., & Wan, J. (2020). Identifying lncRNA-miRNA-mRNA networks to investigate Alzheimer's disease pathogenesis and therapy strategy. *Aging*, 12(3), 2897-2920. <https://doi.org/10.18632/aging.102785>
- MacDonald, Christopher J., Lepage, Kyle Q., Eden, Uri T., & Eichenbaum, H. (2011). Hippocampal "Time Cells" Bridge the Gap in Memory for Discontiguous Events. *Neuron*, 71(4), 737-749. <https://doi.org/10.1016/j.neuron.2011.07.012>
- Macdonald, P. M., & Struhl, G. (1988). Cis- acting sequences responsible for anterior localization of bicoid mRNA in Drosophila embryos. *Nature*, 336(6199), 595-598. <https://doi.org/10.1038/336595a0>
- MacGillavry, H. D., Kerr, J. M., Kassner, J., Frost, N. A., & Blanpied, T. A. (2016). Shank-cortactin interactions control actin dynamics to maintain flexibility of neuronal spines and synapses. *European Journal of Neuroscience*, 43(2), 179-193. <https://doi.org/10.1111/ejn.13129>
- Majewska, A., Brown, E., Ross, J., Yuste, R., Webb, W., Helmchen, F., . . . Thomas, J. (2000). *Mechanisms of Calcium Decay Kinetics in Hippocampal Spines: Role of Spine Calcium Pumps and Calcium Diffusion through the Spine Neck in Biochemical Compartmentalization* (The Journal of Neuroscience, Issue.
- Majewska, A., Tashiro, A., & Yuste, R. (2000). Regulation of Spine Calcium Dynamics by Rapid Spine Motility. *The Journal of Neuroscience*, 20(22), 8262-8268. <https://doi.org/10.1523/JNEUROSCI.20-22-08262.2000>
- Malenka, R. C., & Bear, M. F. (2004). LTP and LTD. *Neuron*, 44(1), 5-21. <https://doi.org/10.1016/j.neuron.2004.09.012>
- Maletic-Savatic, M., Malinow, R., & Svoboda, K. (1999). Rapid Dendritic Morphogenesis in CA1 Hippocampal Dendrites Induced by Synaptic Activity. *Science*, 283(5409), 1923-1927.

- <https://doi.org/10.1126/science.283.5409.1923>
- Malinow, R., & Malenka, R. C. (2002). AMPA Receptor Trafficking and Synaptic Plasticity. *Annual Review of Neuroscience*, 25(1), 103-126.
<https://doi.org/10.1146/annurev.neuro.25.112701.142758>
- Maloney, M. T., Minamide, L. S., Kinley, A. W., Boyle, J. A., & Bamburg, J. R. (2005). Beta-secretase-cleaved amyloid precursor protein accumulates at actin inclusions induced in neurons by stress or amyloid beta: a feedforward mechanism for Alzheimer's disease. *The Journal of neuroscience : the official journal of the Society for Neuroscience*, 25(49), 11313-11321. <https://doi.org/10.1523/JNEUROSCI.3711-05.2005>
- Martin, K. C., & Ephrussi, A. (2009). mRNA localization: gene expression in the spatial dimension. *Cell*, 136(4), 719-730. <https://doi.org/10.1016/j.cell.2009.01.044>
- Martin, S. J., Grimwood, P. D., & Morris, R. G. M. (2000). Synaptic Plasticity and Memory: An Evaluation of the Hypothesis. *Annual Review of Neuroscience*, 23(1), 649-711.
<https://doi.org/10.1146/annurev.neuro.23.1.649>
- Masliah, E., Mallory, M., Alford, M., DeTeresa, R., Hansen, L. A., McKeel, D. W., & Morris, J. C. (2001). Altered expression of synaptic proteins occurs early during progression of Alzheimer's disease. *Neurology*, 56(1), 127-129. <https://doi.org/10.1212/wnl.56.1.127>
- Masliah, E., Mallory, M., Hansen, L., DeTeresa, R., & Terry, R. D. (1993). Quantitative synaptic alterations in the human neocortex during normal aging. *Neurology*, 43(1), 192-197.
https://doi.org/10.1212/wnl.43.1_part_1.192
- Mathys, H., Basquin, J., Ozgur, S., Czarnocki-Cieciura, M., Bonneau, F., Aartse, A., . . . Filipowicz, W. (2014). Structural and biochemical insights to the role of the CCR4-NOT complex and DDX6 ATPase in microRNA repression. *Molecular cell*, 54(5), 751-765.
<https://doi.org/10.1016/j.molcel.2014.03.036>
- Matsuzaki, M., Ellis-Davies, G. C. R., Nemoto, T., Miyashita, Y., Iino, M., & Kasai, H. (2001). Dendritic spine geometry is critical for AMPA receptor expression in hippocampal CA1 pyramidal neurons. *Nature neuroscience*, 4(11), 1086-1086.
<https://doi.org/10.1038/NN736>
- Matsuzaki, M., Honkura, N., Ellis-Davies, G. C. R., & Kasai, H. (2004). Structural basis of long-term potentiation in single dendritic spines. *Nature*, 429(6993), 761-766.
<https://doi.org/10.1038/NATURE02617>
- Matt, L., Kim, K., Hergarden, A. C., Patriarchi, T., Malik, Z. A., Park, D. K., . . . Hell, J. W. (2018). α -Actinin Anchors PSD-95 at Postsynaptic Sites. *Neuron*, 97(5), 1094-1109.e1099.
<https://doi.org/10.1016/j.neuron.2018.01.036>
- Matus, A. (2000). Actin-Based Plasticity in Dendritic Spines. *Science*, 290(5492), 754-758.
<https://doi.org/10.1126/science.290.5492.754>
- Mayer, M. L., Westbrook, G. L., & Guthrie, P. B. Voltage-dependent block by Mg^{2+} of NMDA responses in spinal cord neurones. *Nature*, 309(5965), 261-263.
<https://doi.org/10.1038/309261a0>
- Mayr, C. (2019). What Are 3' UTRs Doing? *Cold Spring Harbor perspectives in biology*, 11(10).
<https://doi.org/10.1101/cshperspect.a034728>

- Mazumder, A., Bose, M., Chakraborty, A., Chakrabarti, S., & Bhattacharyya, S. N. (2013). A transient reversal of miRNA-mediated repression controls macrophage activation. *EMBO reports*, 14(11), 1008-1016. <https://doi.org/10.1038/embor.2013.149>
- McKenzie, A. J., Hoshino, D., Hong, N. H., Cha, D. J., Franklin, J. L., Coffey, R. J., . . . Weaver, A. M. (2016). KRAS-MEK Signaling Controls Ago2 Sorting into Exosomes. *Cell reports*, 15(5), 978-987. <https://doi.org/10.1016/j.celrep.2016.03.085>
- Medina, D. A., Jordán-Pla, A., Millán-Zambrano, G., Chávez, S., Choder, M., & Pérez-Ortín, J. E. (2014). Cytoplasmic 5'-3' exonuclease Xrn1p is also a genome-wide transcription factor in yeast. *Frontiers in Genetics*, 5. <https://doi.org/10.3389/fgene.2014.00001>
- Megías, M., Emri, Z., Freund, T. F., & Gulyás, A. I. (2001). Total number and distribution of inhibitory and excitatory synapses on hippocampal CA1 pyramidal cells. *Neuroscience*, 102(3), 527-540. [https://doi.org/10.1016/S0306-4522\(00\)00496-6](https://doi.org/10.1016/S0306-4522(00)00496-6)
- Meister, G. (2013). Argonaute proteins: functional insights and emerging roles. *Nature Reviews Genetics* 2013 14:7, 14(7), 447-459. <https://doi.org/10.1038/nrg3462>
- Mendoza-Naranjo, A., Contreras-Vallejos, E., Henriquez, D. R., Otth, C., Bamburg, J. R., Maccioni, R. B., & Gonzalez-Billault, C. (2012). Fibrillar amyloid- β 1-42 modifies actin organization affecting the cofilin phosphorylation state: a role for Rac1/cdc42 effector proteins and the slingshot phosphatase. *Journal of Alzheimer's disease : JAD*, 29(1), 63-77. <https://doi.org/10.3233/JAD-2012-101575>
- Meng, Y., Takahashi, H., Meng, J., Zhang, Y., Lu, G., Asrar, S., . . . Jia, Z. (2004). Regulation of ADF/cofilin phosphorylation and synaptic function by LIM-kinase. *Neuropharmacology*, 47(5), 746-754. <https://doi.org/10.1016/j.neuropharm.2004.06.030>
- Meng, Y., Zhang, Y., Tregoubov, V., Janus, C., Cruz, L., Jackson, M., . . . Jia, Z. (2002). Abnormal Spine Morphology and Enhanced LTP in LIMK-1 Knockout Mice. *Neuron*, 35(1), 121-133. [https://doi.org/10.1016/S0896-6273\(02\)00758-4](https://doi.org/10.1016/S0896-6273(02)00758-4)
- Merlini, M., Rafalski, V. A., Rios Coronado, P. E., Gill, T. M., Ellisman, M., Muthukumar, G., . . . Akassoglou, K. (2019). Fibrinogen Induces Microglia-Mediated Spine Elimination and Cognitive Impairment in an Alzheimer's Disease Model. *Neuron*, 101(6), 1099-1108.e1096. <https://doi.org/10.1016/j.neuron.2019.01.014>
- Miles, W. O., Tschöp, K., Herr, A., Ji, J.-Y., & Dyson, N. J. (2012). Pumilio facilitates miRNA regulation of the E2F3 oncogene. *Genes & Development*, 26(4), 356-368. <https://doi.org/10.1101/gad.182568.111>
- Miller, S., Yasuda, M., Coats, J. K., Jones, Y., Martone, M. E., & Mayford, M. (2002). Disruption of dendritic translation of CaMKII α impairs stabilization of synaptic plasticity and memory consolidation. *Neuron*, 36(3), 507-519. [https://doi.org/10.1016/s0896-6273\(02\)00978-9](https://doi.org/10.1016/s0896-6273(02)00978-9)
- Millucci, L., Ghezzi, L., Bernardini, G., & Santucci, A. (2010). Conformations and biological activities of amyloid beta peptide 25-35. *Current protein & peptide science*, 11(1), 54-67. <https://doi.org/10.2174/138920310790274626>
- Minamide, L. S., Striegl, A. M., Boyle, J. A., Meberg, P. J., & Bamburg, J. R. (2000). Neurodegenerative stimuli induce persistent ADF/cofilin-actin rods that disrupt distal

- neurite function. *Nature cell biology*, 2(9), 628-636. <https://doi.org/10.1038/35023579>
- Moolman, D. L., Vitolo, O. V., Vonsattel, J.-P. G., & Shelanski, M. L. (2004). Dendrite and dendritic spine alterations in Alzheimer models. *Journal of neurocytology*, 33(3), 377-387. <https://doi.org/10.1023/B:NEUR.0000044197.83514.64>
- Moreno-Flores, M. T., Lim, F., Martín-Bermejo, M. J., Díaz-Nido, J., Ávila, J., & Wandosell, F. (2003). High level of amyloid precursor protein expression in neurite-promoting olfactory ensheathing glia (OEG) and OEG-derived cell lines. *Journal of Neuroscience Research*, 71(6), 871-881. <https://doi.org/10.1002/jnr.10527>
- Morris, R. G. M. (2006). Elements of a neurobiological theory of hippocampal function: the role of synaptic plasticity, synaptic tagging and schemas. *European Journal of Neuroscience*, 23(11), 2829-2846. <https://doi.org/10.1111/j.1460-9568.2006.04888.x>
- Morris, R. G. M., Anderson, E., Lynch, G. S., & Baudry, M. (1986). Selective impairment of learning and blockade of long-term potentiation by an N-methyl-D-aspartate receptor antagonist, AP5. *Nature*, 319(6056), 774-776. <https://doi.org/10.1038/319774a0>
- Morris, R. G. M., Garrud, P., Rawlins, J. N. P., & O'Keefe, J. (1982). Place navigation impaired in rats with hippocampal lesions. *Nature*, 297(5868), 681-683. <https://doi.org/10.1038/297681a0>
- Mucke, L., Masliah, E., Yu, G. Q., Mallory, M., Rockenstein, E. M., Tatsuno, G., . . . McConlogue, L. (2000). High-Level Neuronal Expression of A β 1–42 in Wild-Type Human Amyloid Protein Precursor Transgenic Mice: Synaptotoxicity without Plaque Formation. *Journal of Neuroscience*, 20(11), 4050-4058. <https://doi.org/10.1523/JNEUROSCI.20-11-04050.2000>
- Muddashetty, R. S., Nalavadi, V. C., Gross, C., Yao, X., Xing, L., Laur, O., . . . Bassell, G. J. (2011). Reversible inhibition of PSD-95 mRNA translation by miR-125a, FMRP phosphorylation, and mGluR signaling. *Molecular cell*, 42(5), 673-688. <https://doi.org/10.1016/j.molcel.2011.05.006>
- Muddashetty, Ravi S., Nalavadi, Vijayalaxmi C., Gross, C., Yao, X., Xing, L., Laur, O., . . . Bassell, Gary J. (2011). Reversible Inhibition of PSD-95 mRNA Translation by miR-125a, FMRP Phosphorylation, and mGluR Signaling. *Molecular Cell*, 42(5), 673-688. <https://doi.org/10.1016/j.molcel.2011.05.006>
- Mullan, M., Crawford, F., Axelman, K., Houlden, H., Lilius, L., Winblad, B., & Lannfelt, L. (1992). A pathogenic mutation for probable Alzheimer's disease in the APP gene at the N-terminus of β -amyloid. *Nature Genetics* 1992 1:5, 1(5), 345-347. <https://doi.org/10.1038/ng0892-345>
- Murray, M. E., Graff-Radford, N. R., Ross, O. A., Petersen, R. C., Duara, R., & Dickson, D. W. (2011). Neuropathologically defined subtypes of Alzheimer's disease with distinct clinical characteristics: a retrospective study. *The Lancet Neurology*, 10(9), 785-796. [https://doi.org/10.1016/S1474-4422\(11\)70156-9](https://doi.org/10.1016/S1474-4422(11)70156-9)
- Murrell, J., Farlow, M., Ghetti, B., & Benson, M. D. (1991). A mutation in the amyloid precursor protein associated with hereditary Alzheimer's disease. *Science (New York, N.Y.)*, 254(5028), 97-99. <https://doi.org/10.1126/science.1925564>

- Myers, A., & McGonigle, P. (2019). Overview of Transgenic Mouse Models for Alzheimer's Disease. *Current Protocols in Neuroscience*, 89(1). <https://doi.org/10.1002/cpns.81>
- Nabavi, S., Fox, R., Proulx, C. D., Lin, J. Y., Tsien, R. Y., & Malinow, R. (2014). Engineering a memory with LTD and LTP. *Nature*, 511(7509), 348-352. <https://doi.org/10.1038/nature13294>
- Nag, S., Sarkar, B., Bandyopadhyay, A., Sahoo, B., Sreenivasan, V. K. A., Kombrabail, M., . . . Maiti, S. (2011). Nature of the amyloid-beta monomer and the monomer-oligomer equilibrium. *The Journal of biological chemistry*, 286(16), 13827-13833. <https://doi.org/10.1074/jbc.M110.199885>
- Nagata-Ohashi, K., Ohta, Y., Goto, K., Chiba, S., Mori, R., Nishita, M., . . . Mizuno, K. (2004). A pathway of neuregulin-induced activation of cofilin-phosphatase Slingshot and cofilin in lamellipodia. *The Journal of cell biology*, 165(4), 465-471. <https://doi.org/10.1083/jcb.200401136>
- Nakanishi, K., Weinberg, D. E., Bartel, D. P., & Patel, D. J. (2012). Structure of yeast Argonaute with guide RNA. *Nature*, 486(7403), 368-374. <https://doi.org/10.1038/nature11211>
- Nelson, P. T., Alafuzoff, I., Bigio, E. H., Bouras, C., Braak, H., Cairns, N. J., . . . Beach, T. G. (2012). Correlation of Alzheimer Disease Neuropathologic Changes With Cognitive Status: A Review of the Literature. *Journal of Neuropathology & Experimental Neurology*, 71(5), 362-381. <https://doi.org/10.1097/NEN.0b013e31825018f7>
- Nicoll, R. A., Kauer, J. A., & Malenka, R. C. (1988). The current excitement in long-term potentiation. *Neuron*, 1(2), 97-103. [https://doi.org/10.1016/0896-6273\(88\)90193-6](https://doi.org/10.1016/0896-6273(88)90193-6)
- Nielson, D. M., Smith, T. A., Sreekumar, V., Dennis, S., & Sederberg, P. B. (2015). Human hippocampus represents space and time during retrieval of real-world memories. *Proceedings of the National Academy of Sciences of the United States of America*, 112(35), 11078-11083. <https://doi.org/10.1073/pnas.1507104112>
- Nikolac Perkovic, M., Videtic Paska, A., Konjevod, M., Kouter, K., Svob Strac, D., Nedic Erjavec, G., & Pivac, N. (2021). biomolecules Epigenetics of Alzheimer's Disease. <https://doi.org/10.3390/biom11020195>
- Niwa, R., Nagata-Ohashi, K., Takeichi, M., Mizuno, K., & Uemura, T. (2002). Control of Actin Reorganization by Slingshot, a Family of Phosphatases that Dephosphorylate ADF/Cofilin. *Cell*, 108(2), 233-246. [https://doi.org/10.1016/S0092-8674\(01\)00638-9](https://doi.org/10.1016/S0092-8674(01)00638-9)
- Noguchi, J., Matsuzaki, M., Ellis-Davies, G. C. R., & Kasai, H. (2005). Spine-neck geometry determines NMDA receptor-dependent Ca²⁺ signaling in dendrites. *Neuron*, 46(4), 609-622. <https://doi.org/10.1016/J.NEURON.2005.03.015>
- Noland, C. L., Ma, E., & Doudna, J. A. (2011). siRNA repositioning for guide strand selection by human Dicer complexes. *Molecular cell*, 43(1), 110-121. <https://doi.org/10.1016/j.molcel.2011.05.028>
- Nowak, L., Bregestovski, P., Ascher, P., Herbet, A., & Prochiantz, A. (1984). Magnesium gates glutamate-activated channels in mouse central neurones. *Nature*, 307(5950), 462-465. <https://doi.org/10.1038/307462a0>
- Nusser, Z., Lujan, R., Laube, G., Roberts, J. D. B., Molnar, E., & Somogyi, P. (1998). Cell Type and

- Pathway Dependence of Synaptic AMPA Receptor Number and Variability in the Hippocampus. *Neuron*, 21(3), 545-559. [https://doi.org/10.1016/S0896-6273\(00\)80565-6](https://doi.org/10.1016/S0896-6273(00)80565-6)
- Nägerl, U. V., Eberhorn, N., Cambridge, S. B., & Bonhoeffer, T. (2004). Bidirectional Activity-Dependent Morphological Plasticity in Hippocampal Neurons. *Neuron*, 44(5), 759-767. <https://doi.org/10.1016/j.neuron.2004.11.016>
- O'Brien, R. J., & Wong, P. C. (2011). Amyloid precursor protein processing and Alzheimer's disease. *Annual review of neuroscience*, 34, 185-204. <https://doi.org/10.1146/annurev-neuro-061010-113613>
- O'Keefe, J., & Dostrovsky, J. (1971). The hippocampus as a spatial map. Preliminary evidence from unit activity in the freely-moving rat. *Brain Research*, 34(1), 171-175. [https://doi.org/10.1016/0006-8993\(71\)90358-1](https://doi.org/10.1016/0006-8993(71)90358-1)
- Okamoto, K. I., Nagai, T., Miyawaki, A., & Hayashi, Y. (2004). Rapid and persistent modulation of actin dynamics regulates postsynaptic reorganization underlying bidirectional plasticity. *Nature neuroscience*, 7(10), 1104-1112. <https://doi.org/10.1038/NN1311>
- Olde Loohuis, N. F. M., Ba, W., Stoerchel, P. H., Kos, A., Jager, A., Schratt, G., . . . Aschrafi, A. (2015). MicroRNA-137 Controls AMPA-Receptor-Mediated Transmission and mGluR-Dependent LTD. *Cell reports*, 11(12), 1876-1884. <https://doi.org/10.1016/j.celrep.2015.05.040>
- Olde Loohuis, N. F. M., Kos, A., Martens, G. J. M., Van Bokhoven, H., Nadif Kasri, N., & Aschrafi, A. (2012). MicroRNA networks direct neuronal development and plasticity. *Cellular and molecular life sciences : CMLS*, 69(1), 89-102. <https://doi.org/10.1007/s00018-011-0788-1>
- Olina, A. V., Kulbachinskiy, A. V., Aravin, A. A., & Esyunina, D. M. (2018). Argonaute Proteins and Mechanisms of RNA Interference in Eukaryotes and Prokaryotes. *Biochemistry. Biokhimiia*, 83(5), 483-497. <https://doi.org/10.1134/S0006297918050024>
- OsBorne, D. J. (1934). The Org:wisation of the Cerebral Cortex. *Lab. Invest. Biol. Univ. Madr*, 29, 145-145.
- Oser, M., & Condeelis, J. (2009). The cofilin activity cycle in lamellipodia and invadopodia. *Journal of Cellular Biochemistry*, 108(6), 1252-1262. <https://doi.org/10.1002/jcb.22372>
- Ossenkoppele, R., Lyoo, C. H., Sudre, C. H., Westen, D., Cho, H., Ryu, Y. H., . . . Hansson, O. (2020). Distinct tau PET patterns in atrophy-defined subtypes of Alzheimer's disease. *Alzheimer's & Dementia*, 16(2), 335-344. <https://doi.org/10.1016/j.jalz.2019.08.201>
- Ostroff, L. E., Fiala, J. C., Allwardt, B., & Harris, K. M. (2002). Polyribosomes redistribute from dendritic shafts into spines with enlarged synapses during LTP in developing rat hippocampal slices. *Neuron*, 35(3), 535-545. [https://doi.org/10.1016/s0896-6273\(02\)00785-7](https://doi.org/10.1016/s0896-6273(02)00785-7)
- Pająk, B., Kania, E., & Orzechowski, A. (2016). Killing Me Softly: Connotations to Unfolded Protein Response and Oxidative Stress in Alzheimer's Disease. *Oxidative Medicine and Cellular Longevity*, 2016, 1-17. <https://doi.org/10.1155/2016/1805304>
- Pantazopoulou, V. I., Georgiou, S., Kakoulidis, P., Giannakopoulou, S. N., Tseleni, S., Stravopodis, D. J., & Anastasiadou, E. From the Argonauts Mythological Sailors to the Argonautes

- RNA-Silencing Navigators: Their Emerging Roles in Human-Cell Pathologies.
<https://doi.org/10.3390/ijms21114007>
- Papadimitriou, C., Celikkaya, H., Cosacak, M. I., Mashkaryan, V., Bray, L., Bhattarai, P., . . . Kizil, C. (2018). 3D Culture Method for Alzheimer's Disease Modeling Reveals Interleukin-4 Rescues A β 42-Induced Loss of Human Neural Stem Cell Plasticity. *Developmental Cell*, 46(1), 85-101.e108. <https://doi.org/10.1016/j.devcel.2018.06.005>
- Paradis-Isler, N., & Boehm, J. (2018). NMDA receptor-dependent dephosphorylation of serine 387 in Argonaute 2 increases its degradation and affects dendritic spine density and maturation. *The Journal of biological chemistry*, 293(24), 9311-9325.
<https://doi.org/10.1074/jbc.RA117.001007>
- Parhizkar, S., Arzberger, T., Brendel, M., Kleinberger, G., Deussing, M., Focke, C., . . . Haass, C. (2019). Loss of TREM2 function increases amyloid seeding but reduces plaque-associated ApoE. *Nature neuroscience*, 22(2), 191-204. <https://doi.org/10.1038/s41593-018-0296-9>
- Park, C. S., & Tang, S.-J. (2009). Regulation of microRNA expression by induction of bidirectional synaptic plasticity. *Journal of molecular neuroscience : MN*, 38(1), 50-56.
<https://doi.org/10.1007/s12031-008-9158-3>
- Park, J. H., Shin, S.-Y., & Shin, C. (2017). Non-canonical targets destabilize microRNAs in human Argonautes. *Nucleic acids research*, 45(4), 1569-1583.
<https://doi.org/10.1093/nar/gkx029>
- Park, M. S., Phan, H.-D., Busch, F., Hinckley, S. H., Brackbill, J. A., Wysocki, V. H., & Nakanishi, K. (2017). Human Argonaute3 has slicer activity. *Nucleic acids research*, 45(20), 11867-11877. <https://doi.org/10.1093/nar/gkx916>
- Parker, J. S. (2010). How to slice: snapshots of Argonaute in action. *Silence*, 1(1), 3-3.
<https://doi.org/10.1186/1758-907X-1-3>
- Pastalkova, E., Serrano, P., Pinkhasova, D., Wallace, E., Fenton, A. A., & Sacktor, T. C. (2006). Storage of Spatial Information by the Maintenance Mechanism of LTP. *Science*, 313(5790), 1141-1144. <https://doi.org/10.1126/science.1128657>
- Penn, A. C., Zhang, C. L., Georges, F., Royer, L., Breillat, C., Hosy, E., . . . Choquet, D. (2017). Hippocampal LTP and contextual learning require surface diffusion of AMPA receptors. *Nature*, 549(7672), 384-388. <https://doi.org/10.1038/nature23658>
- Penzes, P., Cahill, M. E., Jones, K. A., VanLeeuwen, J.-E., & Woolfrey, K. M. (2011). Dendritic spine pathology in neuropsychiatric disorders. *Nature Neuroscience*, 14(3), 285-293.
<https://doi.org/10.1038/nn.2741>
- Perez-Nievas, B. G., Stein, T. D., Tai, H.-C., Dols-Icardo, O., Scotton, T. C., Barroeta-Espar, I., . . . Gómez-Isla, T. (2013). Dissecting phenotypic traits linked to human resilience to Alzheimer's pathology. *Brain*, 136(8), 2510-2526. <https://doi.org/10.1093/brain/awt171>
- Peters, A., & Kaiserman-Abramof, I. R. (1970). The small pyramidal neuron of the rat cerebral cortex. The perikaryon, dendrites and spines. *American Journal of Anatomy*, 127(4), 321-355. <https://doi.org/10.1002/aja.1001270402>
- Peters, C., Espinoza, M. P., Gallegos, S., Opazo, C., & Aguayo, L. G. (2015). Alzheimer's A β

- interacts with cellular prion protein inducing neuronal membrane damage and synaptotoxicity. *Neurobiology of aging*, 36(3), 1369-1377.
<https://doi.org/10.1016/j.neurobiolaging.2014.11.019>
- Pichardo-Casas, I., Goff, L. A., Swerdel, M. R., Athie, A., Davila, J., Ramos-Brossier, M., . . . Vaca, L. (2012). Expression profiling of synaptic microRNAs from the adult rat brain identifies regional differences and seizure-induced dynamic modulation. *Brain research*, 1436, 20-33. <https://doi.org/10.1016/j.brainres.2011.12.001>
- Pickett, E. K., Koffie, R. M., Wegmann, S., Henstridge, C. M., Herrmann, A. G., Colom-Cadena, M., . . . Spires-Jones, T. L. (2016). Non-Fibrillar Oligomeric Amyloid- β within Synapses. *Journal of Alzheimer's Disease*, 53(3), 787-800. <https://doi.org/10.3233/JAD-160007>
- Pike, C. J., Burdick, D., Walencewicz, A. J., Glabe, C. G., & Cotman, C. W. (1993). Neurodegeneration induced by beta-amyloid peptides in vitro: the role of peptide assembly state. *The Journal of neuroscience : the official journal of the Society for Neuroscience*, 13(4), 1676-1687.
- Pleen, J., & Townley, R. (2022). Alzheimer's disease clinical trial update 2019–2021. *Journal of Neurology*, 269(2), 1038-1051. <https://doi.org/10.1007/s00415-021-10790-5>
- Podlisny, M. B., Walsh, D. M., Amarante, P., Ostaszewski, B. L., Stimson, E. R., Maggio, J. E., . . . Selkoe, D. J. (1998). Oligomerization of endogenous and synthetic amyloid beta-protein at nanomolar levels in cell culture and stabilization of monomer by Congo red. *Biochemistry*, 37(11), 3602-3611. <https://doi.org/10.1021/bi972029u>
- Pollard, T. D. (2003). The cytoskeleton, cellular motility and the reductionist agenda. *Nature*, 422(6933), 741-745. <https://doi.org/10.1038/nature01598>
- Pollard, T. D. (2016). Actin and Actin-Binding Proteins. *Cold Spring Harbor Perspectives in Biology*, 8(8), a018226-a018226. <https://doi.org/10.1101/cshperspect.a018226>
- Pozueta, J., Lefort, R., Ribe, E. M., Troy, C. M., Arancio, O., & Shelanski, M. (2013). Caspase-2 is required for dendritic spine and behavioral alterations in J20 APP transgenic mice. *Nature communications*, 4, 1939-1939. <https://doi.org/10.1038/NCOMMS2927>
- Premkumar, D. R. D., & Kalaria, R. N. (1996). Altered Expression of Amyloid β Precursor mRNAs in Cerebral Vessels, Meninges, and Choroid Plexus in Alzheimer's Disease. *Annals of the New York Academy of Sciences*, 777(1), 288-292. <https://doi.org/10.1111/j.1749-6632.1996.tb34434.x>
- Price, J. L., & Morris, J. C. (1999). Tangles and plaques in nondemented aging and ?preclinical? Alzheimer's disease. *Annals of Neurology*, 45(3), 358-368. [https://doi.org/10.1002/1531-8249\(199903\)45:3<358::AID-ANA12>3.0.CO;2-X](https://doi.org/10.1002/1531-8249(199903)45:3<358::AID-ANA12>3.0.CO;2-X)
- Pröschel, C., Blouin, M. J., Gutowski, N. J., Ludwig, R., & Noble, M. (1995). Limk1 is predominantly expressed in neural tissues and phosphorylates serine, threonine and tyrosine residues in vitro. *Oncogene*, 11(7), 1271-1281.
- Purpura, D. P. (1975). Dendritic differentiation in human cerebral cortex: normal and aberrant developmental patterns. *Advances in neurology*, 12, 91-134.
- Qi, H. H., Ongusaha, P. P., Myllyharju, J., Cheng, D., Pakkanen, O., Shi, Y., . . . Shi, Y. (2008). Prolyl 4-hydroxylation regulates Argonaute 2 stability. *Nature*, 455(7211), 421-424.

- <https://doi.org/10.1038/nature07186>
- Quévillon Huberdeau, M., Zeitler, D. M., Hauptmann, J., Bruckmann, A., Fressigné, L., Danner, J., . . . Meister, G. (2017). Phosphorylation of Argonaute proteins affects mRNA binding and is essential for microRNA-guided gene silencing in vivo. *The EMBO journal*, 36(14), 2088-2106. <https://doi.org/10.15252/embj.201696386>
- Raghavan, M., Fee, D., & Barkhaus, P. E. (2019). Generation and propagation of the action potential. In (pp. 3-22). <https://doi.org/10.1016/B978-0-444-64032-1.00001-1>
- Rajgor, D., Sanderson, T. M., Amici, M., Collingridge, G. L., & Hanley, J. G. (2018). NMDAR - dependent Argonaute 2 phosphorylation regulates mi RNA activity and dendritic spine plasticity. *The EMBO Journal*, 37(11). <https://doi.org/10.15252/embj.201797943>
- Reddy, P. H., Tonk, S., Kumar, S., Vijayan, M., Kandimalla, R., Kuruva, C. S., & Reddy, A. P. (2017). A critical evaluation of neuroprotective and neurodegenerative MicroRNAs in Alzheimer's disease. *Biochemical and biophysical research communications*, 483(4), 1156-1165. <https://doi.org/10.1016/j.bbrc.2016.08.067>
- Regehr, W. G., Carey, M. R., & Best, A. R. (2009). Activity-Dependent Regulation of Synapses by Retrograde Messengers. *Neuron*, 63(2), 154-170. <https://doi.org/10.1016/j.neuron.2009.06.021>
- Rehklau, K., Hoffmann, L., Gurniak, C. B., Ott, M., Witke, W., Scorrano, L., . . . Rust, M. B. (2017). Cofilin1-dependent actin dynamics control DRP1-mediated mitochondrial fission. *Cell death & disease*, 8(10), e3063-e3063. <https://doi.org/10.1038/cddis.2017.448>
- Ren, S.-Q., Yan, J.-Z., Zhang, X.-Y., Bu, Y.-F., Pan, W.-W., Yao, W., . . . Lu, W. (2013). PKC λ is critical in AMPA receptor phosphorylation and synaptic incorporation during LTP. *The EMBO Journal*, 32(10), 1365-1380. <https://doi.org/10.1038/emboj.2013.60>
- Reymann, K. G., & Frey, J. U. (2007). The late maintenance of hippocampal LTP: Requirements, phases, 'synaptic tagging', 'late-associativity' and implications. *Neuropharmacology*, 52(1), 24-40. <https://doi.org/10.1016/j.neuropharm.2006.07.026>
- Reza-Zaldivar, E. E., Hernández-Sápiens, M. A., Minjarez, B., Gómez-Pinedo, U., Sánchez-González, V. J., Márquez-Aguirre, A. L., & Canales-Aguirre, A. A. (2020). Dendritic Spine and Synaptic Plasticity in Alzheimer's Disease: A Focus on MicroRNA. *Frontiers in Cell and Developmental Biology*, 8. <https://doi.org/10.3389/fcell.2020.00255>
- Ridge, P. G., Karch, C. M., Hsu, S., Arano, I., Teerlink, C. C., Ebbert, M. T. W., . . . Kauwe, J. S. K. (2017). Linkage, whole genome sequence, and biological data implicate variants in RAB10 in Alzheimer's disease resilience. *Genome Medicine*, 9(1), 100-100. <https://doi.org/10.1186/s13073-017-0486-1>
- Risacher, S. L., Anderson, W. H., Charil, A., Castelluccio, P. F., Shcherbinin, S., Saykin, A. J., & Schwarz, A. J. (2017). Alzheimer disease brain atrophy subtypes are associated with cognition and rate of decline. *Neurology*, 89(21), 2176-2186. <https://doi.org/10.1212/WNL.0000000000004670>
- Rizzoli, S. O., & Betz, W. J. (2005). Synaptic vesicle pools. *Nature Reviews Neuroscience*, 6(1), 57-69. <https://doi.org/10.1038/nrn1583>
- Roh, S.-E., Woo, J. A., Lakshmana, M. K., Uhlar, C., Ankala, V., Boggess, T., . . . Kang, D. E. (2013).

- Mitochondrial dysfunction and calcium deregulation by the RanBP9-cofilin pathway. *FASEB journal : official publication of the Federation of American Societies for Experimental Biology*, 27(12), 4776-4789. <https://doi.org/10.1096/fj.13-234765>
- Roher, A. E., Ball, M. J., Bhawe, S. V., & Wakade, A. R. (1991). β -Amyloid from Alzheimer disease brains inhibits sprouting and survival of sympathetic neurons. *Biochemical and Biophysical Research Communications*, 174(2), 572-579. [https://doi.org/10.1016/0006-291X\(91\)91455-L](https://doi.org/10.1016/0006-291X(91)91455-L)
- Roher, A. E., Palmer, K. C., Capodilupo, J., Wakade, A. R., & Ball, M. J. (1991). New Biochemical Insights to Unravel the Pathogenesis of Alzheimer's Lesions. *Canadian Journal of Neurological Sciences / Journal Canadien des Sciences Neurologiques*, 18(S3), 408-410. <https://doi.org/10.1017/S0317167100032558>
- Rosso, S., Bollati, F., Bisbal, M., Peretti, D., Sumi, T., Nakamura, T., . . . Cáceres, A. (2004). LIMK1 Regulates Golgi Dynamics, Traffic of Golgi-derived Vesicles, and Process Extension in Primary Cultured Neurons. *Molecular Biology of the Cell*, 15(7), 3433-3449. <https://doi.org/10.1091/mbc.e03-05-0328>
- Rothenfluh, A., & Cowan, C. W. (2013). Emerging roles of actin cytoskeleton regulating enzymes in drug addiction: actin or reactin'? *Current opinion in neurobiology*, 23(4), 507-512. <https://doi.org/10.1016/j.conb.2013.01.027>
- Rush, T., Jose Martinez-Hernandez, X., Dollmeyer, M., Frandemiche, M. L., Borel, X., Boisseau, S., . . . Buisson, A. (2018). Cellular/Molecular Synaptotoxicity in Alzheimer's Disease Involved a Dysregulation of Actin Cytoskeleton Dynamics through Cofilin 1 Phosphorylation. <https://doi.org/10.1523/JNEUROSCI.1409-18.2018>
- Rust, M. B., Gurniak, C. B., Renner, M., Vara, H., Morando, L., Görlich, A., . . . Witke, W. (2010). Learning, AMPA receptor mobility and synaptic plasticity depend on n-cofilin-mediated actin dynamics. *The EMBO Journal*, 29(11), 1889-1902. <https://doi.org/10.1038/emboj.2010.72>
- Rybak, A., Fuchs, H., Hadian, K., Smirnova, L., Wulczyn, E. A., Michel, G., . . . Wulczyn, F. G. (2009). The let-7 target gene mouse lin-41 is a stem cell specific E3 ubiquitin ligase for the miRNA pathway protein Ago2. *Nature cell biology*, 11(12), 1411-1420. <https://doi.org/10.1038/ncb1987>
- Rüdel, S., Wang, Y., Lenobel, R., Körner, R., Hsiao, H.-H., Urlaub, H., . . . Meister, G. (2011). Phosphorylation of human Argonaute proteins affects small RNA binding. *Nucleic acids research*, 39(6), 2330-2343. <https://doi.org/10.1093/nar/gkq1032>
- Sabatini, B. L., Maravall, M., & Svoboda, K. (2001). Ca^{2+} signaling in dendritic spines. *Current Opinion in Neurobiology*, 11(3), 349-356. [https://doi.org/10.1016/S0959-4388\(00\)00218-X](https://doi.org/10.1016/S0959-4388(00)00218-X)
- Sabatini, B. L., Oertner, T. G., & Svoboda, K. (2002). The Life Cycle of Ca^{2+} Ions in Dendritic Spines. *Neuron*, 33(3), 439-452. [https://doi.org/10.1016/S0896-6273\(02\)00573-1](https://doi.org/10.1016/S0896-6273(02)00573-1)
- Saganich, M. J., Schroeder, B. E., Galvan, V., Bredesen, D. E., Koo, E. H., & Heinemann, S. F. (2006). Deficits in Synaptic Transmission and Learning in Amyloid Precursor Protein (APP) Transgenic Mice Require C-Terminal Cleavage of APP. *Journal of Neuroscience*, 26(52),

- 13428-13436. <https://doi.org/10.1523/JNEUROSCI.4180-06.2006>
- Sahin, U., Lapaquette, P., Andrieux, A., Faure, G., & Dejean, A. (2014). Sumoylation of Human Argonaute 2 at Lysine-402 Regulates Its Stability. *PLoS ONE*, *9*(7), e102957-e102957. <https://doi.org/10.1371/journal.pone.0102957>
- Saito, T., Matsuba, Y., Mihira, N., Takano, J., Nilsson, P., Itohara, S., . . . Saido, T. C. (2014). Single App knock-in mouse models of Alzheimer's disease. *Nature neuroscience*, *17*(5), 661-663. <https://doi.org/10.1038/nn.3697>
- Sambandan, S., Akbalik, G., Kochen, L., Rinne, J., Kahlstatt, J., Glock, C., . . . Schuman, E. M. (2017). Activity-dependent spatially localized miRNA maturation in neuronal dendrites. *Science*, *355*(6325), 634-637. <https://doi.org/10.1126/science.aaf8995>
- Sananbenesi, F., & Fischer, A. (2015). New friends for Ago2 in neuronal plasticity. *The EMBO Journal*, *34*(17), 2213-2213. <https://doi.org/10.15252/EMBJ.201592466>
- Sarkar, S., Engler-Chiurazzi, E. B., Cavendish, J. Z., Povroznik, J. M., Russell, A. E., Quintana, D. D., . . . Simpkins, J. W. (2019). Over-expression of miR-34a induces rapid cognitive impairment and Alzheimer's disease-like pathology. *Brain research*, *1721*, 146327-146327. <https://doi.org/10.1016/j.brainres.2019.146327>
- Sasahara, M., Fries, J. W., Raines, E. W., Gown, A. M., Westrum, L. E., Frosch, M. P., . . . Collins, T. (1991). PDGF B-chain in neurons of the central nervous system, posterior pituitary, and in a transgenic model. *Cell*, *64*(1), 217-227. [https://doi.org/10.1016/0092-8674\(91\)90223-I](https://doi.org/10.1016/0092-8674(91)90223-I)
- Sasaki, Y. (2020). Local Translation in Growth Cones and Presynapses, Two Axonal Compartments for Local Neuronal Functions. *Biomolecules*, *10*(5). <https://doi.org/10.3390/biom10050668>
- Scheff, S. W., Price, D. A., Schmitt, F. A., & Mufson, E. J. (2006). Hippocampal synaptic loss in early Alzheimer's disease and mild cognitive impairment. *Neurobiology of Aging*, *27*(10), 1372-1384. <https://doi.org/10.1016/j.neurobiolaging.2005.09.012>
- Scheltens, P., De Strooper, B., Kivipelto, M., Holstege, H., Ch  telat, G., Teunissen, C. E., . . . van der Flier, W. M. (2021). Alzheimer's disease. *The Lancet*, *397*(10284), 1577-1590. [https://doi.org/10.1016/S0140-6736\(20\)32205-4](https://doi.org/10.1016/S0140-6736(20)32205-4)
- Schratt, G. M., Tuebing, F., Nigh, E. A., Kane, C. G., Sabatini, M. E., Kiebler, M., & Greenberg, M. E. (2006). A brain-specific microRNA regulates dendritic spine development. *Nature*, *439*(7074), 283-289. <https://doi.org/10.1038/nature04367>
- Schwarz, A. J., Yu, P., Miller, B. B., Shcherbinin, S., Dickson, J., Navitsky, M., . . . Mintun, M. S. (2016). Regional profiles of the candidate tau PET ligand ¹⁸F-AV-1451 recapitulate key features of Braak histopathological stages. *Brain*, *139*(5), 1539-1550. <https://doi.org/10.1093/brain/aww023>
- Sch  ll, M., Lockhart, Samuel N., Schonhaut, Daniel R., O'Neil, James P., Janabi, M., Ossenkoppele, R., . . . Jagust, William J. (2016). PET Imaging of Tau Deposition in the Aging Human Brain. *Neuron*, *89*(5), 971-982. <https://doi.org/10.1016/j.neuron.2016.01.028>
- Scott, R. W., & Olson, M. F. (2007). LIM kinases: function, regulation and association with human

- disease. *Journal of molecular medicine (Berlin, Germany)*, 85(6), 555-568.
<https://doi.org/10.1007/s00109-007-0165-6>
- Scoville, W. B., & Milner, B. (1957). Loss of recent memory after bilateral hippocampal lesions. *Journal of Neurology, Neurosurgery & Psychiatry*, 20(1), 11-21.
<https://doi.org/10.1136/jnnp.20.1.11>
- Seet, B. T., Dikic, I., Zhou, M.-M., & Pawson, T. (2006). Reading protein modifications with interaction domains. *Nature reviews. Molecular cell biology*, 7(7), 473-483.
<https://doi.org/10.1038/nrm1960>
- Sekino, Y., Tanaka, S., Hanamura, K., Yamazaki, H., Sasagawa, Y., Xue, Y., . . . Shirao, T. (2006). Activation of N-methyl-d-aspartate receptor induces a shift of drebrin distribution: Disappearance from dendritic spines and appearance in dendritic shafts. *Molecular and Cellular Neuroscience*, 31(3), 493-504. <https://doi.org/10.1016/j.mcn.2005.11.003>
- Selkoe, D. J. (2002). Alzheimer's Disease Is a Synaptic Failure. *Science*, 298(5594), 789-791.
<https://doi.org/10.1126/science.1074069>
- Seo, G. J., Kincaid, R. P., Phanaksri, T., Burke, J. M., Pare, J. M., Cox, J. E., . . . Sullivan, C. S. (2013). Reciprocal inhibition between intracellular antiviral signaling and the RNAi machinery in mammalian cells. *Cell host & microbe*, 14(4), 435-445.
<https://doi.org/10.1016/j.chom.2013.09.002>
- Serrano-Pozo, A., Das, S., & Hyman, B. T. (2021). APOE and Alzheimer's disease: advances in genetics, pathophysiology, and therapeutic approaches. *The Lancet Neurology*, 20(1), 68-80. [https://doi.org/10.1016/S1474-4422\(20\)30412-9](https://doi.org/10.1016/S1474-4422(20)30412-9)
- Seth, P., Hsieh, P. N., Jamal, S., Wang, L., Gygi, S. P., Jain, M. K., . . . Stamler, J. S. (2019). Regulation of MicroRNA Machinery and Development by Interspecies S-Nitrosylation. *Cell*, 176(5), 1014-1025.e1012. <https://doi.org/10.1016/j.cell.2019.01.037>
- Shankar, G. M., Bloodgood, B. L., Townsend, M., Walsh, D. M., Selkoe, D. J., & Sabatini, B. L. (2007). Neurobiology of Disease Natural Oligomers of the Alzheimer Amyloid-Protein Induce Reversible Synapse Loss by Modulating an NMDA-Type Glutamate Receptor-Dependent Signaling Pathway. <https://doi.org/10.1523/JNEUROSCI.4970-06.2007>
- Shankar, G. M., Li, S., Mehta, T. H., Garcia-Munoz, A., Shepardson, N. E., Smith, I., . . . Selkoe, D. J. (2008). Amyloid-beta protein dimers isolated directly from Alzheimer's brains impair synaptic plasticity and memory. *Nature medicine*, 14(8), 837-842.
<https://doi.org/10.1038/NM1782>
- Shen, J., Xia, W., Khotaskaya, Y. B., Huo, L., Nakanishi, K., Lim, S.-O., . . . Hung, M.-C. (2013). EGFR modulates microRNA maturation in response to hypoxia through phosphorylation of AGO2. *Nature*, 497(7449), 383-387. <https://doi.org/10.1038/nature12080>
- Sheng, M., & Hoogenraad, C. C. (2007). The Postsynaptic Architecture of Excitatory Synapses: A More Quantitative View. *Annual Review of Biochemistry*, 76(1), 823-847.
<https://doi.org/10.1146/annurev.biochem.76.060805.160029>
- Sheppard, P. A. S., Choleris, E., & Galea, L. A. M. (2019). Structural plasticity of the hippocampus in response to estrogens in female rodents. *Molecular Brain*, 12(1), 22-22.
<https://doi.org/10.1186/s13041-019-0442-7>

- Sheu-Gruttadauria, J., & MacRae, I. J. (2017). Structural Foundations of RNA Silencing by Argonaute. *Journal of molecular biology*, 429(17), 2619-2639.
<https://doi.org/10.1016/j.jmb.2017.07.018>
- Sheu-Gruttadauria, J., & MacRae, I. J. (2017c). Structural Foundations of RNA Silencing by Argonaute. *Journal of Molecular Biology*, 429(17), 2619-2639.
<https://doi.org/10.1016/j.jmb.2017.07.018>
- Sheu-Gruttadauria, J., Pawlica, P., Klum, S. M., Wang, S., Yario, T. A., Schirle Oakdale, N. T., . . . MacRae, I. J. (2019). Structural Basis for Target-Directed MicroRNA Degradation. *Molecular Cell*, 75(6), 1243-1255.e1247. <https://doi.org/10.1016/j.molcel.2019.06.019>
- Shi, Y., Pontrello, C. G., DeFea, K. A., Reichardt, L. F., & Ethell, I. M. (2009). Focal Adhesion Kinase Acts Downstream of EphB Receptors to Maintain Mature Dendritic Spines by Regulating Cofilin Activity. *Journal of Neuroscience*, 29(25), 8129-8142.
<https://doi.org/10.1523/JNEUROSCI.4681-08.2009>
- Shi, Y., Pontrello, C. G., DeFea, K. A., Reichardt, L. F., & Ethell, I. M. (2009). Focal adhesion kinase acts downstream of EphB receptors to maintain mature dendritic spines by regulating cofilin activity. *The Journal of neuroscience : the official journal of the Society for Neuroscience*, 29(25), 8129-8142. <https://doi.org/10.1523/JNEUROSCI.4681-08.2009>
- Shigeoka, T., Jung, H., Jung, J., Turner-Bridger, B., Ohk, J., Lin, Julie Q., . . . Holt, Christine E. (2016). Dynamic Axonal Translation in Developing and Mature Visual Circuits. *Cell*, 166(1), 181-192. <https://doi.org/10.1016/j.cell.2016.05.029>
- Shrestha, B. R., Vitolo, O. V., Joshi, P., Lordkipanidze, T., Shelanski, M., & Dunaevsky, A. (2006). Amyloid β peptide adversely affects spine number and motility in hippocampal neurons. *Molecular and Cellular Neuroscience*, 33(3), 274-282.
<https://doi.org/10.1016/j.mcn.2006.07.011>
- Siegel, G., Obernosterer, G., Fiore, R., Oehmen, M., Bicker, S., Christensen, M., . . . Schratt, G. M. (2009). A functional screen implicates microRNA-138-dependent regulation of the depalmitoylation enzyme APT1 in dendritic spine morphogenesis. *Nature Cell Biology*, 11(6), 705-716. <https://doi.org/10.1038/ncb1876>
- Sigel, E., & Steinmann, M. E. (2012). Structure, Function, and Modulation of GABAA Receptors. *Journal of Biological Chemistry*, 287(48), 40224-40231.
<https://doi.org/10.1074/jbc.R112.386664>
- Silva, A. J., Paylor, R., Wehner, J. M., & Tonegawa, S. (1992). Impaired Spatial Learning in α -Calcium-Calmodulin Kinase II Mutant Mice. *Science*, 257(5067), 206-211.
<https://doi.org/10.1126/science.1321493>
- Silva, A. J., Stevens, C. F., Tonegawa, S., & Wang, Y. (1992). Deficient Hippocampal Long-Term Potentiation in α -Calcium-Calmodulin Kinase II Mutant Mice. *Science*, 257(5067), 201-206. <https://doi.org/10.1126/science.1378648>
- Skruber, K., Read, T.-A., & Vitriol, E. A. (2018). Reconsidering an active role for G-actin in cytoskeletal regulation. *Journal of Cell Science*, 131(1).
<https://doi.org/10.1242/jcs.203760>
- Sladeczek, F., Pin, J.-P., Récasens, M., Bockaert, J., & Weiss, S. (1985). Glutamate stimulates

- inositol phosphate formation in striatal neurones. *Nature*, 317(6039), 717-719.
<https://doi.org/10.1038/317717a0>
- Smith, D. L., Pozueta, J., Gong, B., Arancio, O., & Shelanski, M. (2009). Reversal of long-term dendritic spine alterations in Alzheimer disease models. *Proceedings of the National Academy of Sciences*, 106(39), 16877-16882. <https://doi.org/10.1073/PNAS.0908706106>
- Sola, E., Prestori, F., Rossi, P., Taglietti, V., & D'Angelo, E. (2004). Increased neurotransmitter release during long-term potentiation at mossy fibre-granule cell synapses in rat cerebellum. *The Journal of physiology*, 557(Pt 3), 843-861.
<https://doi.org/10.1113/jphysiol.2003.060285>
- Song, Y., Hu, M., Zhang, J., Teng, Z.-Q., & Chen, C. (2019). A novel mechanism of synaptic and cognitive impairments mediated via microRNA-30b in Alzheimer's disease. *EBioMedicine*, 39, 409-421. <https://doi.org/10.1016/j.ebiom.2018.11.059>
- Sperling, R. A., Aisen, P. S., Beckett, L. A., Bennett, D. A., Craft, S., Fagan, A. M., . . . Phelps, C. H. (2011). Toward defining the preclinical stages of Alzheimer's disease: Recommendations from the National Institute on Aging-Alzheimer's Association workgroups on diagnostic guidelines for Alzheimer's disease. *Alzheimer's & Dementia*, 7(3), 280-292.
<https://doi.org/10.1016/J.JALZ.2011.03.003>
- Spies, P. E., Slats, D., Sjogren, J. M. C., Kremer, B. P. H., Verhey, F. R. J., Olde Rikkert, M. G. M., & Verbeek, M. M. (2010). The Cerebrospinal Fluid Amyloid β 42/40 Ratio in the Differentiation of Alzheimers Disease from Non-Alzheimers Dementia. *Current Alzheimer Research*, 7(5), 470-476. <https://doi.org/10.2174/156720510791383796>
- Spires, T. L., Meyer-Luehmann, M., Stern, E. A., McLean, P. J., Skoch, J., Nguyen, P. T., . . . Hyman, B. T. (2005). Dendritic spine abnormalities in amyloid precursor protein transgenic mice demonstrated by gene transfer and intravital multiphoton microscopy. *The Journal of neuroscience : the official journal of the Society for Neuroscience*, 25(31), 7278-7287.
<https://doi.org/10.1523/JNEUROSCI.1879-05.2005>
- Squire, L. R. (2004). Memory systems of the brain: A brief history and current perspective. *Neurobiology of Learning and Memory*, 82(3), 171-177.
<https://doi.org/10.1016/j.nlm.2004.06.005>
- Stagsted, L. V. W., Daugaard, I., & Hansen, T. B. (2017). The agotrons: Gene regulators or Argonaute protectors? *BioEssays*, 39(4), 1600239-1600239.
<https://doi.org/10.1002/BIES.201600239>
- Stamatakou, E., Marzo, A., Gibb, A., & Salinas, P. C. (2013). Activity-Dependent Spine Morphogenesis: A Role for the Actin-Capping Protein Eps8. *Journal of Neuroscience*, 33(6), 2661-2670. <https://doi.org/10.1523/JNEUROSCI.0998-12.2013>
- Steward, O., & Levy, W. B. (1982). *The Journal of Neuroscience Copyright © Society for Neuroscience PREFERENTIAL LOCALIZATION OF POLYRIBOSOMES UNDER THE BASE OF DENDRITIC SPINES IN GRANULE CELLS OF THE DENTATE GYRUS*.
- Stine, W. B., Dahlgren, K. N., Krafft, G. A., & LaDu, M. J. (2003). In vitro characterization of conditions for amyloid-beta peptide oligomerization and fibrillogenesis. *The Journal of biological chemistry*, 278(13), 11612-11622. <https://doi.org/10.1074/jbc.M210207200>

- Stoothoff, W. H., & Johnson, G. V. W. (2005). Tau phosphorylation: physiological and pathological consequences. *Biochimica et Biophysica Acta (BBA) - Molecular Basis of Disease*, 1739(2-3), 280-297. <https://doi.org/10.1016/j.bbadis.2004.06.017>
- Subramanian, J., Savage, J. C., & Tremblay, M. È. (2020). Synaptic Loss in Alzheimer's Disease: Mechanistic Insights Provided by Two-Photon in vivo Imaging of Transgenic Mouse Models. *Frontiers in Cellular Neuroscience*, 14, 445-445. <https://doi.org/10.3389/FNCEL.2020.592607/BIBTEX>
- Sun, J., Gao, X., Meng, D., Xu, Y., Wang, X., Gu, X., . . . Zheng, Y. (2017). Antagomirs Targeting MicroRNA-134 Increase Limk1 Levels After Experimental Seizures in Vitro and in Vivo. *Cellular physiology and biochemistry : international journal of experimental cellular physiology, biochemistry, and pharmacology*, 43(2), 636-643. <https://doi.org/10.1159/000480647>
- Sun, Y., Liang, L., Dong, M., Li, C., Liu, Z., & Gao, H. (2019). Cofilin 2 in Serum as a Novel Biomarker for Alzheimer's Disease in Han Chinese. *Frontiers in aging neuroscience*, 11, 214-214. <https://doi.org/10.3389/fnagi.2019.00214>
- Sun, Y., Rong, X., Lu, W., Peng, Y., Li, J., Xu, S., . . . Wang, X. (2015). Translational study of Alzheimer's disease (AD) biomarkers from brain tissues in A β PP/PS1 mice and serum of AD patients. *Journal of Alzheimer's disease : JAD*, 45(1), 269-282. <https://doi.org/10.3233/JAD-142805>
- Sungur, A. Ö., Stemmler, L., Wöhr, M., & Rust, M. B. (2018). Impaired Object Recognition but Normal Social Behavior and Ultrasonic Communication in Cofilin1 Mutant Mice. *Frontiers in behavioral neuroscience*, 12, 25-25. <https://doi.org/10.3389/fnbeh.2018.00025>
- Sutton, M. A., Ito, H. T., Cressy, P., Kempf, C., Woo, J. C., & Schuman, E. M. (2006). Miniature Neurotransmission Stabilizes Synaptic Function via Tonic Suppression of Local Dendritic Protein Synthesis. *Cell*, 125(4), 785-799. <https://doi.org/10.1016/j.cell.2006.03.040>
- Swarts, D. C., Makarova, K., Wang, Y., Nakanishi, K., Ketting, R. F., Koonin, E. V., . . . van der Oost, J. (2014). The evolutionary journey of Argonaute proteins. *Nature structural & molecular biology*, 21(9), 743-753. <https://doi.org/10.1038/nsmb.2879>
- Tabner, B. J., El-Agnaf, O. M. A., Turnbull, S., German, M. J., Paleologou, K. E., Hayashi, Y., . . . Allsop, D. (2005). Hydrogen Peroxide Is Generated during the Very Early Stages of Aggregation of the Amyloid Peptides Implicated in Alzheimer Disease and Familial British Dementia. *Journal of Biological Chemistry*, 280(43), 35789-35792. <https://doi.org/10.1074/jbc.C500238200>
- Tada, T., & Sheng, M. (2006). Molecular mechanisms of dendritic spine morphogenesis. *Current Opinion in Neurobiology*, 16(1), 95-101. <https://doi.org/10.1016/j.conb.2005.12.001>
- Takeuchi, T., Duszkievicz, A. J., & Morris, R. G. M. (2014). The synaptic plasticity and memory hypothesis: encoding, storage and persistence. *Philosophical Transactions of the Royal Society B: Biological Sciences*, 369(1633). <https://doi.org/10.1098/RSTB.2013.0288>
- Takumi, Y., Matsubara, A., Rinvik, E., & Ottersen, O. P. (1999). The Arrangement of Glutamate Receptors in Excitatory Synapses. *Annals of the New York Academy of Sciences*, 868(1

- MOLECULAR AND), 474-482. <https://doi.org/10.1111/j.1749-6632.1999.tb11316.x>
- Tang, Y.-P., Shimizu, E., Dube, G. R., Rampon, C., Kerchner, G. A., Zhuo, M., . . . Tsien, J. Z. (1999). Genetic enhancement of learning and memory in mice. *Nature*, *401*(6748), 63-69. <https://doi.org/10.1038/43432>
- Tavana, J., Rosene, M., Jensen, N., Ridge, P. G., Kauwe, J. S. K., & Karch, C. M. (2018). RAB10: an Alzheimer's disease resilience locus and potential drug target. *Clinical Interventions in Aging*, *Volume 14*, 73-79. <https://doi.org/10.2147/CIA.S159148>
- Taylor, A. M., Wu, J., Tai, H. C., & Schuman, E. M. (2013). Axonal Translation of β -Catenin Regulates Synaptic Vesicle Dynamics. *Journal of Neuroscience*, *33*(13), 5584-5589. <https://doi.org/10.1523/JNEUROSCI.2944-12.2013>
- Terry, R. D., Masliah, E., Salmon, D. P., Butters, N., DeTeresa, R., Hill, R., . . . Katzman, R. (1991). Physical basis of cognitive alterations in alzheimer's disease: Synapse loss is the major correlate of cognitive impairment. *Annals of Neurology*, *30*(4), 572-580. <https://doi.org/10.1002/ANA.410300410>
- Thal, D. R., Rüb, U., Orantes, M., & Braak, H. (2002). Phases of A β -deposition in the human brain and its relevance for the development of AD. *Neurology*, *58*(12), 1791-1800. <https://doi.org/10.1212/WNL.58.12.1791>
- Thelen, M. P., & Kye, M. J. (2020). The Role of RNA Binding Proteins for Local mRNA Translation: Implications in Neurological Disorders. *Frontiers in Molecular Biosciences*, *6*. <https://doi.org/10.3389/fmolb.2019.00161>
- Thomas, K. T., Gross, C., & Bassell, G. J. (2018). microRNAs Sculpt Neuronal Communication in a Tight Balance That Is Lost in Neurological Disease. *Frontiers in molecular neuroscience*, *11*, 455-455. <https://doi.org/10.3389/fnmol.2018.00455>
- Thompson, P. M., Hayashi, K. M., de Zubicaray, G., Janke, A. L., Rose, S. E., Semple, J., . . . Toga, A. W. (2003). Dynamics of Gray Matter Loss in Alzheimer's Disease. *The Journal of Neuroscience*, *23*(3), 994-1005. <https://doi.org/10.1523/JNEUROSCI.23-03-00994.2003>
- Tian, Y., Simanshu, D. K., Ma, J.-B., & Patel, D. J. (2011). Structural basis for piRNA 2'-O-methylated 3'-end recognition by Piwi PAZ (Piwi/Argonaute/Zwille) domains. *Proceedings of the National Academy of Sciences of the United States of America*, *108*(3), 903-910. <https://doi.org/10.1073/pnas.1017762108>
- Todorovski, Z., Asrar, S., Liu, J., Saw, N. M. N., Joshi, K., Cortez, M. A., . . . Jia, Z. (2015). LIMK1 Regulates Long-Term Memory and Synaptic Plasticity via the Transcriptional Factor CREB. *Molecular and Cellular Biology*, *35*(8), 1316-1328. <https://doi.org/10.1128/MCB.01263-14>
- Tolar, M., Abushakra, S., & Sabbagh, M. (2020). The path forward in Alzheimer's disease therapeutics: Reevaluating the amyloid cascade hypothesis. *Alzheimer's & dementia : the journal of the Alzheimer's Association*, *16*(11), 1553-1560. <https://doi.org/10.1016/j.jalz.2019.09.075>
- Tolia, N. H., & Joshua-Tor, L. (2007). Slicer and the Argonautes. *Nature Chemical Biology*, *3*(1), 36-43. <https://doi.org/10.1038/nchembio848>
- Tsai, J., Grutzendler, J., Duff, K., & Gan, W. B. (2004). Fibrillar amyloid deposition leads to local

- synaptic abnormalities and breakage of neuronal branches. *Nature neuroscience*, 7(11), 1181-1183. <https://doi.org/10.1038/NN1335>
- Tsien, J. Z., Huerta, P. T., & Tonegawa, S. (1996). The Essential Role of Hippocampal CA1 NMDA Receptor–Dependent Synaptic Plasticity in Spatial Memory. *Cell*, 87(7), 1327-1338. [https://doi.org/10.1016/S0092-8674\(00\)81827-9](https://doi.org/10.1016/S0092-8674(00)81827-9)
- Tsuboyama, K., Tadakuma, H., & Tomari, Y. (2018). Conformational Activation of Argonaute by Distinct yet Coordinated Actions of the Hsp70 and Hsp90 Chaperone Systems. *Molecular Cell*, 70(4), 722-729.e724. <https://doi.org/10.1016/J.MOLCEL.2018.04.010>
- Um, Ji W., Kaufman, Adam C., Kostylev, M., Heiss, Jacqueline K., Stagi, M., Takahashi, H., . . . Strittmatter, Stephen M. (2013). Metabotropic Glutamate Receptor 5 Is a Coreceptor for Alzheimer A β Oligomer Bound to Cellular Prion Protein. *Neuron*, 79(5), 887-902. <https://doi.org/10.1016/j.neuron.2013.06.036>
- Um, J. W., Nygaard, H. B., Heiss, J. K., Kostylev, M. A., Stagi, M., Vortmeyer, A., . . . Strittmatter, S. M. (2012). Alzheimer amyloid- β oligomer bound to postsynaptic prion protein activates Fyn to impair neurons. *Nature Neuroscience*, 15(9), 1227-1235. <https://doi.org/10.1038/nn.3178>
- Vadukul, D. M., Vrancx, C., Burguet, P., Contino, S., Suelves, N., Serpell, L. C., . . . Kienlen-Campard, P. (2021). An evaluation of the self-assembly enhancing properties of cell-derived hexameric amyloid- β . *Scientific Reports*, 11(1), 11570-11570. <https://doi.org/10.1038/s41598-021-90680-y>
- van der Flier, W. M. (2005). Epidemiology and risk factors of dementia. *Journal of Neurology, Neurosurgery & Psychiatry*, 76(suppl_5), v2-v7. <https://doi.org/10.1136/jnnp.2005.082867>
- van Kouwenhove, M., Kedde, M., & Agami, R. (2011). MicroRNA regulation by RNA-binding proteins and its implications for cancer. *Nature Reviews Cancer*, 11(9), 644-656. <https://doi.org/10.1038/nrc3107>
- Vargas, L. M., Leal, N., Estrada, L. D., González, A., Serrano, F., Araya, K., . . . Alvarez, A. R. (2014). EphA4 activation of c-Abl mediates synaptic loss and LTP blockade caused by amyloid- β oligomers. *PloS one*, 9(3), e92309-e92309. <https://doi.org/10.1371/journal.pone.0092309>
- Vogel, J. W., Iturria-Medina, Y., Strandberg, O. T., Smith, R., Levitis, E., Evans, A. C., . . . Wollmer, P. (2020). Spread of pathological tau proteins through communicating neurons in human Alzheimer's disease. *Nature Communications*, 11(1), 2612-2612. <https://doi.org/10.1038/s41467-020-15701-2>
- Vogel, J. W., Young, A. L., Oxtoby, N. P., Smith, R., Ossenkoppele, R., Strandberg, O. T., . . . Hansson, O. (2021). Four distinct trajectories of tau deposition identified in Alzheimer's disease. *Nature medicine*, 27(5), 871-881. <https://doi.org/10.1038/s41591-021-01309-6>
- Wakiyama, M., Takimoto, K., Ohara, O., & Yokoyama, S. (2007). Let-7 microRNA-mediated mRNA deadenylation and translational repression in a mammalian cell-free system. *Genes & development*, 21(15), 1857-1862. <https://doi.org/10.1101/gad.1566707>
- Walsh, D. M., Hartley, D. M., Condron, M. M., Selkoe, D. J., & Teplow, D. B. (2001). In vitro

- studies of amyloid beta-protein fibril assembly and toxicity provide clues to the aetiology of Flemish variant (Ala692-->Gly) Alzheimer's disease. *The Biochemical journal*, 355(Pt 3), 869-877. <https://doi.org/10.1042/bj3550869>
- Walsh, D. M., Klyubin, I., Fadeeva, J. V., Cullen, W. K., Anwyl, R., Wolfe, M. S., . . . Selkoe, D. J. (2002). Naturally secreted oligomers of amyloid β protein potently inhibit hippocampal long-term potentiation in vivo. *Nature*, 416(6880), 535-539. <https://doi.org/10.1038/416535a>
- Walsh, D. M., Klyubin, I., Shankar, G. M., Townsend, M., Fadeeva, J. V., Betts, V., . . . Selkoe, D. J. (2005). The role of cell-derived oligomers of Abeta in Alzheimer's disease and avenues for therapeutic intervention. *Biochemical Society transactions*, 33(Pt 5), 1087-1090. <https://doi.org/10.1042/BST20051087>
- Walsh, D. M., & Teplow, D. B. (2012). Alzheimer's Disease and the Amyloid β -Protein. In (pp. 101-124). <https://doi.org/10.1016/B978-0-12-385883-2.00012-6>
- Walsh, K. P., Minamide, L. S., Kane, S. J., Shaw, A. E., Brown, D. R., Pulford, B., . . . Bamburg, J. R. (2014). Amyloid- β and proinflammatory cytokines utilize a prion protein-dependent pathway to activate NADPH oxidase and induce cofilin-actin rods in hippocampal neurons. *PloS one*, 9(4), e95995-e95995. <https://doi.org/10.1371/journal.pone.0095995>
- Wang, H. W., Pasternak, J. F., Kuo, H., Ristic, H., Lambert, M. P., Chromy, B., . . . Trommer, B. L. (2002). Soluble oligomers of beta amyloid (1-42) inhibit long-term potentiation but not long-term depression in rat dentate gyrus. *Brain research*, 924(2), 133-140. [https://doi.org/10.1016/S0006-8993\(01\)03058-X](https://doi.org/10.1016/S0006-8993(01)03058-X)
- Wang, X. B., Yang, Y., & Zhou, Q. (2007). Independent expression of synaptic and morphological plasticity associated with long-term depression. *The Journal of neuroscience : the official journal of the Society for Neuroscience*, 27(45), 12419-12429. <https://doi.org/10.1523/JNEUROSCI.2015-07.2007>
- Wang, Y., Zhang, Y., Hu, W., Xie, S., Gong, C.-X., Iqbal, K., & Liu, F. (2015). Rapid alteration of protein phosphorylation during postmortem: implication in the study of protein phosphorylation OPEN. *Nature Publishing Group*. <https://doi.org/10.1038/srep15709>
- Wang, Z., Jackson, R. J., Hong, W., Taylor, W. M., Corbett, G. T., Moreno, A., . . . Walsh, D. M. (2017). Human Brain-Derived A β Oligomers Bind to Synapses and Disrupt Synaptic Activity in a Manner That Requires APP. *The Journal of Neuroscience*, 37(49), 11947-11966. <https://doi.org/10.1523/JNEUROSCI.2009-17.2017>
- Webster, S. J., Bachstetter, A. D., Nelson, P. T., Schmitt, F. A., & Van Eldik, L. J. (2014). Using mice to model Alzheimer's dementia: an overview of the clinical disease and the preclinical behavioral changes in 10 mouse models. *Frontiers in genetics*, 5(APR). <https://doi.org/10.3389/FGENE.2014.00088>
- Weinmann, L., Höck, J., Ivacevic, T., Ohrt, T., Mütze, J., Schwille, P., . . . Meister, G. (2009). Importin 8 Is a Gene Silencing Factor that Targets Argonaute Proteins to Distinct mRNAs. *Cell*, 136(3), 496-507. <https://doi.org/10.1016/j.cell.2008.12.023>
- Westholm, J. O., & Lai, E. C. (2011). Mirtrons: microRNA biogenesis via splicing. *Biochimie*, 93(11), 1897-1904. <https://doi.org/10.1016/j.biochi.2011.06.017>

- Whitehouse, P. J., Price, D. L., Struble, R. G., Clark, A. W., Coyle, J. T., & DeLong, M. R. (1982). Alzheimer's Disease and Senile Dementia: Loss of Neurons in the Basal Forebrain. *Science*, 215(4537), 1237-1239. <https://doi.org/10.1126/science.7058341>
- Whitlock, J. R., Heynen, A. J., Shuler, M. G., & Bear, M. F. (2006). Learning Induces Long-Term Potentiation in the Hippocampus. *Science*, 313(5790), 1093-1097. <https://doi.org/10.1126/science.1128134>
- Whitwell, J. L., Dickson, D. W., Murray, M. E., Weigand, S. D., Tosakulwong, N., Senjem, M. L., . . . Josephs, K. A. (2012). Neuroimaging correlates of pathologically defined subtypes of Alzheimer's disease: a case-control study. *The Lancet Neurology*, 11(10), 868-877. [https://doi.org/10.1016/S1474-4422\(12\)70200-4](https://doi.org/10.1016/S1474-4422(12)70200-4)
- Wibbrand, K., Pai, B., Siripornmongkolchai, T., Bittins, M., Berentsen, B., Ofte, M. L., . . . Bramham, C. R. (2012). MicroRNA regulation of the synaptic plasticity-related gene Arc. *PloS one*, 7(7), e41688-e41688. <https://doi.org/10.1371/journal.pone.0041688>
- Wibbrand, K., Panja, D., Tiron, A., Ofte, M. L., Skaftnesmo, K.-O., Lee, C. S., . . . Bramham, C. R. (2010). Differential regulation of mature and precursor microRNA expression by NMDA and metabotropic glutamate receptor activation during LTP in the adult dentate gyrus in vivo. *The European journal of neuroscience*, 31(4), 636-645. <https://doi.org/10.1111/j.1460-9568.2010.07112.x>
- Wiegert, J. S., & Oertner, T. G. (2013). Long-term depression triggers the selective elimination of weakly integrated synapses. *Proceedings of the National Academy of Sciences*, 110(47). <https://doi.org/10.1073/pnas.1315926110>
- Wilcox, K. S., Buchhalter, J., & Dichter, M. A. (1994). Properties of inhibitory and excitatory synapses between hippocampal neurons in very low density cultures. *Synapse*, 18(2), 128-151. <https://doi.org/10.1002/syn.890180206>
- Wilde, M. C., Overk, C. R., Sijben, J. W., & Masliah, E. (2016). Meta-analysis of synaptic pathology in Alzheimer's disease reveals selective molecular vesicular machinery vulnerability. *Alzheimer's & Dementia*, 12(6), 633-644. <https://doi.org/10.1016/j.jalz.2015.12.005>
- Willkomm, S., Oellig, C. A., Zander, A., Restle, T., Keegan, R., Grohmann, D., & Schneider, S. (2017). Structural and mechanistic insights into an archaeal DNA-guided Argonaute protein. *Nature microbiology*, 2, 17035-17035. <https://doi.org/10.1038/nmicrobiol.2017.35>
- Woo, J.-A. A., Liu, T., Fang, C. C., Cazzaro, S., Kee, T., LePochat, P., . . . Kang, D. E. (2019). Activated cofilin exacerbates tau pathology by impairing tau-mediated microtubule dynamics. *Communications biology*, 2, 112-112. <https://doi.org/10.1038/s42003-019-0359-9>
- Woo, J. A., Boggess, T., Uhlar, C., Wang, X., Khan, H., Cappos, G., . . . Kang, D. E. (2015). RanBP9 at the intersection between cofilin and A β pathologies: rescue of neurodegenerative changes by RanBP9 reduction. *Cell Death and Disease*, 6. <https://doi.org/10.1038/cddis.2015.37>
- Woo, J. A., Jung, A. R., Lakshmana, M. K., Bedrossian, A., Lim, Y., Bu, J. H., . . . Kang, D. E. (2012). Pivotal role of the RanBP9-cofilin pathway in A β -induced apoptosis and

- neurodegeneration. *Cell death and differentiation*, 19(9), 1413-1423.
<https://doi.org/10.1038/CDD.2012.14>
- World Health, O. Dementia Factsheet. In
<https://www.who.int/news-room/fact-sheets/detail/dementia>. Accessed on:
 05.04.2020.
- Wright, A. L., Zinn, R., Hohensinn, B., Konen, L. M., Beynon, S. B., Tan, R. P., . . . Vissel, B. (2013). Neuroinflammation and Neuronal Loss Precede A β Plaque Deposition in the hAPP-J20 Mouse Model of Alzheimer's Disease. *PLoS ONE*, 8(4).
<https://doi.org/10.1371/JOURNAL.PONE.0059586>
- Wu, C.-C., Chawla, F., Games, D., Rydel, R. E., Freedman, S., Schenk, D., . . . Bloom, F. E. (2004). Selective vulnerability of dentate granule cells prior to amyloid deposition in PDAPP mice: Digital morphometric analyses. *Proceedings of the National Academy of Sciences*, 101(18), 7141-7146. <https://doi.org/10.1073/pnas.0402147101>
- Wu, J. e., Yang, J., Cho, W. C., & Zheng, Y. (2020). Argonaute proteins: Structural features, functions and emerging roles. *Journal of Advanced Research*, 24, 317-317.
<https://doi.org/10.1016/J.JARE.2020.04.017>
- Xing, L., & Bassell, G. J. (2013). mRNA Localization: An Orchestration of Assembly, Traffic and Synthesis. *Traffic*, 14(1), 2-14. <https://doi.org/10.1111/tra.12004>
- Xu, W., Tan, L., Wang, H.-F., Jiang, T., Tan, M.-S., Tan, L., . . . Yu, J.-T. (2015). Meta-analysis of modifiable risk factors for Alzheimer's disease. *Journal of Neurology, Neurosurgery & Psychiatry*, jnnp-310548. <https://doi.org/10.1136/jnnp-2015-310548>
- Yang, G., Pan, F., & Gan, W.-B. (2009). Stably maintained dendritic spines are associated with lifelong memories. *Nature*, 462(7275), 920-924. <https://doi.org/10.1038/nature08577>
- Yang, M., Haase, Astrid D., Huang, F.-K., Coulis, G., Rivera, Keith D., Dickinson, Bryan C., . . . Tonks, Nicholas K. (2014). Dephosphorylation of Tyrosine 393 in Argonaute 2 by Protein Tyrosine Phosphatase 1B Regulates Gene Silencing in Oncogenic RAS-Induced Senescence. *Molecular Cell*, 55(5), 782-790.
<https://doi.org/10.1016/j.molcel.2014.07.018>
- Ye, X., Huang, N., Liu, Y., Paroo, Z., Huerta, C., Li, P., . . . Zhang, H. (2011). Structure of C3PO and mechanism of human RISC activation. *Nature structural & molecular biology*, 18(6), 650-657. <https://doi.org/10.1038/nsmb.2032>
- Yi, R., Qin, Y., Macara, I. G., & Cullen, B. R. (2003). Exportin-5 mediates the nuclear export of pre-microRNAs and short hairpin RNAs. *Genes & development*, 17(24), 3011-3016.
<https://doi.org/10.1101/gad.1158803>
- Yoon, S.-J., Elahi, L. S., Paşca, A. M., Marton, R. M., Gordon, A., Revah, O., . . . Paşca, S. P. (2019). Reliability of human cortical organoid generation. *Nature Methods*, 16(1), 75-78.
<https://doi.org/10.1038/s41592-018-0255-0>
- Yuste, R. (2011). Dendritic Spines and Distributed Circuits. *Neuron*, 71(5), 772-781.
<https://doi.org/10.1016/j.neuron.2011.07.024>
- Yuste, R. (2015). The discovery of dendritic spines by Cajal. *Frontiers in neuroanatomy*, 9, 18-18.
<https://doi.org/10.3389/fnana.2015.00018>

- Zablah, B. Y., Merovitch, N., & Jia, Z. (2020). The Role of ADF/Cofilin in Synaptic Physiology and Alzheimer's Disease. *Frontiers in cell and developmental biology*, 8. <https://doi.org/10.3389/FCELL.2020.594998>
- Zampa, F., Bicker, S., & Schratt, G. (2018). Activity-Dependent Pre-miR-134 Dendritic Localization Is Required for Hippocampal Neuron Dendritogenesis. *Frontiers in molecular neuroscience*, 11. <https://doi.org/10.3389/FNMOL.2018.00171>
- Zeng, Y., Sankala, H., Zhang, X., & Graves, Paul R. (2008). Phosphorylation of Argonaute 2 at serine-387 facilitates its localization to processing bodies. *Biochemical Journal*, 413(3), 429-436. <https://doi.org/10.1042/BJ20080599>
- Zhang, H., Wang, Y., Dou, J., Guo, Y., He, J., Li, L., . . . Yu, J. (2019). Acetylation of AGO2 promotes cancer progression by increasing oncogenic miR-19b biogenesis. *Oncogene*, 38(9), 1410-1431. <https://doi.org/10.1038/s41388-018-0530-7>
- Zhang, K., Zhang, X., Cai, Z., Zhou, J., Cao, R., Zhao, Y., . . . Fu, X.-D. (2018). A novel class of microRNA-recognition elements that function only within open reading frames. *Nature Structural & Molecular Biology*, 25(11), 1019-1027. <https://doi.org/10.1038/s41594-018-0136-3>
- Zhang, X.-h., & Poo, M.-m. (2002). Localized Synaptic Potentiation by BDNF Requires Local Protein Synthesis in the Developing Axon. *Neuron*, 36(4), 675-688. [https://doi.org/10.1016/S0896-6273\(02\)01023-1](https://doi.org/10.1016/S0896-6273(02)01023-1)
- Zhao, W.-Q., & Townsend, M. (2009). Insulin resistance and amyloidogenesis as common molecular foundation for type 2 diabetes and Alzheimer's disease. *Biochimica et Biophysica Acta (BBA) - Molecular Basis of Disease*, 1792(5), 482-496. <https://doi.org/10.1016/j.bbadis.2008.10.014>
- Zheng, K., Hu, F., Zhou, Y., Zhang, J., Zheng, J., Lai, C., . . . Zhu, L.-Q. miR-135a-5p mediates memory and synaptic impairments via the Rock2/Adducin1 signaling pathway in a mouse model of Alzheimer's disease. <https://doi.org/10.1038/s41467-021-22196-y>
- Zhou, Q., Homma, K. J., & Poo, M. M. (2004). Shrinkage of dendritic spines associated with long-term depression of hippocampal synapses. *Neuron*, 44(5), 749-757. <https://doi.org/10.1016/J.NEURON.2004.11.011>
- Zovoilis, A., Agbemenyah, H. Y., Agis-Balboa, R. C., Stilling, R. M., Edbauer, D., Rao, P., . . . Fischer, A. (2011). microRNA-34c is a novel target to treat dementias. *The EMBO Journal*, 30(20), 4299-4308. <https://doi.org/10.1038/emboj.2011.327>

Appendix 1: South West Dementia Brain Bank human sample data

| MRC ID | AGE | SEX | Histological Diagnosis | Secondary diagnosis | Tertiary diagnosis | PM DELAY (hours) | Braak tangle stage |
|----------|-----|-----|--|----------------------------|--------------------|------------------|--------------------|
| BBN_8739 | 93 | F | NO PL,SC T(HIPPO&MT CORTEX) | NO | NO | 18 | 2 |
| BBN_8751 | 82 | M | NO PL OR T | NO | NO | 30 | 2 |
| BBN_8770 | 89 | F | AGE(SC PL TF CORTEX,T ENTOR) | NO | NO | 15 | 2 |
| BBN_8848 | 77 | F | AD | NO | NO | 43 | 4 |
| BBN_8917 | 91 | M | AD | NO | NO | 43 | 3 |
| BBN_8923 | 82 | M | AGE | NO | NO | 3 | 2 |
| BBN_8968 | 89 | F | AD | NO | NO | 14 | 4 |
| BBN_8989 | 90 | M | AD | NO | NO | 13 | 3 |
| BBN_9028 | 76 | M | NORMAL BRAIN | NO | NO | 23 | 2 |
| BBN_9050 | 90 | F | AD | NO | NO | 21 | 4 |
| BBN_9078 | 78 | F | AD(SEV) | NO | NO | 26 | 4 |
| BBN_9092 | 75 | M | NORMAL FOR SHELLEY | NO | NO | 6 | 3 |
| BBN_9189 | 78 | F | AD(SEV) | NO | NO | 21 | 6 |
| BBN_9222 | 90 | M | AD,DLBD | DLBD | NO | 32 | 6 |
| BBN_9284 | 76 | F | AD, LBD | LBD | NO | 43.5 | 6 |
| BBN_9299 | 90 | M | NORMAL | NO | NO | 5.5 | 2 |
| BBN_9311 | 93 | M | No AD, CONTROL | NO | NO | 37.75 | 3 |
| BBN_9317 | 79 | F | AD definite, moderate CVD, very limited cortical LBD | CVD | LBD | 27.25 | 5 |
| BBN_9325 | 90 | F | AD possible, Argyrophilic grain disease, mod CVD | Argyrophilic grain disease | CVD | 18 | 4 |
| BBN_9329 | 80 | M | Mod CAA, mild to mod cerebrovascular disease | NO | NO | 45.75 | 0 |
| BBN_9338 | 95 | M | AD probable, mod CAA, mod small vessel disease | NO | NO | 27 | 4 |
| BBN_9340 | 94 | F | Mod atherosclerosis, CAA | NO | NO | 21 | 2 |
| BBN_9343 | 80 | M | AD probable, moderate CAA | NO | NO | 24 | 4 |

| | | | | | | | |
|----------|----|---|--|-----|-----------------------|------|---|
| BBN_9354 | 85 | M | Control, no significant abnormalities | NO | NO | 30.5 | 2 |
| BBN_4213 | 88 | M | AD probable, very mild limbic LBD | LBD | NO | 5 | 5 |
| BBN_4215 | 80 | F | AD probable, moderate CAA | NO | NO | 26 | 4 |
| BBN_9357 | 92 | F | Braak tangle stage IV but does not fulfil CERAD criteria for AD | NO | NO | 34.5 | 4 |
| BBN_4220 | 86 | F | AD possible, moderate to severe CAA, small vessel CVD with microinfarcts | CVD | NO | 13.5 | 3 |
| BBN_4229 | 87 | F | Apart from mild small vessel disease, no abnormalities seen | NO | NO | 47 | 3 |
| BBN_9375 | 96 | F | AD definite, moderate arteriosclerotic small vessel disease, mild CAA, hippocampal sclerosis | CVD | Hippocampal sclerosis | 26 | 5 |
| BBN_9394 | 81 | M | AD probable, severe capillary CAA | CAA | NO | 32 | 4 |
| BBN_4238 | 85 | F | AD definite, moderate arteriosclerotic small vessel disease, moderate to marked CAA | CVD | CAA | 14 | 5 |
| BBN_9407 | 90 | F | Mild argyrophilic grain disease, moderate CAA, fine to use as control brain | NO | NO | 41 | 2 |
| BBN_9408 | 87 | M | Moderate cerebrovascular disease (atherosclerosis and small vessel disease) use as control but not for comparison with VaD | CVD | NO | 42 | 2 |
| BBN_9422 | 74 | F | Control, no significant abnormalities | NO | NO | 39.5 | 1 |
| BBN_9426 | 81 | M | AD definite, moderately severe arteriosclerotic vascular | CVD | CAA | 32 | 6 |

| | | | | | | | |
|--|--|--|--|--|--|--|--|
| | | | disease (small vessel disease, atheroma), moderate CAA | | | | |
|--|--|--|--|--|--|--|--|

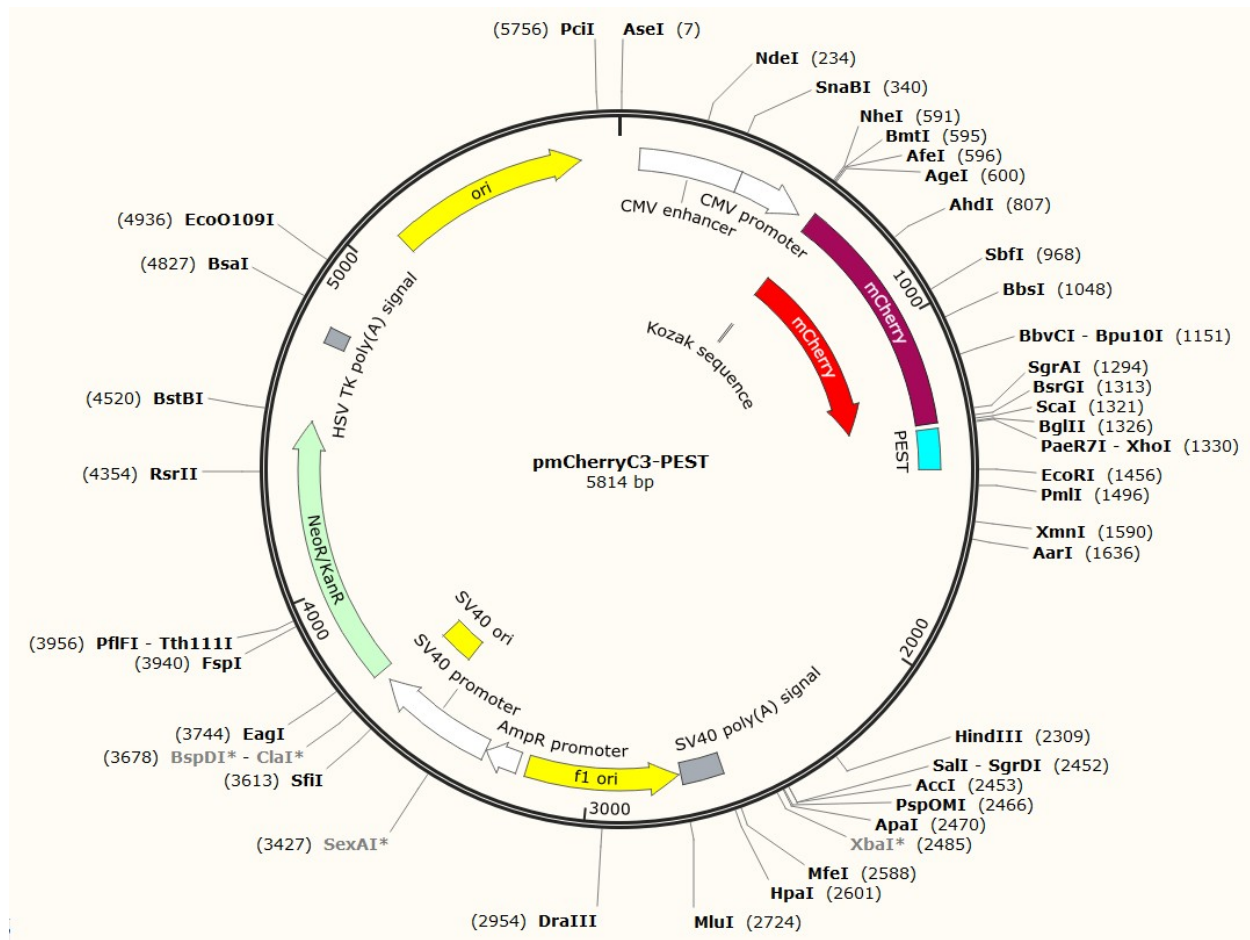
| | | | | | | | |
|-----------|----|---|--|----------------------------|----------------------|-------|---|
| BBN_9432 | 74 | F | Fine to use as control. Argyrophilic grain disease, severe CAA, mild to moderate arteriosclerotic cerebrovascular disease | Argyrophilic grain disease | CAA, CVD | 27.5 | 2 |
| BBN_9433 | 88 | M | AD probable, moderately severe atheromatous large vessel disease and arteriosclerotic small vessel disease, severe CAA | CVD | CAA | 36 | 4 |
| BBN_14398 | 90 | F | AD probable, moderate small vessel disease, moderate CAA | CVD | CAA | 46.75 | 5 |
| BBN_19608 | 96 | M | Control, no significant abnormalities, TDP43 pathology | TDP43 pathology | NO | 21 | 2 |
| BBN_19615 | 75 | M | AD definite, moderate SVD, moderate CAA | CVD | CAA | 7 | 5 |
| BBN_19626 | 81 | M | Fine to use as control. Argyrophilic grain disease | Argyrophilic grain disease | NO | 35.75 | 3 |
| BBN_19627 | 94 | F | Control, moderate CAA | CAA | NO | 29.5 | 2 |
| BBN_19632 | 91 | M | AD definite, hippocampal sclerosis, severe CVD with several infarcts, TDP43 pathology | Hippocampal sclerosis | CVD, TDP43 pathology | 43 | 6 |
| BBN_24309 | 92 | M | AD definite, moderately severe arteriosclerotic SVD | CVD | NO | 30.5 | 5 |
| BBN_24311 | 82 | F | Fine to use as control. Mild | Argyrophilic grain | NO | 36 | 2 |

| | | | | | | | |
|--------------|----|---|----------------------------|---------|----|-------|---|
| | | | argyrophilic grain disease | disease | | | |
| BBN_26015 | 90 | F | AD definite, moderate CAA | CAA | NO | 21.25 | 6 |
| BBN006.27017 | 93 | F | AD definite | NO | NO | 31.75 | 5 |
| BBN006.28766 | 87 | F | AD definite | NO | NO | 40.5 | 5 |
| BBN006.29018 | 89 | F | Nil of note | NO | NO | 26.5 | 2 |

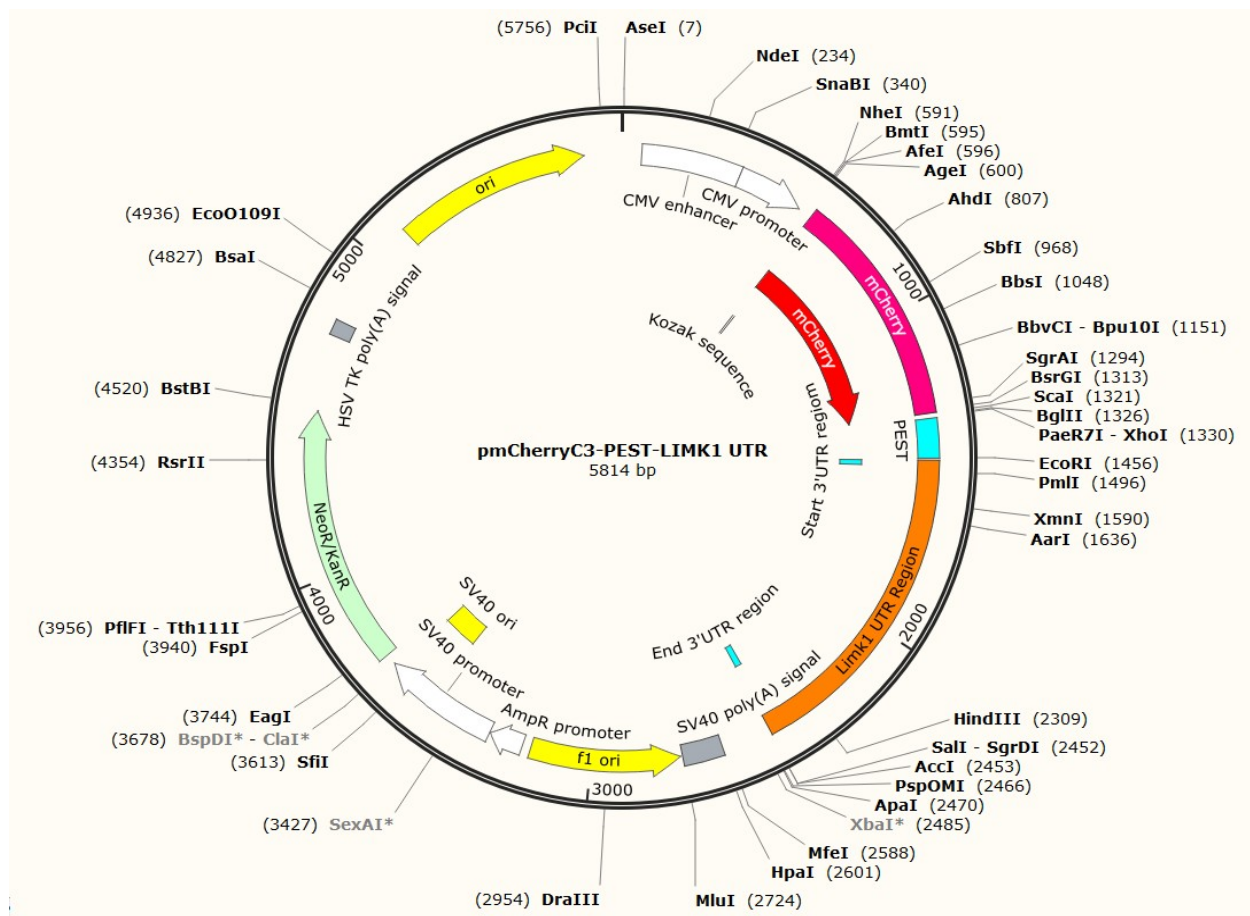
| | | | | | | | |
|--------------|----|---|---|-------------------------|-------------------------------------|-------|---|
| BBN006.29614 | 85 | M | AD definite, severe CAA & capillary CAA with multiple microinfarcts, VCING low likelihood | CAA & capillary CAA | Multiple microinfarcts | 31 | 6 |
| BBN006.29723 | 92 | F | AD probable, VCING high likelihood, multiple subacute cerebral infarcts | VaD | Multiple subacute cerebral infarcts | 16 | 5 |
| BBN006.30024 | 84 | F | AD definite, moderately severe SVD, subarachnoid haemorrhage | CVD | Subarachnoid haemorrhage | 10.25 | 6 |
| BBN006.30165 | 93 | M | No significant abnormalities apart from microinfarct in putamen | Microinfarct in putamen | NO | 34.5 | 2 |
| BBN006.31445 | 86 | M | AD definite, AD-associated TDP43 pathology, hippocampal sclerosis | TDP43 pathology | Hippocampal sclerosis | 34.5 | 4 |
| BBN006.32514 | 80 | M | AD definite, TDP43 pathology associated with AD | TDP43 pathology | NO | 21.25 | 6 |
| BBN006.32578 | 86 | F | Normal brain, moderate CAA | CAA | NO | 36.25 | 2 |

| | | | | | | | |
|------------------|----|---|--|-----------------|----------------------|-------|---|
| BBN006.32845 | 92 | M | CONTROL, severe CAA | CAA | NO | 47.25 | 2 |
| BBN006.3366 6 | 80 | M | AD probable, TDP43 pathology associated with AD/ageing | TDP43 pathology | NO | 43 | 5 |
| BBN006.3368 2 | 91 | F | Moderately severe SVD, severe CAA, mild AD pathology | CAA | Mild AD pathology | 43.5 | 3 |

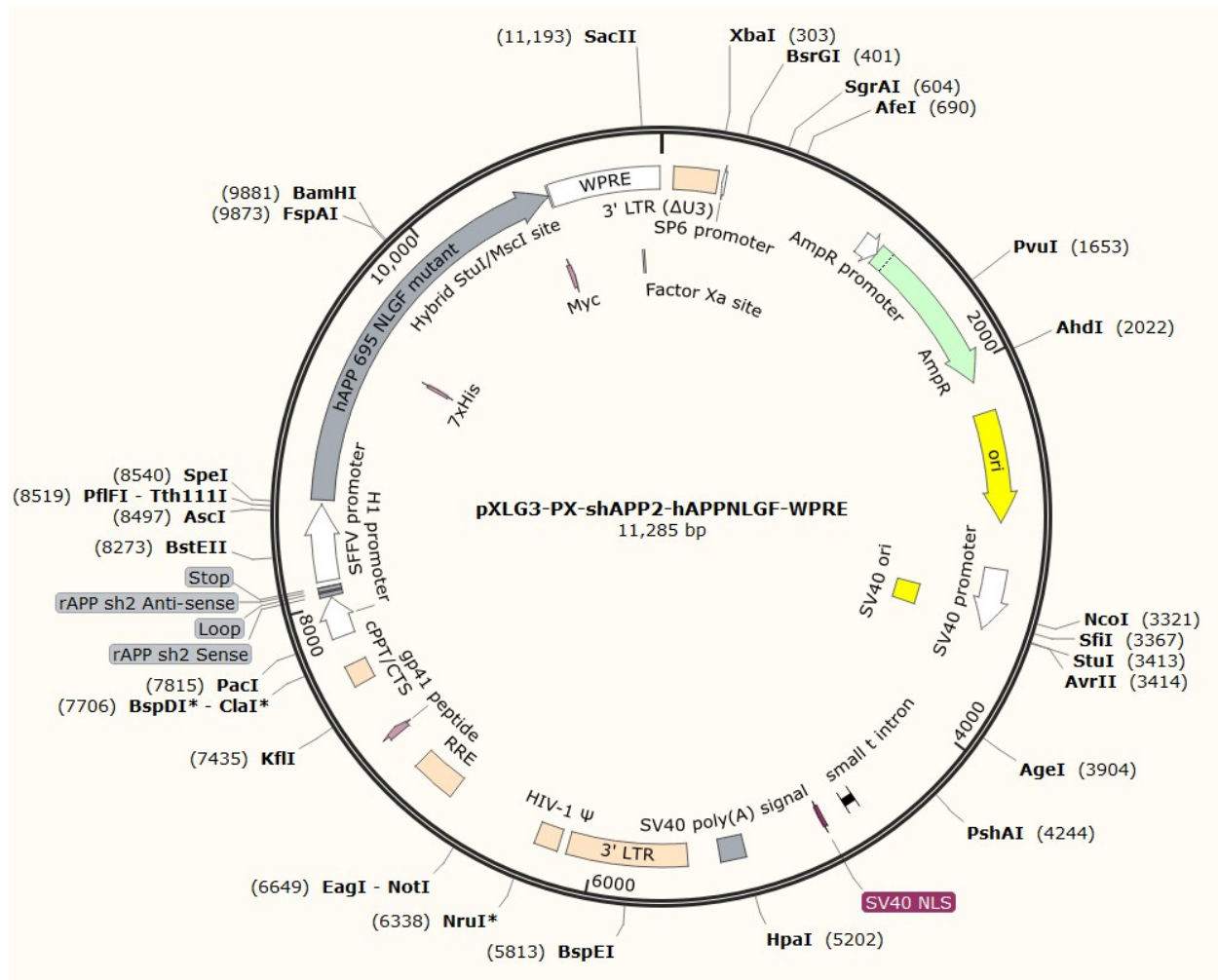
Appendix 2: Plasmid maps



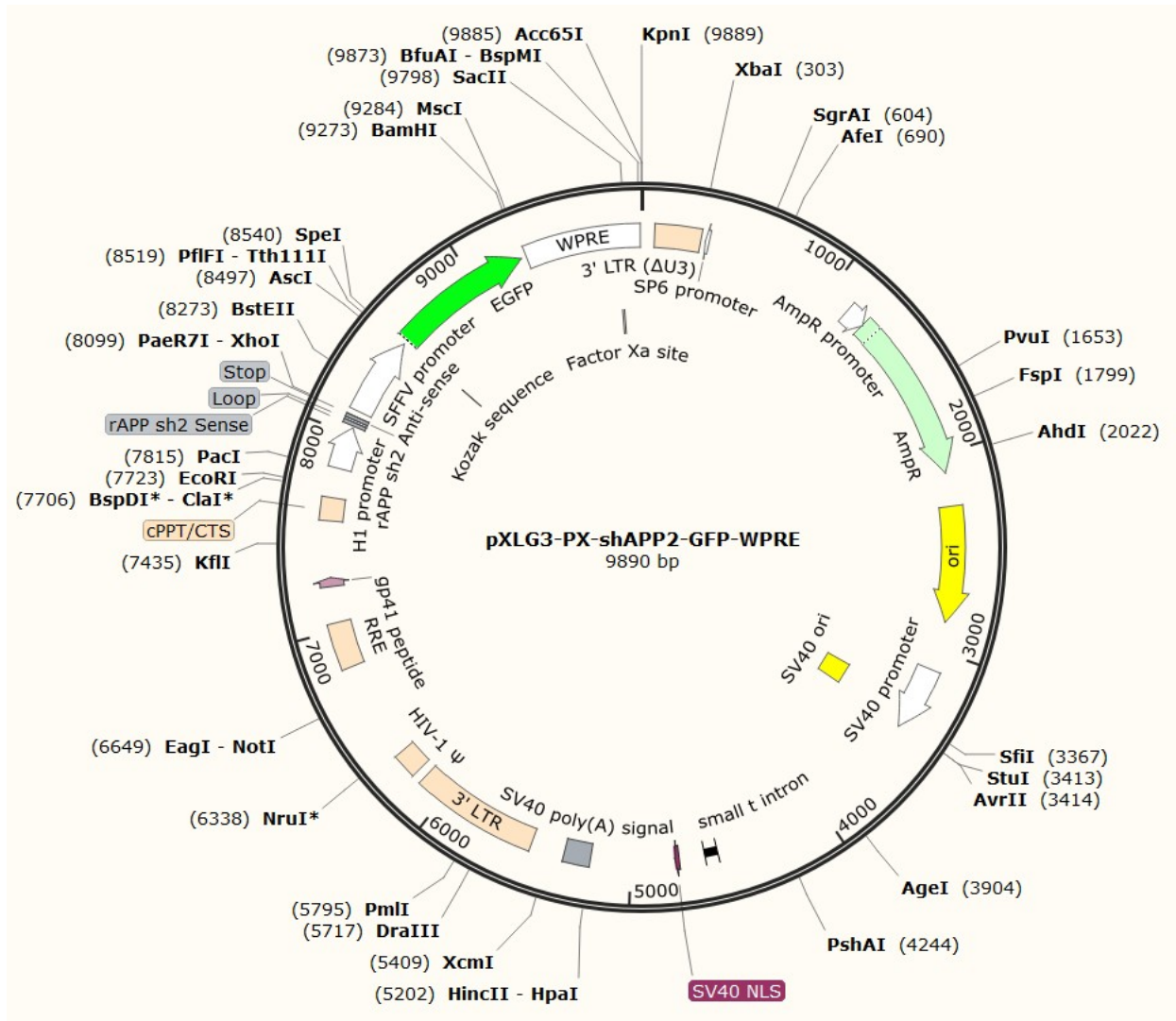
Appendix 2A:



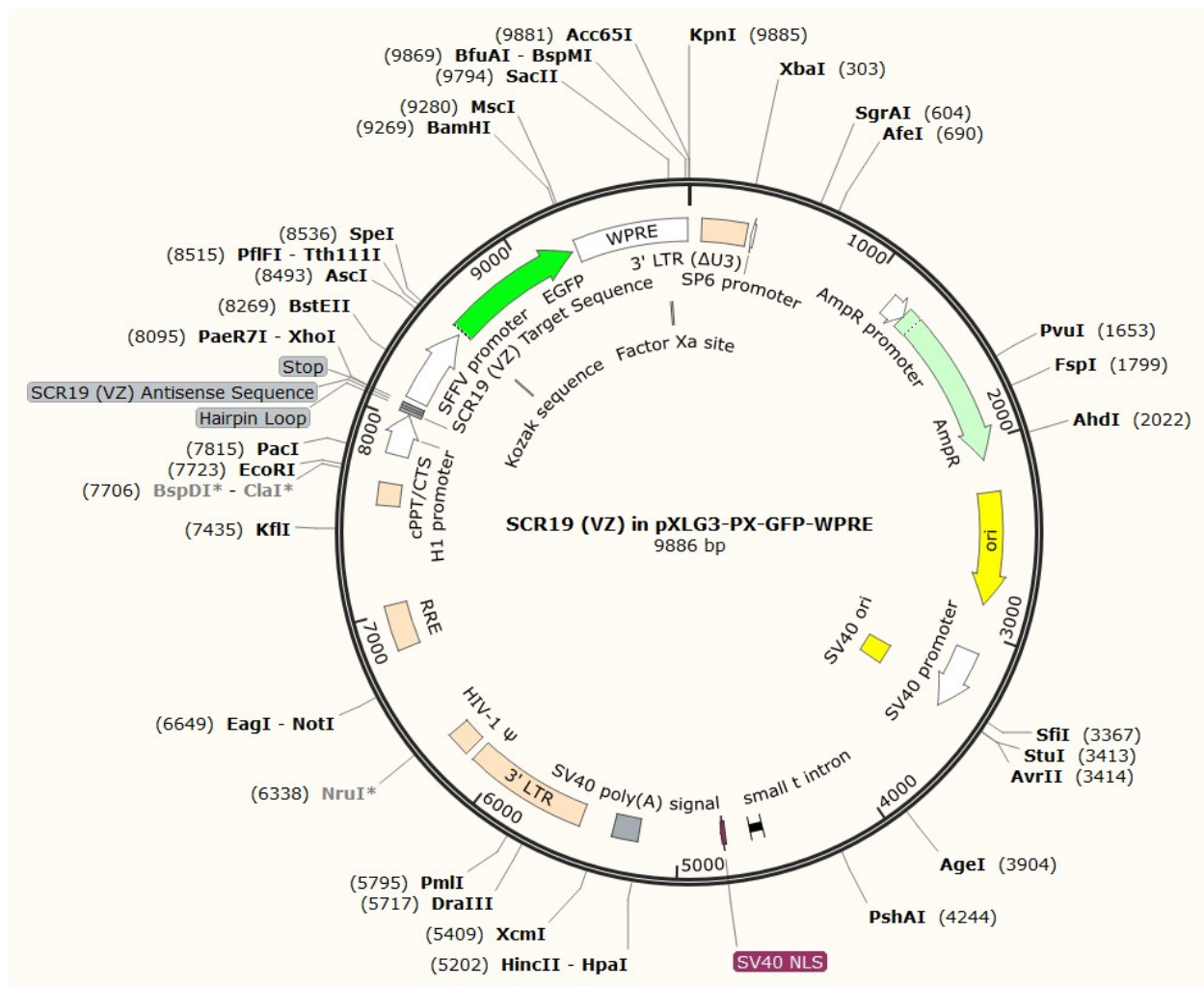
Appendix 2B:



Appendix 2C:



Appendix 2F:



Appendix 2A:

